Titre: Title:	Phase Morphology Development and Rheological Behavior of Non-Plasticized and Plasticized Thermoplastic Elastomer Blends
Auteur: Author:	Shant Shahbikian
Date:	2010
Type:	Mémoire ou thèse / Dissertation or Thesis
Référence: Citation:	Shahbikian, S. (2010). Phase Morphology Development and Rheological Behavior of Non-Plasticized and Plasticized Thermoplastic Elastomer Blends [Thèse de doctorat, École Polytechnique de Montréal]. PolyPublie. https://publications.polymtl.ca/363/

UNIVERSITÉ DE MONTRÉAL

PHASE MORPHOLOGY DEVELOPMENT AND RHEOLOGICAL BEHAVIOR OF NON-PLASTICIZED AND PLASTICIZED THERMOPLASTIC ELASTOMER BLENDS

SHANT SHAHBIKIAN

DÉPARTEMENT DE GÉNIE CHIMIQUE

ÉCOLE POLYTECHNIQUE DE MONTRÉAL

THÈSE PRÉSENTÉE EN VUE DE L'OBTENTION

DU DIPLÔME DE PHILOSOPHIAE DOCTOR (Ph.D.)

(GÉNIE CHIMIQUE)

AOÛT 2010

UNIVERSITÉ DE MONTRÉAL

ÉCOLE POLYTECHNIQUE DE MONTRÉAL

Cette thèse intitulée:

PHASE MORPHOLOGY DEVELOPMENT AND RHEOLOGICAL BEHAVIOR OF NON-PLASTICIZED AND PLASTICIZED THERMOPLASTIC ELASTOMER BLENDS

présentée par: SHAHBIKIAN Shant

en vue de l'obtention du diplôme de: Philosophie Doctor

a été dûment acceptée par le jury d'examen constitué de:

M. DUBOIS Charles, Ph.D., président

M. CARREAU Pierre, Ph.D., membre et directeur de recherche

Mme HEUZEY Marie-Claude, Ph.D., membre et codirectrice de recherche

M. AJJI Abdellah, Ph.D., membre

M. BAIRD Donald G., Ph.D., membre

DEDICATION

To My Beloved Parents

ACKNOWLEDGMENTS

I would like to express my deep and sincere gratitude to my research supervisors, Prof. Pierre J. Carreau and Prof. Marie-Claude Heuzey for providing me the fabulous and gratifying opportunity to study under their supervision. I am truly indebted to their support, kind guidance and encouragements throughout my studies at the École Polytechnique de Montréal. Their guidance, patience and confidence on me had an extraordinary and remarkable impact on developing my scientific and professional foundations. I shall also thank the Center for Applied Research on Polymers and Composites (CREPEC) at École Polytechnique de Montréal, a multidisciplinary research center where this project has been realized.

My especial thanks to Dr. Maria D. Ellul, Dr. John Cheng, Dr. Pradeep P. Shirodkar and Dr. Hari P. Nadella from ExxonMobil Chemical Co. for their support, technical advices and follow-ups. Among them, I shall express my sincere gratitude to Dr. John Cheng and specially Dr. Maria D. Ellul not only for their great scientific vision but also for their magnificent encouragements and concerns regarding this project and my future.

Thanks to all other professors at Chemical Engineering department of École Polytechnique de Montréal, especially Prof. Miroslav Grmela, Prof. Basil D. Favis and Prof. Charles Dubois and Prof. Paula Wood-Adams from Mechanical & Industrial Engineering department of Concordia University with whom I had my wonderful courses during my studies.

I would also like to thank all the technical and administrative staff of Chemical Engineering department, especially Ms. Martine Lamarche, Mr. Lionel Valero, Mr. Jacques Beausoleil, Mr. Carol Painchaud, Mr. Gino Robin and Mr. Guillaume Lessard among the technical staff and Ms. Chantal Bénard, Ms. Lyne Henley and Ms. Diane Héroux among the

administrative staff. An especial thank to Ms. Mélina Hamdine the responsible of our rheology and processing laboratories who besides being a brilliant research associate, she has also been a splendid and magnificent friend. I would also like to show my appreciation to Ms. Rachel Falcon and Ms. Alex Tahan, the two undergraduate students who partly assisted me in carrying out this research project as a part of their final undergraduate project.

Many thanks to all my colleagues and friends specially Mr. Babak Esmaeili, Mr. Amirhossein Maani, Mr. Marc Vidal and Mr. Salim Samsam who were there, present during my studies, and were ready to help in any condition; the friends with whom I had wonderful and pleasant time all along these years.

Ultimately, I would like to express my special, unique and deepest gratitude to my beloved parents not only for their encouragements during each and every step of my life, but also for their unconditional love, understanding and support to pursue my interests even when the interests went beyond boundaries of language, field and geography. A special thank to my brother and his family who have always been a unique symbol of perseverance, hard work and hope.

RÉSUMÉ

Le développement de la morphologie et les propriétés rhéologiques finales d'un mélange de polymères immiscible sont généralement connues pour être influencées par les propriétés viscoélastiques et interfaciales de chacun des polymères constituants ainsi que des paramètres de mise en œuvre. Cette thèse a pour but principale de déterminer la relation entre la morphologie et la rhéologie de mélanges immiscibles réticulés et non réticulés basés sur le terpolymère d'éthylène-propylène-diène (EPDM) et sur le polypropylène (PP), en présence et en absence d'un plastifiant parafinique de faible masse molaire. Ces mélanges constituent une catégorie importante d'un plus grand groupe de matériaux polymères connus sous le nom d'élastomères thermoplastiques (TPEs). Durant les dernières décennies les mélanges EPDM/PP ont, en raison de leur importance commerciale, attirés l'attention des milieux industriels et académiques afin de mieux comprendre et maîtriser le développement de leur morphologie et donc leur propriétés physiques et mécaniques.

Pour ce travail, deux paires EPDM/PP avec des ratios de viscosité (η_{EPDM}/η_{PP}) variant entre 2.04 et 5.53 ont été choisies. Des versions non réticulées (ou polyoléfines thermoplastiques (TPOs)) et réticulés (ou thermoplastiques vulcanisés (TPVs)) des deux paires EPDM/PP ont été étudiées. Pour examiner l'effet du plastifiant et le développement de la co-continuité des mélanges non réticulés, des TPOs de différentes compositions ont été mis en œuvre à l'état fondu dans un mélangeur interne. Une méthode d'extraction par solvant a permis de constater que la plastification favorise une percolation plus rapide du composant élastomère pour les mélanges en faible teneur en EPDM mais en conservant un début de co-continuité identique en comparant aux homologues non plastifiés , i.e. à 40% en poids d'EPDM. La percolation rapide observée en

présence de plastifiant a été attribuée à la forme non sphérique des domaines EPDM et donc à la présence d'un certain niveau de connectivité, comme observé par microscopie électronique à balayage (SEM) et par microscopie à force atomique (AFM). De l'autre côté de la plage de composition, la présence du plastifiant retarde la percolation de la phase PP et donc réduit l'intervalle de co-continuité d'environ 15 unités de la fraction massique. Outre les analyses d'extraction par solvant, les propriétés viscoélastiques linéaires de ces TPOs ont été examinées pour la détermination de la co-continuité. Cependant, à cause de la relativement faible tension interfaciale entre le EPDM et le PP, i.e. environ 0.3 mN/m, les effets de l'élasticité interfaciale dans les TPOs non plastifiés a été masquée par ceux de l'élasticité de la phase EPDM. Par conséquent, seulement les données de la tangente delta basées sur l'approche de gel chimique ont fourni des résultats plus satisfaisants sur l'intervalle de la co-continuité. De plus, parmi les modèles semi-empiriques d'inversion de phase, les modèles basés sur le ratio de viscosité dont la composition de l'inversion de phase présente une dépendance minimal au ratio de viscosité sont connus pour être les plus appropriés.

En outre, pour élucider le développement morphologique des systèmes EPDM/PP réticulés et non réticulés, le comportement viscoélastique non linéaire et l'évolution de la morphologie des mélanges EPDM/PP à bas rapport de viscosité ont été étudiés dans un champ d'écoulement de cisaillement simple. Les précurseurs réactifs et non réactifs ont été préparés dans un mélangeur interne et par la suite soumis à des expériences de démarrage multi-étape dans un rhéomètre rotationnel.

Dans les mélanges non réactifs, le plastifiant favorise le gonflement et la coalescence, augmentant la taille des domaines polymériques et diminuant l'aire interfaciale spécifique (telle que mesurée par AFM). En même temps, l'effet de coalescence semble être plus prononcé dans les mélanges à faible teneur en EPDM. D'un autre coté, à cause d'une contrainte de cisaillement

plus élevée exercée par le composant élastomère sur la phase PP, une morphologie fibrillaire stable a été obtenue pour les mélanges non plastifiés à haute teneur en élastomère. Il est intéressant de remarquer que ni instabilités interfaciales, ni rupture, ni relaxation de forme vers une sphéricité n'ont été observées dans les mélanges non réactifs. Ceci est principalement dû à la faible tension interfaciale entre l'EPDM et le PP.

Dans les mélanges réactifs, la réaction de réticulation in-situ conduit à des domaines polymériques moins allongés avec une interface irrégulière et une plus grande aire interfaciale spécifique comparé aux mélanges non réactifs. La phase EPDM dans les systèmes non plastifiés à haute teneur en élastomère sujets à de longs temps de cisaillement fut transformée en des domaines grossiers et rugueux d'EPDM réticulé encapsulés par la phase thermoplastique, ce qui montre une tendance à l'inversion de phase. La présence du plastifiant réduit le taux de réticulation initiale du composant élastomère dans les premiers stades du cisaillement, ce qui abouti en de larges domaines d'EPDM coalescés sans tendance à l'encapsulation ou à l'inversion de phase.

En générale, le développement de la morphologie dans un écoulement simple est sensiblement différent de celui généré dans un équipement conventionnel de mise en œuvre des polymères. Ceci est principalement dû à la présence d'écoulements complexes dans ce dernier. Une étude comparative sur le développement de la morphologie des mélanges non réticulés et dynamiquement réticulés à base d'EPDM/PP à haut taux de viscosité a donc été effectuée en utilisant un mélangeur interne et une extrudeuse bivis co-rotative. Comme indiqué précédemment, la présence du plastifiant donne lieu à une phase EPDM gonflée et coalescée dans les mélanges non réticulés (TPOs). De plus, l'étude comparative a montré que la majorité du plastifiant dans les TPOs extrudés se trouve dans la phase EPDM, ce qui permet sa déformation dans le sens de l'écoulement. D'autre part, malgré un taux moyen de cisaillement similaire dans

les deux équipements utilisés, l'écoulement dans l'extrudeuse bivis a abouti à une morphologie plus fine comparée au mélangeur interne. Pour les mélanges réticulés dynamiquement (TPVs), la plastification montre aussi un effet de grossissement, aboutissant à des domaines EPDM réticulés interconnectés dans une certaine mesure. Malgré un temps de résidence plus court dans l'extrudeuse bivis, en comparaison avec le mélangeur interne, la réaction de réticulation s'est avérée plus rapide durant l'extrusion, ce qui entraîne un plus haut taux de gel et de plus grands domaines EPDM réticulés et dispersés de façon hétérogène dans la phase thermoplastique. Outre les caractéristiques morphologiques globales observées pour la plupart des TPVs, un phénomène interfacial intéressant a eu lieu où la surface des domaines PP a été érodée et dépouillée, résultant en des domaines, de l'ordre du nanomètre, encapsulés par la phase EPDM réticulé.

Sur la base des résultats obtenus dans cette étude, la plastification semble avoir un effet significatif sur le développement de la morphologie et sur les propriétés viscoélastiques des TPEs. Par conséquent, la plastification doit être prise en compte afin d'obtenir des produits avec les propriétés optimales désirées.

ABSTRACT

The phase morphology development and the final rheological properties of an immiscible polymer blend are generally known to be influenced by the intrinsic viscoelastic and interfacial properties of the constituent polymers and the processing parameters. This dissertation mainly intends to cover the relationship between morphology and rheology of uncross-linked and cross-linked immiscible blends based on ethylene-propylene-diene-terpolymer (EPDM) and polypropylene (PP), in the presence and absence of a low molecular weight paraffinic plasticizer. These blends constitute an important category of a larger group of polymeric materials known as Thermoplastic Elastomers (TPEs). During the last few decades the EPDM/PP-based blends, due to their commercial importance, have drawn significant attention of both industrial and academic world to better understand and control their phase morphology development and, therefore, their ultimate physical and mechanical properties.

For this work, two EPDM/PP pairs with viscosity ratios (η_{EPDM}/η_{PP}) ranging from 2.04 to 5.53 were chosen. Uncross-linked (or Thermoplastic Polyolefins (TPOs)) and cross-linked (or Thermoplastic Vulcanizates (TPVs)) versions of the two EPDM/PP pairs were investigated. To study the effect of the plasticizer on the co-continuity development of the uncross-linked blends, TPOs at various compositions were melt blended inside an internal mixer. Based on a solvent extraction method, it was found that the plasticization promoted a more rapid percolation of the elastomeric component on the low EPDM side of the composition diagram, but keeping an identical onset of co-continuity as compared to the non-plasticized counterparts, i.e. at 40 wt% EPDM. The observed rapid percolation in the presence of the plasticizer was attributed to the non-spherical shape of the EPDM domains and, therefore, to the presence of a certain level of

connectivity, as observed by scanning electron microscopy (SEM) and atomic force microscopy (AFM). On the other side of the composition range, the presence of the plasticizer delayed the percolation of the PP phase and, therefore, reduced the co-continuity interval by ~15 compositional units. Besides the solvent extraction analyses, the linear viscoelastic properties of these TPOs were examined for co-continuity determination. However, due to the relatively low interfacial tension between EPDM and PP, i.e. ~0.3 mN/m, the interfacial excess elasticity in the non-plasticized TPOs was overshadowed by the elasticity of the EPDM phase and, therefore, only the frequency independence of loss tangent data, based on the chemical gel approach, provided a comparable information on the co-continuity interval. In addition, among the existing semi-empirical phase inversion models, the viscosity ratio-based models with minimum dependency of the phase inversion composition to the viscosity ratio appeared to be the most appropriate.

Additionally, to elucidate the morphology development of uncross-linked and cross-linked EPDM/PP systems, the non-linear viscoelastic behaviour and morphology evolution of the low viscosity ratio EPDM/PP blends were investigated in a homogeneous shear flow field. The non-reactive and reactive precursors were prepared inside an internal mixer and subsequently subjected to single and multiple start-up transient experiments in a rotational rheometer.

In the non-reactive blends the plasticizer promoted swelling and coalescence, enlarging the size of the polymeric domains and decreasing the specific interfacial area (as measured by AFM) throughout the multiple shearing steps. Meanwhile, the coalescence effect appeared to be more pronounced in low EPDM content blends. On the other hand, due to the higher shear stress exerted by the elastomeric component on the PP phase, a stable fibrilar morphology was obtained at high elastomer content for non-plasticized blends. Interestingly, neither interfacial instabilities

and breakup, nor shape relaxation towards sphericity was observed in the non-reactive blends, mainly due to the low interfacial tension between EPDM and PP.

In the reactive blends, the insitu cross-linking reaction resulted in less elongated polymeric domains with an irregular interface and larger specific interfacial area as compared to the non-reactive blends. The EPDM phase in the non-plasticized systems with high elastomer content subjected to long shearing times was transformed into coarse cross-linked EPDM domains encapsulated by the thermoplastic phase showing a tendency towards phase inversion. The presence of the plasticizer reduced the initial curing rate of the elastomeric component in the early shearing stage and resulted in large coalesced EPDM domains, with no tendency towards encapsulation or phase inversion.

Generally, the morphology development inside a homogeneous flow field is quite different from the one generated inside a conventional melt mixing equipment, mainly due the presence of complex flow fields in the latter. Therefore, a comparative study on the morphology development of uncross-linked and dynamically cross-linked high viscosity ratio EPDM/PP blends was performed using an internal mixer and co-rotating twin-screw extrusion. As previously reported, the presence of the plasticizer resulted in a swollen and coalesced EPDM phase in uncross-linked blends (TPOs). The processing comparative study showed furthermore that the majority of the plasticizer in the extruded TPOs resided in the EPDM phase, enabling its deformation in the flow direction. On the other hand, despite a similar average apparent shear rate employed in both mixing equipments, the intensive flow field inside the twin screw extruder resulted in a finer morphology in comparison to the internal mixer. For dynamically cross-linked blends (TPVs), the plasticization showed again a similar coarsening effect, resulting into cross-linked EPDM domains interconnected to some extent. Despite the shorter residence time inside the twin screw extruder as compared to the internal mixer, the cross-linking reaction was found to

proceed comparably faster during twin screw extrusion, resulting in a higher level of gel content and larger cross-linked EPDM domains heterogeneously dispersed in the thermoplastic phase. Besides the overall morphological features observed for most TPVs, an interesting interfacial phenomenon also took place, where the surface of the PP domains was eroded and stripped off, resulting into nanometre-size occluded PP domains encapsulated by the cross-linked EPDM phase.

Based on the results obtained in this study, the plasticization appeared to have a significant coarsening effect on the morphology development and to decrease the viscoelastic properties of TPEs and hence shall be taken into account in order to achieve products with optimum desired properties.

CONDENSÉ EN FRANÇAIS

Les élastomères thermoplastiques (TPEs) représentent un groupe important de matériaux polymères contenant des liens thermoréversible faciles à manipuler via des procédés de mise en œuvre des plastiques, et qui possèdent un comportement élastique similaire aux caoutchoucs vulcanisés (i.e. chimiquement réticulés). Une catégorie importante de TPEs consiste en des matériaux à base de polyoléfine combinant à la fois une polyoléfine thermoplastique semi-cristalline et un composant élastomère amorphe. Dans cette catégorie, les TPEs à base de polypropylène (PP) et de terpolymère éthylène-propylène-diène (EPDM) ont été reconnus dans le marché pour leurs propriétés physiques et mécaniques obtenues par la mise en œuvre à l'état fondu, et principalement dues à leur faible tension interfaciale (~0.3 mN/m) et à leur compatibilité de phase. En plastifiant ces TPEs on pourrait améliorer leur gonflement dans l'huile, leur stabilité thermique, leur hystérésis, et leur déformation permanente. Aussi, on pourrait améliorer les propriétés mécaniques à basse température, la mise en œuvre à l'état fondu, ainsi bien que l'apparence finale des produis. Et donc, en raison de leur importance commerciale, ces matériaux ont été largement étudiés au cours de ces dernières décennies.

L'objectif de cette thèse consiste en l'étude, d'une part, du développement morphologique, et d'autre part, de la relation entre les propriétés viscoélastiques et la morphologie des mélanges non miscibles composés d'EPDM et de PP. Plus précisément, il s'agit ici de l'étude approfondie des effets d'un plastifiant à faible poids moléculaire et de la réticulation sélective de la phase élastomère sur la relation entre morphologie et la rhéologie de ces mélanges.

Pour atteindre ces objectifs, deux paires différentes d'EPDM/PP ont été choisies. Une paire est composée d'un EPDM de viscosité de Mooney élevée et d'un homopolymère PP (E1/P1), tandis que l'autre paire est composée d'un EPDM de faible viscosité de Mooney et d'un co-polymère PP aléatoire (E2/P2), avec des rapports de viscosité (η_{EPDM}/η_{PP}) de 5.53 et de 2.04 à 180°C respectivement. L'effet du plastifiant sur le développement de la continuité a été étudié pour les deux systèmes non réticulé E1/P1 et E2/P2, aussi connus en tant que polyoléfines thermoplastiques (TPOs). Les TPOs à base de E1/P1 et E2/P2 plastifiés et non plastifiés ont été mélangés à l'état fondu dans un mélangeur interne. Pour les TPOs plastifiés, 100 phr (partie par cent de caoutchouc) d'huile de paraffine ont été ajoutées durant l'étape de mise en œuvre à l'état fondu. Une technique d'extraction par solvant a été effectuée sur les échantillons pour déterminer l'intervalle de co-continuité et de la percolation par une dissolution sélective de la phase EPDM.

Il est intéressant à noter que dans les mélanges à faibles teneurs en EPDM, une percolation rapide a été observée, contrairement à la lente percolation classique caractéristique des mélanges à très forte tension interfaciale. La microscopie électronique à balayage (SEM) des TPOs à faible teneur en EPDM a confirmé la présence de domaines élastomères irrégulièrs et non sphériques avec un certain niveau d'interconnectivité. La présence d'un plastifiant a permis de promouvoir davantage la coalescence et le gonflement, et elle a conduit ainsi à une percolation plus rapide de la phase à faible teneur en EPDM. Par conséquent, chez les TPOs plastifiés contenant 25% (en poids) d'EPDM, il y a ~80% de la phase EPDM qui contribue au réseau élastomérique continue, alors que dans le système non plastifié, la continuité de l'EPDM se situe seulement entre 48-59%. Malgré cet effet sur la percolation, il paraît que la plastification n'affecte pas de début de la co-continuité qui a été observée à 40% en poids d'EPDM dans tous les mélanges.

On signale également que dans les mélanges à faibles quantités de PP, une percolation beaucoup plus rapide de cette phase a été observée par rapport aux mélanges à faible teneur en EPDM. En plus, la plastification a retardé la percolation de la phase PP semi-cristalline, et ainsi elle a réduit l'intervalle de co-continuité par ~15% unités de fraction massique, i.e. de 40 à ~75% (en poids) en EPDM, contrairement à ce qu'on trouve chez les TPOs non plastifiés qui ont un intervalle de 40 à ~90% (en poids) en EPDM.

En parallèle avec les analyses d'extraction par solvant, les propriétés viscoélastiques linéaires de ces TPOs ont été également étudiées pour la détermination de la co-continuité. Toutefois, en raison de la faible tension interfaciale entre l'EPDM et le PP, i.e. ~0.3 mN/m, et en l'absence du plastifiant, les effets de l'élasticité interfaciale a été bien masquée par ceux de l'élasticité de l'EPDM. Par conséquent, la réponse du module de stockage, à faible fréquence, des TPOs non plastifiés semble être insensible aux changements morphologiques. L'addition du plastifiant a fait diminuer de manière drastique la viscosité et l'élasticité des polymères et des TPOs résultants, tout en améliorant la réponse interfaciale de ces mélanges. Malgré cette amélioration en présence du plastifiant, seulement les données de la tangente delta basés sur l'approche de gel chimique ont fourni des résultats sur l'intervalle de co-continuité comparable avec les analyses d'extraction par solvant.

En plus, les intervalles de co-continuité déterminés expérimentalement et obtenus par la technique d'extraction par solvant, ont été comparés avec les prédictions des modèles d'inversion de phase semi-empiriques. Parmi ces modèles, ceux qui prédisent une composition d'inversion de phase moins dépendante au rapport de viscosité, semblent être plus appropriés. D'autres tentatives ont été faites dans le but de modéliser les propriétés viscoélastiques de ces TPOs, possédant une morphologie co-continue, en utilisant un modèle micromécanique de Veenstra-D.

Ceci a amené à conclure qu'une certaine quantité de plastifiant pourrait être présente à l'interface entre les composants polymériques entraînant une interphase plastifiée.

Pour élucider le développement morphologique des mélanges EPDM/PP réticulés et non réticulés, le comportement viscoélastique non linéaire ainsi que l'évolution morphologique des mélanges E2/P2 ont été étudiés dans champ d'écoulement de cisaillement homogène. Pour cet effet, des mélanges non réactifs et des précurseurs réactifs contenant 5 phr d'une résine phénolique ont été préparés dans un mélangeur interne et soumis par la suite à des démarrages multi-étapes dans un rhéomètre rotationnel. Les mélanges non réactifs ont été soumis à des cisaillements multi-étapes dans le sens horaire et anti-horaire pour une durée de 450 s à 0.1 s^{-1} chacune, séparées par un temps de repos de 600 s. Durant la première étape dans le sens horaire, la magnitude de pic de contrainte et le temps nécessaire pour atteindre l'état stationnaire a aussi augmenté avec le contenu en EPDM. À la fin de cette étape, une morphologie élongée et coalescée a été obtenue pour tous les mélanges non réactifs, indépendamment de la plastification. En outre, une morphologie fibrillaire stable a été également observée par microscopie à force atomique (AFM) pour des mélanges non plastifiés à haute teneur en EPDM à cause de la contrainte de cisaillement élevée exercée par la phase élastomère sur la phase thermoplastique. Plus intéressant, ni les instabilités interfaciales et la rupture, ni la relaxation de forme vers une morphologie sphérique ont été observés dans ces mélanges, principalement dûs à la faible tension interfaciale entre les composants polymériques. La présence du plastifiant à travers les multiples étapes de cisaillement a bien favorisé le gonflement et la coalescence en élargissant la taille des domaines polymériques, et en diminuant la surface interfaciale spécifique. En plus, l'évolution des surfaces interfaciales spécifiques expérimentales des mélanges non réactifs a été prédite en utilisant le modèle phénoménologique modifié de Lee et Park.

Par ailleurs, les mélanges réactifs ont été soumis uniquement à des démarrages, en une seule étape, dans le sens horaire à 0.1 s^{-1} pour des durées de 450, 2700 et 7200 s. La réaction de réticulation in-situ a généré des domaines polymériques moins élongés avec une interface irrégulière et une surface interfaciale spécifique plus large par rapport aux mélanges non réactifs. La phase EPDM dans les mélanges réactifs non plastifiés avec 50 à 60 % (en poids) en EPDM, et soumis à un cisaillement à 2700 s, a été transformée à des domaines rugueux d'EPDM réticulés et encapsulés par la phase thermoplastique tout en montrant une tendance vers l'inversion de phase. La présence du plastifiant semble avoir un effet retardant sur la réaction de réticulation de la phase EPDM durant le début de cisaillement. Cet effet a permis ainsi de produire des larges domaines coalescés d'EPDM à des temps longs, i.e. 2700 s, sans aucune tendance vers l'encapsulation ou de l'inversion de phase.

Puisque le champ d'écoulement à l'intérieur des équipements conventionnels de mise en œuvre des polymères est très complexe comparé a l'écoulement homogène à l'intérieur des rhéomètres rotationnels, une étude comparative du développement morphologique a été effectuée sur les mélanges non-réticulés et dynamiquement réticulés à base de mélanges E1/P1 obtenus à partir d'un mélangeur interne et une extrudeuse bivis co-rotative. La technique AFM a été employée pour étudier les effets du plastifiant et des méthodes de mise en œuvre sur le développement morphologique. Sans tenir compte de l'équipement de mise en œuvre utilisé, la présence de plastifiant a généré une phase EPDM gonflée et coalescée dans les mélanges non réticulés (TPOs) en réduisant de manière significative la moyenne des surfaces interfaciales spécifiques. De plus, les micrographes SEM des TPOs extrudés ont révélés que la majorité du plastifiant se trouvait dans la phase EPDM permettant sa déformation dans la direction de l'écoulement. D'autre part, malgré la valeur similaire du taux de cisaillement apparent employé dans les deux équipements, le champ d'écoulement intensif à l'intérieur de l'extrudeuse bivis a

abouti à une morphologie plus fine. Ainsi, les rapports de la moyenne de la surface interfaciale spécifique des TPOs obtenus à partir de l'extrudeuse bivis par rapport à ceux préparés dans le mélangeur interne ont été, respectivement, de l'ordre de 2,25 et de 1,77 pour les TPOs plastifiés et non plastifiés.

Pour les mélanges dynamiquement réticulés aussi connus sous le nom de vulcanisats thermoplastiques (TPVs), différents facteurs comme la plastification, l'intensité du champ d'écoulement et, de façon plus importante, la cinétique de réticulation du composant élastomère, affectent simultanément le développement morphologique. Dans les TPVs, la plastification a résulté encore une fois un aspect rugueux des domaines d'EPDM réticulés interconnectés. En revanche dans les TPVs non plastifiés, ces domaines élastomères ont été bien distingués. En outre, sans tenir compte de la plastification, et malgré un temps de résidence plus court à l'intérieur de l'extrudeuse bivis par rapport au mélangeur interne, la réaction de réticulation s'est avérée plus rapide durant l'extrusion bivis, ce qui entraîne un plus haut taux de gel et de plus larges domaines d'EPDM réticulés dispersés de manière hétérogène dans la phase PP.

En addition à l'ensemble de ces aspects morphologiques observés dans les TPVs, un phénomène interfacial intéressant a été également observé entre les phases EPDM et PP. La surface de la phase PP a été érodée et dépouillée, résultant en des domaines de l'ordre du nanomètre encapsulés par la phase EPDM réticulée. L'apparition de ce phénomène a été nettement marquée pour les TPVs plastifiés obtenus par l'extrusion bivis. Ceci est dû à l'augmentation de l'élasticité de la phase EPDM durant l'étape de la réticulation dynamique et à la diminution simultanée de la viscosité locale de la surface PP en présence du plastifiant.

En se basant sur les résultats de cette étude, tout en soulignant le rôle crucial de la microstructure du mélange sur les propriétés ultimes des TPEs, il paraît que la plastification parmi d'autres paramètres possède un effet énorme sur le développement morphologique et sur

les propriétés viscoélastiques des mélanges TPVs et TPOs. Ainsi, pour finaliser un produit plastifié bien optimisé, la quantité et la méthode d'incorporation du plastifiant devraient être considérées avec précaution.

TABLE OF CONTENTS

LIST OF TABLES

LIST OF FIGURES

NOMENCLATURE

English letters:

a	Geometric parameter associated to one of the phases in Veenstra-D model
b	Geometric parameter associated to one of the phases in Veenstra-D model
c_1	The degree of total relaxation in Lee and Park model
c_2	The degree of size relaxation in Lee and Park model
c_3	The degree of break-up and shape relaxations in Lee and Park model
d_1	The coalescence relaxation dimensionless rate constant in Lee and Park model
d_2	The shape relaxation dimensionless rate constant in Lee and Park model
d_3	The break-up and shape relaxations dimensionless rate constant in Lee and Park model
$k_{\alpha\beta}$	The components of the velocity gradient tensor
n	Unit normal vector to the interface
q	The anisotropy tensor
$q_{\alpha\beta}$	The components of the anisotropy tensor
r_1	The coalescence relaxation rate in Lee and Park model
r_2	The shape relaxation rate in Lee and Park model
r_3	The break-up and shape relaxations rate in Lee and Park model
t	Time
t_b	Break-up time
t_c	Film drainage time

t_d	Characteristic time of the diffusion process
t_{gel}	Time at gel point (crossover point of G' and G'')
t_x	Time required to reach x% modulus increase during cross-linking reaction
$w_{\text{oil,EPDM}}$	Weight fraction of oil (plasticizer) in the EPDM phase
$w_{\text{oil,PP}}$	Weight fraction of oil (plasticizer) in the PP phase
B_{A}	Specific interfacial perimeter
Ca	Capillary number
$Ca_{\text{crit.}}$	Critical capillary number
D	Droplet diameter
$\mathbf{D}$	The volume average rate of deformation tensor
$\mathbf{D_d}$	The volume average rate of deformation tensor in the dispersed phase
$\mathbf{D_m}$	The volume average rate of deformation tensor in the matrix phase
D_b	Deborah diffusion number
E_a	Activation energy of cross-linking reaction
G'	Storage modulus
G'_0	Storage modulus prior cross-linking reaction
G'_f	Storage modulus at the end of reaction
G'_{NR}	Storage modulus of non-reactive blend
G''	Loss modulus
G''_{NR}	Loss modulus of non-reactive blend
G^*	Complex modulus
G^*_d	Complex modulus of dispersed phase

G^*_m	Complex modulus of dispersed phase
I	The unit tensor
K	Plasticizer distribution coefficient
N1(t)	First normal stress growth function
P	Hydrostatic pressure
Q	Specific interfacial area
R	Droplet radius
R_n	Number average droplet radius
R_v	Volume average droplet radius
S	Area
T	Temperature
T_g	Glass transition temperature
T_m	Melting temperature
V	Volume

Greek letters:

γ	Strain
$\dot{\gamma}$	Shear rate
$\dot{\gamma}_{eff.}$	Effective shear rate
δ	Phase angle
δ_d	Phase angle of the dispersed phase

δ_m	Phase angle of the matrix phase
$\delta_{\alpha\beta}$	The Kronecker delta
η	Viscosity
η_i	Viscosity of component *i*
η_d	Viscosity of dispersed phase
η_m	Viscosity of matrix phase
η_r	Viscosity ratio (η_d/η_m)
η_s	Viscosity at the steady state
$\eta^+(t)$	Shear stress growth coefficient
η^*	Complex viscosity
η^*_{NR}	Complex viscosity of the non-reactive blend
$[\eta]$	Intrinsic viscosity
λ_m	Characteristic relaxation time of the fluid
ξ	The pre-factor used in several semi-empirical phase inversion models
τ	Mixing torque
$\tau_{eff.}$	Effective matrix shear stress
$\boldsymbol{\tau}$	The volume average total stress tensor
$\boldsymbol{\tau_d}$	The volume average total stress tensor in the dispersed phase
$\boldsymbol{\tau_m}$	The volume average total stress tensor in the matrix phase
ϕ	Volume fraction
ϕ_c	Percolation threshold volume fraction
ϕ_m	Maximum packing volume fraction

$\phi_{I,\mathrm{i}}$	Phase inversion composition of component *i*
$\phi_{Onset,\mathrm{i}}$	Onset of co-continuity composition of component *i*
ψ	The exponent used in several semi-empirical phase inversion models
ω	Oscillating frequency
Γ	Interfacial tension
Δ	The power law exponent for storage and loss moduli at gel point
Δ'	The power law exponent for storage modulus
Δ''	The power law exponent for loss modulus
Ω	Complex function of viscosity ratio and wave length in Tomotika's theory

LIST OF ABBREVIATIONS

phr	Parts per hundred parts of rubber
AFM	Atomic force microscopy
ASTM	The American Society For Testing and Materials
CCW	Counter-clockwise
CI	Continuity index
COPEs	Co-polyester elastomers
CW	Clockwise
DRS	Dielectric relaxation spectroscopy
EMA	Ethylene methyl acrylate co-polymer
ENB	Ethylidene norbornene
EPDM	Ethylene-propylene-diene-terpolymer
EPDM-g-MA	Maleic anhydride grafted ethylene-propylene-diene-terpolymer
EPR	Ethylene propylene rubber
EVA	Ethylene vinyl acetate co-polymer
HDPE	High density polyethylene
LLDPE	Linear low density polyethylene
MFI	Melt flow index
NMR	Nuclear magnetic resonance
NP	Non-plasticized

NR	Non-reactive
P	Plasticized
PA, PA6	Polyamide, Polyamide-6
PBT	Poly(butylenes terephthalate)
PC	Polycarbonate
PDMS	Poly(dimethylsiloxane)
PEO	Polyethylene oxide
PES	Polyethersulfone
PMI	Partially mobile interface
PMMA	Poly(methyl methacrylate)
PP	Polypropylene
PP-RCP	Polypropylene random co-polymer
PS	Polystyrene
PVdF-HFP	Polyvinylidenefluoride-hexafluoropropylene
R	Reactive
SBCs	Styrenic block co-polymers
SEBS	Polystyrene-poly(ethylene-co-butylene)-polystyrene triblock co-polymer
SEM	Scanning electron microscopy
$SnCl_2$	Stannous chloride
TEM	Transmission electron microscopy
TPEs	Thermoplastic elastomers
TPOs	Thermoplastic polyolefins
TPUs	Thermoplastic polyurethanes

TPVs	Thermoplastic vulcanizates
ZnO	Zinc oxide

CHAPTER 1

INTRODUCTION

The development of polymeric materials has always been driven towards the production of new high performance materials at minimum cost. These goals have so far been achieved either by chemical synthesis at a commercial scale, or by blending different existing polymers. Generally the cost of developing a new polymeric material through chemical synthesis is comparably higher than conventional melt blending processes, where by employing a suitable blending technology a wide range of physical and mechanical properties can be attained for a specific end-use application with the advantage of a unique performance/cost ratio. As a result, polymer blends have played a significant revolutionary role in advancing the polymer science and technology during the last few decades.

In the literature the term *Polymer Blend* has been assigned to any combination/mixture of two (or more) structurally different polymers being miscible or immiscible, giving rise to a material with a range of properties which could not have been achieved by any of the constituents alone (Paul and Bucknall, 2000). Similar to the expression used in the field of material science, the immiscibility refers to the existence of a phase separated structure in a blend.

As a general rule, the main thermodynamic function that indicates the miscibility of solutions is the variation of the Gibbs free energy of mixing ($\Delta G_{\text{mix.}}$), along with its enthalpic ($\Delta H_{\text{mix.}}$) and enthropic ($\Delta S_{\text{mix.}}$) contributions:

$$\Delta G_{mix.} = \Delta H_{mix.} - T\Delta S_{mix.} \tag{1.1}$$

The first criterion for the occurrence of miscibility at the equilibrium state (e.g. polymer in solvent, polymer in polymer, etc.), is that the Gibbs free energy must be minimum, which in turn implies that the change in the Gibbs free energy of mixing must be negative ($\Delta G_{\text{mix.}}<0$). Furthermore, in addition to a negative change in the Gibbs free energy of mixing, a second condition is required for complete miscibility, where the second derivative of $\Delta G_{mix.}$ with respect to the composition (i.e., $\partial^2 \Delta G_{mix.} / \partial \phi_A^{\,2} > 0$) should be positive at a constant temperature and pressure (Paul and Bucknall, 2000).

Generally for blends composed of at least two polymeric constituents with large degrees of polymerization and low interactive forces, the positive mixing enthalpy overcomes the negligible negative mixing entropy, resulting in an immiscible or phase separated structure. It is noteworthy to mention that depending on the final applications, immiscibility and, therefore, a phase separated structure has never been considered as a drawback. In the following chapters, the main focus will be devoted to a specific category of polymeric materials known as thermoplastic elastomers (TPEs), where the immiscibility and phase separated structure is an indispensable factor for their specific end-use applications.

From a technological point of view, thermoplastic elastomers (TPEs) have drawn significant attention of researchers since their introduction in the market in the 1960s (Drobny, 2007). They can exhibit an elastic behavior identical to that of vulcanized (chemically cross-linked) conventional elastomers, with the ease of processing by conventional melt processing machineries. Furthermore, in contrast to elastomers where the elastic properties are gained via vulcanization of the polymeric chains, i.e. an irreversible chemical reaction, the physical and mechanical properties of TPEs are generally attained through phase separated morphologies (De and Bhowmick, 1990; Holden, 2000; Drobny, 2007).

As a result, they offer the following advantages over conventional cross-linked elastomers (Drobny, 2007): simpler polymer processing using conventional methods used for thermoplastics, shorter fabrication times, limited or no compounding needs, recyclability and re-use of scraps, lower energy consumption, better and lower cost quality control and closer tolerances of finished parts and lower volume cost due to their lower density compared to conventional elastomers. However, they also present some disadvantages as compared to conventional elastomers (Drobny, 2007): melting at elevated temperatures, the existence of limited low hardness products (lower than 80 Durometer A), and the need for drying prior to processing.

In order to tackle with the problem of lowering the hardness of TPEs, a proper plasticizer (processing oil or extender oil) has been regularly used in TPE industry. The addition of plasticizer generally reduces the overall cost and improves the resistance to oil swell, heat stability, hysteresis, elastic recovery and permanent set of the TPEs, as well as the low temperature mechanical properties, melt processability and the final appearance of the products (Abdou-Sabet and Fath, 1982).

It is worth nothing that according to a study entitled "*World thermoplastic elastomers*" conducted by Freedonia Group, Inc. (2005), the global demand for TPEs in November 2005 was 2,300,000 metric tons, with styrenic block co-polymers and thermoplastic polyolefins (TPOs) representing the two largest groups in volume (Table 1.1). The study also showed that the world demand for TPEs is expanding by ~6.2% per year, most probably up to 4,200,000 metric tons in 2014.

Table 1.1. World thermoplastic elastomers (TPEs) demand (x10^{-3} metric tons) (Freedonia Group, Inc. (2005) and (Drobny, 2007)

Item	2004	2009	2014	% Annual growth, Sep. 2004

Thermoplastic elastomer demand	2300.0	3100.0	4200.0	6.2
By type:				
Styrenic block copolymers (SBCs)	1081.0	1409.0	1847.0	5.4
Thermoplastic polyolefins (TPOs)	506.2	687.0	936.0	6.3
Thermoplastic polyurethanes (TPUs)	320.1	442.0	609.0	6.7
Thermoplastic vulcanizates (TPVs)	161.7	233.0	332.0	7.6
Co-polyester elastomers (COPEs)	120.9	175.0	256.0	7.7
Other TPEs	110.1	154.0	220.0	6.9
By region:				
North America	628.7	785.5	980.5	4.6
Western Europe	503.4	608.0	726.5	3.8
China	690.0	1052.0	1587.0	8.8
Japan	153.0	183.5	220.5	3.7
Other Asia/Pacific	237.0	342.5	497.5	7.6
Other regions	87.9	128.5	188.0	7.9

According to the mentioned report, among different industries using TPEs, the motor vehicle industry will remain the largest market. On the other hand, smaller sectors such as medical products and sporting goods will become the fastest growing market through 2011. Furthermore, worldwide, China represents the largest market in volume based on the country's key position in the production of different TPE-based products. However, the main global TPE demand remains in the developed countries such as United States, Western Europe and Japan, particularly for high performance TPEs such as co-polyester elastomers (COPEs) and thermoplastic vulcanizates (TPVs).

A schematic of the cost/performance of different types of TPEs is presented in Figure 1.1. Accordingly, among different types of TPEs, thermoplastic polyolefins (TPOs) and thermoplastic vulcanizates (TPVs) offer an acceptable performance at a reasonable cost.

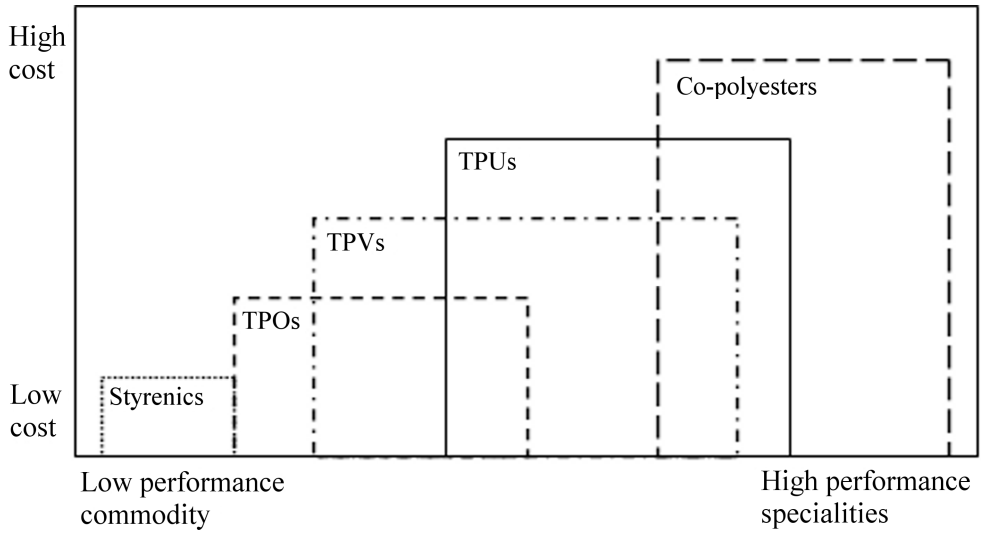

Figure 1.1. Cost/performance of thermoplastic elastomers (TPEs). (De and Bhowmick, 1990)

These two categories of TPEs, i.e. thermoplastic polyolefins (TPOs) and thermoplastic vulcanizates (TPVs), are combinations of a hard semi-crystalline thermoplastic phase and an elastomeric component produced through melt blending. TPOs are uncross-linked immiscible blends, while TPVs are obtained through a process known as "*dynamic vulcanization*" (Gessler and Haslett, 1962). Throughout this process, the elastomeric phase (usually the major phase) is dynamically vulcanized/cross-linked during melt mixing with a semi-crystalline thermoplastic material. Eventually, the thermoplastic minor phase becomes the matrix and the cross-linked major elastomeric phase is transformed into the dispersed one. This morphological transformation is known as "*phase inversion*" where two phases respectively exchange their functions (Steinmann et al., 2001).

Both TPOs and TPVs can be generally obtained from any combination of elastomeric and thermoplastic components. However, Coran and Patel (1981) explored various combinations of elastomers and thermoplastic polymers, where the combination of polypropylene (PP) and ethylene-propylene-diene-terpolymer (EPDM) resulted in one of the most promising polymeric

pairs, mainly due to their phase compatibility. Furthermore, the use of a proper plasticizer has been shown to lower the hardness of TPOs and TPVs in the range of 60 and 35 Shore *A*, respectively (Holden, 2000; Abraham et al., 2007).

As a result, throughout the past few decades a great number of studies have been conducted on the EPDM/PP-based TPEs in order to better understand and control their phase morphology development, the plasticizer distribution and, therefore, their ultimate physical and mechanical properties.

Considering the technological and economical importance of TPEs, the main effort of this dissertation is to investigate the effect of plasticization on the morphology/rheology relationship of EPDM/PP-based uncross-linked and dynamically cross-linked thermoplastic elastomers (TPEs).

This dissertation is based on three scientific articles that have been accepted for publication or submitted, and is organized as follows:

- In **Chapter 2**, the literature review;
- The objectives are presented in **Chapter 3**;
- **Chapter 4** represents the organization of the articles;
- **Chapters 5, 6 and 7** contain respectively the three articles;
- In **Chapter 8**, a general discussion is introduced;
- Finally conclusions and recommendations are presented in **Chapter 9**.

CHAPTER 2

LITERATURE REVIEW

2.1 Modes of Dispersion in Emulsions

The microstructure evolution in polymer blends is closely related to the modes of dispersion of the constituent components. To control and to understand the morphology development, it is indispensable to understand the main affecting parameters on the dispersion process by closely looking at certain phenomena such as breakup and coalescence of complex interfaces. As a first step towards this goal, it is crucial to comprehend the deformation and break-up phenomena in simple droplet/matix emulsions. In these systems, a strict correlation exists between the break-up and coalescence phenomena with the rheological and interfacial properties of the components. Taylor's pioneering work was probably the first published quantitative analyses on the dispersion mechanism of emulsions (Taylor, 1932; 1934).

Considering a single Newtonian droplet dispersed in a Newtonian fluid, Taylor defined a non-dimensional parameter known as capillary number (*Ca*) representing the ratio of viscous to interfacial tension forces,

$$Ca = \frac{\eta_m \dot{\gamma} R}{\Gamma} \tag{2.1}$$

where R is the radius of dispersed phase, η_m is the viscosity of matrix phase, $\dot{\gamma}$ is the shear rate and Γ is the interfacial tension between two phases.

In a pure shear flow field, for all viscosity ratios (η_d / η_m), i.e. viscosity of dispersed phase divided by the viscosity of matrix, the droplet shape is nearly spherical providing the

capillary number is adequately small. In this condition ($Ca << 1$), the deformation of a single droplet is linear with capillary number (Taylor, 1934). Furthermore, when the viscosity ratio is extremely large ($\eta_d / \eta_m >> 1$), a droplet will sustain its nearly spherical shape at all capillary numbers. On the other hand at very low viscosity ratios ($\eta_d / \eta_m << 1$), an emulsion subjected to a very high shear rates and consequently large capillary numbers ($Ca >> 1$) may form steady, highly elongated slender type droplets. In the intermediate viscosity ratio range, i.e. $\eta_d / \eta_m \approx 10^{-3}$-$10^{0}$, the droplet deformation increases with the capillary number and the dispersed phase becomes more and more elongated. Exceeding a certain capillary number, a stable droplet is unable to sustain its steady shape and, therefore, undergoes a continuous transient deformation, thins and eventually breaks up. The capillary number where this critical situation emerges is known as the critical capillary number for breakup (Ca_{crit}). Throughout this process, if the droplet radius becomes adequately small before breakup, capillary waves can cause the highly elongated drop to fragment during flow (Tomotika, 1935). However, this requires a highly elongated droplet with large length over diameter ratio, i.e. $L/D > 20$ (Mikami et al., 1975).

In contrast to a shear flow field, the extensional flow field is known to be more efficient in deforming and breaking up a single droplet (Grace, 1982). The extensional flow field is known for its ability to break up droplets regardless of the viscosity ratio. As a result, droplets in high viscosity ratio systems, which generally can not be broken up in a simple shear flow, can be easily deformed and broken up in an extensional flow field.

It is worth mentioning that the majority of existing emulsions are generally far from an ideal Newtonian fluid. Hence, the elasticity of the either phases may play an important role in the dispersion process. Mighri et al. (1997; 1998) have studied the emulsions of purely elastic components in both shear and extensional flow fields. Using a constant viscosity elastic (Boger)

fluid and by defining an elasticity ratio based on the ratio between the drop and matrix relaxation times, these authors found that in a simple shear flow field the droplet resistance to deformation and breakup increases with the elasticity ratio. Furthermore, the matrix elasticity appeared to facilitate the deformation of the droplets, whereas the droplet elasticity resisted deformation (Mighri et al., 1998). Similarly, in an extensional flow field, Mighri et al. (1997) found that droplet deformation decreases as its elasticity increases, whereas the increasing the matrix elasticity increases the droplet deformation.

The dispersion process in emulsions may evolve even after cessation of the flow where the interfacial tension drives two competing processes. One is the relaxation towards sphericity and the other is the development of capillary waves (Janssen, 1993). These two phenomena may depend on the extent of droplet deformation and the time scales corresponding to droplet relaxation and to growth of the capillary waves. If the droplet has been slightly stretched, the pressure difference over the interface will force the droplet towards spherical shape. On the contrary, for highly extended droplets as soon as the capillary waves are initiated on the interface, a pressure difference will develop periodically between the centers of disturbance and subsequently will break up the highly extended droplet. As a result, if the time scale for the growth of capillary waves is less than the time scale for relaxation, the droplet will break up through capillary instabilities. Otherwise, relaxation will occur with no breakup (Janssen, 1993).

Along with the deformation and breakup, coalescence is another important phenomenon particularly in semi-dilute and concentrated emulsions where the interaction between droplets can not be neglected. Several theoretical works have already been conducted on droplet coalescence (Elmendorp, 1986; Chesters, 1991; Janssen, 1993). According to Roland and Bohm (1984), the shear flow induced coalescence of two Newtonian droplets consists of the following steps: at first, two droplets approach each other and slightly rotate in the shear flow field and subsequently

the matrix phase in between two droplets drains away resulting coalescence. Throughout the mentioned process, the final film drainage step is known to be the rate determining step in coalescence phenomenon. The important parameters controlling coalescence are the volume fraction of the dispersed phase, the intensity of the flow field and the rheological and interfacial properties of the constituents. These parameters determine the frequency of droplet collisions, the contact force and the interaction time which indeed are the driving force for the film drainage process. Several models have been proposed to describe the film drainage process based on the mobility of the interface. One assuming fully mobile interfaces (Janssen, 1997) , the other based on the assumption of partially mobile interfaces (Chesters, 1991), and finally immobile interfaces (Janssen and Meijer, 1995). The predicted coalescence time based on each of these models appears to depend on viscosity ratio. Accordingly, the model based on the fully mobile interfaces is valid when the viscosity ratio is low ($\eta_d / \eta_m << 1$), whereas the model for immobile interfaces is mostly appropriate for high viscosity ratio systems ($\eta_d / \eta_m >> 1$). In between, the model based on the partially mobile interfaces shall be used for systems with viscosity ratio close to unity.

To conclude, many parameters are affecting the deformation process of a single droplet emulsion. Therefore, one shall expect a more complicated situation during the morphology development of an immiscible polymer blend consisted of highly complex interfaces. However, it is worth mentioning that the majority of the basic correlations obtained for simple emulsions are still fundamentally useful to describe certain phenomena even in complex immiscible polymer blends.

2.2 Morphology Development in Immiscible Polymer Blends

As mentioned earlier, the blending technology provide significant advantageous over chemical synthesis. In addition to the wide range of physical and mechanical property improvements through a suitable blending process, the polymer blends may as well improve processing behavior and lower cost. Earlier was mentioned that the majority of commercial polymer blends are immiscible due to thermodynamic limitations essentially related to the negligible mixing entropy and unfavourable mixing enthalpy. Hence, blending usually leads to multiphase heterogeneous morphologies where the properties of the polymeric constituents, interface adhesion and the final morphology often dictate the ultimate properties of these materials (Utracki, 1998). The morphology development during melt mixing stage, i.e. the size, shape and distribution of one polymeric phase into another, strictly depends on the rheological properties of the constituent polymers, the presence of different types of additives, the interfacial tension and processing conditions (Favis, 2000). Consequently, for a given blending pair and processing condition different types of morphologies can be tailored for various end use applications (Figure 2.1). For instance, droplet/matrix morphology is known to improve the toughness and impact properties; fibrillar morphology improves the strength and tensile properties; lamellar morphology enhances the barrier properties and eventually the co-continuous morphology toughness and stiffness mainly due to the contribution of both polymeric constituents to the overall bulk properties and provides a means of controlled electrical conductivity (Potschke and Paul, 2003; Harrats et al., 2006).

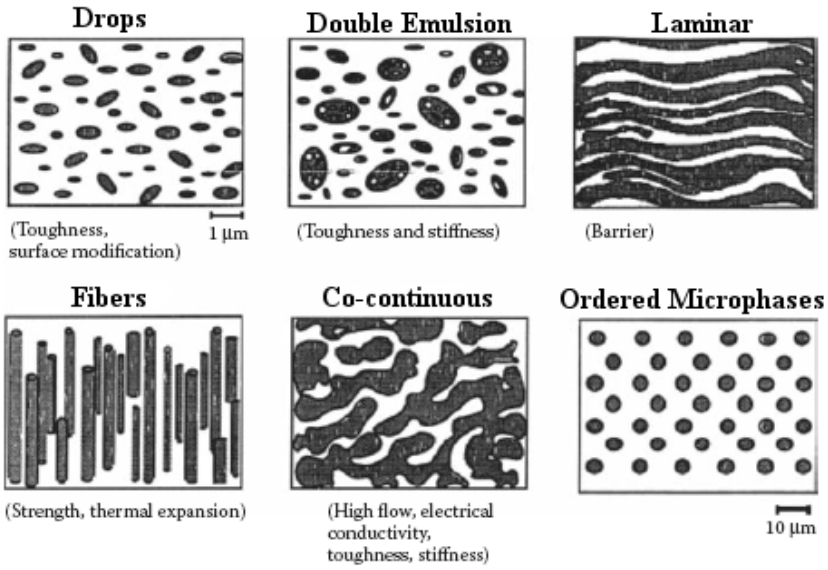

Figure 2.1. Schematic of various types of morphologies in immiscible polymer blends.

(Harrats et al., 2006)

In addition to the aforementioned parameters affecting the morphology development, the possibility of an in-situ cross-linking reaction may further change the morphology evolution. This situation particularly arises during several reactive blending processes such as an in-situ reactive compatibilization and dynamic vulcanization/cross-linking (Harrats et al., 2006). Although in most of these processes, e.g. dynamic cross-linking, the in-situ reaction is the major step dictating the final morphological state, but the initial morphology evolution prior to the reaction step is as crucial as the reactive blending itself.

Therefore, one needs to study first the effects of different parameters on the morphology development of the non-reactive blends.

2.2.1 Non-Reactive Immiscible Blends

In the scientific literature, extensive efforts have been devoted to improve the existing knowledge on the morphology development of non-reactive immiscible blends. Generally melt blending starts in the solid state where the neat polymeric components as pellets, powder or bales are mixed inside a mixing equipment, e.g. extruder or batch internal mixer. In such an intensive mixing environment the polymeric materials are heated, sheared and, therefore, melted during the first stage of the mixing process. According to Shih et al. (1991), throughout the blending process the polymeric components individually experiences the four following sequential states: elastic solid pellets, softened or deformed pellets, transitional material and eventually viscoelastic fluid.

In the initial softening stage, Scott and Macosko (1991) showed that the initial morphology development from pellets to micron size particles are through sheet formation. According to the authors, the mechanism involves the dragging of a large solid particle of the dispersed phase along the hot surface of the barrel resulting in the formation of sheets or ribbons of the dispersed phase. The mentioned sheets of the dispersed phase are transformed into cylinders and eventually broke-up into smaller spherical droplets through Rayleigh instabilities. The schematic of the aforementioned initial morphology development is shown in Figure 2.2. Later working on several model systems, Sundararaj et al. (1995) illustrated that the sheet formation process may also occur in the molten state well above the melting point of the polymeric components. Hence, the sheet formation in the molten state is highly dependent on the viscoelastic properties of the components. Sundararaj et al. (1995) developed a map where different mechanisms such as sheet or cylinder formations were represented by the Deborah number and the ratio of the first normal stress difference of the matrix to the restoring stress of

the pellet or droplet (sum of the surface stress resulting from interfacial tension and the first normal stress difference of the droplet).

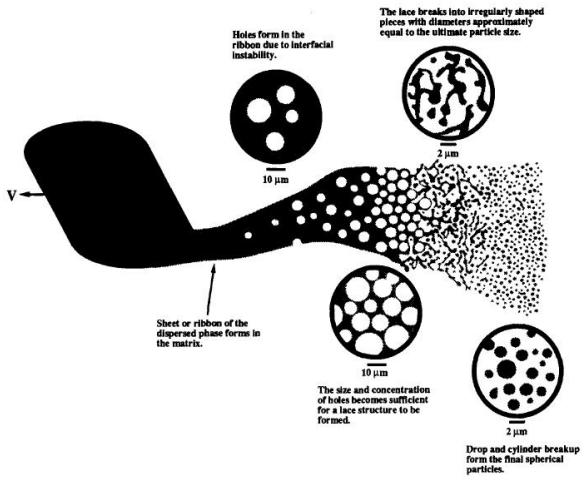

Figure 2.2. A schematic mechanism for initial morphology development in polymer blends. (Scott and Macosko, 1995)

In the transition zone, i.e. during the first few minutes of the mixing process, the melting order of the polymeric components has an important consequence on the morphology development (Shih et al., 1991; Ratnagiri and Scott, 1998; Lazo and Scott, 1999). If the minor component softens first, it will initially encapsulate the solid particles of the major phase and forms the matrix. However, at elevated temperature after the major component is melted, it becomes the matrix phase and the minor phase transformed into dispersed phase. This situation may not occur if the major phase softens first.

Following the step where all polymeric components are in the molten state, the blending medium is composed of a mixture of viscoelastic fluids. At this stage, the morphology development depends on several factors such as processing parameters (i.e. mixing temperature, mixing time, shear and elongational rates), rheological properties of the constituents, blending composition, interfacial properties and the presence of different types of additives (Favis, 2000).

As mentioned earlier, in the molten state the rheological properties of constituents have an important role in the morphology development. Favis and Chalifoux (1987; 1988) studied the effects of viscosity ratio (η_r) and composition in PP/PC blends. The authors concluded that the size of the polymeric domains is closely related to the viscosity ratio (η_r). According to their observation in the range of $\eta_r > 1$, regardless of the composition of the dispersed phase, the size of the polymeric domains appeared to increase monotonically with viscosity ratio. Furthermore in contrast to Newtonian dispersions, it was still possible to deform a viscoelastic dispersed phase at $\eta_r = 17$. For low viscosity ratio range, i.e. $\eta_r < 1$, a composition dependency was observed (Favis and Chalifoux, 1987; Favis and Chalifoux, 1988). For low composition of dispersed phase, a minimum domain size was observed at $\eta_r \sim 0.15$ where below this value, the size of the polymeric domains remained constant. On the other hand for slightly higher composition, a minimum domain size was observed at $\eta_r \sim 0.2\text{-}0.3$ where below and above the mentioned range, the particle size had the tendency to increase.

Karger-Kocsis et al. (1984) investigated the effect of viscosity ratio on the dispersion of EPDM in PP matrix. Their observations led to a conclusion similar to Favis and Chalifoux (1987), where the average domain size and polydispersity of the EPDM phase appeared to increase with the viscosity ratio. In addition to the viscosity ratio, Wu (1987) demonstrated that the size of the dispersed phase in EPR/PA and EPR/PET-based blends depends on the interfacial tension as well. According to the author, the droplet size of the dispersed phase (EPR) was smaller for low interfacial tension system with viscosity ratio close to unity.

The composition effect of components on the phase morphology was also studied by Favis and Chalifoux (1988). The authors reported that at low composition range, the main morphology consisted of dispersed droplet/matrix type with low polydispersity; however, by

further addition of the minor phase, the morphology began changing towards co-continuity while the polydispersity increased simultaneously. Eventually at higher composition range, the phases inverted and the former matrix transformed into the dispersed phase and the dispersed one became the matrix. In contrast to classical description of the phase inversion defined by a single phase inversion composition, the blends of highly viscous and elastic polymers show a composition interval where both polymeric components are co-continuous and the inversion occurs on either sides of the co-continuity interval. The mentioned interval may itself be influenced by many parameters. Favis and Chalifoux (1988) studied the effect of torque ratio (viscosity ratio) on the co-continuity interval of PP/PC blends. The co-continuity interval was found to be shifted towards higher composition as viscosity ratio decreases. Since this type of behavior could not be explained by viscosity ratio-based phase inversion models (discussed in section 2.4), the authors concluded that in addition to the viscosity ratio, one must also consider the elasticity of the components in order to be able to predict the phase morphology.

Willemse et al. (1998) and Willemse et al. (1999) studied the effect of interfacial tension on the range of co-continuity. The authors chose different polymer pairs with various interfacial tensions but identical viscosity ratios. According to them, the broadness of the co-continuity interval was directly related to the interfacial tension. In systems with relatively higher interfacial tension, the onset of percolation appeared at higher composition, and the co-continuity range was slightly narrower. Furthermore, the morphology was less stable and the phase dimensions were larger compared to systems with low interfacial tension. The observed behaviors were similar for both high and low viscosity ratio blends. A similar trend was also reported by Li et al. (2002). The authors proposed different mechanisms for co-continuity development: thread-thread coalescence for low-interfacial tension systems, while droplet-droplet coalescence for high interfacial tension systems. Hence, the shift in the onset of dual phase continuity is not only

associated with the rheological properties of the polymeric constituents, but also with the mobility of the interface and the possibility of coalescence and, therefore, the percolation of the dispersed phase. Hence, any phenomenon suppressing the coalescence in a polymer blend may shift the onset of percolation to a higher composition (Bourry and Favis, 1998).

The co-continuous structure may also be affected by annealing (Veenstra et al., 2000; Yuan and Favis, 2005). This phenomenon is more common in high interfacial tension blends compared to low interfacial tension ones such as EPDM and PP.

The effect of mixing time on the morphology development has also been investigated by several authors (Karger-Kocsis et al., 1984; Favis, 1990; Sundararaj et al., 1992; Bu and He, 1996; Potente et al., 2001). Bu and He (1996) investigated two immiscible polymer blends, a low viscosity ratio blend ($\eta_r \sim 0.03$) composed of PA/PES, and a blend composed of PBT/PS with a viscosity ratio equal to unity ($\eta_r = 1$). The authors observed that the morphologies were not only affected by the composition of the components and the viscosity, but also by the mixing time. According to their observation, the effect of viscosity ratio became negligible with the mixing time and the morphology at longer times was mainly determined by the blend composition (Figure 2.3). However at the early mixing stage, the morphology of the low viscosity component in the low viscosity ratio blend passed through dispersed particle type, fibrillar morphology and eventually became co-continuous at relatively low compositions (Figure 2.3a). On the other hand, the high viscosity phase in the same blending system appeared mainly in the form of dispersed particles and directly transformed into continuous phase at higher compositions (Figure 2.3a). For blends with viscosity ratio equal to unity, the dispersed phases from both composition sides appeared to be in the form of particles up to the co-continuous composition range (Figure 2.3b).

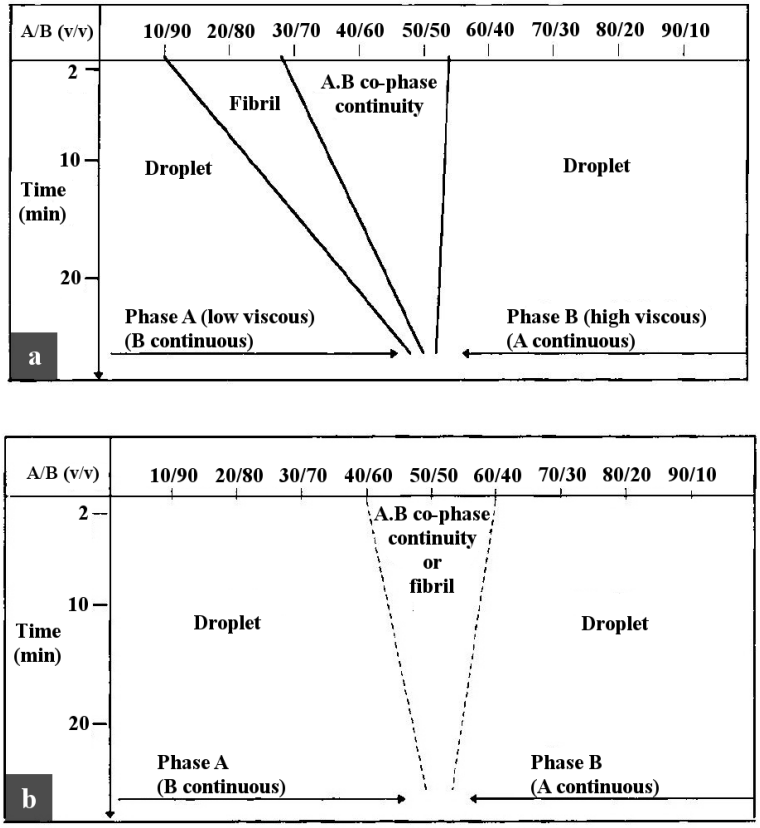

Figure 2.3. Diagram of morphology development in a blend of A/B as a function of composition, viscosity ratio and mixing time: (a) $\eta_r \sim 0.03$, (b) $\eta_r = 1$. (Bu and He, 1996)

On the other hand, Favis (1990) demonstrated that the main deformation and disintegration processes took place within the first two minutes of mixing and, therefore, mixing time did not play a significant role on the particle size of the dispersed phase. Sundararaj et al. (1992) also observed a similar trend for blends prepared by twin screw extrusion where according to them the major morphology changes occurred within first minute of mixing. However, it is worth noting that the blends investigated by Favis (1990) and Sundararaj et al. (1992) were high viscosity ratio ($\eta_d > \eta_m$, where η_d and η_m are the viscosities of disperse and matrix phases, respectively) blends which according to Bu and He (1996), the morphology of the minor high viscosity phase shall not be sensitive to mixing time. Earlier, a similar condition has been

reported in the elastomer/thermoplastic blends such as EPDM in PP, where no morphology changes has been observed as a function of mixing time (Karger-Kocsis et al., 1984).

Shear rate is another important parameter in the morphology development. However, despite the expected effect of increasing shear rate or the mixing rotational speed in reducing the size of the polymeric domains and creating finer morphology, it appears not to play a significant role. Working with high and low viscosity ratios PC/PP blends, Favis (1990) demonstrated that an increase in the mixing rotational speed did not have any effect on the morphology development of low viscosity ratio blends; whereas for high viscosity ratio blends the morphology was slightly affected at low rotational speed. Ghodgaonkar and Sundararaj (1996) used a force balance taking into account both viscous and elastic properties of the polymeric components to illustrate the effect of shear rate on the phase morphology. Among different blending pairs studied by Ghodgaonkar and Sundararaj (1996), only a single low viscosity ratio blend appeared to be affected by the shear rate where a minimum droplet size was observed at an intermediate range of shear rate. Concerning the effect of mixing equipment, i.e. batch internal mixer vs. twin-screw extruder, on the morphology development, Sundararaj et al. (1992); Thomas and Groeninckx (1999) and Goharpey et al. (2008) reported that the morphology development and the final morphology at matched conditions are identical in both mixing devices.

In this section, the effects of several different parameters on the morphology development of non-reactive immiscible blends have been described. It is noteworthy to mention that the importance of controlling the morphology of a non-reactive immiscible blend is not only limited to the possible physical and mechanical properties obtained through a well designed morphology. In the following section, one may realize that the morphology of a non-reactive blend plays a significant role as an initial morphological state for a possible subsequent reactive processing.

2.2.2 Reactive Immiscible Blends

The phase morphology development in the reactive polymer blends requires that either the rheological, interfacial, or thermodynamic properties of at least one of the polymeric constituents changes. The reaction may generally occur on the interface between the polymeric constituents such as in reactive compatibilization, or within one of the components such as in the case of in-situ selective cross-linking of the elastomeric component during dynamic vulcanization step. This section mainly covers the morphology development in the dynamically vulcanized thermoplastic vulcanizates (TPVs).

The morphology development during dynamic vulcanization of TPVs is not only affected by the parameters mentioned in the previous section, but also by the selective crosslinking of the elastomeric component during melt mixing with a semi-crystalline thermoplastic polymer. The formation of cross-linked elastomeric network increases both the viscosity and the elasticity of the elastomer phase, changes the interfacial properties, the viscosity and elasticity ratios of the blend and consequently drastically affects the morphology development of the TPVs (Chung and Nadella, 2001; Goharpey et al., 2001; Dufaure et al., 2005). Throughout this process, the cross-linked elastomer (usually the major component) is transformed into a dispersed phase and the thermoplastic minor phase becomes the matrix. This morphology transformation is known as "phase inversion" where two phases respectively exchange their functions. The major interest in this field is to identify and control the affecting parameters on the phase inversion process and, therefore, to control and optimize the morphology development of TPVs.

While studying the morphology development in 80/20 (wt/wt%) EPDM/PP blend, Abdou-Sabet et al. (1996) demonstrated that prior dynamic vulcanization stage, a co-continuous

morphology is formed and as the cross-linking reaction proceeds the continuous elastomeric network brakes up and cross-linked elastomeric particles becomes dispersed in the thermoplastic continuous phase (Figure 2.4).

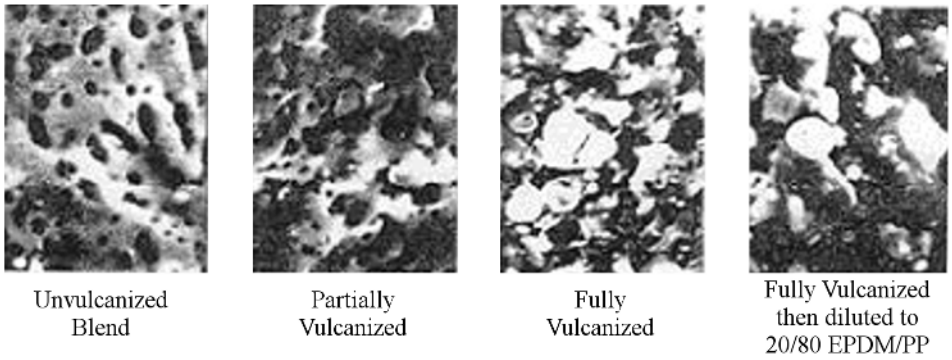

Figure 2.4. Morphology development in 80/20 (wt/wt%) EPDM/PP TPV. (Bright phase: EPDM) (Abdou-Sabet et al., 1996)

A similar morphological transformation has also been reported by several other researchers (Radusch and Pham, 1996; Goharpey et al., 2001; Joubert et al., 2002; Dufaure et al., 2005). A schematic of phase morphology development is presented in Figure 2.5. According to Radusch (2006), at the initial stage of dynamic vulcanization the co-continuous morphology is strongly deformed into continuous elastomeric threads and eventually breaks up and forms the final dispersed cross-linked elastomeric domains.

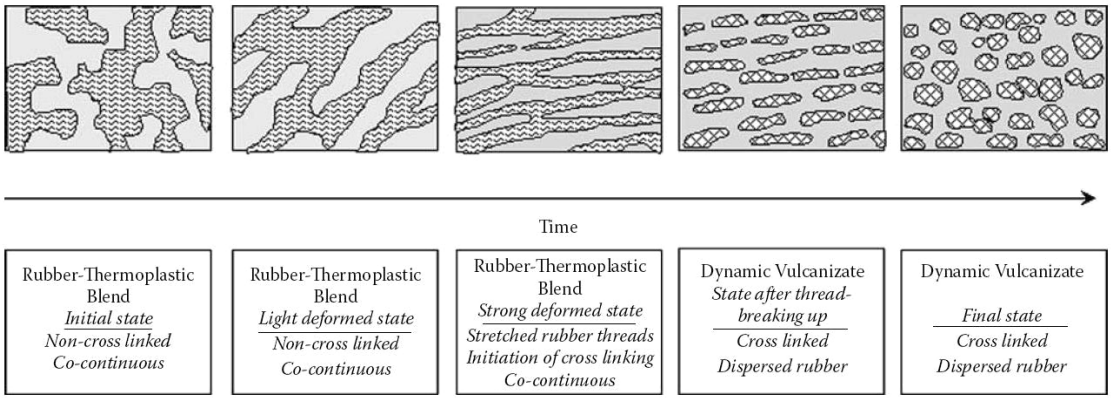

Figure 2.5. Schematic of phase morphology transformation during the dynamic vulcanization process. (Radusch, 2006)

It is worth noting that the presence of co-continuous morphology prior to dynamic vulcanization step is a prerequisite to obtain dispersed cross-linked elastomer phase at the end (Naskar and Noordermeer, 2005; Radusch, 2006). In connection with the mentioned prerequisite morphological condition, only an initial co-continuous structure allows the effective transfer of the shear and elongational stresses from one phase to the other and guarantees the breakup of the elastomeric component during the dynamic vulcanization stage (Radusch, 2006). However, if the co-continuous morphology at the intermediate stage of dynamic vulcanization process is comparably stable, the phase inversion phenomenon would possibly be hindered. The appearance of stable co-continuous morphology has already been reported by Bouilloux et al. (1997) in EMA/LLDPE blending system.

Hence, the initial morphological state prior dynamic vulcanization has a great importance and is mainly controlled by the parameters mentioned earlier in the previous section. For instance, the elastomeric component in the blends with extremely low viscosity thermoplastic minor phase (low viscosity ratio systems) may already form the dispersed phase, which indeed is not the desired morphological state prior dynamic vulcanization (Joubert et al., 2002; Oderkerk

and Groeninckx, 2002; Dufaure et al., 2005). The initial morphologies of high and low viscosity ratio EVA/PP 60/40 (wt/wt%) blends are shown in Figure 2.6. One may observe that for low and high viscosity ratio blends the matrix consists of the thermoplastic minor and elastomer major phases, respectively. Moreover as mentioned earlier, in contrast to high viscosity ratio blend the morphology of the blend with low viscosity minor phase is composed of coarse elastomeric domains already dispersed in the thermoplastic phase (Figure 2.6).

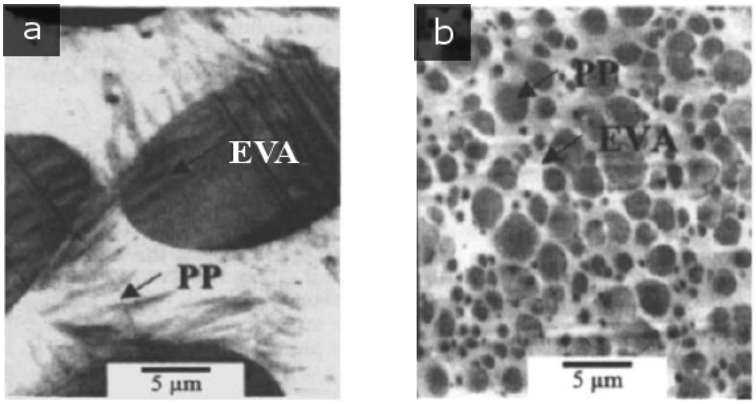

Figure 2.6. Initial morphology of EVA/PP 60/40 (wt/wt%) at different viscosity ratios: (a) η_{PP}/η_{EVA} = 0.09, (b) η_{PP}/η_{EVA} = 17.5. (Joubert et al., 2002)

On the other hand, Oderkerk and Groeninckx (2002) observed that during dynamic vulcanization, it was not possible to disperse the elastomer phase in highly viscous thermoplastic minor phase (Figure 2.7)

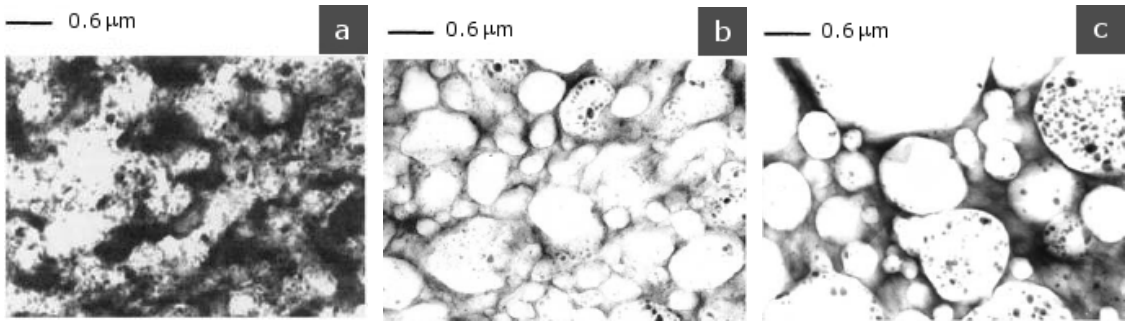

Figure 2.7. The viscosity effect of the minor phase prior dynamic vulcanization on the morphology of EPDM-g-MA/PA6 60/40 (wt/wt%) TPVs: (a) High viscosity PA6, (b) Medium-low viscosity PA6, (c) Low viscosity PA6. (Bright phase: EPDM-g-MA) (Oderkerk and Groeninckx, 2002)

Generally by lowering the viscosity ratio of a blending system prior to dynamic vulcanization (excluding the elasticity effects), one would expect to shift the co-continuity range towards lower volume fraction of the minor phase, meaning that a larger amount of major phase (in this case elastomer) can be dispersed in the minor one (thermoplastic in this case) (Jordhamo et al., 1986). According to Bu and He (1996), the lower the viscosity of minor phase is, the lower would be the volume fraction of the percolation and faster would be the percolation of the mentioned phase. Hence, due to the mentioned differences in the viscosity ratios and the initial morphologies of different blending systems, the mixing curves of their corresponding dynamically vulcanized blends are expected to be substantially different (Joubert et al., 2002). The mixing curves of EVA/PP 60/40 (wt/wt%) blends during dynamic vulcanization are shown in Figure 2.8. Blends with initial high viscosity ratio (with dispersed/matrix initial morphology) demonstrate a shoulder in their mixing curve, whereas the moderate viscosity ratio blends (with co-continuous initial morphology) demonstrate a smoother transition with a maximum almost identical to the intensity of the shoulders observed in the high viscosity ratio blends. On the other hand, the blends with low viscosity ratio do not show any sharp maximum due to their initial

morphology which is mainly dispersed elastomer major phase in a continuous thermoplastic minor phase.

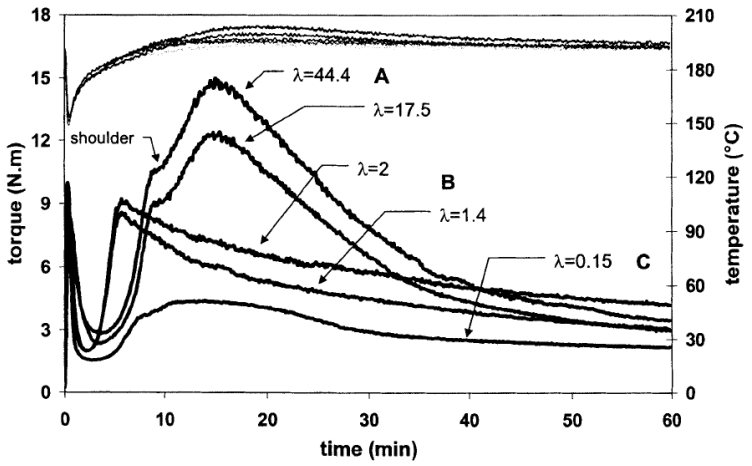

Figure 2.8. The effect of initial viscosity ratio (λ) on the mixing curves of several EVA/PP 60/40 (wt/wt%) blends. (Joubert et al., 2002)

The shoulders observed in Figure 2.8 have been attributed to the onset of phase inversion, where the initial dispersed/matrix morphology is transformed into a co-continuous morphology (Joubert et al., 2002). The appearance of a shoulder has also been reported by Verbois et al. (2004) and Dufaure et al. (2005). From industrial point of view and based on the mixing curves observed in Figure 2.8, the initial co-continuous morphology is the desired morphological state prior dynamic vulcanization, mainly due to lower energy consumption (lower torque) and shorter processing time required for dynamic vulcanization.

Although for blends with high viscosity dispersed minor phase subjected to dynamic vulcanization process, one would expect to observe a shoulder passing through co-continuous morphology, but according to Goharpey et al. (2001) the shoulder may disappear and the phase inversion could not be easily recognized in the case of rapid cross-linking reaction. Therefore, in addition to the parameters affecting the initial morphological state prior dynamic vulcanization

step, the cross-linking kinetics may also play a major role on the morphology development of TPVs. Generally the rate of cross-linking reaction increases with temperature, especially in heat reactive curing systems, e.g. phenolic curing resin. Verbois et al. (2004) studied the effect of temperature on the cross-linking rate of EVA used in the preparation of the TPVs. The authors observed that the storage modulus of the elastomeric component increases comparably faster at higher temperature and the time required reaching the gel point decreases with temperature, meaning that the increase in temperature provokes a faster reaction in the elastomeric phase.

Dufaure et al. (2005) observed a similar behavior. Based on the storage modulus of the TPVs prepared at different temperatures, the authors concluded that the increase in the mixing temperature increased the reaction rate and the gel content of the elastomer and, therefore, hindered the complete disintegration and dispersion of the cross-linked elastomer phase. According to Dufaure et al. (2005), the smoother the phase inversion process and, therefore, the better the dispersion of the elastomer is, the lower would be the elastic modulus. In another study, Martin et al. (2009) investigated the importance of the gel content on the dispersion of precross-linked elastomeric domains in a thermoplastic phase. According to the authors, it is crucial to disperse the EPDM phase before the gel content reaches 70%. Beyond that, the cross-linked EPDM phase can no longer be fragmented and finely dispersed into the PP phase. Studying the morphology development of in-situ cured epoxy in PS, Fenouillot and Perier-Camby (2004) also observed a similar trend where for gel content larger than 70%, a coalesced and agglomerated structure was formed.

The mixing intensity may also affect the morphology development. According to Joubert et al. (2002) the effect of mixing intensity can not be dissociated from the temperature effect. The increase in the mixing intensity (shear rate), may rapidly increase the blending temperature through viscous dissipation and consequently affect the morphology development by rapidly

increasing the rate of cross-linking reaction. In such condition, the phase inversion is mainly controlled by the fragmentation of the cross-linked elastomer domains, rather than by the transient equilibrium between coalescence and break-up (Joubert et al., 2002). According to Bouilloux et al. (1997) and Dufaure et al. (2005), the mixing intensity does not have a significant effect on the morphology development unless affecting the curing rate of the elastomeric component.

Concerning the effect of mixing equipment, the correlation between the phase morphology evolution in TPVs and the level of gel content has been reported to be almost identical in both discontinuous batch and continuous mixing equipments (Verbois et al., 2004). According to Verbois et al. (2004), regardless of the mixing equipment, the transition from co-continuous to dispersed cross-linked elastomer morphologies appears to depend merely on the gel content of the elastomeric component. Furthermore, regardless of the mixing equipment the mentioned transition appears to occur comparably fast within one minute of the addition of curing system (Radusch, 2006). However, despite the rapid onset of transition, the final morphology of the TPVs is closely affected by the rate of cross-linking reaction and the total amount of shear exerted on the blend (Sengupta and Noordermeer, 2004). As a result, Sengupta and Noordermeer (2004) observed a coarser morphology and larger cross-linked elastomeric domains for TPVs obtained from twin-screw extruder in comparison the ones obtained from internal mixer, mainly due to the faster cross-linking reaction and shorter residence time in the extrusion process.

To conclude, one may already realize that in order to achieve a finely dispersed cross-linked elastomeric domains in the range of 1 to 3 μm, which results in optimum physical and mechanical properties, several processing and material related parameters such mixing time,

shear rate, the rate of the crosslinking reaction, the viscosity and elasticity ratios and, therefore, the initial morphological state of the uncross-linked blend have to be well controlled throughout the dynamic vulcanization process.

2.2.3 Plasticization in TPOs and TPVs

Plasticizers have long been employed in the thermoplastic elastomer industry. In addition to lowering the overall cost of the products and improving the low temperature mechanical properties, the presence of a proper plasticizer is known to improve the melt processability and the final appearance of the products (Abdou-Sabet and Fath, 1982). The mentioned improvements are directly associated with the effect of plasticizer on lowering the melt rheological properties of the polymeric constituents (described in section 2.3) and, therefore, potentially affecting the morphology development of TPEs.

The morphology development of both TPOs and TPVs share an additional level of complexity in the presence of a plasticizer. Generally, in order to avoid certain problems such as migration of a low molecular weight plasticizer from bulk to surface, highly compatible plasticizers are usually chosen. As a result of this compatibility and small polarity difference between the chosen plasticizer and the polymeric components, the plasticizer is usually expected to be well distributed and to swell both phases in the molten state (Lei et al., 2007). As a result, in order to better understand the microstructure evolution in the plasticized TPOs and TPVs, the diffusion and distribution processes of the plasticizer between the polymeric constituents have to be well understood.

The diffusion process is generally characterized by a dimensionless group known as Deborah diffusion number (D_b) which is defined as the ratio of the characteristic relaxation time

of the fluid (λ_m) over the characteristic time of the diffusion process (t_d) (Vrentas and Duda, 1977). For large Deborah numbers, the mass transport is called elastic diffusion, and the plasticizer diffuses and swells the polymer without inducing substantial disentanglements (Ponsard-Fillette et al., 2005). On the other hand for low Deborah numbers, the diffusion process is most likely Fickian and due to comparably shorter relaxation time of the fluid, the diffusion process results in disentanglements of the polymeric chains (Ponsard-Fillette et al., 2005). Accordingly in the elastomer/thermoplastic blends such as EPDM/PP, the diffusion process of a low molecular weight plasticizer into each and every polymeric constituent would be considerably different due to the elasticity difference between components. Studying the diffusion process of a paraffinic oil separately into the EPDM and PP, Ponsard-Fillette et al. (2005) have demonstrated that the incorporation of a plasticizer in PP is more of a Fickian type resulting in a reduction of disentanglements. However, the same authors concluded that the Fickian diffusion process is less appropriate for EPDM/plasticizer binary system, indicating stronger intermolecular interactions and entanglements between EPDM chains which are not totally released in the presence of plasticizer and, therefore, showing an elastic diffusion process. Furthermore, between EPDM and PP, the plasticizer diffusion kinetics appeared to be faster in EPDM indicating the importance of elastic diffusion and, therefore, the presence of swollen elastomeric phase in comparison to less swollen PP during melt processing step (Ponsard-Fillette et al., 2005).

On the other hand besides the diffusion process, the second important parameter is the plasticizer distribution into polymeric constituents, which may directly affect the rheological properties and, therefore, the morphology evolution. Based on the depression of T_g in the PP phase, Ohlsson et al. (1996) defined a distribution coefficient (K) as the ratio of the oil

concentration in the semi-crystalline thermoplastic phase over the concentration of oil in the elastomer phase. The authors reported a distribution coefficient ranging from 0.33 to 0.47 for blends with 10 to 90 wt% of the semi-crystalline PP phase, indicating a preferential distribution of the plasticizer in the elastomeric phase. Winters et al. (2001) used solid state NMR spectroscopy to estimate the plasticizer distribution. However, according to the authors, about 30 wt% of the plasticizer could not be traced either in the thermoplastic or in the elastomeric phase. Jayaraman et al. (2004) used TEM microscopy method along with image analysis to measure the area fraction of the swollen plasticized elastomer domains and to subsequently quantify the plasticizer distribution in the EPDM/PP-based TPVs. Sengers et al. (2004) used a micro-mechanical modeling approach to obtain the distribution coefficient. To do so, the mentioned coefficient (K) was introduced as an additional model parameter. The obtained values for the distribution coefficient varied between 0.04 and 1.1 depending on the composition. Later, Sengers et al. (2005) used dielectric relaxation spectroscopy (DRS) for the same purpose and average values of 0.6 and 0.63 were obtained for the same coefficient in the SEBS/PP-based TPOs and EPDM/PP-based TPVs, respectively. Recently, Abraham et al. (2007) used AFM imaging in order to qualitatively describe the distribution of the plasticizer. The authors claimed that a substantial amount of plasticizer was present as a separate phase surrounded by the amorphous thermoplastic phase, a result similar to what had been previously reported by Winters et al. (2001). Following the literature data presented above, the outcome of the majority of these studies was a plasticizer distribution coefficient of less than unity, meaning that generally the plasticizer has a larger preference towards the elastomeric phase. This tendency may drastically affect the morphology development. On one hand, the plasticizer tends to swell the elastomeric component (Jayaraman et al., 2004; Ponsard-Fillette et al., 2005; Abraham et al., 2007) and, on the other the viscoelastic properties of both polymeric components and especially the elastomer

phase may drastically decrease in the presence of plasticizer, changing the ratios of the viscoelastic properties.

Although the work of Abraham et al. (2007) was primarily aimed to qualitatively describe the plasticizer distribution, but the coarsening and swelling effects of the plasticizer on the phase morphology observed in the AFM micrographs were clear indications of how a plasticizer may possibly affect the morphology development of a thermoplastic elastomer (Figure 2.9).

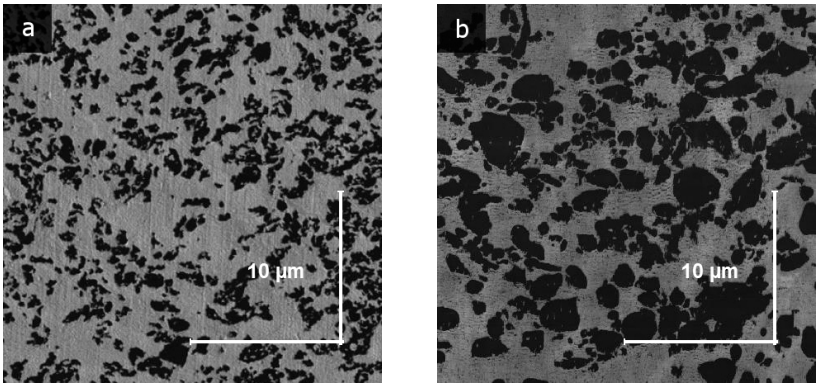

Figure 2.9. AFM phase micrographs of EPDM/PP 33/66 (wt/wt%) TPVs: (a) Non-plasticized, (b) Plasticized. (Dark phase: EPDM; Bright phase: PP) (Abraham et al., 2007)

2.3 Rheology of Immiscible Polymer Blends

Rheology has always been considered a strong characterization tool due to the existing highly reciprocal relationship between rheology and morphology. Generally several factors such as the composition, the intrinsic rheological properties of the constituent polymers, the interfacial properties, the blend morphology and eventually the presence of several additives such as plasticizer drastically affect the rheological response of the polymeric materials.

According to the literature, the viscoelastic response of the non-reactive immiscible polymer blends subjected to small amplitude oscillatory shear flow greatly depends on the

interface deformation (Tucker and Moldenaers, 2002). One of the fundamental features observed at low frequencies is the enhancement of the elastic response of the blends through the storage of the mechanical energy due to deformation of the interface (Palierne, 1990). For blends with droplet/matrix morphology, i.e. at low composition of dispersed phase, the mentioned enhancement of the elastic properties occurs through the relaxation of deformed droplets towards sphericity which is generally observed in the form of a shoulder in the G' curve (Palierne, 1990; Graebling et al., 1993). The critical frequency where this shoulder appears depends on the size of the droplets and, therefore, their deformability and corresponding shape relaxation times. The shoulder shifts to the lower frequencies, i.e. longer times, as the droplet size of the dispersed phase increases (Graebling et al., 1993). However, if the relaxation times of the matrix and dispersed phases are greater than the shape relaxation of the droplets, no shoulder will appear on the storage modulus curve (Tucker and Moldenaers, 2002).

As the concentration of the minor phase in an immiscible blend increases, the dispersed phase begins to coalesce and forms a percolated structure. Subsequently, the viscoelastic response of the blend begins to deviate from the typical response of a droplet/matrix system. Prior to the complete percolation of the minor phase and formation of co-continuous morphology, the specific interfacial area and the low frequency storage modulus of the blend increases with the composition of the minor phase (Figures 2.10 and 2.11) (Galloway et al., 2002).

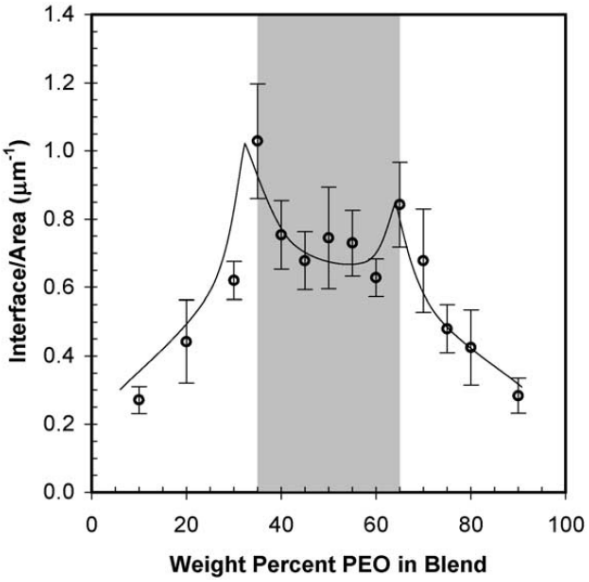

Figure 2.10. The specific interfacial area as function of PEO concentration in PEO/PS blend. (Galloway et al., 2002)

Meanwhile, the shoulder in the G' curve becomes less visible and the power law exponent of G', i.e. Δ' in $G' \sim \omega^{\Delta'}$, decreases resulting in plateau storage modulus while the same exponent for the loss modulus, i.e. Δ'', remains relatively constant as for the pure polymer components ($\Delta'' \sim 1$) (Castro et al., 2005). In concentrated polymer blends, after the complete percolation of the dispersed phase and formation of co-continuous morphology, the decrease in surface/volume ratio of the interface results in less elasticity enhancement due to less specific interfacial area (Steinmann et al., 2002; Castro et al., 2004; Galloway and Macosko, 2004).

Therefore, the initial increase in dynamic rheological properties prior to co-continuity formation and the decreasing trend afterwards in the co-continuous composition range, generally results in an extremum (Castro et al., 2004; Galloway and Macosko, 2004). According to Castro et al. (2004) the two extrema observed in the viscoelastic properties of the blends in either sides of the composition diagram correspond to the onsets of the co-continuity (Figure 2.11). However, some authors have merely observed a single extremum associated with the onset of co-continuity

(Steinmann et al., 2002; Peon et al., 2003). The discrepancies observed through the use of rheology as a characterization tool for determining the co-continuity interval may largely depend on the viscoelastic properties of the constituent polymers and the interfacial tension between them. In blends with low interfacial tension, the presence of a highly elastic component may overshadow the elasticity caused by the interface deformation and consequently mask the extrema.

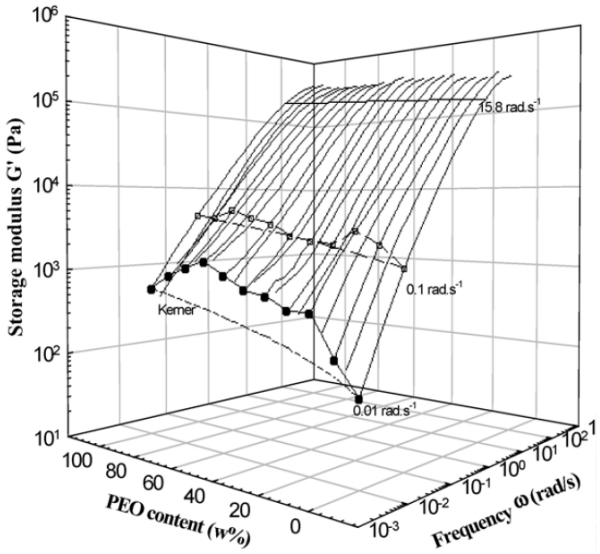

Figure 2.11. Storage modulus as function of frequency for complete composition range at 150°C in PEO/PVdF-HFP blend. (Castro et al., 2004)

An alternative approach to study the rheology/morphology relationship of the percolated co-continuous networks is based on the chemical gel approach (Castro et al., 2005). In a chemical gel, the viscoelastic moduli cross each other, and depending on the type of reaction, a frequency independent crossover point can be observed at the gel point (Muller et al., 1991). In addition, at the gel point both moduli obey a power-law relation with the same exponent Δ over the entire frequency range ($G' \sim G'' \sim \omega^{\Delta}$). According to Muller et al. (1991), the value of Δ depends on the type of chemical reaction, ranging from $1/2 \leq \Delta \leq 2/3$ (it could also approach unity). Generally in

polymer blends, the power-law exponent and consequently the loss tangent (tan δ) as a function of blend composition decreases from both extremities and reaches a somehow constant value in the intermediate co-continuous composition range (Figure 2.12) (Castro et al., 2005).

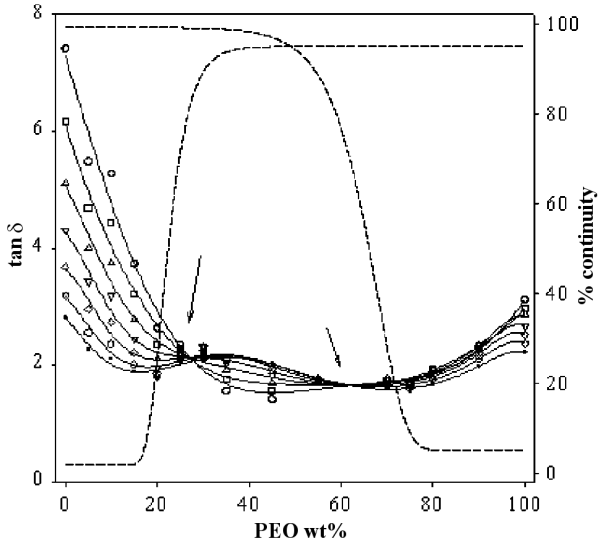

Figure 2.12. The tan(δ) and the solvent extraction continuity data (dashed lines) as a function of PEO concentration in PEO/PVdF-HFP blend at 150°C and at different frequencies (rad/s): (○) 0.01, (□) 0.0159, (△) 0.0251, (▽) 0.0398, (◇) 0.0631, (▪) 0.1 and (+) 0.1585 (Castro et al., 2005)

On the other hand, the viscoelastic properties of the reactive blends such as TPVs are largely affected by the presence of vulcanized elastomeric domains. Similar to the non-reactive blends, e.g. TPOs, TPVs are generally shear thinning. Studying the melt rheological properties of EVA/LLDPE blends, Moly et al. (2002) demonstrated that the shear thinning behavior and, therefore, the power law index was considerably smaller in the dynamically vulcanized blends in comparison to the uncross-linked ones and furthermore, among TPVs, it was smaller in the blends with larger cross-link density. Earlier in a separate study, Goettler et al. (1982) had also reported the shear thinning behavior in EPDM/PP-based TPVs where the power law index was slightly larger for TPVs with larger amount of thermoplastic phase (PP).

One of the most important rheological aspects of TPVs is their continuous shear thinning behavior even at low shear rates with no tendency towards zero shear viscosity (Goettler et al., 1982; Han and White, 1995). This behavior has been associated with the existence of a three dimensional network of cross-linked elastomeric domains, similar to particle-filled systems (Han and White, 1995). The mentioned strong viscosity enhancement can also be observed through dynamic linear viscoelastic measurements at low frequencies where the slope and the magnitude of the complex viscosity increases with the elastomer content (Figure 2.13) (Goharpey et al., 2005).

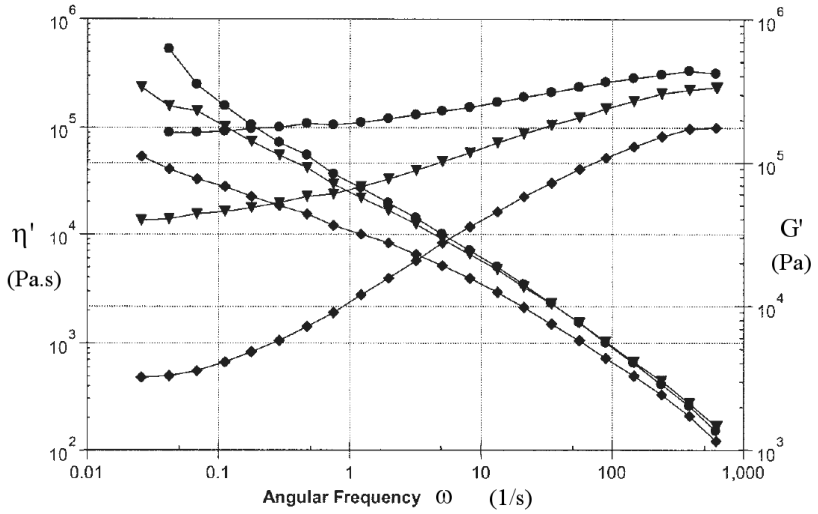

Figure 2.13. Storage modulus and dynamic viscosity of EPDM/PP-based TPVs at different EPDM/PP (wt/wt%) compositions: (◆) 20/80, (▼) 40/60, (●) 60/40. (Goharpey et al., 2005)

The high elastomer content TPVs generally exhibit a plateau storage modulus at low frequencies which has been associated with the network-type structure formed by the cross-linked elastomeric domains (Han and White, 1995; Shi et al., 2002; Dufaure et al., 2005; Goharpey et al., 2005). Bousmina and Muller (1993) demonstrated that the aggregation of the elastomeric particles directly affects the storage modulus of the blend. Although their study was not directly performed on TPVs, their results obtained based on rubber-toughened PMMA clearly

showed that the appearance of a plateau storage modulus was directly associated with the extent of aggregation and was more pronounced when a network type structure was formed.

The mentioned behaviors are identical to those observed in systems exhibiting yield stress (Araki and White, 1998). Consequently at low stresses, TPVs behave mostly like an elastic material due to the special network-like morphology. Undoubtedly, several factors such as the amount of elastomeric phase, the cross-link density and the presence of additional modifiers such as plasticizer affect the elasticity of TPVs. Steeman and Zoetelief (2000) and Zoetelief (2001) demonstrated the yield stress behavior by studying the rheological behavior of several commercial EPDM/PP-based TPVs with different hardness levels (Figure 2.14). According to Steeman and Zoetelief (2000), TPVs at low stress levels behave mostly elastic due to the presence of an interacting network of elastomeric domains; at intermediate stresses passing the yield stress, the elastomeric network is broken and the material behaves as a stiff elastomer filled thermoplastic system similar to the behavior observed in the concentrated suspensions; eventually in the high stress region, the rheological properties are mostly governed by the thermoplastic phase.

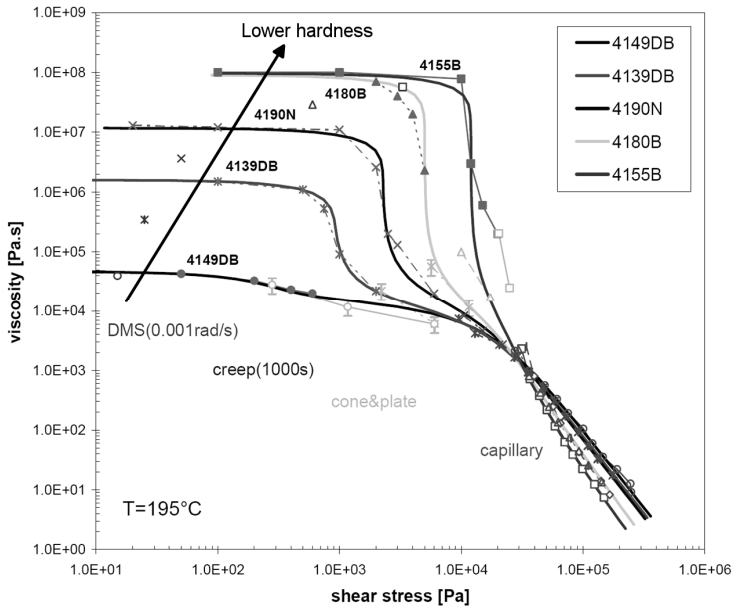

Figure 2.14. The shear viscosity of several different commercial EPDM/PP-based TPVs as a function of shear stress at 195°C. (Zoetelief, 2001)

Saroop and Mathur (1997); Jain et al. (2000) studied the melt rheological properties of different uncross-linked (TPOs) and dynamically cross-linked (TPVs) blends. According to them, TPVs had higher melt viscosity but lower melt elasticity in comparison to their corresponding TPOs. Furthermore, the melt elasticity in the TPVs appeared to decrease with the elastomer content. This important characteristic of the TPVs confirms the appearance of considerably smaller die swell in dynamically cross-linked EPDM/PP-based TPVs in comparison to neat PP or their corresponding uncross-linked TPOs previously observed by Goettler et al. (1982).

Furthermore as mentioned earlier in section 2.2.3, the rheological properties of the polymeric components in a thermoplastic elastomer blend may considerably be altered in the presence of different additives such as a low molecular weight plasticizer due its diffusion and distribution into the polymeric constituents. It is known that in the melt state, the plasticizer is absorbed and distributed between the thermoplastic and the elastomeric phases (Jayaraman et al.,

2004). Therefore, Sengers et al. (2004) employed the concentration-time superposition principle, originally suggested by Nakajima and Harrell (1982), to study the viscoelastic properties of oil extended PP/SEBS-based TPOs and EPDM/PP-based TPVs. According to Nakajima and Harrell (1982), the presence of a plasticizer results in a reduction of entanglements, decreases the value of moduli and consequently shifts the relaxation times of the polymeric chains to lower values. The effect of plasticizer on reducing the storage modulus of a neat polypropylene and the master curve obtained based on the concentration-time superposition is shown in Figure 2.15. Sengers et al. (2004) further employed the Veenstra-D micro-mechanical model (Veenstra et al., 2000) along with the concentration-time superposition to model the viscoelastic properties of plasticized TPOs and TPVs.

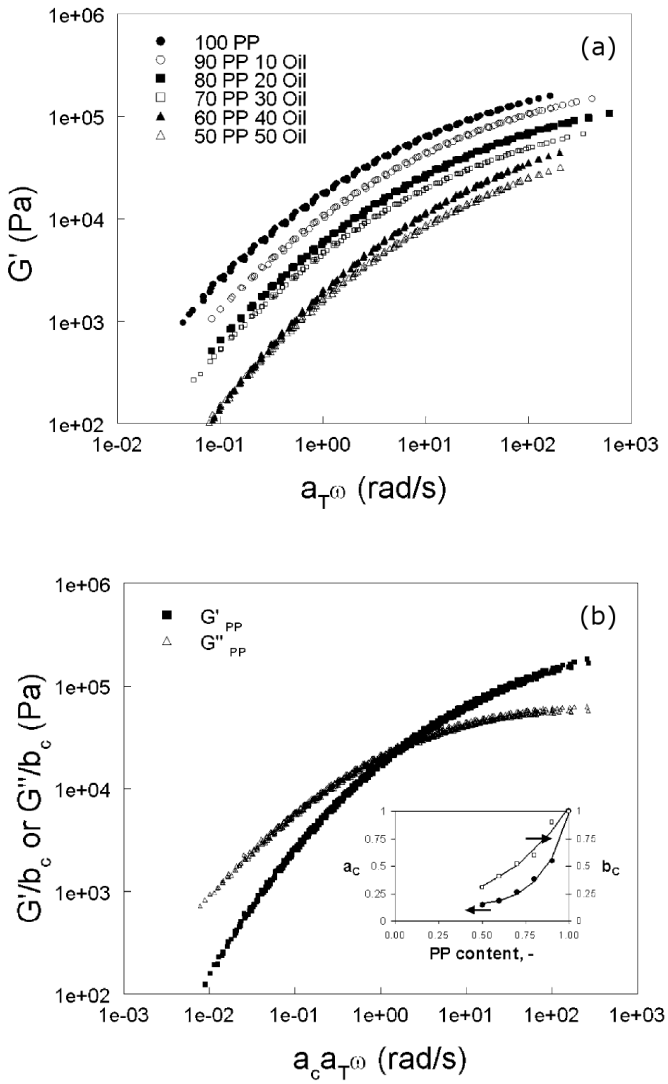

Figure 2.15. Storage modulus of PP/oil binary mixture at 190°C: (a) At various oil contents, (b) After concentration-time superposition. In the insert of (b) are the values for the concentration-time shift factors and their empirical fits (lines). (Sengers et al., 2004)

In a separate study, Jayaraman et al. (2004) investigated the shear viscosity of different plasticized EPDM/PP-based TPVs. They as well applied the Nakajima and Harrell's concentration-time superposition principle to investigate the effect of plasticizer on the viscosity of continuous medium thermoplastic phase, i.e. polypropylene. They concluded that the shear

flow behavior of the plasticized TPVs is closer to the effective flow behavior of the plasticized PP phase rather than the neat PP phase alone.

According to the above discussion, several factors such as composition, morphology, interfacial properties and the presence of different additives may directly affect the rheological response of an immiscible blend. Meanwhile due to the reciprocal interrelationship between the rheology and morphology, the unique rheological response of these blending systems offers a great deal of information concerning their microstructure and morphological state.

2.4 Semi-empirical Phase Inversion Predicting Models

In the course of the last few decades, numerous studies have been devoted to predict the phase morphology of immiscible polymer blends, especially the phase inversion composition, i.e. $\phi_{I,1}$ or $\phi_{I,2}$, and the co-continuity interval (Potschke and Paul, 2003). The results of these studies were largely based on empirical and semi-empirical models using the rheological properties of the constituent polymers. Due to the semi-empirical nature of these models, they mostly rely on the experimental co-continuity and in certain cases on prior morphological data. In the following paragraphs and in Table 2.1, a summary of these semi-empirical phase inversion models is presented.

Avgeropoulos et al. (1976) were the first to propose a simple relationship describing the phase inversion composition while employing the mixing torque ratio. Paul and Barlow (1980) and later Jordhamo et al. (1986) proposed a similar equation for the phase inversion point, where the torque ratio was replaced by the zero shear viscosity ratio. Miles and Zurek (1988) modified the existing equations assuming that the phase inversion composition shall be calculated using the effective viscosity ratio, evaluated at the processing shear rate. Others have introduced a pre-

factor and/or exponent while using the effective viscosity ratio concept (Ho et al., 1990; Everaert et al., 1999; Kitayama et al., 2000). Utracki (1991) proposed a different approach based on the emulsion theory, where at the phase inversion point the viscosity of the dispersion of one component into the other is equal to the viscosity of the inverse blend. For their part, Metelkin and Blekht (1984) used the Tomotika (1935) capillary instability theory and considered that at the inversion point, the break-up time of a filament composed of either components of the blend surrounded by the other polymeric phase should be equal. In a similar approach, Luciani and Jarrin (1996) considered that the co-continuity is mainly governed by the stability of the fibrillar structures. By equating the instability parameter described in Tomotika's theory, they assumed identical stability for both fibrillar structures. According to the authors, the validity of the model is limited to viscosity ratios ranging from 0.25 to 4. Steinmann et al. (2002) proposed a different approach based on the shape relaxation times of the constituent components, where the shape relaxation times of the components reach a maximum at the phase inversion point.

On the other hand, Van Oene (1972) developed an equation for the dynamic interfacial tension, which described the stability condition of an emulsion in a flowing condition. The outcome of the mentioned equation was that a stable phase morphology can be obtained when the elasticity (i.e., first normal stress difference) of the dispersed phase is equal or larger than the elasticity of the matrix phase. Whereas in the reverse case, there exists a critical domain size above which no stable dispersed phase can exist (Utracki, 1988). Accordingly, a preferential encapsulation of one phase by another might be induced due to the reduction of the dynamic interfacial tension. Considering the Van Oene's approach, Boury and Favis (1998) proposed a model employing the storage moduli and loss tangent ratios instead of viscosity ratios. According to them, the phase inversion composition obtained in this way was well fitted to their

experimental data, and as a result they concluded that the elastic contribution of the blends is an essential element to be considered.

All the above mentioned models result in a single phase inversion composition; whereas the immiscible polymer blends with highly viscous and elastic components demonstrate a co-continuous interval. Willemse et al. (1998) were the first to develop a semi-empirical equation defining the lower and upper limits of the co-continuity interval based on the continuity of elongated rods and maximum packing volume fraction (ϕ_m). However, the use of this model requires that the domain size of the dispersed phase to be known a priori. Later Lyngaae-Jorgensen et al. (1999) derived an equation predicting the range of co-continuity based on the percolation theory.

Table 2.1. The summary of semi-empirical phase inversion models

Equation*		Reference
Viscosity ratio based models		
$\frac{\phi_{I,1}}{\phi_{I,2}} = \frac{\tau_1}{\tau_2}$		Avgeropoulos et al. (1976)
$\frac{\phi_{I,1}}{\phi_{I,2}} = \xi\left(\frac{\eta_1}{\eta_2}\right)^{\psi}$	$\xi = 1$, $\psi = 1$ η_1/η_2 ~ zero shear viscosity ratio	Paul and Barlow (1980)
	$\xi = 1$, $\psi = 1$ η_1/η_2 ~ zero shear viscosity ratio	Jordhamo et al. (1986)
	$\xi = 1$, $\psi = 1$ η_1/η_2 ~ evaluated at mixing apparent shear rate	Miles and Zurek (1988)
$\frac{\phi_{I,1}}{\phi_{I,2}} = \xi\left(\frac{\tau_1}{\tau_2}\right)^{\psi}$	$\xi = 1.22$, $\psi = 0.29$	Ho et al. (1990)
$\phi_{I,1}$ ... $\left(\eta\right)^{\psi}$	$\xi = 1$, $\psi = 0.3$	Everaert et al. (1999)

	$\xi = 0.887$, $\psi = 0.29$	Kitayama et al. (2000)
$\phi_{I,2} = \frac{1}{1+\frac{\eta_1}{\eta_2}F(\frac{\eta_1}{\eta_2})}$ $F(\frac{\eta_1}{\eta_2}) = 1.25\log\frac{\eta_1}{\eta_2} + 1.81(\log\frac{\eta_1}{\eta_2})^2$		Metelkin and Blekht (1984)
$\frac{\eta_1}{\eta_2} = \left[\frac{\phi_m - \phi_{I,2}}{\phi_m - \phi_{I,1}}\right]^{[\eta]\phi_m}$	$[\eta]$ (intrinsic viscosity) ~ 1.9 ϕ_m (maximum packing volume fraction)	Utracki (1991)
$\phi_{I,2} = \frac{1-\left(\frac{\eta_1}{\eta_2}\right)^2\Omega^2\left(\frac{\eta_1}{\eta_2}\right)}{\left(\frac{\eta_1}{\eta_2}\right)^2\Omega^2\left(\frac{\eta_1}{\eta_2}\right)+\Omega^2\left(\frac{\eta_2}{\eta_1}\right)}$	$0.25 < \frac{\eta_1}{\eta_2} < 4$	Lucuani and Jarrin (1996)
$\phi_{I,2} = \frac{1}{(\frac{\eta_1}{\eta_2}^{1/Z}+1)}$	*"Z"* depends on the specific interfacial area and the relaxation rate of the structure	Steinmann et al. (2002)
$\frac{1}{\phi_{Onset,1}} = 1.38 + 0.0213\left(\frac{\eta_2\dot{\gamma}}{\Gamma}R\right)^{4.2}$	First model to predict the range of co-continuity interval based on the continuity of elongated rods and maximum packing density. (Requires prior morphological data)	Willemse et al. (1998)
$\phi_{I,1} = k(\phi_1 - \phi_c)^{0.45}$	Model predicting the range of co-continuity based on the percolation theory.	Lyngaae-Jorgensen et al. (1999)
Elasticity ratio based Models		
$\frac{\phi_{I,1}}{\phi_{I,2}} = \frac{G_2'}{G_1'}$		Bourry and Favis (1998)

$$\frac{\phi_{I,1}}{\phi_{I,2}} = \frac{\tan(\delta)_1}{\tan(\delta)_2}$$

* The symbol definitions are given in the *Nomenclature* section.

2.5 Rheological Models for Emulsions

The first model for emulsion of slightly deformable spherical droplets was developed by Taylor (1932) considering dilute emulsion of Newtonian droplet in Newtonian matrix during creeping shear flow. The viscosity of Taylor's model is presented as follows,

$$\eta = \eta_m \left(1 + \frac{5(\eta_d / \eta_m) + 2}{2(\eta_d / \eta_m) + 2} \phi \right) \tag{2.2}$$

where ϕ, η_d and η_m are the volume fraction, the viscosities of dispersed and matrix phases, respectively. In the limit of very high viscosity ratio, i.e. $\eta_d / \eta_m >> 1$, this model reduces to Einstein's equation for dilute suspensions. Following the same trend and taking into account the effect of interfacial tension and droplet size, Schowalter et al. (1968) developed a new constitutive equation expressing the stress tensor of dilute emulsions subjected to simple shear flow.

The first viscoelastic emulsion model for polymer blends accounting for interfacial tension was probably developed by Oldroyd (1953). This model describes the response of a dilute emulsion by considering two Newtonian components restricted to small droplet deformations. The complex viscosity of this model excluding the interface effect and considering a constant interfacial tension is presented as follows,

$$\eta^* = \eta_m \left(\frac{1 + 3\phi H^*(\omega)}{1 - 2\phi H^*(\omega)} \right) \tag{2.3}$$

where $H^*(\omega)$ is a complex function of matrix viscosity, viscosity ratio, droplet size and interfacial tension. The Taylor's equation can be retrieved at the limit of low frequencies ($\omega \to 0, \eta^* = \eta_{Taylor}$). Scholz et al. (1989) developed another constitutive equation for dilute emulsion of non-interacting, spherical and mono-disperse Newtonian droplets. The storage and loss moduli of this model in the linear viscoelastic region are presented as follows,

$$G'(\omega) = \frac{{\eta_m}^2 R\phi}{80\Gamma}\left(\frac{19(\eta_d/\eta_m)+16}{(\eta_d/\eta_m)+1}\right)^2 \omega^2$$
$$G''(\omega) = \eta_m \omega\left(1+\phi\frac{5(\eta_d/\eta_m)+2}{2(\eta_d/\eta_m)+2}\right) \tag{2.4}$$

where η_m is the viscosity of matrix phase, η_d is the viscosity of dispersed phase, R is the droplet radius, Γ is the interfacial tension, and ϕ is the volume fraction of the dispersed phase.

Odlroyd's theory was later extended by Palierne (1990) considering two viscoelastic components where the interfacial tension was responsible for an excess elasticity due to interface deformation. Palierne (1990) provided a detail derivation including the distribution of droplet sizes as well as possible interfacial tension variation caused by a surfactant. Palierne's equation has been one of the most frequently cited models used for predicting the viscoelastic behavior of dilute and semi-dilute immiscible polymer blends. The complex modulus G^* of this model is presented as follows,

$$G^* = G_m^* \frac{1+3\sum_i \phi_i H_i}{1-2\sum_i \phi_i H_i} \tag{2.5}$$

$$H_i = \frac{4(\Gamma/R_i)\left(2G_m^*+5G_d^*\right)+\left(G_d^*-G_m^*\right)\left(16G_m^*+19G_d^*\right)}{40(\Gamma/R_i)\left(G_m^*+G_d^*\right)+\left(2G_d^*+3G_m^*\right)\left(16G_m^*+19G_d^*\right)} \tag{2.6}$$

where G_m^* is the complex modulus of the matrix phase, G_d^* is the complex modulus of the dispersed phase , Γ is the interfacial tension, and ϕ_i is the volume fraction of dispersed phase (droplets) of radius R_i. This model contains no empirical fitting parameters and, therefore, it has been extensively used to estimate the interfacial tension or droplet size of emulsions (Mekhilef et al., 2000; Xing et al., 2000; Tucker and Moldenaers, 2002). Although Paliern's model is based on droplet size distribution, but as long as the polydispersity (described by the ratio of volume to number average radiuses, i.e. R_v/R_n) of an emulsion system is less than two, the volume average droplet radius (R_v) could be employed instead of R_i (Graebling et al., 1993). This simplification is based on the assumption that the volume average droplet radius takes into account a wide range of the droplet size distribution (Bousmina and Muller, 1993).

Although this model has several advantages over previous cited models in covering the viscoelastic response of semi-concentrated emulsions, it only describes the viscoelastic response of dispersed droplet/matrix type morphology. Therefore, none of the aforementioned models are capable of predicting the viscoelastic response of concentrated emulsions in the co-continuous region and, therefore, one needs to consider the contribution of complex interfaces to the total stress.

In any emulsion system, generally both stress and rate of deformation vary significantly in the micro-scale. However, only their average values are measured through conventional rheometers. Therefore, to model the rheological behaviour of concentrated emulsions, it is possible to determine the volume average stress ($\boldsymbol{\tau}$) and rate of deformation ($\mathbf{D}$) tensors based on the same quantities in the dispersed and matrix phases: i.e. $\boldsymbol{\tau}_d$ and $\mathbf{D}_d$ in the dispersed phase, and $\boldsymbol{\tau}_m$ and $\mathbf{D}_m$ in the matrix phase.

As a result, in the absence of interfacial slip, the volume average rate of deformation (**D**) can be expressed according to a simple mixing rule (Tucker and Moldenaers, 2002),

$$\mathbf{D} = (1-\phi)\mathbf{D}_m + \phi\mathbf{D}_d \tag{2.7}$$

A similar equation can be written for the stress tensor with an additional term expressing the contribution of the interface (Batchelor, 1970),

$$\boldsymbol{\tau} = -P\mathbf{I} + (1-\phi)\boldsymbol{\tau}_m + \phi\boldsymbol{\tau}_d - \Gamma\mathbf{q} \tag{2.8}$$

where ϕ is the volume fraction of dispersed phase, P is the hydrostatic pressure, Γ is the interfacial tension and finally **I** and **q** are the unit and anisotropy tensors, respectively. The last two equations do not rely on any specific microstructure. The last term in Equation 2.8 known as the excess stress ($-\Gamma\mathbf{q}$) is the direct contribution of the interface to the total stress. The anisotropy tensor which appears in the excess stress has been defined by Onuki (1987) in the following way,

$$q_{\alpha\beta} = \frac{1}{V}\int\left(n_\alpha n_\beta - \frac{1}{3}\delta_{\alpha\beta}\right)dS \tag{2.9}$$

where $q_{\alpha\beta}$ are the components of anisotropy tensor, $\delta_{\alpha\beta}$ is the Kronecker delta, **n** is the unit normal vector to the interface, V and S are, respectively, the volume and the integration surface area.

The theory of concentrated emulsions subjected to higher order of deformation was originally proposed by Doi and Ohta (1991) describing the time evolution of complex interfaces in a creeping flow. The authors employed the aforementioned anisotropy tensor (**q**) to express the orientation of the interface and the specific interfacial area (Q) to quantify the overall interfacial area per unit volume of the interface.

$$Q = \frac{1}{V}\int dS \tag{2.10}$$

Doi and Ohta (1991) mainly considered a mixture of two immiscible liquids having an identical constant viscosity and density, mixed with the volume ratio of 50/50. According to the authors, the microstructure evolution in immiscible blends is mainly affected by the flow field which enlarges and orients the interface, and the interfacial tension which opposes the deformation. Furthermore, for the interfacial contribution part, they merely considered two modes of relaxations: size and shape with no effect of break-up coming into the picture. This model was further extended by Lee and Park (1994) to account for the viscosity difference between the constituents and to incorporate the interface break-up phenomenon as an additional relaxation mode. The authors slightly modified the stress tensor originally proposed by Batchelor (1970) to incorporate the contribution of the rheological properties of the polymeric components. The complete stress tensor of Lee and Park model can be written as follows,

$$\tau_{\alpha\beta} = \left(1 + \frac{6}{10}\left(\frac{\eta_d - \eta_m}{\eta_d + \eta_m}\right)\phi\right)\eta_m(k_{\alpha\beta} + k_{\beta\alpha}) - \Gamma q_{\alpha\beta} - P\delta_{\alpha\beta} \tag{2.11}$$

where $k_{\alpha\beta}$ are the components of the velocity gradient tensor.

To completely describe the stress tensor, the time evolution equations of both anisotropy tensor and the specific interfacial area must be known. These two quantities are greatly affected by the flow field and the interfacial tension. As mentioned earlier the flow field tends to enlarge and orient the interface to an anisotropic state, whereas the interfacial tension opposes the deformation, minimizes the interfacial area and forces the system towards isotropic state. Hence, the time evolution of these two quantities are presented as follows,

$$\frac{\partial Q}{\partial t} = \left.\frac{\partial Q}{\partial t}\right|_{Flow} + \left.\frac{\partial Q}{\partial t}\right|_{\substack{Interfacial \\ tension}} \tag{2.12}$$

$$\frac{\partial q_{\alpha\beta}}{\partial t} = \left.\frac{\partial q_{\alpha\beta}}{\partial t}\right|_{Flow} + \left.\frac{\partial q_{\alpha\beta}}{\partial t}\right|_{\substack{Interfacial \\ tension}} \tag{2.13}$$

Assuming affine deformation, the time evolution equations of the anisotropy tensor and the specific interfacial area for the flow contribution part could be written as follows,

$$\begin{aligned} \left.\frac{\partial Q}{\partial t}\right|_{Flow} &= -\kappa_{\alpha\beta} q_{\alpha\beta} \\ \left.\frac{\partial q_{\alpha\beta}}{\partial t}\right|_{Flow} &= -q_{\alpha\gamma}\kappa_{\gamma\beta} - q_{\beta\gamma}\kappa_{\gamma\alpha} + \frac{2}{3}\delta_{\alpha\beta}\kappa_{\mu\nu}q_{\mu\nu} - \frac{Q}{3}(\kappa_{\alpha\beta} + \kappa_{\beta\alpha}) + \frac{q_{\mu\nu}\kappa_{\mu\nu}}{Q} q_{\alpha\beta} \end{aligned} \tag{2.14}$$

To describe the interfacial tension contribution on the interface evolution, Lee and Park (1994) considered three different relaxation mechanisms: coalescence, shape relaxation/interface retraction and break-up relaxations where each was characterized by Γ, η_m and Q (Figure 2.16).

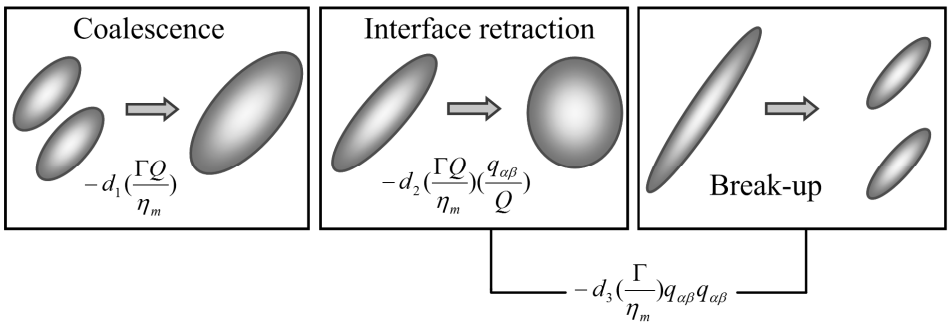

Figure 2.16. The schematic of coalescence, interface retraction (shape) and break-up relaxations along with their corresponding rate equations (Lee and Park, 1994).

Using dimensional analysis and by taking into account the aforementioned relaxation mechanisms, Lee and Park (1994) derived the following time evolution equations for the interfacial contribution part,

$$\left.\frac{\partial Q}{\partial t}\right|_{\substack{Interfacial\\tension}} = -r_1 - r_3 q_{\alpha\beta} = -d_1 \frac{\Gamma Q}{\eta_m} Q - d_3 \frac{\Gamma}{\eta_m} q_{\alpha\beta} q_{\alpha\beta} \tag{2.15}$$

$$\left.\frac{\partial}{\partial t}\left(\frac{q_{\alpha\beta}}{Q}\right)\right|_{\substack{Interfacial\\tension}} = -r_2\left(\frac{q_{\alpha\beta}}{Q}\right) = -d_2 \frac{\Gamma Q}{\eta_m}\left(\frac{q_{\alpha\beta}}{Q}\right) \tag{2.16}$$

$$r_1 = d_1 \frac{\Gamma Q}{\eta_m} \quad , \quad r_2 = d_2 \frac{\Gamma Q}{\eta_m} \quad , \quad r_3 = d_3 \frac{\Gamma}{\eta_m} q_{\alpha\beta} \tag{2.17}$$

where r_1, r_2 and r_3 are the relaxation rates representing coalescence, shape and break-up mechanisms, respectively. The authors further rearranged the above equations using dimensionless c_1, c_2 and c_3 parameters to describe the degree of total relaxation, size relaxation, and break-up and shape relaxations, respectively.

$$\left.\frac{\partial Q}{\partial t}\right|_{\substack{Interfacial\\tension}} = -c_1 c_2 \frac{\Gamma Q}{\eta_m} Q - c_1 c_3 \frac{\Gamma}{\eta_m} q_{\alpha\beta} q_{\alpha\beta} \tag{2.18}$$

$$\left.\frac{\partial q_{\alpha\beta}}{\partial t}\right|_{\substack{Interfacial\\tension}} = -c_1 \frac{\Gamma Q}{\eta_m} q_{\alpha\beta} - c_1 c_3 \frac{\Gamma}{\eta_m} \frac{q_{\mu\nu} q_{\mu\nu}}{Q} q_{\alpha\beta} \tag{2.19}$$

$$c_1 = d_1 + d_2 \qquad c_2 = d_1/(d_1 + d_2) \qquad c_3 = d_3/(d_1 + d_2) \tag{2.20}$$

In a dilute emulsions with no coalescence occurring in the system, the shape relaxation is the dominant relaxation mode. However, in concentrated emulsions with co-continuous morphology, it is expected to observe both shape and size relaxations simultaneously. The complete constitutive equation of Lee and Park model is the combination of total stress ($\boldsymbol{\tau}$) (Equation 2.11) and the time evolution equations of $\mathbf{q}$ and Q (Equations 2.12 to 2.20). Lee and Park (1994) satisfactorily employed the model to predict the viscoelastic properties of an immiscible blend composed of PS and LLDPE with a relatively high interfacial tension, i.e. ~4.7

mN/m. Grmela and Aitkadi (1994; 1998); Grmela et al. (1998); Lacroix et al. (1999) further reworked the equations of Doi and Ohta model keeping the same morphological parameters, i.e. Q and **q**, and employed the general form of Poisson-Bracket and Onsager reciprocity formalism called GENERIC (General equation for non-equilibrium reversible non-reversible coupling) (Grmela and Ottinger, 1997; Ottinger and Grmela, 1997).

Despite the advantages associated with the emulsion models based on the deformation of complex interfaces such as Lee and Park's model, these models were later found not to be appropriate to predict the rheological behavior of TPVs or TPOs with co-continuous morphology (Sengers et al., 2004). According to Sengers et al. (2004), the Lee-Park's model fails to predict the viscoelastic behavior of TPVs in the low frequency range, when the difference between viscosity or elasticity of the phases are large and the interfacial tension between the thermoplastic and the elastomer components is relatively low. According to the authors, in blends with low interfacial tension, the interfacial elasticity arisen from the interface deformation can be overshadowed by the elasticity of the elastomeric phase. As a result, Sengers et al. (2004) used an alternative approach based on the micro-mechanical models reflecting the morphology with series and parallel mixtures rules. They particularly employed the Veenstra-D model (Veenstra et al., 2000) to predict the viscoelastic properties of SEBS/PP and EPDM/PP blends. This model has exclusively been used for co-continuous morphologies where the co-continuity has been represented and visualized by two uniformly interconnected phases in a unit cube. Hence, the complex modulus of Veenstra-D model taking into account the contribution of each of those phases in the co-continuous morphology is presented as follows,

$$G^* = \frac{a^2 b G_1^* + (a^3 + 2ab + b^3) G_1^* G_2^* + ab^2 G_2^*}{bG_1^* + aG_2^*} \qquad (2.21)$$

$$\phi_1 = 3a^2 - 2a^3 \quad , \quad b = 1\text{-}a$$

where both *a* and *b* are geometric parameters associated to the volume fraction of phase one and two, respectively.

To conclude, each of the presented models possesses certain advantages and specific predictive capabilities. As a result, a complete insight into the blending system is required prior to the use of any of the aforementioned models.

2.6 Concluding Remarks

In this chapter, first an overview of the major important variables such as processing parameters, interfacial and rheological properties affecting the morphology development of non-reactive and reactive immiscible blends in general, or thermoplastic elastomer blends has been presented. In addition to the discussion on the morphology development, the importance of rheology as an essential microstructure characterization tool has also been pointed out. It has been a long time since the unique reciprocal relationship between rheology and morphology assisted researchers, on the one hand, to better understand the microstructure and, on the other hand, to optimize the design of the polymer processing equipments based on the rheological response of these materials.

However, despite the mentioned points described in this chapter and the existing large amount of information in the literature regarding the morphology development and more specifically the rheology/morphology relationship of immiscible polymer blends, numerous questions are still remain unanswered. In this regard, due to the special role played by plasticizers in the thermoplastic elastomer industry, no systematic study has yet been conducted with the aim of understanding the possible effect of plasticizer on the morphology development of non-reactive TPOs and their corresponding dynamically cross-linked TPVs.

More specifically:

- There is no direct information on how the plasticization may affect the co-continuity interval and the rheological response of non-reactive TPO blends;

- There is no systematic study on how the morphology of the non-reactive and reactive thermoplastic elastomer blends may evolve in the presence of plasticizer;

- Concerning the reactive thermoplastic elastomer blends, i.e. TPVs, there is no detail study on how the plasticization may affect the rate of cross-linking reaction and, therefore, the morphology transformation from an uncross-linked blend (TPO) to a dynamically cross-linked one (TPV).

According to what has been described, the complexities associated with the presence of different additives such as plasticizer in polymer blending science and technology are indeed very vast and, therefore, a large amount of research work is still required to improve the existing knowledge.

CHAPTER 3

OBJECTIVES

Considering the technological and economical importance of plasticization in the thermoplastic industry, and due to the limited literature data and the lack of systematic study on the effect of plasticization on the morphology development of TPEs and the existing gap between the rheology/morphology relationship of these materials in the presence of plasticizer, the main objective of this dissertation is:

"To elucidate the effect of plasticization on the morphology development and rheological behavior of EPDM/PP-based uncross-linked and dynamically cross-linked thermoplastic elastomers (TPEs)"

To achieve this goal, the effects of different parameters such as blending composition, viscosity ratio and the presence of plasticizer on the co-continuity development and the viscoelastic properties of uncross-linked EPDM/PP-based blends are examined initially.

Subsequently, the morphology development of uncross-linked and insitu cross-linked EPDM/PP blends is investigated through transient shear experiments in a rotational rheometer and a well controlled flow field. Particular attention is paid to the effects of plasticization and the insitu selective cross-linking of the EPDM phase on the morphology development and the rheolgical response of these TPEs.

Finally, the effects of complex flow fields inside conventional mixing equipments and plasticization on the morphology development of the uncross-linked and dynamically cross-

linked EPDM/PP-based blends are investigated through melt mixing inside an internal mixer and twin-screw extruder.

CHAPTER 4

ORGANIZATION OF THE ARTICLES

The following three chapters contain the articles submitted in the scope of this work:

The first article presented in Chapter 5 is entitled "*Rheology/Morphology Relationship of Plasticized and Non-Plasticized Thermoplastic Elastomers Based on Ethylene-Propylene-Diene-Terpolymer and Polypropylene*". It investigates the effect of plasticizer on the morphology, especially the co-continuity interval of the uncross-linked TPE blends, and associates the observed morphological features to the materials rheological response. Two different EPDM/PP-based non-plasticized/plasticized TPEs with a wide composition range are studied. Different techniques such as solvent extraction, scanning electron microscopy (SEM), atomic force microscopy (AFM) and rheological characterization are employed to achieve this goal. This paper has been submitted to *Polymer Engineering & Science* and is now in press.

The second article presented in Chapter 6 is entitled "*Morphology and Rheology of Non-Reactive and Reactive EPDM/PP Blends in Transient Shear Flow: Plasticized vs. Non-Plasticized*" presents the effect of plasticizer on the non-linear viscoelastic behavior and morphology evolution of non-reactive and reactive TPE blends. This study is conducted in a homogeneous shear flow field inside a rotational rheometer through single and multiple start-up transient experiments. The resulting morphologies are examined by atomic force microscopy (AFM). This work has been submitted to *Rubber Chemistry & Technology* and is currently under review.

The third and last article is presented in Chapter 7 and is entitled "*Morphology Development of EPDM/PP Uncross-linked and Dynamically Cross-linked Blends*". It compares the morphology development and viscoelastic properties of uncross-linked (TPOs) and dynamically cross-linked (TPVs) obtained from two different processes, an internal mixer and a co-rotating twin-screw extruder. AFM phase morphology imaging is used to investigate the effects of plasticizer and processing method on the morphology development. In addition, the linear viscoelastic properties of all blending systems are correlated to their corresponding morphology and curing state (where applicable). This paper has been submitted to *Polymer Engineering & Science* and is currently under review.

CHAPTER 5

RHEOLOGY/MORPHOLOGY RELATIONSHIP OF PLASTICIZED AND NON-PLASTICIZED THERMOPLASTIC ELASTOMERS BASED ON ETHYLENE-PROPYLENE-DIENE-TERPOLYMER AND POLYPROPYLENE

S. Shahbikian,[1] P.J. Carreau,[1*] M.-C. Heuzey,[1] M. D. Ellul,[2] H. P. Nadella[3], J. Cheng,[3] P. Shirodkar[3]

[1] Center for Applied Research on Polymers and Composites (CREPEC), Department of Chemical Engineering, École Polytechnique de Montréal, Quebec H3T 1J4, Canada

[2] ExxonMobil Chemical Co., Global Specialty Polymers Technology, Akron, Ohio 44311, USA

[3] ExxonMobil Chemical Co., Global Specialty Polymers Technology, Baytown, Texas 77520, USA

*Corresponding author: pierre.carreau@polymtl.ca

"*Polymer Engineering and Science*", in press (2010)

5.1 Abstract

The rheology/morphology relationship of plasticized and non-plasticized ethylene-propylene-diene-terpolymer/polypropylene (EPDM/PP) TPOs was studied. The aim was to investigate the effect of a plasticizer on the morphology, specially on the co-continuity interval of these blends. The addition of a plasticizer increased the interconnectivity of the elastomeric phase, resulting in a rapid percolation of the EPDM at a relatively low composition range as compared to the non-plasticized counterparts. However, the addition of the plasticizer did not change the onset of the co-continuity interval in the low EPDM content side of the composition diagram. Moreover, due to plasticization, the percolation of the PP phase was delayed on the other side of the composition diagram. Large differences between the viscous and elastic properties of the constituent polymers were observed. Hence, a combination of low frequency measurements and a gel approach were crucial to characterize the co-continuity interval using rheology. The phase inversion compositions were fairly well described by existing semi-empirical viscosity ratio-based models. Furthermore, a satisfactory prediction was obtained for the viscoelastic properties of the non-plasticized TPOs using a micro-mechanical model. However, this model failed in the case of the plasticized TPOs, due to the probable presence of a plasticized interphase.

5.2 Introduction

Blending technology provides a more flexible and accessible route to develop new sets of polymeric materials with desired properties, as compared to chemical synthesis. However, due to the high molecular weight of polymers and their thermodynamic limitation mainly caused by the

vanishing mixing entropy, blending almost always leads to immiscible multiphase systems with heterogeneous morphologies [1]. In such immiscible blends, four general types of morphology can be observed through blending: matrix/dispersed, matrix/fibers, lamellar and co-continuous morphologies. Accordingly, by controlling the phase morphology, a wide range of materials with tailored physical and mechanical properties can be achieved. The existence of the different morphologies depends on many factors such as the rheological properties of the constituent polymers, the interfacial tension, the blending composition, the processing conditions and the presence of various modifiers or additives [2]. Among them, interfacial modifiers can affect the morphology, rheology and mechanical properties of the blends.

Thermoplastic elastomeric blends (TPOs) are obtained through melt mixing of a semi-crystalline thermoplastic polyolefin and an elastomer. They are also considered as immiscible blends and have been studied to a great extent due to their growing industrial and economic importance. Among them, TPOs based on polypropylene (PP) and ethylene-propylene-diene-terpolymer (EPDM) are commercially recognized for their unique physical and mechanical properties. In the thermoplastic elastomer industry, it is common practice to incorporate about 70 to 200 phr (parts per hundred parts of rubber) by weight of a proper plasticizer (or processing oil) during the melt processing step. Plasticizers are commonly paraffinic, naphthenic or aromatic oils derived from petroleum fractions. They generally improve the heat stability, hysteresis, cost and permanent set of the thermoplastic elastomer, as well as the low temperature mechanical properties, melt processability and the final appearance of the products [3,4]. Furthermore, the addition of a plasticizer is indispensable to obtain softer TPO compositions with hardness in the range of 60 Shore *A* [5,6]. It is generally believed that a proper plasticizer possessing a relatively high affinity with both polymeric components is distributed in both phases and subsequently swells them in the molten state. Hence, it reduces the viscoelastic properties of the constituent

polymers and consequently affects the morphology development of these blends [7]. Upon cooling, due to the crystallization of the semi-crystalline polymer, the majority of plasticizer is redistributed and absorbed by the elastomeric component and the amorphous fraction of the semi-crystalline polymer [8]. In order to understand the relationship between rheology and morphology of these plasticized TPOs, the distribution of the plasticizer in each polymeric component has to be determined. Several studies have intended to obtain an accurate measure of the oil distribution in both the solid and melt states [3,9-13]. Most of these studies agreed for a slight preferential oil distribution in the elastomeric component.

Regardless of plasticization, a dispersed/matrix type of morphology has been generally observed for immiscible polymer blends, including TPOs, at low volume fraction of either one of the components. The shape and size of the minor phase is believed to be mainly dictated by the interfacial tension, viscosity ratio, elasticity ratio and mixing time and intensity. In blends with low interfacial tension, stable elongated fibers have been observed [14,15], whereas in blends with high interfacial tension, droplets of the minor phase were generally formed [16,17]. By increasing the composition of the minor phase, the dispersed domains may coalesce and form larger domains. Further increase of the minor phase, exceeding the percolation threshold, extends the inter-connectivity of the phases and leads to the formation of a co-continuous morphology. This can be visualized by an intertwining morphology where both polymeric components have a three-dimensional spatial continuity. The co-continuity composition range differs from one blend to another, depending on the compatibility of the components and the presence of an interfacial modifier. Usually, in the absence of any interfacial modifier, compatible blends with low interfacial tension demonstrate a low percolation threshold and broad co-continuity range, whereas blends possessing high interfacial tension usually displayed a delayed percolation with narrower co-continuity range [14]. Beyond the co-continuity composition range, further addition

of the initially minor phase results in a complete morphological change, where the former polymeric component constituting the matrix phase becomes the dispersed one. The mentioned overall morphology transformation is known as the phase inversion phenomenon, where the dispersed and matrix phases switch their roles. In the case of polymeric blends with high molecular weight chains, the phase inversion occurs over a wide composition range known as the co-continuity interval. The presence of any phase modifier or additive in a binary blend might affect the percolation and, consequently, the co-continuity development through its effect on the viscoelastic and interfacial properties of the constituent polymers.

Several experimental techniques have already been exploited to characterize the morphology of immiscible polymer blends, especially in the co-continuity composition range [18]. The combination of solvent extraction, morphology analysis and rheological characterization are among the techniques, which have been widely used and considered as the most reliable methods. Generally, dynamic rheological measurements provide a faster route to investigate the state of an emulsion. It has been known that the droplet/matrix morphology results in a characteristic relaxation mode at longer times, corresponding to the droplet deformation, which enhances the elastic properties of the blend in the low frequency range [19]. On the other hand, it is generally believed that in blends with a co-continuous morphology, the lower surface/volume ratio of the interface results in less elasticity enhancement due to less specific interfacial area [18,20,21].

In the course of the last few decades, numerous studies have been devoted to phase morphology predictions of immiscible polymer blends, aiming at predicting phase inversion and more recently the co-continuity interval [2]. The results of these studies were largely based on empirical and semi-empirical models mainly using the rheological properties of the constituent polymers. Despite all efforts dedicated to improve the existing knowledge of phase morphology

predictions and to understand the relationship between rheology/morphology of immiscible polymer blends, the interdependency of the linear viscoelastic properties of these blends and their morphological features such as the co-continuity interval has not yet been satisfactorily understood.

In this work, the rheology/morphology relationship of non-plasticized and plasticized EPDM/PP immiscible blends has been studied. Two sets of EPDM/PP blends consisting of components of highly different rheological properties have been investigated. In addition, the effect of a low molecular weight plasticizer on the phase morphology and rheology of these TPOs is investigated. Particular attention has been devoted to the study of the co-continuity interval and the effect of the plasticizer on the latter.

5.3 Experimental

5.3.1 Materials

In this work, two EPDM and two PP grades provided by ExxonMobil Chemical Company were used as the elastomeric and semi-crystalline polyolefin components, respectively. The nomenclatures and properties of these polymeric components are given in Table 5.1. Different non-plasticized and plasticized EPDM/PP (wt/wt%) compositions were studied over the whole composition range. In the case of the plasticized blends, 100 phr (based on the EPDM content) of paraffinic oil (Sunpar® 150M from Sunoco, Inc.) was used. Furthermore, in order to prevent the thermal degradation of the polymeric components during the melt mixing stage, an antioxidant (Irganox® B-225, 1 wt% based on the weight of EPDM + PP) was used.

Table 5.1. Characteristics of the neat polymeric components.

Polymer	*Symbol*	*MFI,* dg/60 s (ASTM D-1238)	T_m °C	*Mooney Viscosity* (ASTM D-1646)	*ENB** wt%	C_2+ wt%
EPDM	E1	-	-	76 (ML 1+4, @ 125°C)	5.8	45
EPDM	E2	-	-	25 (ML 1+4, @ 125°C)	4.7	57.5
PP	P1	5.3 (230°C/2.16 kg)	165	-	-	-
*PP (RCP)***	P2	3 (-)	141	-	-	4

* ENB: ethylidene norbornene.

+ C_2: ethylene content.

** PP (RCP): Polypropylene (random co-polymer).

5.3.2 Melt Mixing

The melt mixing was carried out using a small scale laboratory internal mixer (Brabender® Plasti-corder®) equipped with a 30 mL chamber. The E1/P1 TPOs were merely blended at 180°C and the E2/P2 blends were blended at 165°C and 180°C. The rotation speed was set at 100 rpm and the mixing was performed for 12 min. The mentioned rotor speed corresponds to an apparent shear rate of ~50 s^{-1} [22]. In the case of the plasticized blends, 75 wt% of the plasticizer was added during the first 8 min of the mixing process, and the remaining was added at the latest mixing stage (last 4 min). This process was carried out under a nitrogen atmosphere to prevent the thermal degradation of the polymeric components. Subsequently, at the end of the mixing process, the blends were immediately quenched in liquid nitrogen to freeze the morphology.

5.3.3 Rheological Measurements

For the rheological characterization the blends were compression molded at their corresponding melt mixing temperature in the form of 25 mm diameter disks with ~1.5 mm thickness. The rheological measurements were also carried out at their corresponding melt mixing temperature using a stress controlled rheometer (TA Instruments® AR2000) with a parallel plate flow geometry under a nitrogen atmosphere. Time sweep and frequency sweep experiments were carried out in the linear viscoelastic range to characterize the thermal stability and overall rheological behavior of the blends, respectively.

5.3.4 Morphological Analyses

The blended samples were cryo-microtomed at -150°C ~ -170°C using a Leica® RM 2165 instrument equipped with a Leica® LN 21 cryo-chamber. For the scanning electron microscopy (SEM) analysis, the samples were subjected to fresh *n*-heptane to create the necessary contrast by extracting the EPDM phase at the surface. The samples were then dried and coated with a gold-palladium layer and scanning electron microscopy was carried out using a Jeol® JSM 840 system operated at 10 kV.

In addition to SEM, atomic force microscopy (AFM) was used to clearly identify and distinguish the interface in the co-continuous composition range. The AFM imaging was performed on the cryo-microtomed sections using a Dimension™ 3100 microscope from Veeco Instruments, in tapping mode. The experiments were carried out under ambient conditions using a scanning rate of ~0.3-0.7 (Hz), integral gain of ~0.3-0.7 and proportional gain of ~0.6-1.4.

5.3.5 Solvent Extraction and Gravimetric Analyses

To determine the composition window where a complex co-continuous morphology exists, solvent extraction analyses have been performed. Due to the importance of the surface/volume ratio in these experiments, uniform samples with pre-defined shapes were prepared [23]. Accordingly, the blends were compression molded in the form of 25 mm diameter disks and ~1.5-1.8 mm thickness. Rectangular samples with width and length of ~8-10 mm were cut from the molded disks and placed in 50 mL centrifugal tubes containing 35-40 mL of fresh *n*-heptane to dissolve the elastomeric phase. The tubes were placed on a shaking table for 7 days. Afterward, the samples were taken out and dried in a vacuum oven at 60°C, and their weights were subsequently measured. The whole process was repeated several times to achieve a constant sample weight. The continuity index (*CI*) of the extracted EPDM phase was then calculated based on the following correlation:

$$\%\ \text{Continuity Index of EPDM} = \frac{W_{EPDM,Initial} - W_{EPDM,After\ Extraction}}{W_{EPDM,Initial}} \tag{4.1}$$

where $W_{EPDM,\ initial}$ and $W_{EPDM,\ After\ Extraction}$ represent the initial and final weight of the EPDM during the extraction experiment, respectively. In the case where the sample is not disintegrated, the PP phase is considered 100% continuous, and the amount of weight lost during the experiments corresponds to the elastomeric phase that belongs to the percolated structure. On the other hand, a total sample disintegration confirms a 100% continuity of the EPDM phase.

5.4 Results and Discussion

5.4.1 Rheology of Neat Polymers

The thermal stability of the unprocessed and processed pure polymeric components was examined by performing time sweep rheological measurements in the linear viscoelastic domain, and all the materials were shown to be thermally stable. The storage modulus and the complex of the neat polymeric constituents are presented in Figures 5.1 and 5.2, respectively. The storage modulus and complex viscosity of the PPs exhibit a classical viscoelastic behavior with a tendency to reach the terminal zone at low frequencies, where G' is proportional to $\omega^{1.26}$ (Figure 5.1).

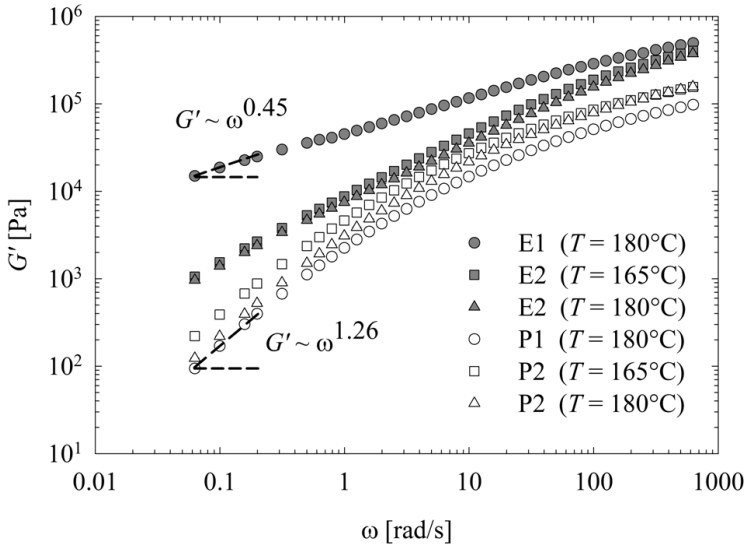

Figure 5.1. Storage modulus (G') as a function of frequency at different temperatures.

In the same frequency range, η^* exhibits a tendency towards a typical Newtonian plateau (Figure 5.2). In the case of the EPDMs, for both high and low Mooney viscosity elastomers (E1 and E2) the terminal zone is not reached even at the lowest frequency. The complex viscosities of

the two elastomers are also far from a Newtonian plateau with E1 exhibiting a typical yield stress behavior (Figure 5.2).

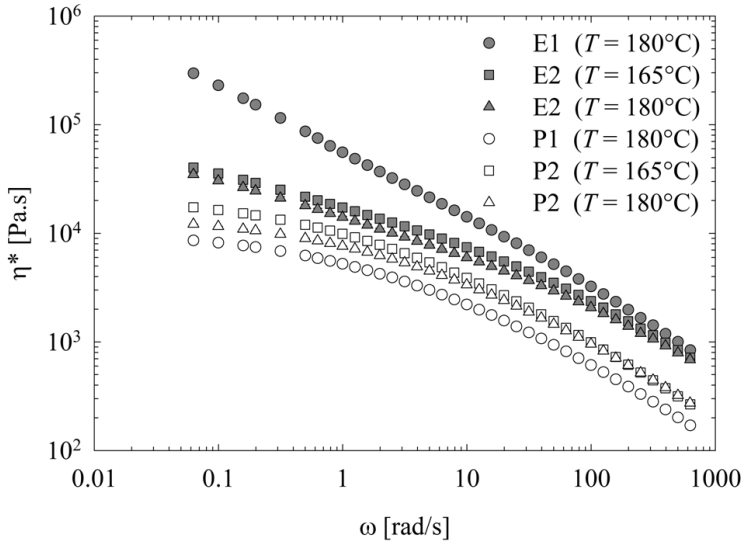

Figure 5.2. Complex viscosity (η*) as a function of frequency at different temperatures.

At each designated temperature, the EPDMs are more viscous and more elastic in comparison to the PPs. Nevertheless, regardless of temperature, the rheological properties of E2 and P2 components are closer due to low Mooney viscosity of the elastomer. Assuming the Cox-Merz [24] relation to be valid for the neat polymeric components [25], the complex viscosity can be interpreted as the steady shear viscosity. As a result, from high to low frequencies (or shear rate) the viscosity ratios (η_{EPDM}/η_{PP}) of E1/P1 and E2/P2 blends lie between 3.5-32 and 1.7-2.7, respectively (Table 5.2). Accordingly, at the apparent shear rate of the mixing equipment (i.e., ~50 s^{-1}), the viscosity and elasticity values of the different non-plasticized neat polymeric components decrease based on the following trend: E1 (180°C) > E2 (165°C) > E2 (180°C) > P2 (165°C) > P2 (180°C) > P1 (180°C). Regardless of temperature, all the ratios of the rheological properties are larger than unity. As a result, the EPDMs shall always be considered less deformable than the PPs.

Table 5.2. Ratios of rheological properties for the TPO blends prepared under various mixing conditions.

Blends	T [°C]	Phases		Matrix shear stress[+]	At constant shear rate			At constant shear stress		
		Matrix	Dispersed	[kPa]	η_d/η_m [-]	G'_d/G'_m [-]	$tan\delta_d/tan\delta_m$ [-]	η_d/η_m [-]	G'_d/G'_m [-]	$tan\delta_d/tan\delta_m$ [-]
E1/P1	180	E1	P1	258.88	0.18	0.17	1.31	0.0016*	-	-
		P1	E1	46.77	5.53	5.99	0.76	81.71	1.03	1.10
E2/P2	180	E2	P2	147.73	0.49	0.55	0.77	0.13	1.28	2.04
		P2	E2	72.53	2.04	1.81	1.29	3.61	0.78	0.61
E2/P2	165	E2	P2	174.89	0.44	0.50	0.75	0.07	-	-
		P2	E2	77.62	2.25	2.02	1.33	4.64	0.75	0.54

[+] Calculated at 50 s^{-1}.

[*] Based on data extrapolation.

As mentioned before, the viscoelastic properties of polymers in the molten state are generally decreased in the presence of a plasticizer [10]. However, upon cooling, especially in the case of semi-crystalline polymers, the plasticizer is depleted from the crystalline domains. As a result, the rheological characterization performed on quenched samples do not generally represent the viscoelastic properties of the plasticized polymers in the molten state. An alternative reliable approach is, therefore, sought to estimate the viscosity ratio of the plasticized blends. According to Bousmina et al. [22], the mixing torque ratio can be assumed to be equal to viscosity ratio ($\tau_{EPDM}/\tau_{PP} = \eta_{EPDM}/\eta_{PP}$). The torque ratio of the non-plasticized components was found to be equal to the viscosity ratio measured by the rheometer ($\tau_{E2}/\tau_{P2} = 2.04$). Furthermore, the mixing of the individual polymeric components (EPDM and PP) separately with 25 and 50 phr plasticizer resulted in an approximately identical torque reduction in mixtures containing the same amount of oil. Consequently, the torque ratios for 0, 25 and 50 phr plasticized components remained approximately in the same range: 2.04, 2.14 and 2.22, respectively. In the literature, the

affinity has been interpreted in terms of solubility parameters, with values of 16.77 $MPa^{½}$ [26], 16.40 $MPa^{½}$ [27] and 14.11-16.36 $MPa^{½}$ [28] for the PP, EPDM and the plasticizer, respectively. Considering a relatively high affinity between the plasticizer and the polymeric components, a uniform distribution of the plasticizer in the molten state can be assumed. Hence, the torque ratio of the individually plasticized components, which is approximately equal to the ratio of the non-plasticized pairs, can be considered as the viscosity ratio of the plasticized TPO medium.

5.4.2 Solvent Extraction and Continuity Development

The continuity index (*CI*) of the EPDM phase in the non-plasticized and plasticized TPOs is reported in Figure 5.3. Prior to the continuity determination, the results obtained from the *n*-heptane exposure of the neat polymeric components (PP and EPDM) and processing oil revealed that the PP, EPDM and processing oil were respectively 0%, 100% and 100% soluble in *n*-heptane. It has to be mentioned that 18 h were adequate to dissolve a neat EPDM sample of identical dimensions. Figure 5.3 clearly shows that the co-continuity interval (the dual-continuity composition range) for both plasticized and non-plasticized blends covers a wide composition range.

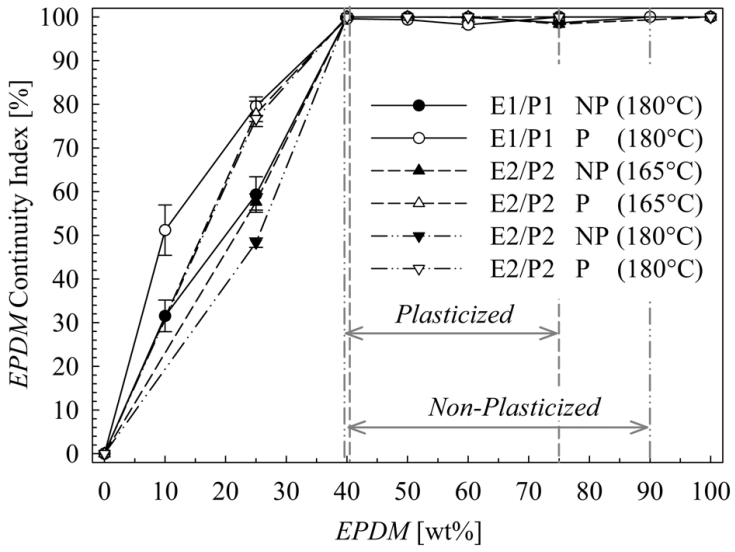

Figure 5.3. Continuity index of EPDM and co-continuity interval in non-plasticized and plasticized TPOs. (Lines are guide lines)

Regardless of the blending system (i.e., E1/P1 or E2/P2) and the mixing temperature, the co-continuity interval extends from 40 up to ~90 wt% of EPDM in the non-plasticized systems, and from 40 up to 75 wt% of EPDM in the plasticized blends, resulting in an asymmetric co-continuity interval. Due to the difficulty of dissolving selectively the PP phase, the upper level of the co-continuity interval has been merely defined based on the complete disintegration of the EPDM phase. As a result, the actual upper level of the co-continuity shall lie between 75 to 90 wt% of EPDM in the non-plasticized and 60 to 75 wt% of EPDM in the plasticized blends.

At the low composition range of the EPDM, the classical sigmoidal continuity curve with slow percolation known for relatively high interfacial tension polymer blends is not observed [16], regardless of plasticization. On the contrary, a rapid percolation is seen, which could be attributed to the non-spherical shape of the dispersed phase, mainly a fibrillar or irregular morphology forming a certain level of connectivity, as will be reported in the next section. Furthermore, the mentioned rapid percolation is more pronounced in the plasticized blends,

where at 25 wt% EPDM in the plasticized blends ~80% of the EPDM phase contributes to the continuous network as compared to the non-plasticized TPOs where the continuity of the EPDM lies between 48 to 59%. The viscosity ratios of the neat EPDM/PP components (i.e., η_{EPDM}/η_{PP}) calculated at the apparent shear rate of the mixing equipment are all greater than unity (Table 5.2). Accordingly, at low EPDM content, especially for the non-plasticized TPOs, the matrix shear stress is possibly not sufficient to disperse the highly viscous and elastic EPDM phase. As a result, the PP tends to encapsulate the EPDM phase rather than to disperse it [29]. On the other hand, it is generally known that the elasticity of the dispersed phase stabilizes the morphology, whereas the elasticity of the matrix phase has an opposite effect. Accordingly, it is more difficult to deform and disperse a highly elastic dispersed phase in the presence of a lower elastic matrix [30,31]. Moreover, according to Van Oene [32], under dynamic flow conditions, the difference between the elasticity of the components, defined by their first normal stress difference, can influence the interfacial deformation through the dynamic interfacial tension. When the dispersed phase consists of the more elastic phase (i.e., EPDM in this case), the difference in the elasticity of the components increases the interfacial resistance, manifesting itself on the dynamic interfacial tension, which would consequently affect the dispersion of the elastomeric component. Therefore, both the high viscosity ratio and large elasticity difference would probably result in a relatively rapid initial percolation, as well as a non-sigmoidal continuity formation. Besides the mentioned effect of the rheological properties, the diffusion of the low molecular weight plasticizer from the EPDM to the PP may result in a plasticized interphase. According to Tufano et al. [33], the diffusion of low molecular weight species from one phase to another, in an extremely diffusive system, results in faster coalescence. Hence, the diffusion of the plasticizer

could possibly result in a faster coalescence of the elastomeric domains and, therefore, favoring a higher continuity index for plasticized TPOs, as seen in Figure 5.3.

At the other side of the composition diagram, and based on the complete disintegration of the EPDM phase, the onset for the 100% continuity of the PP phase was ~10 and 25 wt% of PP in the non-plasticized and plasticized blends, respectively (Figure 5.3). Compared to the continuity development of the EPDM, a more rapid percolation has been observed on the low polypropylene content side of the co-continuity curve. Based on the earlier discussion, the viscosity ratio (η_{PP}/η_{EPDM}) is lower than unity for this high EPDM composition range and the matrix (i.e., EPDM) is more elastic. Moreover, the EPDM/PP blends possess a relatively low interfacial tension (~0.3 mN/m @ 190°C) [15,34,35], and according to Van Oene [32] this could be further reduced in a dynamic flow situation due to the larger elasticity of the matrix phase. Hence, the relatively high shear stress in the matrix and low interfacial tension under flow conditions could result in a stable fibrillar morphology, ease of percolation and formation of a co-continuous structure. The stability of a PP fiber in an EPDM matrix can be readily calculated using Tomotika's theory [36]. Recently, Bhadane et al. [15] investigated the stability of fibers formed in EPDM/PP blends of various viscosity ratios, where the reported thread breakup time of a PP in an EPDM matrix fell far beyond the mixing time, confirming the formation of a stable fibrillar morphology. A similar rapid percolation of a fibrillar morphology has also been observed in a low interfacial tension PS/SBR blend, during the addition of the PS phase [37]. According to the authors, the thermoplastic phase (PS) immediately tended to become the continuous phase by fiber formation with an asymmetric co-continuity interval.

5.4.3 Morphology of TPOs

SEM micrographs of the non-plasticized and plasticized E1/P1 25/75 wt/wt% TPOs are shown in Figure 5.4. The common morphological feature in both micrographs is the presence of interconnections between the extracted EPDM domains. The presence of large extracted domains with interior holes is in accordance with the erosion-based mechanism expressing the presence of simultaneous fibrillar and dispersed type morphologies in high viscosity ratio EPDM/PP blends [38], which may be responsible for the rapid percolation and co-continuity development.

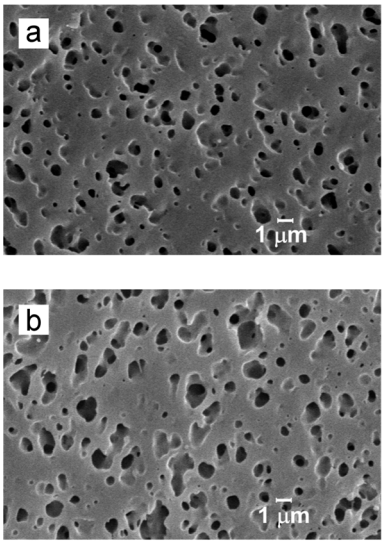

Figure 5.4. SEM micrographs of non-plasticized and plasticized E1/P1 25/75 (wt/wt%) TPO blends: (a) Non-plasticized, (b) Plasticized.

In the co-continuous composition range, the interface of the existing features is generally hard to detect in the SEM micrographs [39]. To overcome this problem, atomic force microscopy (AFM) provides a relatively sharp contrast between phases by relying on the viscoelastic properties of the different constituent polymers. AFM phase micrographs of the non-plasticized and plasticized TPOs in the mid composition range (50/50) are shown in Figure 5.5. The addition of the plasticizer results in a coarser morphology, with coalesced and swollen EPDM domains.

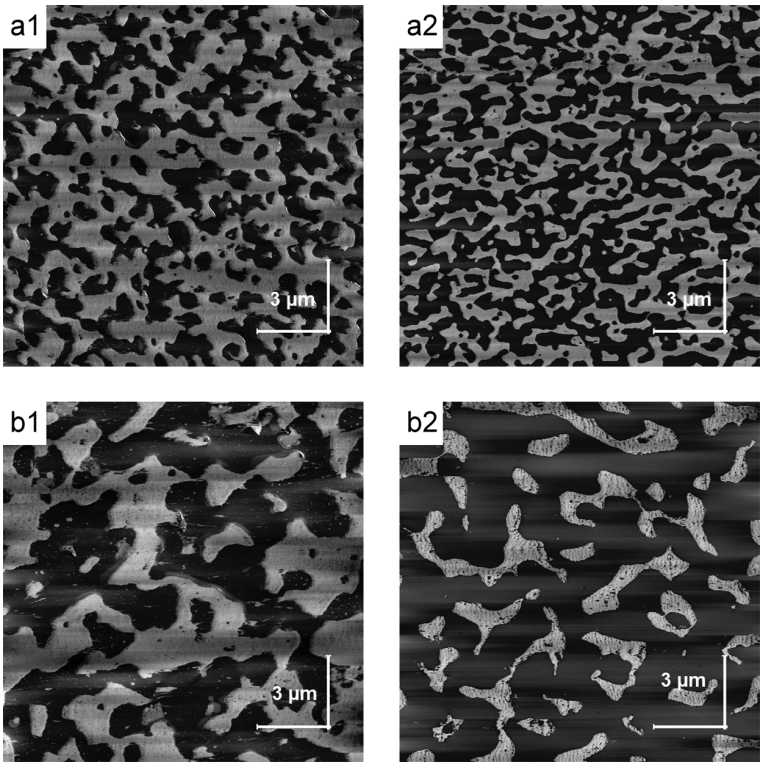

Figure 5.5. AFM phase micrographs of non-plasticized and plasticized 50/50 (wt/wt%) TPOs blended at 180°C: (1) E1/P1, (2) E2/P2. (Row *a*: non-plasticized; Row *b*: plasticized; Dark phase: EPDM; Bright phase: PP)

A similar phenomenon can be observed for the TPOs of low EPDM content (25 wt% of EPDM) (Figure 5.6). Note that similar results were obtained for the E1/P1 and E2/P2 systems. However, the morphology of the non-plasticized E2/P2 blend is much finer than that of the non-plasticized E1/P1 blend. The trend observed in the AFM micrographs is in accordance with the solvent extraction results, confirming a more rapid percolation of the elastomeric phase in the low EPDM composition range of the plasticized TPOs (Figure 5.3).

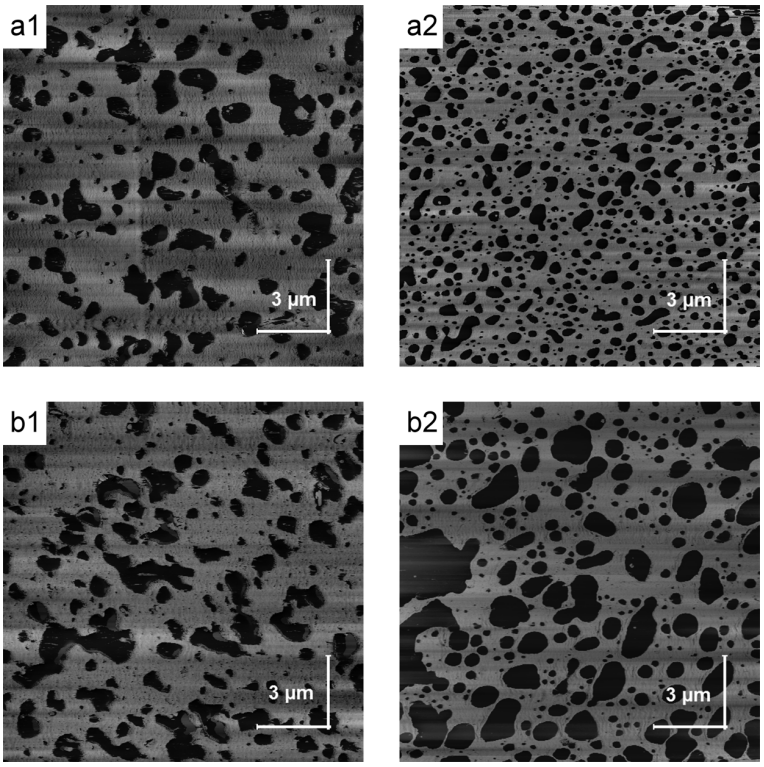

Figure 5.6. AFM phase micrographs of non-plasticized and plasticized 25/75 (wt/wt%) TPOs blended at 180°C: (1) E1/P1, (2) E2/P2. (Row *a*: non-plasticized; Row *b*: plasticized; Dark phase: EPDM; Bright phase: PP)

5.4.4 Rheology of TPOs and Co-continuity Interval

The complex viscosities of the non-plasticized and plasticized E1/P1 TPOs are shown in Figure 5.7. The complex viscosity of the non-plasticized blends increases with the elastomer content while the tendency to reach the terminal zone vanishes (Figure 5.7a). Consequently, the complex viscosity curves do not overlap.

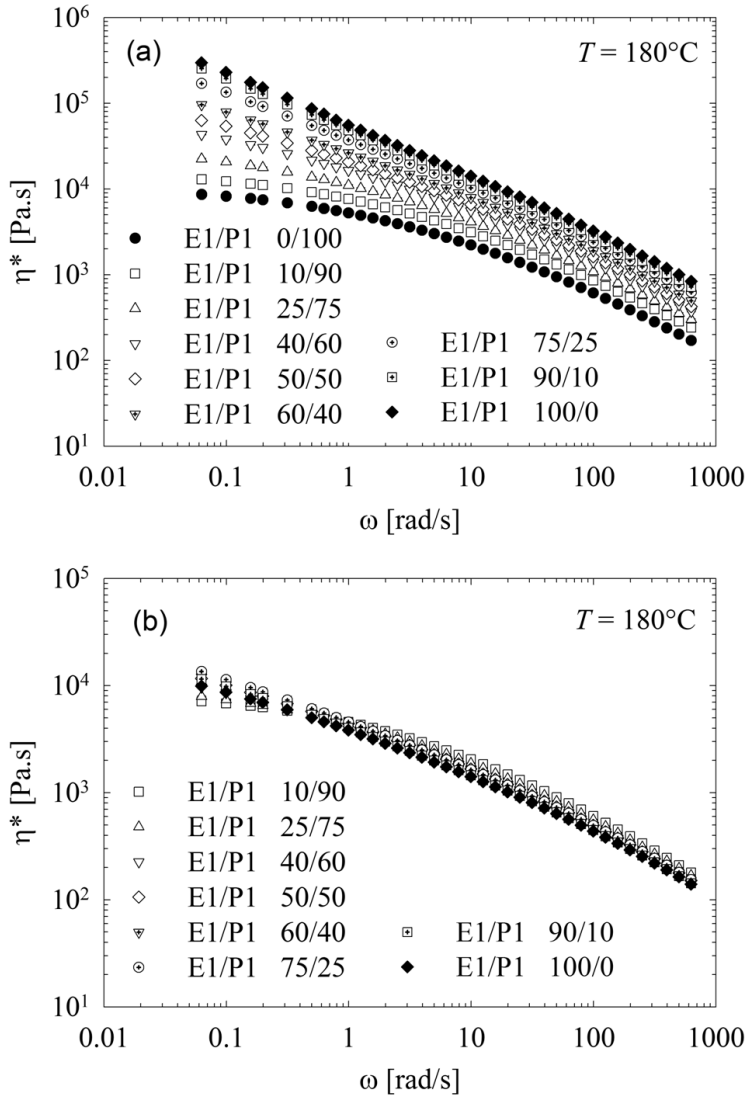

Figure 5.7. Complex viscosity data at 180C: (a) Non-plasticized E1/P1 (wt/wt%) TPO blends, (b) Plasticized E1/P1 (wt/wt%) TPO blends.

On the other hand, the presence of a plasticizer results in a considerable change on the rheological behavior of these blends. As Figure 5.7b, the complex viscosity of the blends is only slightly affected by the EPDM content and an inverse viscosity trend as a function of EPDM content is observed at low frequency, where the complex viscosity decreases with EPDM content. Consequently, in the plasticized E1/P1 blends (Figure 5.7b), the rheological properties overlap at

a certain composition range, which could potentially be used to estimate the onset of the co-continuity interval [40].

To this end, the interfacial driven relaxation of the interface enhancing the elastic response (G') of the blends at low frequencies provides, however, a better insight into the rheology/morphology relationship of immiscible blends [19]. The interfacial area reflecting the excess elasticity is directly related to the existing type of morphology. In the low frequency range, a blend with a finely dispersed droplet/matrix morphology generally possesses a larger specific interfacial area and, therefore, displays a larger excess elasticity as compared to a blend with an identical composition but with a certain degree of interconnected morphology. In the literature, the variation of the storage modulus as a function of blend composition at the lowest possible frequency and the appearance of extrema have been attributed to the onset of co-continuity from both extremities of the composition diagram [18,20,29,41,42]. Figures 5.8 and 5.9 show the composition effect on the low frequency storage modulus of the non-plasticized and plasticized E1/P1 and E2/P2 TPOs, respectively, along with the predictions of the Kerner model for the non-plasticized systems.

This model describes the rheological behavior of a droplet/matrix type morphology with a perfect interphase adhesion [43]. It further assumes a zero interfacial tension and, therefore, has been considered as a mixing rule taking into account only the composition dependency with no excess interfacial elasticity [29]. As a result, in the low composition range, deviations from the Kerner model predictions would imply a departure from the droplet/matrix type morphology.

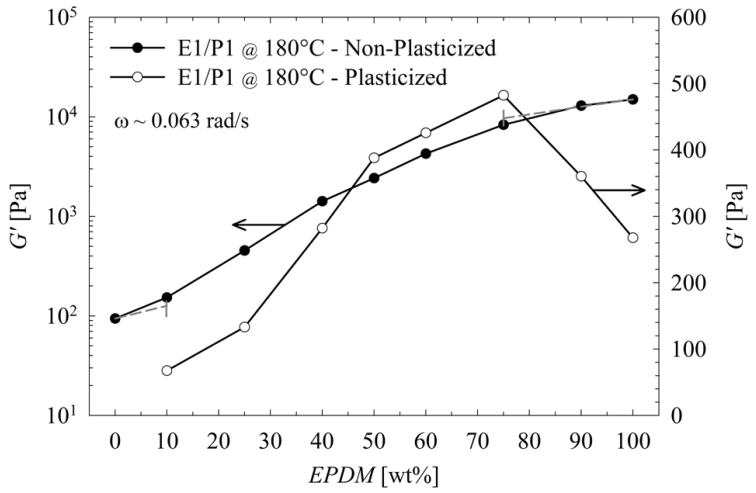

Figure 5.8. Storage modulus versus composition at the lowest frequency: non-plasticized and plasticized E1/P1 TPOs at 180°C. (Solid lines are guide lines; dashed lines are the predictions of the Kerner model up to 10% deviation from experimental data)

It has to be mentioned that due to the lack of rheological data for the highly plasticized semi-crystalline polypropylene, this model could not be used for the plasticized TPOs. As shown in Figures 5.8 and 5.9, the addition of a highly elastic elastomeric component in the non-plasticized TPOs results in a uniform increase of G' with no appearance of any extremum. This represents the general behavior of an immiscible polymer blend possessing a highly elastic three dimensional polymeric network with a plateau storage modulus. For the non-plasticized blends (Figure 5.8) the storage modulus is close to the prediction of the Kerner model at both extremities of the composition diagram, indicating the existence of a semi-dispersed morphology. However, from 10 to 75 wt% EPDM, a divergence larger than 10% was observed between the model prediction and the experimental data, possibly indicating the existence of a complex interconnected morphology. The non-plasticized E2/P2 TPOs blended at 180°C demonstrate an identical trend with no extrema (Figure 5.9). Furthermore, the deviations from the Kerner model

starts from 40 to 75 wt% EPDM (Table 5.3), which corresponds to the co-continuity results by solvent extraction (Figure 5.3).

Table 5.3. Co-continuity interval composition data obtained from different techniques

Blends	Type*	T [°C]	Solvent extraction EPDM [wt%]			Dynamic rheological exp. based on *G'* EPDM [wt%]		Dynamic rheological exp. based on *tan(δ)* EPDM [wt%]	
			Onset	End	Mid point of co-continuity +	Onset	End	Onset	End
E1/P1	NP	180	40	75-90	~57.5-65	~10**	~75**	~40-50	-
	P	180	40	60-75	~50-57.5	-	75	40	75
E2/P2	NP	165	40	75-90	~57.5-65	~40**	~75**	~40-50	-
	P	165	40	60-75	~50-57.5	-	75	~40-50	75
E2/P2	NP	180	40	75-90	~57.5-65	~40**	~75**	~40-50	-
	P	180	40	60-75	~50-57.5	-	75	~40-50	75

* *NP*: Non-plasticized; *P*: Plasticized.

+ Calculated based upon mid-points obtained using the onset and two end compositions of co-continuity interval.

** Based on the maximum 10% deviation observed between the experimental data and the predictions of the Kerner model.

The plasticization decreases the elasticity of the elastomeric phase, especially for the TPOs with larger EPDM content and, therefore, the effect of the interfacial elasticity becomes more pronounced. In all the plasticized TPOs, regardless of the blending pairs, an extremum appears at 75 wt% EPDM, corresponding to the complete disintegration observed in the solvent extraction experiments (Figure 5.3).

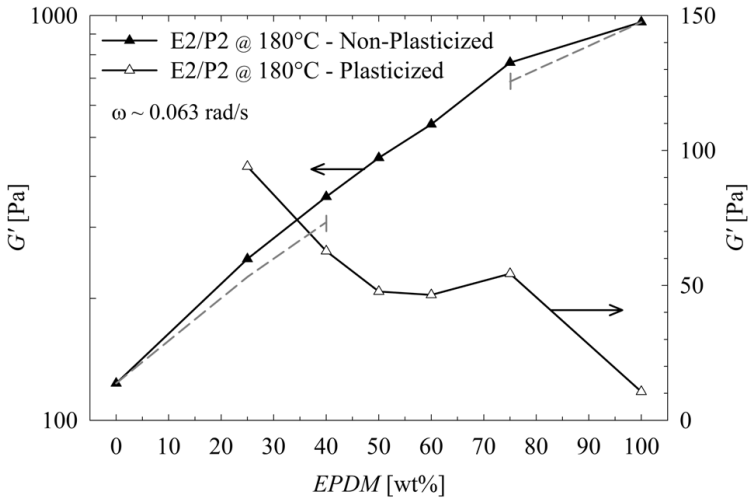

Figure 5.9. Storage modulus versus composition at the lowest frequency: non-plasticized and plasticized E2/P2 TPOs at 180°C. (Solid lines are guide lines; dashed lines are the predictions of the Kerner model up to 10% deviation from experimental data)

Due to the lack of two distinct extrema defining the boundaries of the co-continuity interval, an alternative approach shall be employed, which would not be merely based on the storage modulus of the highly elastic immiscible blends. According to Castro et al. [44], the rheology of a co-continuous network can be described by a chemical gel approach. In a chemical gel, the viscoelastic moduli cross each other, and depending on the type of reaction, a frequency independent cross-over point can be observed at the gel point [45]. In addition, at the gel point both moduli obey a power-law relation with the same exponent Δ over the entire frequency range ($G' \sim G'' \sim \omega^{\Delta}$). According to Muller et al. [45], the value of Δ depends on the type of chemical reaction, ranging from $1/2 \leq \Delta \leq 2/3$ (it could also approach unity). A similar trend can be expected for an immiscible polymer blend at the percolation composition, where the formation of a co-continuous network can be perceived as a chemical gel (or percolated structure). Generally in polymer blends, the power-law exponent and consequently the loss tangent as a function of blend composition decreases from both extremities of the composition diagram and reaches a

somehow constant value in the intermediate co-continuous composition range [44]. Figure 5.10 reports the loss tangents of the non-plasticized and plasticized E1/P1 and E2/P2 TPOs. The frequency independent range of the loss tangent for the non-plasticized TPOs, and consequently the onset of the co-continuity interval begins between 40 to 50 wt% EPDM. However, using this approach, the upper range of the co-continuity interval can not be detected. According to Sengers et al. [13], for blends with relatively low interfacial tension the excess elasticity caused by the interface deformation is overshadowed by the elasticity of the elastomeric phase. Hence, the loss tangent for high elastomer content non-plasticized blends remains frequency independent up to 100 wt% of EPDM.

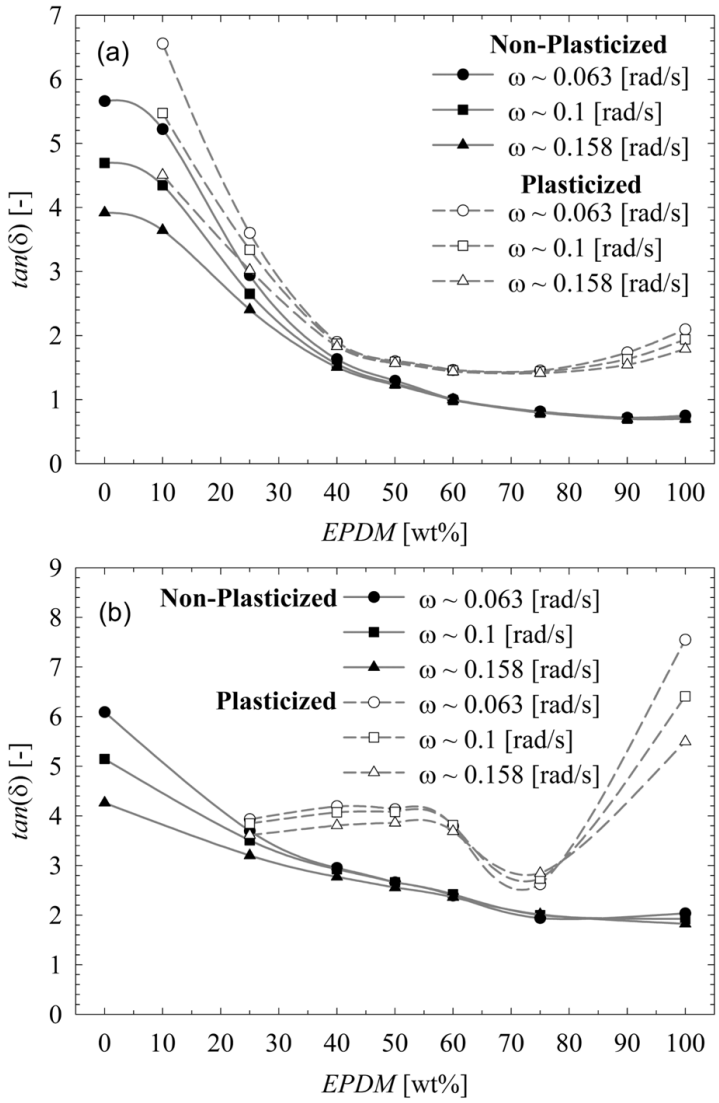

Figure 5.10. Loss tangent of non-plasticized and plasticized TPOs blended and characterized at 180°C: (a) E1/P1, (b) E2/P2. (Solid and dashed lines are guide lines)

For the plasticized TPOs, similarly to what was previously observed in the co-continuity interval measurements, the dual continuity range of the E1/P1-based TPOs begins at 40 wt% EPDM and extends up to ~75 wt%. The plasticization decreases the gap between the viscous and the elastic properties of the polymeric components, and consequently avoids the overcoming effect of the major elastomeric phase on the overall properties of the blend at low frequencies.

For the plasticized E2/P2 TPOs, the onset of a frequency independent region begins from a composition between 40 and 50 wt% EPDM and extends up to 75 wt% EPDM.

A summary of the co-continuity data obtained by different techniques is presented in Table 5.3. Among the rheology-based analyses, the loss tangent data leads to extensive information and reasonable agreement with the solvent extraction results. On the other hand, the use of the storage modulus data was mainly useful for the non-plasticized blends, along with the use of the Kerner model.

5.4.5 Semi-empirical Phase Inversion Modeling

During the last few decades, several empirical and semi-empirical models have been developed to predict the phase inversion composition and the co-continuity interval by employing the rheological properties of the constituent polymers. The majority of these models have been mainly constructed based on the viscosity ratio [21,46-55]. However, elasticity shall play a major role, especially in blends with large elasticity differences between the components [16,32,56]. Due to the semi-empirical nature of these models, they rely on experimental co-continuity data and in certain cases on prior morphological data [57]. Hence, they are not considered as predictive models.

The midpoint of the phase inversion composition obtained experimentally from solvent extraction (Table 5.3) as a function of their corresponding viscosity ratios (Table 5.2) are presented in Figure 5.11 along with the predictions of those semi-empirical models.

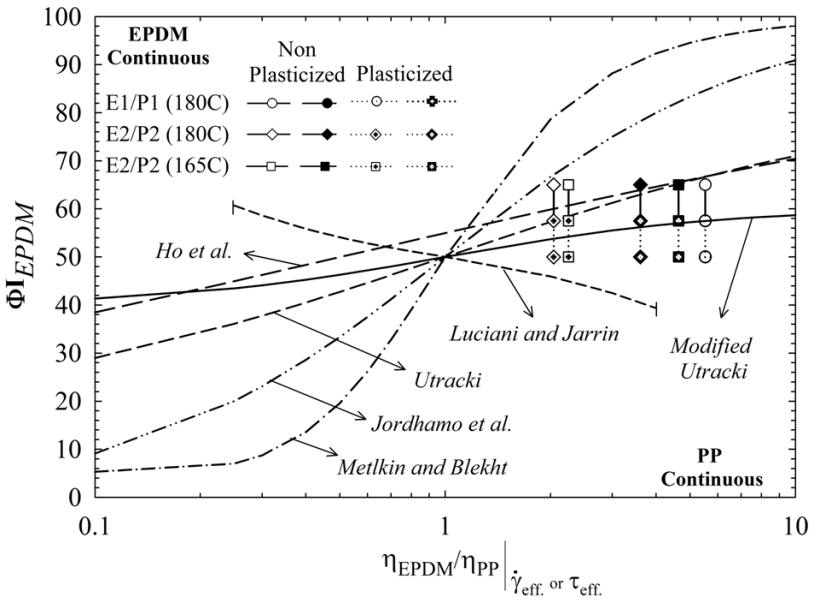

Figure 5.11. Phase inversion predictions for different viscosity based-models as well as the experimental mid-composition of phase inversion for non-plasticized and plasticized TPOs: Open symbols: at constant apparent shear rate, i.e. 50s^{-1}; Filled symbols: at constant matrix shear stress evaluated at 50s^{-1}.

The shear viscosity ratios were both evaluated at a constant apparent shear rate of the mixing equipment, i.e. 50 s^{-1} (open symbols), and at a constant matrix shear stress corresponding to the same apparent shear rate (filled symbols). Because the onset of the co-continuity for the low PP content could not be accurately defined (due to the lack of a selective solvent dissolving the PP), no single mid-composition could be defined for phase inversion. Therefore, the estimated experimental mid-composition of phase inversion is represented by vertical lines covering a composition range. As mentioned earlier, the experimental composition range of the co-continuity interval was not affected by the viscosity ratio, i.e. both E1/P1 and E2/P2 non-plasticized blends demonstrated an identical co-continuity interval. However, the plasticization narrowed the mentioned interval and, therefore, shifted the mid-composition of the phase inversion to lower EPDM content.

As seen in Figure 5.11, the viscosity ratio-based models predict a shift of the phase inversion point to low EPDM content below $\eta_{EPDM}/\eta_{PP} < 1$. On the other side of the viscosity ratio range, these models predict a large EPDM content for the phase inversion point. This tendency is in accordance with our experimental data, where the viscosity ratio is larger than unity and the phase inversion midpoint is in the range of 50 to 57.5 and 57.5 to 65 wt% EPDM in the case of the plasticized and the non-plasticized TPOs, respectively. Among the viscosity ratio-based models, the model of Metelkin and Blekht [54] overestimates the phase inversion composition. Their approach is, however, limited to viscosity ratios close to unity (i.e., iso-viscous components) [2,58]. On the other hand, the model presented by Utracki [53] yields the best agreement among the viscosity-based models, as previously reported for blends with viscosity ratio widely different from unity [58]. This model predicts both an upper and lower level for the phase inversion composition, depending on how the maximum packing density (Φ_m) is defined. Originally this value has been set based on homogeneously dispersed hard spheres, resulting in a maximum packing density of 84 vol% (i.e., the percolation threshold (Φ_c) is equal to 16 vol%). The percolation threshold for immiscible blends could reach a larger value due to the deformability and inhomogeneity of the phases. Accordingly, the Utracki model parameters were modified and the best fit was obtained by setting the percolation threshold (Φ_c) equal to 39.9 vol% (Figure 5.11). This mentioned value is equal to the onset of the co-continuity interval in the low EPDM content region of the continuity graph (Figure 5.3). Furthermore, this procedure resulted in a curve with a weak dependency on the viscosity ratio already observed by Utracki [53], Steinmann et al. [58] and Bhadane et al. [38].

Due to experimental difficulties in isolating the effect of elasticity and viscosity ratios for an immiscible blend, very limited experimental data are available in the literature explaining the

effect of the elasticity ratio on the phase inversion. Using the ratios of G' and/or $tan(\delta)$, Bourry and Favis [16] concluded that the more elastic component tends to encapsulate the less elastic one, forming the matrix phase. The experimental midpoint of the phase inversion (Table 5.3) as a function of their corresponding ratios of G' and $tan(\delta)$ (Table 5.2) are presented in Figure 5.12 along with the prediction of Bourry and Favis model. The overall trend of the model does not agree with the experimental data; the model underestimates the midpoint of the phase inversion, especially for the elasticity ratios defined by the storage modulus (G') at constant shear rate. Similarly to what was seen for the viscosity ratios, a plateau-like behavior is as well observed for the experimental data, with no sensitivity on the elasticity ratio. From Figure 5.12, one can notice that among the experimental data evaluated at a constant shear rate the best agreement is achieved by using the ratio of $tan(\delta)$ rather than that of the G'.

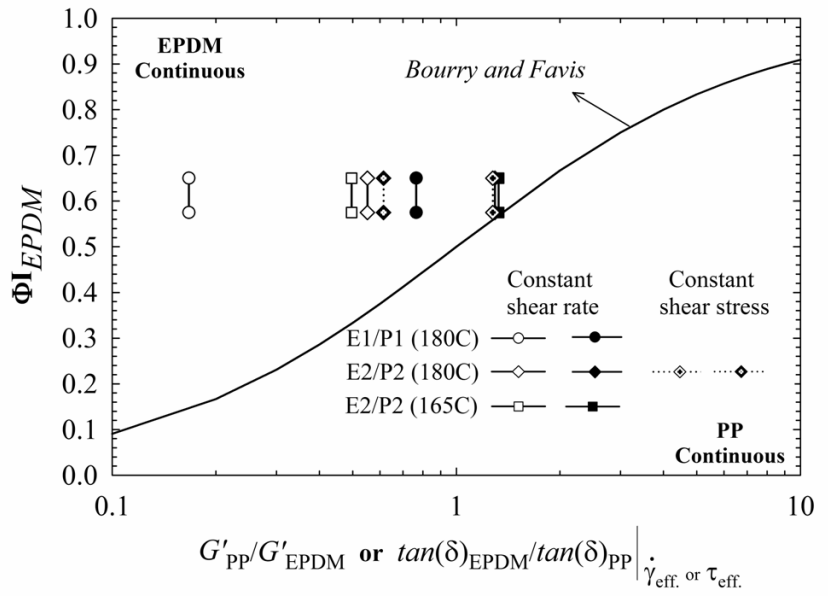

Figure 5.12. Experimental mid-composition of phase inversion for non-plasticized TPOs calculated at both constant apparent shear rate (non-crossed symbols) and shear stress (crossed symbols). (Open symbols: based on G´ ratio; Filled symbols: based on the tan(δ) ratio)

Therefore, we conclude that *tan*(δ), which incorporates both viscous and elastic contributions of an immiscible blend, provides a better agreement with the predictions of the Bourry and Favis model. The mentioned behavior has also been observed by Sarazin and Favis [59] and Prochazka et al. [60]. In contrast, the experimental G' ratio at constant matrix shear stress provides a better agreement with the Bourry and Favis model (Figure 5.12). Similar observations have been reported by Steinmann et al. [58]. In another study, Astruc and Navard [61] separated the effect of elasticity and viscosity ratios in a well defined polymeric system. The authors verified the effect of the elasticity ratio on the phase inversion composition by keeping a constant viscosity ratio. Based on their observations, the resultant steady-state morphology was not significantly influenced by the variation of the elasticity ratio and the best agreement with the model of Bourry and Favis was only achieved at high shear rates.

5.4.6 Micromechanical Modeling

Despite of the progression in viscoelastic modelling of emulsions in the last few decades, the majority of existing models are only capable of predicting the properties of dilute or semi-dilute emulsions [19]. To model the viscoelastic properties of co-continuous blends, one needs to incorporate the inter-connectivity of existing phases by assuming a proper length scale describing such morphologies. Accordingly, several modeling approaches have been proposed based on the pioneering work of Doi and Ohta [62] by incorporating the free energy of the interface deformation [20,63]. These models fail to describe the viscoelastic responses of low interfacial tension blends composed of components with relatively large viscosity and elasticity differences [13]. Recently, Sengers et al. [13] used a micro-mechanical model (Veenstra-D) originally proposed by Veenstra et al. [64] to describe the viscoelastic properties of plasticized PP/SEBS

blends in the co-continuous composition range. The same approach was used in this work to model the viscoelastic properties of the plasticized and non-plasticized E2/P2-based TPOs. The model considers a spatial arrangement of the two polymeric components in a unit cube with a dual inter-connectivity. As a result, the only parameters involved are the dynamic moduli and the weighted volume fractions of the constituent polymers. Moreover, if the total amount of the plasticizer in the blend is known, its distribution within each phase is unknown. This is generally described by the distribution coefficient K, which in this work is the ratio of the plasticizer content in the PP phase over that in the EPDM phase. Hence, $K = 0$ represents a blend where the plasticizer is entirely distributed in the elastomeric phase, whereas $K = \infty$ is the opposite case. By incorporating the distribution coefficient in the model, Sengers et al. [13] obtained the plasticizer distribution in both polymeric phases. The predicted storage moduli of the non-plasticized E2/P2 TPO at various compositions are shown in Figure 5.13. Since this model was originally developed for a co-continuous composition range, an acceptable prediction is obtained for 40 to 60 wt% EPDM.

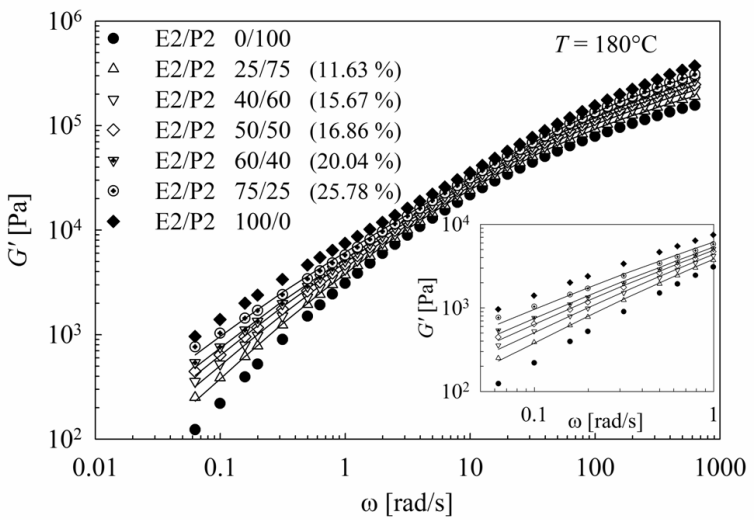

Figure 5.13. Storage modulus of non-plasticized E2/P2 TPOs (wt/wt%) blended and characterized at 180°C. (The values in parenthesis are the square root of the objective function used for data fitting and the solid lines represent the predictions of the Veenstra-D model)

In contrast to what has been reported in the literature, the same analysis does not lead to a satisfactory result for the plasticized blends as shown in Figure 5.14. Two extreme cases for the plasticized E2/P2 50/50 (wt/wt%) TPOs are illustrated. In Figure 5.14a, it is assumed that the plasticizer has been entirely distributed in the EPDM phase with a distribution coefficient of $K = 0$ while in Figure 5.14b the opposite scenario is used ($K = \infty$). In both cases the model predictions overestimate the storage moduli of the plasticized TPOs. The predicted storage modulus of the model always lies in between the storage moduli of the constituent polymers and, therefore, in none of these cases, the extent of plasticization of the constituent polymers is sufficient to obtain a suitable result.

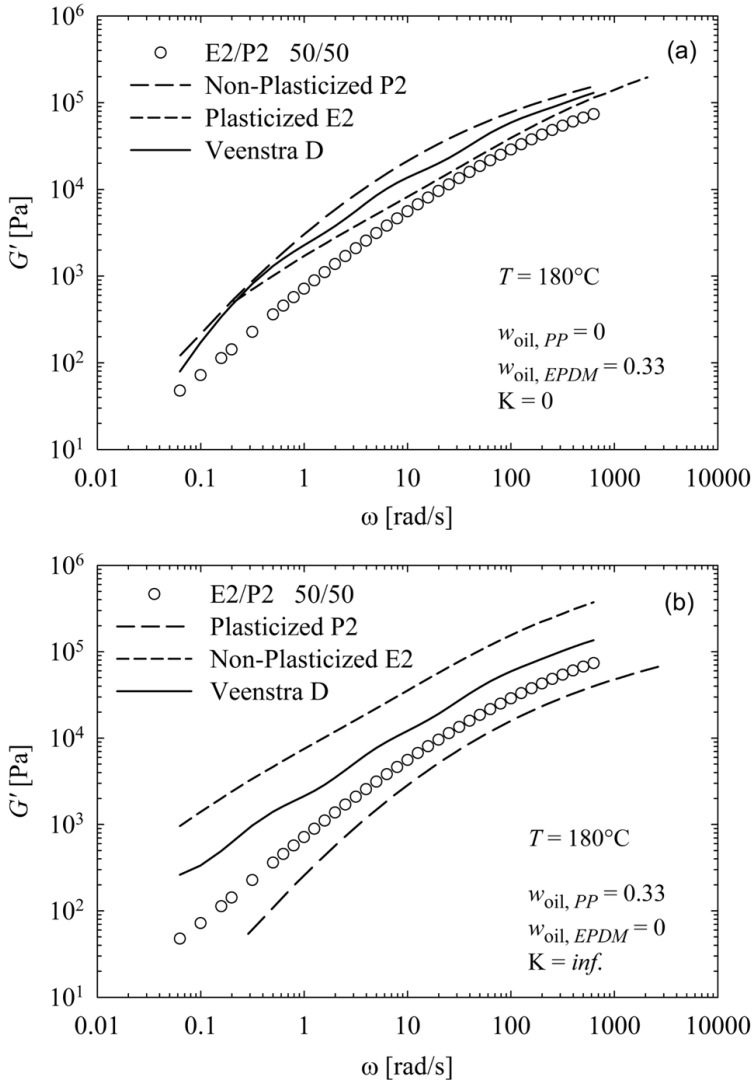

Figure 5.14. Storage modulus of plasticized E2/P2 50/50 (wt/wt%) blended and characterized at 180°C: (a) The plasticizer is distributed in EPDM, $w_{oil,PP}$ = 0 and $w_{oil,EPDM}$=0.33 (*K*=0); (b) The plasticizer is distributed in PP, $w_{oil,PP}$ = 0.33 and $w_{oil,EPDM}$=0 (*K*=inf.). (The dashed lines are the G´ data of neat polymeric components including the plasticization effect and the solid line represents the predictions of the Veenstra-D model)

Here we assume that upon heating, due to the entropic nature of the rubber elasticity, the elastomeric chains in their corresponding phase are retracted and possibly a certain amount of the plasticizer is desorbed. The desorbed plasticizer would diffuse and be absorbed in the molten

polyolefin. However, the diffusion process itself depends on the molecular weight of the polyolefin chains, the nature and the affinity with the plasticizer, the temperature, etc. As a result, a slow diffusion process might lead to a relatively thick plasticized interphase. The presence of a plasticized interphase could reduce the rheological properties of the interface and, consequently, the overall properties of the blend. Despite of the absence of any experimental proof, the discrepancies observed between the model predictions and the data may potentially be associated with the absence of a sharp interface.

5.5 Conclusions

In this work, the continuity development of two different EPDM/PP-based non-plasticized and plasticized TPOs was studied. The main purpose was to investigate the effect of a low molecular weight plasticizer on the morphology, especially on the co-continuity interval of these blends, and to associate the rheological response of these blends to their morphological features. The addition of a plasticizer was seen to decrease the viscoelastic proprieties of both constituent polymers and increase the interconnectivity of the elastomeric phase. Consequently, for all TPOs encountered in this work, the plasticization promoted the rapid percolation of the elastomeric component on the low EPDM side of the composition diagram, with an identical onset of the co-continuity as compared to their non-plasticized counterparts (at 40 wt% of EPDM). On the high EPDM content side, the plasticizer delayed the percolation of the semi-crystalline phase. Consequently, its presence reduced the co-continuity interval by ~15 compositional units. On the other hand, due to the relatively low interfacial tension between EPDM and PP (~ 0.3 mN/m), the interfacial excess elasticity was overshadowed by the elasticity of the elastomeric phase. Consequently, the variation of the low frequency storage modulus (G')

as a function of composition resulted in limited information on the co-continuity interval. The frequency independent loss tangent data (chemical gel approach) led to more extensive information and reasonable agreement with the solvent extraction results, in contrast to the storage modulus data, which were merely capable of detecting the end composition of the co-continuity interval in the plasticized TPOs. The results for both types of EPDM/PP blends were quite similar.

Furthermore, the mid-composition of the phase inversion was compared with the predictions of semi-empirical phase inversion models. Among the existing models, despite the large differences between the viscous and elastic properties of the constituent polymers, the viscosity ratio-based models predicting a plateau dependency of phase inversion composition were more appropriate. Accordingly, a limited viscosity ratio change could not dramatically alter the co-continuity interval. To model the viscoelastic properties of these TPOs, especially in the co-continuous composition range, a micro-mechanical model (Veenstra-D) was employed. A satisfactory prediction was obtained for the non-plasticized TPOs, whereas the model overestimated the viscoelastic properties of the plasticized blends. The failure of the model in predicting the viscoelastic properties of the plasticized TPOs was associated with the diffusion of the plasticizer and consequently the possible presence of a plasticized interphase.

5.6 References

1. D.R. Paul, and C.B. Bucknall, *Polymer blends*, Wiley, New York (2000).

2. P. Potschke, and D.R. Paul, *J. Macromol. Sci., Polym. Rev.*, **43(1)**, 87-141 (2003).

3. C.H. Lei, X.B. Huang, and F.Z. Ma, *Polym. Adv. Technol.*, **18(12)**, 999-1003 (2007).

4. S. Sabet-Abdou, and M.A. Fath, U.S. Patent, 4,311,628 (1982).

5. T. Abraham, K.-S. Shen, and N.G. Barber, U.S. Patent, 7,276,559 (2007).

6. G. Holden, *Understanding thermoplastic elastomers*, Hanser Gardner Pub., Inc., Cincinnati (2000).

7. T. Abraham, and N.G. Barber, U.S. Patent, 7,504,458 (2009).

8. M.D. Ellul, *Rubber Chem. Technol.*, **71(2)**, 244-276 (1998).

9. R. Winters, J. Lugtenburg, V.M. Litvinov, M. van Duin, and H.J.M. de Groot, *Polymer*, **42(24)**, 9745-9752 (2001).

10. K. Jayaraman, V.G. Kolli, S.-Y. Kang, S. Kumar, and M.D. Ellul, *J. Appl. Polym. Sci.*, **93(1)**, 113-121 (2004).

11. W.G.F. Sengers, M. Wubbenhorst, S.J. Picken, and A.D. Gotsis, *Polymer*, **46(17)**, 6391-6401 (2005).

12. T. Abraham, N.G. Barber, and M.P. Mallamaci, *Rubber Chem. Technol.*, **80(2)**, 324-339 (2007).

13. W.G.F. Sengers, P. Sengupta, J.W.M. Noordermeer, S.J. Picken, and A.D. Gotsis, *Polymer*, **45(26)**, 8881-8891 (2004).

14. J.M. Li, P.L. Ma, and B.D. Favis, *Macromolecules*, **35(6)**, 2005-2016 (2002).

15. P.A. Bhadane, M.F. Champagne, M.A. Huneault, F. Tofan, and B.D. Favis, *Polymer*, **47(8)**, 2760-2771 (2006).

16. D. Bourry, and B.D. Favis, *J. Polym. Sci., Part B: Polym. Phys.*, **36(11)**, 1889-1899 (1998).

17. N. Mekhilef, P.J. Carreau, B.D. Favis, P. Martin, and A. Ouhlal, *J. Polym. Sci., Part B: Polym. Phys.*, **38(10)**, 1359-1368 (2000).

18. J.A. Galloway, and C.W. Macosko, *Polym. Eng. Sci.*, **44(4)**, 714-727 (2004).

19. C.L. Tucker, and P. Moldenaers, *Annu. Rev. Fluid Mech.*, **34**, 177-210 (2002).

20. M. Castro, C. Carrot, and F. Prochazka, *Polymer*, **45(12)**, 4095-4104 (2004).

21. S. Steinmann, W. Gronski, and C. Friedrich, *Rheol. Acta*, **41(1-2)**, 77-86 (2002).

22. M. Bousmina, A. Ait-Kadi, and J.B. Faisant, *J. Rheol.*, **43(2)**, 415-433 (1999).

23. J.A. Galloway, K.J. Koester, B.J. Paasch, and C.W. Macosko, *Polymer*, **45(2)**, 423-428 (2004).

24. W.P. Cox, and E.H. Merz, *J. Polym. Sci.*, **28**, 619-622 (1958).

25. O. Chung, and A.Y. Coran, *Rubber Chem. Technol.*, **70(5)**, 781-797 (1997).

26. A.S. Michaels, W.R. Vieth, and H.H. Alcalay, *J. Appl. Polym. Sci.*, **12(7)**, 1621-1624 (1968).

27. R. Guo, A.G. Talma, R.N. Datta, W.K. Dierkes, and J.W.M. Noordermeer, *Eur. Polym. J.*, **44(11)**, 3890-3893 (2008).

28. G. Wypych, *Handbook of plasticizers*, ChemTec Pub. - William Andrew Pub., Toronto - New York (2004).

29. S. Chaput, C. Carrot, M. Castro, and F. Prochazka, *Rheol. Acta*, **43(5)**, 417-426 (2004).

30. J. Reignier, B.D. Favis, and M.C. Heuzey, *Polymer*, **44(1)**, 49-59 (2003).

31. P. Van Puyvelde, and P. Moldenaers, "Rheology-Morphology Relationships in Immiscible Polymer Blends", C. Harrats, S. Thomas, and G. Groeninckx, In: *Micro- and nanostructured polymer blend systems: phase morphology and interfaces*, CRC/Taylor & Francis, (2006).

32. H. Van Oene, *J. Colloid Interface Sci.*, **40(3)**, 448-467 (1972).

33. C. Tufano, G.W.M. Peters, P. van Puyvelde, and H.E.H. Meijer, *J. Colloid Interface Sci.*, **328(1)**, 48-57 (2008).

34. M. Hemmati, H. Nazokdast, and H.S. Panahi, *J. Appl. Polym. Sci.*, **82(5)**, 1129-1137 (2001).

35. H. Shariatpanahi, H. Nazokdast, B. Dabir, K. Sadaghiani, and M. Hemmati, *J. Appl. Polym. Sci.*, **86(12)**, 3148-3159 (2002).

36. S. Tomotika, *Proc. R. Soc. London, A*, **150**, 322-337 (1935).

37. L.E. Nielsen, *Rheol. Acta*, **13(1)**, 594-600 (1974).

38. P.A. Bhadane, M.F. Champagne, M.A. Huneault, F. Tofan, and B.D. Favis, *J. Polym. Sci., Part B: Polym. Phys.*, **44(14)**, 1919-1929 (2006).

39. J.A. Galloway, M.D. Montminy, and C.W. Macosko, *Polymer*, **43(17)**, 4715-4722 (2002).

40. J. Peon, J.F. Vega, B. Del Amo, and J. Martinez-Salazar, *Polymer*, **44(10)**, 2911-2918 (2003).

41. T.S. Omonov, C. Harrats, P. Moldenaers, and G. Groeninckx, *Polymer*, **48(20)**, 5917-5927 (2007).

42. J. Portal, C. Carrot, J.C. Majeste, S. Cocard, V. Pelissier, K. Baran, and I. Anselme-Bertrand, *Polym. Eng. Sci.*, **48(6)**, 1068-1076 (2008).

43. E.H. Kerner, *Proc. R. Soc. London, A*, **69**, 808-813 (1956).

44. M. Castro, F. Prochazka, and C. Carrot, *J. Rheol.*, **49(1)**, 149-160 (2005).

45. R. Muller, E. Gerard, P. Dugand, P. Rempp, and Y. Gnanou, *Macromolecules*, **24(6)**, 1321-1326 (1991).

46. G.N. Avgeropoulos, F.C. Weissert, P.H. Biddison, and G.G.A. Boehm, *Rubber Chem. Technol.*, **49(1)**, 93-104 (1976).

47. D.R. Paul, and J.W. Barlow, *J. Macromol. Sci., Rev. Macromol. Chem.*, **C18(1)**, 109-168 (1980).

48. G.M. Jordhamo, J.A. Manson, and L.H. Sperling, *Polym. Eng. Sci.*, **26(8)**, 517-524 (1986).

49. I.S. Miles, and A. Zurek, *Polym. Eng. Sci.*, **28(12)**, 796-805 (1988).

50. V. Everaert, L. Aerts, and G. Groeninckx, *Polymer*, **40(24)**, 6627-6644 (1999).

51. R.M. Ho, C.H. Wu, and A.C. Su, *Polym. Eng. Sci.*, **30(9)**, 511-518 (1990).

52. N. Kitayama, H. Keskkula, and D.R. Paul, *Polymer*, **41(22)**, 8041-8052 (2000).

53. L.A. Utracki, *J. Rheol.*, **35(8)**, 1615-1637 (1991).

54. V.I. Metelkin, and V.S. Blekht, *Kolloidn. Zh.*, **46(3)**, 476-480 (1984).

55. A. Luciani, and J. Jarrin, *Polym. Eng. Sci.*, **36(12)**, 1619-1626 (1996).

56. L.A. Utracki, "Analysis of Polymer Blends by Rheological Techniques", M.A. Kohudic, In: *Advances in Polymer Blends and Alloys Technology, Vol. 1*, (1988).

57. R.C. Willemse, A.P. De Boer, J. Van Dam, and A.D. Gotsis, *Polymer*, **39(24)**, 5879-5887 (1998).

58. S. Steinmann, W. Gronski, and C. Friedrich, *Polymer*, **42(15)**, 6619-6629 (2001).

59. P. Sarazin, and B.D. Favis, *Biomacromolecules*, **4(6)**, 1669-1679 (2003).

60. F. Prochazka, R. Dima, J.C. Majeste, and C. Carrot, *E Polymer*, **(040)** (2003).

61. M. Astruc, and P. Navard, *Macromol. Symp.*, **149**, 81-85 (2000).

62. M. Doi, and T. Ohta, *J. Chem. Phys.*, **95(2)**, 1242-1248 (1991).

63. H.M. Lee, and O.O. Park, *J. Rheol.*, **38(5)**, 1405-1425 (1994).

64. H. Veenstra, P.C.J. Verkooijen, B.J.J. van Lent, J. van Dam, A.P. de Boer, and A. Nijhof, *Polymer*, **41(5)**, 1817-1826 (2000).

CHAPTER 6

MORPHOLOGY AND RHEOLOGY OF NON-REACTIVE AND REACTIVE EPDM/PP BLENDS IN TRANSIENT SHEAR FLOW: PLASTICIZED VS. NON-PLASTICIZED BLENDS

S. Shahbikian,[1] P.J. Carreau,[1*] M.-C. Heuzey,[1] M. D. Ellul,[2] H. P. Nadella[3], J. Cheng,[3] P. Shirodkar[3]

[1] Center for Applied Research on Polymers and Composites (CREPEC), Department of Chemical Engineering, École Polytechnique de Montréal, Quebec H3T 1J4, Canada

[2] ExxonMobil Chemical Co., Global Specialty Polymers Technology, Akron, Ohio 44311, USA

[3] ExxonMobil Chemical Co., Global Specialty Polymers Technology, Baytown, Texas 77520, USA

*Corresponding author: pierre.carreau@polymtl.ca

Submitted to "*Rubber Chemistry and Technology*".

6.1 Abstract

In this work, non-plasticized and plasticized EPDM/PP (ethylene-propylene-diene-terpolymer/polypropylene) based thermoplastic elastomers (TPEs) were prepared in the presence and absence of a curing system (i.e., reactive vs. non-reactive TPEs). The non-linear viscoelastic behavior and morphology evolution of these blends were investigated through single and multiple start-up transient experiments to find out the effects of composition, plasticizer and the presence of the curing system in a homogeneous shear flow field. Due to the highly elastic nature of the elastomeric component, the shear rate was set to 0.1 s^{-1} and in the case of multiple start-up experiments a 10 min rest time was set between consecutive shearing cycles. The specific interfacial areas (Q) of TPEs were analyzed prior to and after shearing and subsequently correlated to the corresponding rheological response of these blends. The magnitude and the width of the stress overshoot were correlated to the morphology of the blends, elastomer content, the presence of plasticizer and curing system. The presence of a plasticizer (paraffinic oil) drastically decreased the viscosity and elasticity of both neat polymers and consequently the resulting TPEs, and it further reduced the initial curing rate of the elastomeric component at the early shearing stage of the reactive TPEs. Moreover, the plasticization promoted swelling and coalescence enlarging the size of the polymeric domains and decreasing the specific interfacial area. Furthermore, the insitu curing reaction in the reactive TPE blends resulted in less elongated polymeric domains with an irregular and larger interface compared to non-reactive blends. A Phase inverted morphology has also been observed for non-plasticized high elastomer content reactive TPEs sheared for long periods. The obtained experimental morphology data of the non-reactive blends subjected to multiple start-up experiments was fairly well predicted using a phenomenological model proposed by Lee and Park (J. Rheo. 38(5), 1994).

6.2 Introduction

Blending technology provides a flexible and accessible route towards the production of new, high performance and in certain cases lower cost polymeric materials.[1] Depending on the final application, different polymeric pairs can be blended, tailoring the desired properties. Among different commonly used polymers, blending of an elastomer with a semi-crystalline thermoplastic polymer results in blends known as thermoplastic elastomers (TPEs).[2] They possess rubber like properties with processability identical to conventional thermoplastic polymers. Along with the polymeric components in TPEs, it is a common practice to incorporate a low molecular weight plasticizer (processing oil) to reduce the hardness and to improve the processability of these materials.[3, 4] Plasticizers chosen for this purpose usually have small polarity differences with the polymeric components and are entirely mixed and distributed in the polymeric constituents, swelling them during the melt mixing stage.[3-6] However, upon cooling, due to crystallization of the semi-crystalline thermoplastic, the plasticizer is redistributed and predominantly absorbed by the elastomeric component with a limited content residing in the amorphous region of the thermoplastic phase.[6] The distribution of oil in the melt stage and its redistribution upon cooling affects the rheological properties in the liquid state and the microstructure, physical and mechanical properties in the solid state.[3, 6-9]

Regardless of composition and plasticization, due to the high molecular weight of polymeric components and the consequent thermodynamic limitations, the outcome of the mixing process of most polymeric materials is an immiscible blend with a complex morphology.[10] It is known that numerous factors, such as composition, interfacial tension, rheological properties of the constituent polymers, the presence of low molecular weight additives and modifiers, thermal

history, flow and deformation field govern the mentioned complex morphology evolution of these blends.[11] On the other hand, the final properties of these blends such as rheological, physical, chemical and mechanical properties to large extent depend on their morphology and micro-structure represented by the size, shape and distribution of one phase into another.[10] As a result, a strong and complex, however, still mysterious relationship exists between the rheology and morphology of immiscible polymer blends, knowledge of which would be essential for the optimization of blending processes.

The rheological behavior of immiscible polymer blends can be generally evaluated by means of their linear and non-linear viscoelastic responses, each of those providing essential information on the micro-structure evolution and final morphology. Probing the linear viscoelastic behavior, by imposing a small amplitude strain solicitation results in a stress response linear in strain.[12] Dynamic rheological measurements performed in the linear viscoelastic range fully satisfy this requirement. In such a condition, it has been known that the state of morphology remains unchanged especially in the case of stable low interfacial tension blends.[13] Furthermore, key information such as average droplet size and interfacial tension in the case of dilute and semi-dilute emulsions, and co-continuity interval in the case of concentrated emulsions could be obtained through the use of a suitable rheological constitutive equation.

On the other hand, in non-linear rheological measurements, depending on the type and intensity of the flow field, the microstructure of an immiscible emulsion undergoes a dynamic and continuous evolution comprising deformation, orientation, disintegration or breakup and coalescence up to a new steady state morphology. The initial morphology state of emulsions along with the occurrence of the mentioned phenomena results in a specific stress response. Accordingly, the mentioned transient flows are sensitive to morphology and can be used to probe the morphology evolution in immiscible emulsions. Hence the non-linear viscoelastic behavior of

immiscible blends is of scientific as well as technological interest.[13, 14] However, the description of the dynamics involved during the morphology evolution could only be expressed through highly non-linear, complex time-dependent constitutive equations.

After the Taylor pioneering work on the deformation of a single Newtonian droplet in a Newtonian medium,[15, 16] several theoretical models have been developed to relate the morphology/rheology of emulsions in the low deformation range and in the dilute and semi-dilute regimes (up to approximately 15 vol%).[17-21] On the other hand, a theory of concentrated emulsions subjected to higher order of deformation was originally proposed by Doi and Ohta,[22] describing the time evolution of complex interfaces. The authors used an anisotropy tensor (**q**) to express the orientation of the interface,[23] and a scalar (Q) quantifying the overall interfacial area per unit volume (specific interfacial area) of the interface. The dynamics of morphology evolution, i.e. orientation, coalescence and breakup of the interface, were expressed by separate kinetic equations. This approach has already been employed in several studies and few modifications have been proposed to improve the predictions.[24-28]

In this work, the effects of composition, plasticizer and the presence of a curing agent on the rheological properties and morphology evolution of non-plasticized and plasticized EPDM/PP TPEs under various transient shear flows such as single and multiple-step stress growths have been studied. The morphology evolution of these blends was tracked analyzing the specific interfacial areas (Q), and a semi-phenomenological kinetic model originally proposed by Lee and Park[28] was employed to predict the morphology evolution of non-reactive TPE blends under multiple start-up experiments.

6.3 Experimental

6.3.1 Materials

In this work, an ethylene-propylene-diene-terpolymer (EPDM) and a polypropylene (PP) random co-polymer both provided by ExxonMobil Chemical Co. were used as elastomeric and semi-crystalline polyolefin polymeric components, respectively. The nomenclatures and the key properties of these polymeric components are given in Table 6.1. The investigated blending systems were composed of: non-reactive and reactive both non-plasticized and plasticized EPDM/PP TPE blends. Different EPDM/PP (wt/wt%) compositions were studied: 25/75, 40/60, 50/50, 60/40, 75/25 and 40/60, 50/50, 60/40 for non-reactive and reactive blends, respectively. In the case of plasticized blends, 100 phr paraffinic oil (based on elastomer content) was used. Furthermore, in order to prepare the reactive precursor TPE blends, 5 phr (based on elastomer content) phenolic resin (SP-1045) was added. An antioxidant, Irganox® B-225, (1 wt% based on the weight of EPDM + PP) was used for all blending systems to prevent the thermal degradation of the polymeric components during the melt mixing stage.

Table 6.1. Characteristics of the neat polymeric components

Polymer	Symbol	MFI, dg/60 s (ASTM D-1238)	Mooney Viscosity (ML 1+4, @ 125°C)	T_m, °C	ENB[a], wt%	C_2[b], wt%
EPDM	E	-	25	-	4.7	57.5
PP (RCP)[c]	P	3	-	141	-	4

[a] Ethylidene norbornene.

[b] Ethylene content.

[c] Polypropylene (random co-polymer).

6.3.2 Melt Mixing

The melt mixing was carried out using a small scale laboratory internal mixer (Brabender® Plasti-corder® equipped with 30 mL chamber) at 165°C and 100 rpm for 12 min. The mentioned rotor speed corresponds to an apparent shear rate of ~50 s^{-1}.[29] The temperature was high enough to melt process the polyolefin component (PP), but low enough to reduce the extent of cross-linking of the elastomeric phase in the reactive TPE blends throughout the mixing stage. In the case of plasticized blends, the total amount of plasticizer was added during the first 8 min of the mixing process. For the reactive non-plasticized/plasticized TPEs, the curing agent (phenolic resin) was added at the latest mixing stage (last 4 min) and the mixing torque was monitored to insure the prevention of excessive cross-linking reaction at this stage. To prevent the thermal degradation of the polymeric components, the mixing process was carried out under nitrogen atmosphere. Subsequently, at the end of the mixing process, the blends were immediately quenched in liquid nitrogen to freeze the morphology and to instantly stop any ongoing cross-linking reaction in reactive blends.

6.3.3 Rheological Measurements

For rheological characterization, the blends were compression molded at 165°C in the form of 25 mm diameter disks with ~1.5 mm thickness. The hot molding cycle was minimized to 4 min to insure the least amount of possible static curing during this step in the reactive blends. Time sweep and frequency sweep experiments were carried out in the linear viscoelastic range using a stress controlled rheometer (TA Instruments® AR2000) with parallel plate geometry under nitrogen atmosphere at 165°C and 180°C to characterize the thermal stability and overall rheological properties of the pure polymeric components as well as the non-reactive blends. The

curing behaviour of non-plasticized/plasticized EPDM containing 5 phr phenolic resin was investigated using a stress-controlled rheometer (Physica MCR 501, Anton Paar) by time sweep experiment at 10.43 rad/s (frequency stated in ASTM-D2084 for vulcanization of rubbery materials using Oscillatory disk cure meter)[30] with a strain $\gamma \leq 0.1$ and in the temperature range between 135°C and 180°C (with 15°C intervals).

The morphology evolution of non-reactive and insitu reactive blends was studied under well defined start-up (stress growth) transient shear flows in the stress-controlled rheometer (Physica MCR-501, Anton Paar) using a parallel plate geometry. Initially various shear rates and flow histories were investigated on the pure polymeric components to obtain the optimum conditions to avoid the ejection of polymeric components during the experiments. As a result, the optimum shear rate was fixed at 0.1 s^{-1}.

Non-reactive blends were exposed to two different sets of start-up experiments: single and multiple steps (forward and reverse) at 165°C. Single step experiment consisted of 450 s at 0.1 s^{-1} and the multiple steps consisted of 450 s clockwise (1^{st} *CW*), 10 min rest, 450 s counter-clockwise (*CCW*), 10 min rest and eventually 450 s clockwise (2^{nd} *CW*), all at 0.1 s^{-1}. The multiple step start-up experiments were performed to observe the effect of relaxation and reverse flow on the rheological behavior and morphology development of these TPEs. To minimize the shear history of the polymeric components on the rheological response of these blends, a rest period was indispensable between each consecutive shearing step. As a result, different rest periods between 0 to 10 min. were tested during preliminary experiments on the neat polymeric components, and 10 min. rest time was chosen as a sufficient period assuring both polymeric phases were adequately relaxed.

On the other hand, due to the reactive nature of the reactive TPEs, no rest time and consequently no multiple start-up experiments were performed and these blends were only

exposed to single step start-up experiments with different durations: 450 s, 2700 s and 7200 s at 0.1 s^{-1} and 165°C. To verify the effect of temperature and consequently the curing rate on the morphology evolution, the reactive blends were also tested at 180°C for 2700 s.

At the end of each transient experiment, the temperature was set to 25°C and the sample was rapidly quenched inside the rheometer using air-jet to freeze the morphology. In the absence of air-jet, the cooling rate of testing environment (Peltier) alone was ~52 °C/min. Therefore, the combination of air-jet and the cooling capacity of the testing environment was largely sufficient to rapidly quench and freeze the morphology inside the rheometer.

6.3.4 Morphological Analyses

To study the microstructure evolution during start-up experiments in both non-reactive and reactive blends, the morphology was examined in the flow direction, i.e., in a plane perpendicular to the radial direction. Due to the end effects, secondary flows and high curvature at the plate center and at the edge, all samples were cut at 3/4 of disk radius, and the middle section of this area was cryo-microtomed at -150°C~-170°C using a Leica® RM 2165 equipped with Leica® LN 21 cryo-chamber.[31] The atomic force microscope (AFM) imaging was performed on the cryo-microtomed sections using a DimensionTM 3100 from Veeco Instruments in tapping mode. The experiments were carried out under ambient conditions using scanning rate of ~0.3-0.7 (Hz), integral gain of ~0.3-0.7 and proportional gain of ~0.6-1.4. The height, phase and amplitude channels were recorded. Subsequently, due to the intrinsic large difference between the viscoelastic properties of EPDM and PP at room temperature, the phase images were used for subsequent morphological analyses. A semi-automatic technique consisting of a digitalizing table and image analysis software (SigmaScan Pro Ver.5) was employed to trace the interface between

polymeric phases. Accordingly, the measured interface representing the perimeter between the two polymeric phases was divided by the area of the micrograph to obtain the specific interfacial perimeter (B_A). To do so, between three to four AFM micrographs with various scan sizes ranging between 10 to 25 μm were employed. The specific interfacial perimeters obtained from each of those micrographs were further used to calculate the specific interfacial area or the average interfacial area per unit volume (Q) of the blends:[32]

$$Q = \frac{4B_A}{\pi} \tag{6.1}$$

the calculated specific interfacial area holds for any cross-sectional orientation of imaged photos and for any type of non-lamellar morphology.[33]

6.4 Results and Discussion

6.4.1 Dynamic Rheological Measurements

Prior to conducting any experiments, the thermal stability of un-processed and processed neat polymeric components was verified. The polymeric materials were thermally stable. In Figure 6.1, the complex viscosity and the storage modulus of the neat polymeric constituents are shown at 165°C and 180°C, respectively. Both polymeric components (PP and EPDM) do not reach the terminal zone where G' is proportional to ω^2.

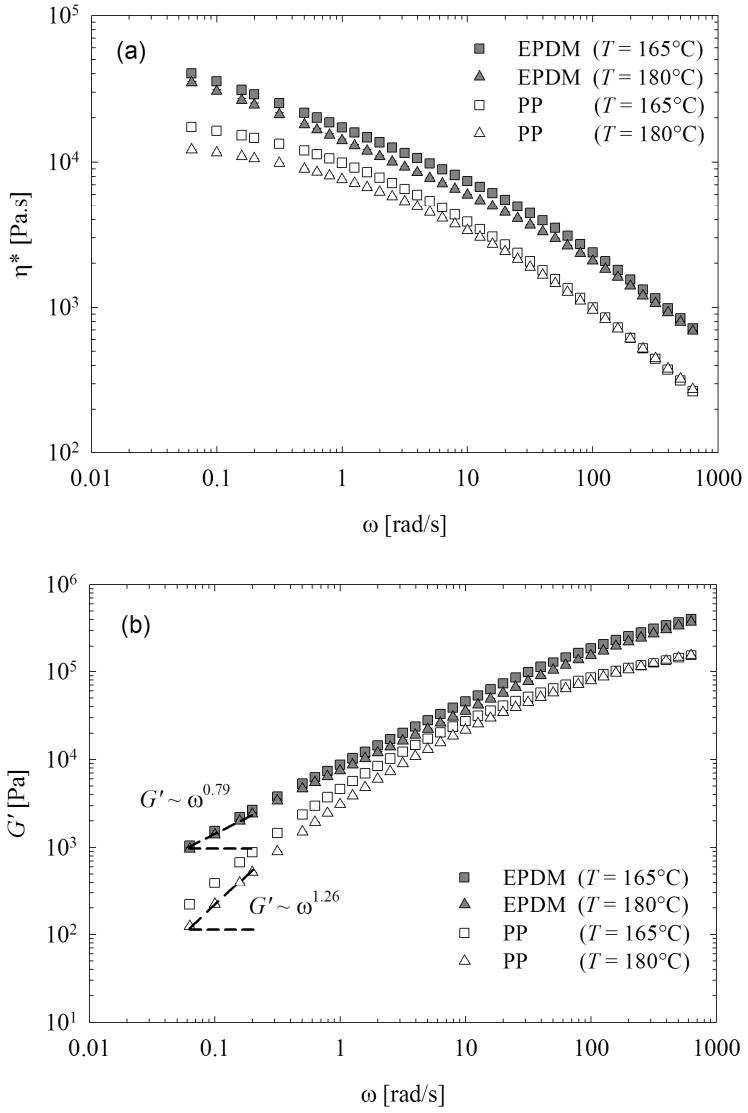

Figure 6.1. Rheological properties of pure polymeric components as a function of frequency: (a) Complex viscosity (η^*), (b) Storage modulus (G').

However, the storage modulus and complex viscosity of PP compared to EPDM exhibit a classical viscoelastic behavior with a tendency to reach the terminal zone at low frequencies, with G' being proportional to $\omega^{1.26}$ (Figure 6.1). In the same frequency range, the complex viscosity (η^*) exhibits the tendency towards a typical Newtonian plateau. At each designated temperature, the EPDM is more viscous and elastic compared to the PP. Furthermore, the increase in

temperature does not significantly change the viscoelastic properties of the polymeric components, especially in the high frequency range. Assuming the Cox-Merz[34] relation to be valid for the neat polymeric components,[35] the frequency data can be interpreted as the results obtained from steady shear experiments. Therefore, regardless of the temperature, the rheological property ratios, e.g. viscosity ratio (η_{EPDM}/η_{PP}), of the mentioned polymeric pairs at processing condition (50 s^{-1}) is larger than unity (Table 6.2).

Table 6.2. Rheological properties at different conditions

T, °C	Shear rate, s^{-1}	Phases		η_d/η_m [c]
		Matrix	Dispersed	
165	50 [a]	E	P	0.44
		P	E	2.25
165 & 180	0.1	E	P	0.46
		P	E	2.17
165 & 180	0.075 [b]	E	P	0.44
		P	E	2.27

[a] Apparent mixing shear rate inside the internal mixer.

[b] Shear rate at ¾ of the rim of the parallel plate geometry.

[c] In the absence of plasticizer (η_d: the viscosity of dispersed phase, η_m: the viscosity of matrix phase).

As a result, the EPDM can be considered less deformable than the PP throughout the whole range of frequency or shear rate. To reduce the difference between the rheological properties of the pure polymeric components and to improve the processability of the elastomeric phase, a proper plasticizer is usually employed during the melt processing step. During the melt mixing stage, the plasticizer is distributed in both polymeric phases and reduces the viscoelastic properties of the neat polymeric components and their corresponding blends. Consequently, this might affect the viscoelastic properties and morphology of the plasticized TPEs in comparison to

the non-plasticized ones. The complex viscosity data of different non-plasticized/plasticized non-reactive TPEs at 165°C are shown in Figure 6.2. Compared to the neat PP, in the non-plasticized blends the complex viscosity increases with the elastomer content while the tendency to reach the terminal zone decreases with no significant viscosity overlap (Figure 6.2a). On the other hand, the presence of a plasticizer results in a considerable change in the rheological behaviour of the blends. Figures 6.2b shows that the complex viscosity decreases in the presence of plasticized elastomer and, therefore, throughout the whole frequency range, the complex viscosity of the TPEs decreases with EPDM content.

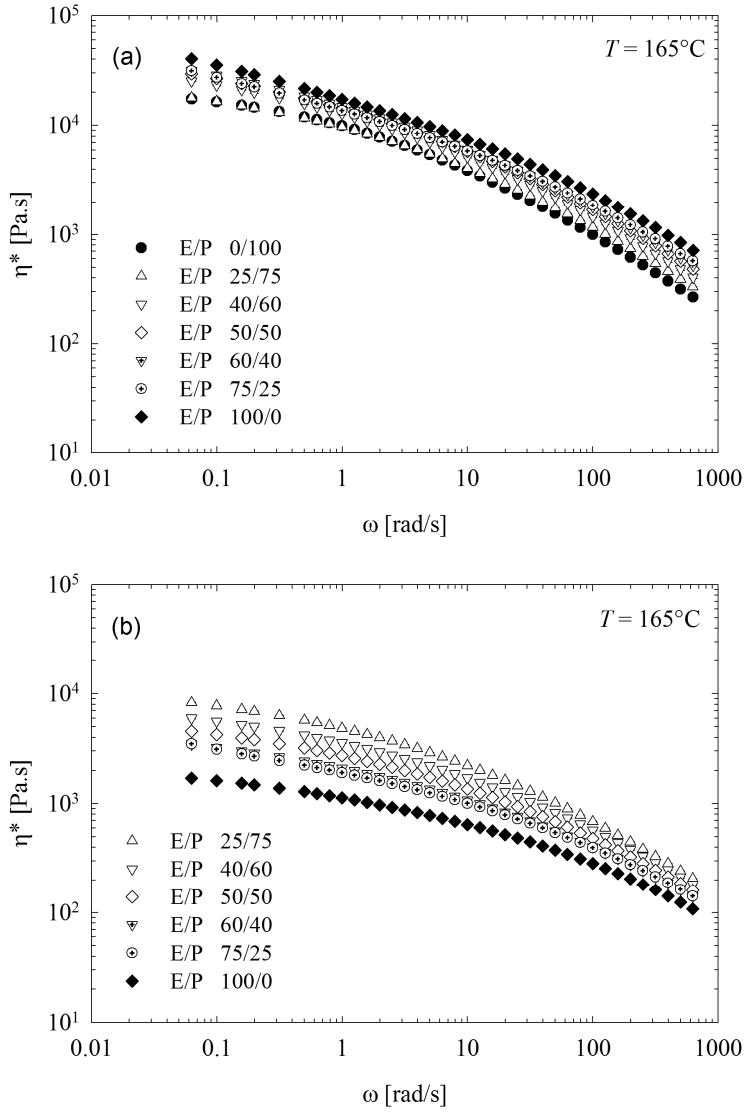

Figure 6.2. Complex viscosity data of non-reactive E/P (wt/wt%) TPEs at 165°C: (a) Non-plasticized, (b) Plasticized.

In a previous work done in our laboratory, the effect of plasticizer on the viscoelastic properties and morphology of the non-reactive TPE blends was investigated and coarser blend morphology with more coalesced plasticized elastomeric domains was observed in the presence of plasticizer. Furthermore, since the amount of the plasticizer was based on the elastomeric component, the blends with larger EPDM content contained a larger amount of plasticizer and,

therefore, the overall viscoelastic properties were mainly influenced by the coalesced plasticized elastomeric domains, resulting in an inverse viscosity trend.

6.4.2 Curing Behavior of Non-Plasticized and Plasticized EPDM

Different methods such as chemical, rheological or thermal (by means of differential scanning calorimetry) can be used to characterize the curing behaviour of an elastomer. In this work, the curing behavior of non-plasticized/plasticized EPDM has been mainly characterized by a rheological method. The aim was to investigate the effect of the plasticizer on the curing behavior of the EPDM. During the curing reaction, a three dimensional network of chemically cross-linked chains is usually obtained. The formation of such three dimensional network reduces the mobility of the polymeric chains resulting in increased viscosity and elasticity. To obtain comparable results between the non-plasticized and plasticized EPDM, the linear viscoelastic properties were normalized by their non-reactive counterparts. This approach has been previously employed to obtain the curing kinetics of ethylene vinyl acetate (EVA) and ethylene methyl acrylate (EMA).[36] Generally, the linear viscoelastic properties such as η^*, G' and G'' for a thermally stable non-reactive elastomer are time independent and could be referred as η^*_{NR}, G'_{NR} and G''_{NR} (*NR*: non-reactive). Therefore, prior to curing, the ratio of any viscoelastic property to its corresponding non-reactive counterpart shall be equal to one. Values larger than one would indicate that a slight cross-linking had already occurred prior to the rheological characterization (especially during mixing stage); whereas values lower than unity might indicate a plasticization effect of the molten curing system prior to the cross-linking reaction. The normalized storage modulus of non-plasticized/plasticized EPDM at various temperatures is shown in Figure 6.3.

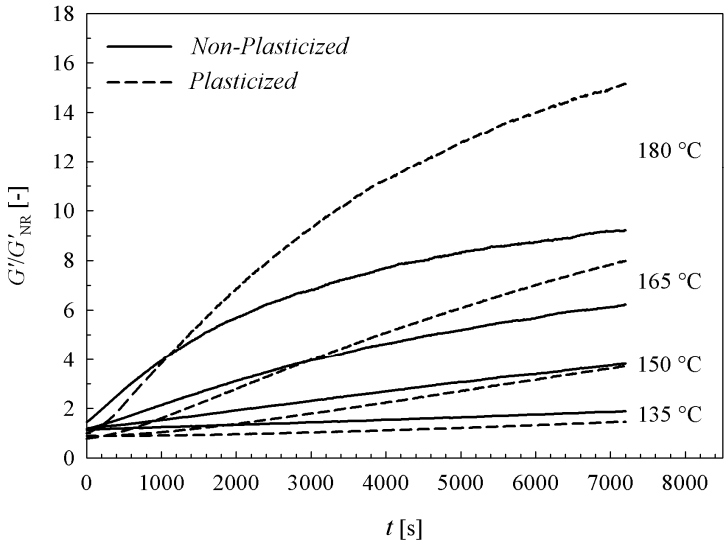

Figure 6.3. The evolution of storage modulus during cross-linking reaction of non-plasticized/plasticized EPDM at various temperatures.

Regardless of plasticization, the increase in temperature results in a faster curing reaction manifested by a rapid rise of the viscoelastic properties. At low temperatures (e.g., the lowest temperature in this case 135°C), the storage modulus of the plasticized EPDM is lower than the non-plasticized elastomer throughout the whole curing period (i.e. 7200 s) indicating the plasticization effect of the curing agent at low temperatures. By increasing the temperature, the normalized storage modulus of the plasticized EPDM exceeds the non-plasticized one after an initial delay. The mentioned delay could not be observed if the viscoelastic data were normalized based on their initial value at the beginning of curing reaction (G'_0). Furthermore, this can also be shown by the conventional gelling point, i.e. the crossover point of G' and G'' as shown in Figure 6.4. Regardless of plasticization, the required time to reach the cross-over point decreases with temperature. Moreover, the delaying effect of the plasticizer is clearly evident by comparing the gel time (crossover time). At each corresponding temperature, the gel point of the cross-linking reaction shifts to longer times in the presence of the plasticizer.

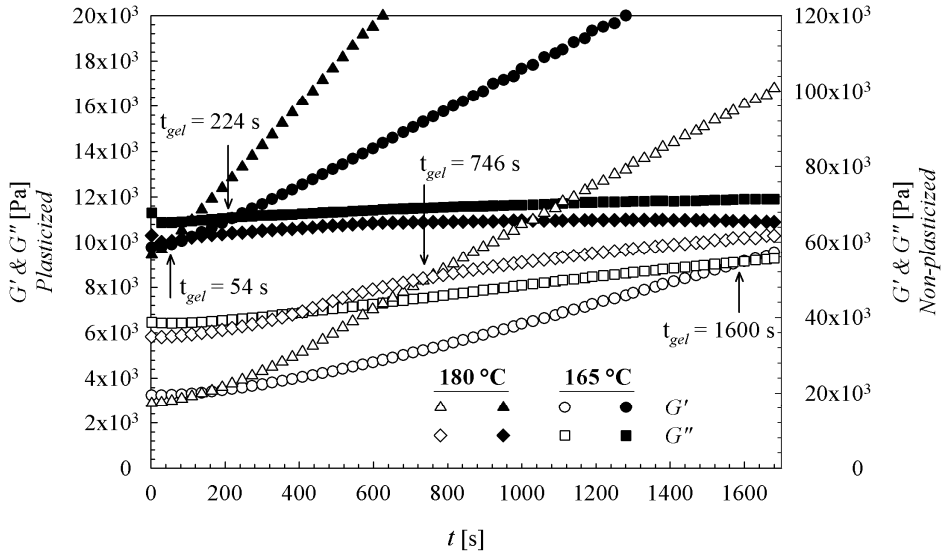

Figure 6.4. The curing behavior of non-plasticized (filled symbols) and plasticized (open symbols) EPDM at 165°C and 180°C. (The arrows indicate the crossover point of *G′* and *G″*)

In addition to the gel point method, the curing behavior was also analyzed based on the required time for obtaining a 50% and 90% modulus increase (i.e., "Cure time" or t_x where x=50% and 90%). This method of determining the "Cure time" is identical to what is stated as the standard test method in ASTM-D2084.[30] In Figure 6.5 the "Cure Rate Index" (i.e., 100/(t_x-scorch time), scorch time has been considered zero in this case) of the non-plasticized and plasticized EPDM evaluated based on G' and G'/G'_{NR} are shown at 165 and 180°C. Regardless of the normalization and "Cure time", at each designated temperature, plasticization reduces the curing rate. However, the differences between the "cure rate indices" of the non-plasticized and plasticized elastomers are larger when evaluated at t_x=50% rather than t_x=90%, indicating a delayed curing behavior in the presence of the plasticizer at the initial stage.

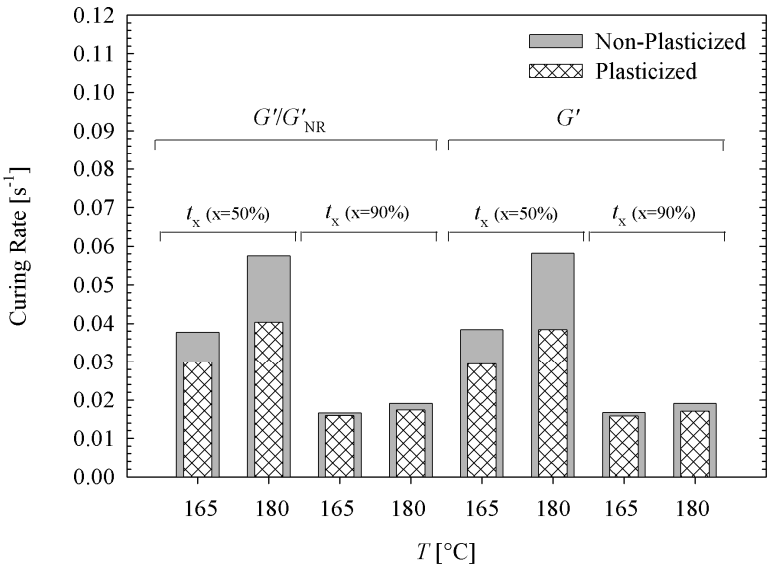

Figure 6.5. Cure rate index of non-plasticized and plasticized EPDM calculated based on the time required to reach 50% and 90% increase in the viscoelastic properties during curing step.

In spite of the delaying effect, the cross-linking reaction had a larger effect on the final viscoelastic properties of the plasticized elastomer than on the non-plasticized one (Figure 6.6). The normalized storage modulus of plasticized EPDM cured at high temperatures ($T \geq 150$°C) is larger than the non-plasticized ones when frequency sweep experiments were performed immediately after the curing reaction. The effect could be clearly observed at low frequencies. However at high frequencies (shorter times), for which the relaxation processes of short chain segments of macromolecules is accounted for,[37] the effect still persisted. This might be an indication of a denser cross-link network in the presence of the plasticizer. However due to the plasticization, despite the larger values of normalized storage modulus (Figure 6.6), the actual storage modulus (elasticity) of the plasticized elastomer is lower and the substance is much softer than the non-plasticized one.

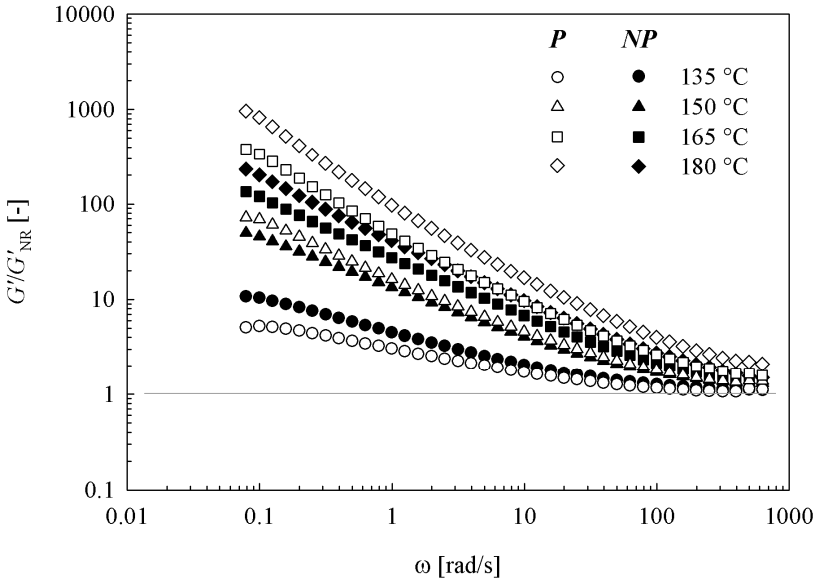

Figure 6.6. The normalized storage moduli of non-plasticized (NP) and plasticized (P) EPDM obtained from frequency sweep experiment immediately after the cross-linking reaction.

6.4.3 Transient Rheological Measurements and Morphology Development

6.4.3.1 Neat Polymeric Components

Prior to any transient rheological measurements on non-reactive/reactive EPDM/PP blends, the effect of plasticization on the stress growth of the neat EPDM and PP was investigated. Figure 6.7 reports merely the multiple step start-up (stress growth) data of the non-plasticized/plasticized EPDM. The shear rate was set to 0.1 s^{-1} to provide sufficient amount of shear (45 units of shear) at each step, and to avoid the appearance of significant non-linear effects through an overshoot. Due to the highly elastic nature of the non-plasticized EPDM, neither the viscosity nor the first normal stress difference reach a complete steady state during the multiple startups (Figure 6.7).

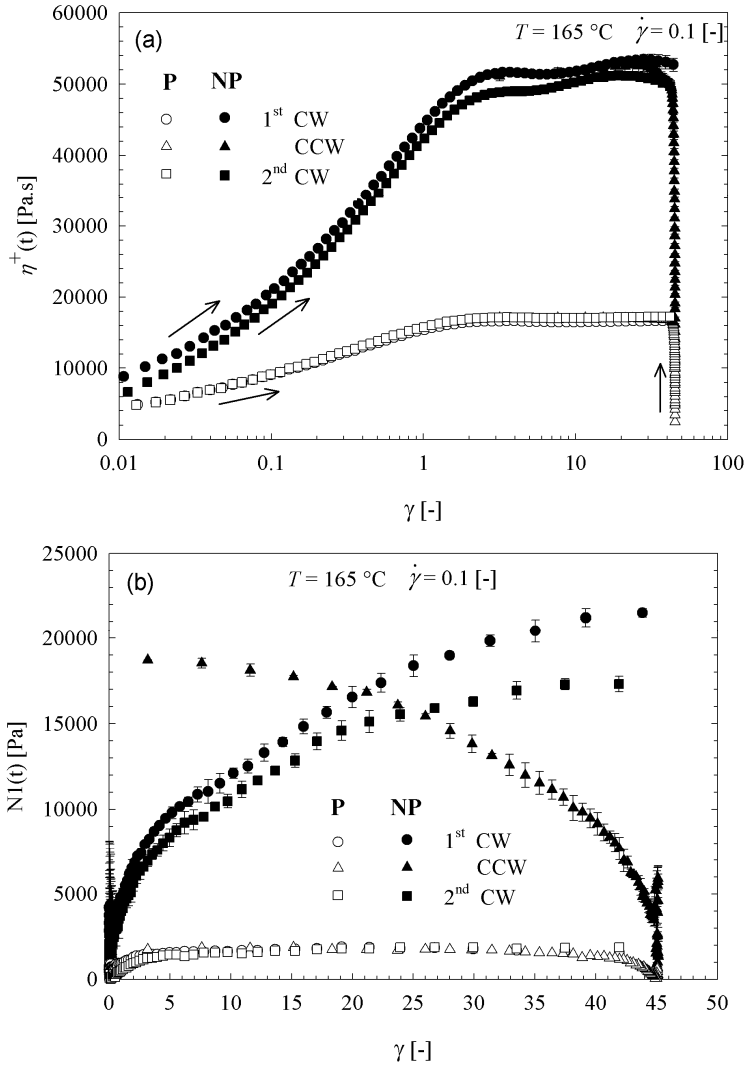

Figure 6.7. Multiple start-up (stress growth) curves of non-plasticized (NP) and plasticized (P) (25 phr plasticizer) EPDM: (a) Viscosity, (b) First normal stress difference.

On the contrary, the non-plasticized PP reached its steady state stress level and recovered its elasticity at the end of each shearing step (results not shown here). The effect of plasticization on the EPDM can be readily observed in Figure 6.7. It can be seen that only a small amount of plasticizer (25 phr in this case) is sufficient to drastically decrease the viscoelastic properties and to reduce or eliminate the non-linear viscoelastic effects. A similar plasticization effect was also seen for the PP. It is well known that the addition of a low molecular weight and low volatile

miscible liquid to polymers increases the free volume and mobility of polymeric chains and reduces the glass transition temperature (T_g) of the polymer.[6, 38] Hence, it decreases the viscosity and results in a faster relaxation of polymeric chains and lowers the elasticity.[8]

6.4.3.2 Non-Reactive EPDM/PP Blends

The normalized transient shear viscosities of these blends during single step startups are shown in Figure 6.8. All TPE blends were subjected to 0.1 s^{-1} for 450 s. For all the mentioned blends, a stress overshoot followed by a steady state region can be observed representing the non-linear viscoelastic behaviour at short times. The appearance of the stress overshoot in immiscible polymer blends has been mainly attributed to the orientation and deformation of the interface, with its peak and the steady state region representing the maximum orientation state and the continuation of interface stretching, respectively.[24, 39] In Figure 6.8, regardless of the plasticization, the magnitude of the normalized overshoot and the time required to reach the steady state increase with the elastomer content (except in the case of non-plasticized E/P 75/25 wt/wt%).

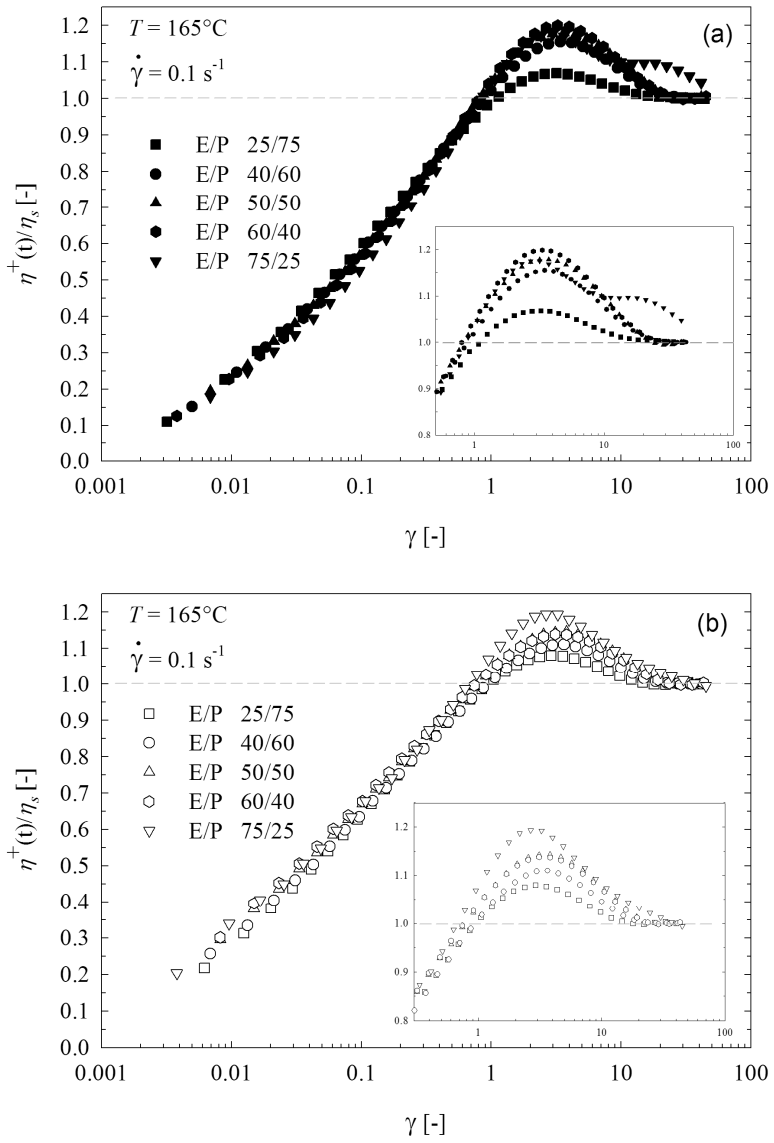

Figure 6.8. Single start-up (stress growth) curves of non-reactive E/P (wt/wt%) TPEs: (a) Non-plasticized, (b) Plasticized. (η_s: the viscosity at the steady state condition)

Despite the composition effect (EPDM content), the amplitude of the overshoot is larger for blends with a substantially interconnected morphology. This can be clearly observed by looking at the differences between the magnitude of the overshoots in TPEs with 25 and 40 wt% of EPDM in the non-plasticized blends compared to the plasticized ones (Figure 6.8). The differences are larger in the case of the non-plasticized blends, which could be attributed to the

initial morphology of these blends before shearing as the plasticized blends generally possess coarser and larger polymeric domains compared to the non-plasticized blends (Figure 6.9). The initial coarser morphology of plasticized blends with large polymeric domains could be mainly attributed to the swelling effect of the plasticizer and the coalescence took place during the blending step of these TPEs. It is known that in the melt state, the plasticizer is distributed and absorbed by both polymeric phases resulting in swollen polymeric domains.[7] Furthermore, the coalescence phenomenon is promoted in the presence of low molecular weight species (e.g., a plasticizer), during its diffusion from one phase to another.[40] Hence, the combination of swelling and coalescence phenomena could have been responsible for an initial coarser morphology in the plasticized TPEs.

In a previous study,[41] it has been shown that both non-plasticized and plasticized TPEs with EPDM content larger than 40 wt% possess a co-continuous morphology with a continuity index (*CI*) of 100% for both polymeric phases. However, at low EPDM content (25 wt% of EPDM), the non-plasticized blend showed a finer morphology with less interconnectivity and lower continuity index of EPDM, i.e. *CI*=57.6 % compared to 77.8 % in the case of the plasticized blend.

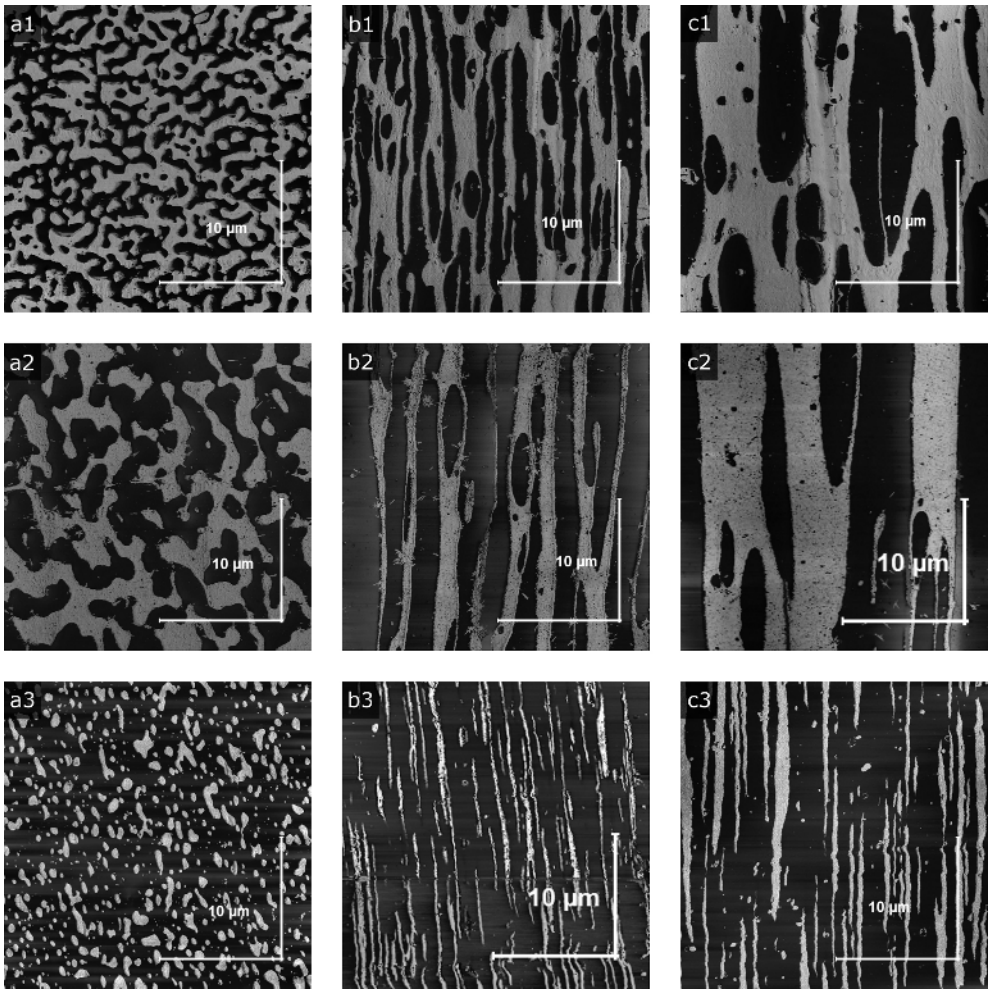

Figure 6.9. AFM phase morphologies of non-reactive E/P (wt/wt%) TPEs during start-up experiment at 0.1 s^{-1} and 165°C: (1) 50/50 Non-plasticized, (2) 50/50 Plasticized, (3) 75/25 Non-plasticized. (Column *a*: Prior shearing; Column *b*: After 1st CW step; Column *c*: After 2nd CW step; Dark phase: EPDM; Bright phase: PP)

In a non-plasticized TPE blend, deforming a network of interconnected EPDM phase is harder than deforming a finely dispersed elastomeric phase. As a result, the difference between the interconnectivity of the elastomeric phase in the non-plasticized blends compared to the plasticized one might possibly cause the larger difference between the overshoot magnitude between TPEs with 25 and 40 wt% of EPDM. On the other hand, the time required to reach the overshoot is equal or slightly larger in the case of the plasticized blends, indicating a slower

interface orientation. In a different study on the non-linear viscoelastic behaviour of polystyrene/polypropylene blends by Macaubas et al.[39], the longer overshoot times were as well attributed to a slower interface orientation. Figure 6.9 shows a few AFM phase morphologies of the non-plasticized and plasticized TPEs at the end of 450 s. Hence, the effect of shear on the orientation of the polymeric phases can be clearly observed. These TPEs possess a relatively low interfacial tension (~0.3 mN/m)[42-44] which would possibly lead to the formation of an extended stable fibrilar morphology with a relatively long thread break-up time.[42] Therefore, in the absence of a significant breakup during the start-up experiment, depending on the composition, coalescence would play a major role. The phase morphologies of 50/50 wt/wt% TPEs indicate the shearing and coalescence effect, where the initial co-continuous morphology has coalesced and formed ellipsoidal domains (Figure 6.9). On the other hand, in blends with high elastomer content (especially non-plasticized E/P 75/25 wt/wt%), the high matrix shear stress exerted on the PP resulted in finely elongated fibrilar morphology, with limited coalescence (Figure 6.9). The quantitative morphology data of these blends through their specific interfacial areas (Q) show a similar trend, where regardless of the composition, coalescence resulted in a decrease in the specific interfacial area of both non-plasticized and plasticized TPEs at the end of single and multiple start-up experiments (Figure 6.10). However, the decrease in Q was more pronounced for the low elastomer content non-plasticized blends, indicating the importance of coalescence over other interfacial phenomena.

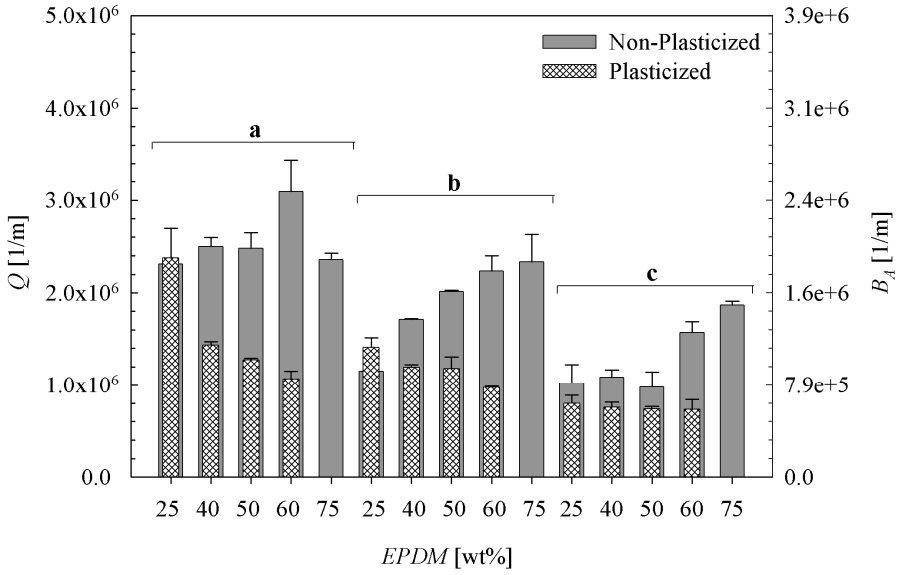

Figure 6.10. The evolution of specific interfacial areas (*Q*) of non-reactive TPEs during start-up experiments at 165°C: (a) Prior shearing, (b) At the end of 450 s or 1st CW step, (c) At the end of 2nd CW step.

Figure 6.11 reports the transient shear viscosities of TPEs containing 40, 50 and 60 wt% of EPDM subjected to multiple startups. During the 1st *CW* step, one would observe a similar trend observed in the case of single step start-up experiments, where the magnitude of the overshoot and the required time to reach the steady state increase with elastomer content. In TPEs with identical EPDM content, the magnitude of the overshoot is larger for the non-plasticized blends compared to the plasticized ones. Furthermore, the differences in magnitude of the overshoot increase with the elastomer content. This might be due the presence of the plasticizer and its preferential distribution in the elastomeric component. Furthermore, the amount of the plasticizer in plasticized TPEs has a constant proportionality with the elastomer content (100 phr plasticizer based on the EPDM content) and blends with higher EPDM content contain larger amounts of plasticizer distributed essentially in the elastomeric component.

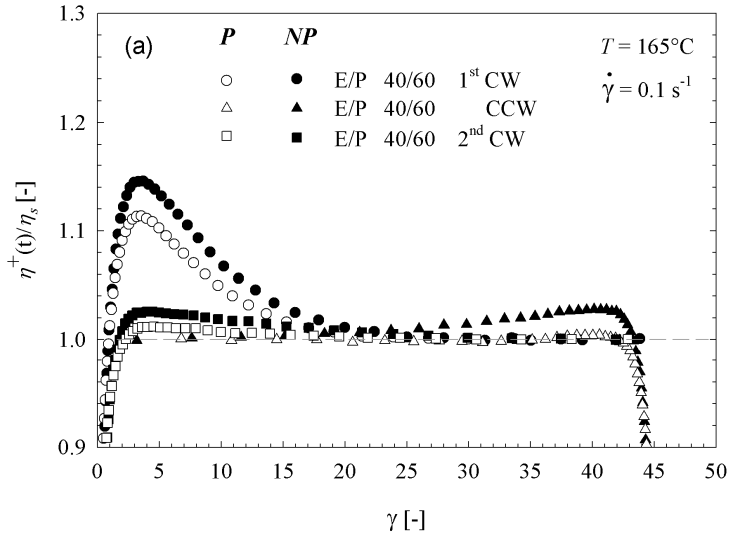
(a)
P
NP
T = 165°C
γ̇ = 0.1 s-1
E/P 40/60 1st CW
E/P 40/60 CCW
E/P 40/60 2nd CW
η+(t)/ηs [-]
γ [-]

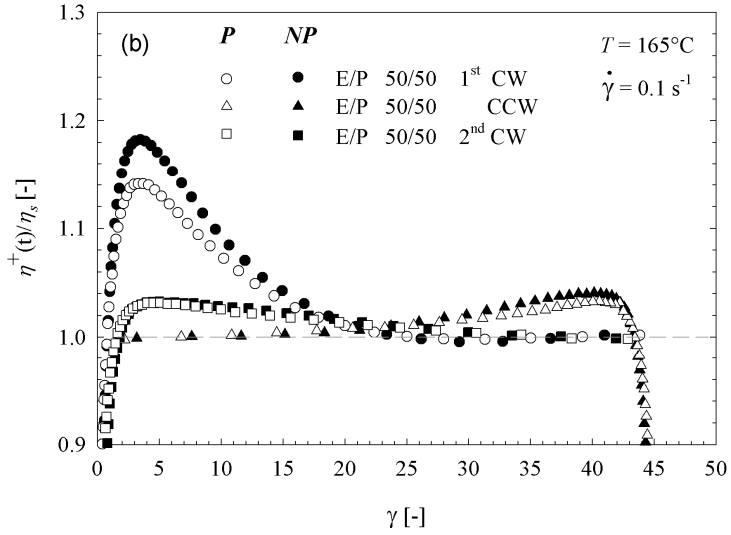
(b)
P
NP
T = 165°C
γ̇ = 0.1 s-1
E/P 50/50 1st CW
E/P 50/50 CCW
E/P 50/50 2nd CW
η+(t)/ηs [-]
γ [-]

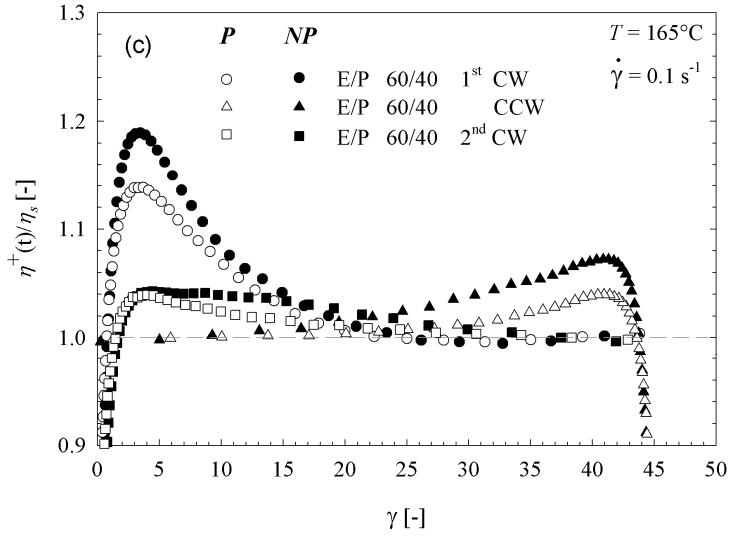

Figure 6.11. Multiple start-up (stress growth) curves of non-reactive E/P (wt/wt%) TPEs: (a) 40/60, (b) 50/50, (c) 60/40. (*NP*: non-plasticized; *P*: plasticized; η_s: the viscosity at steady state condition)

Prior to the *CCW* step, the blends were subjected to 10 min rest time between each consecutive shearing step. Accordingly, during the mentioned rest period, the excess stress in both polymeric components and the interface between them would relax. The more the excess stress is relaxed during this period, the less would be the effect of the shear history of the neat polymeric components on the consequent shearing steps. Consequently, during the flow reversal, the stress buildup would be mainly governed by the morphology evolution of the blend. Therefore, the appearance of stress overshoots in the non-plasticized and plasticized TPEs during the *CCW* step (Figure 6.11) and the absence of such non-linear effects for their corresponding neat components (Figure 6.7) indicate the dominant effect of the interface orientation and phase deformation on the non-linear behavior of these blends through overshoots. However, the magnitude of the overshoots at this step is smaller, and the required time to reach the steady state is longer compared to the 1st *CW* step. In the absence of any experimental proof, the larger time required to reach the overshoot might possibly be due to the re-orientation of the interface in the

reverse direction. On the other hand, the smaller overshoot might be explained based on differences between the initial morphological states of the TPEs prior to the 1st *CW* and the *CCW* shearing steps. According to morphological results, the largest stress that built up during the first *CW* step is mainly due to the presence of an initial co-continuous network structure in contrast to elongated coalesced morphology at the beginning of the *CCW* step (Figures 6.9). Taking the inverse of the specific interfacial area as a length scale, the deformability of the interface and the stress response during the *CCW* and 2nd *CW* steps could be explained through the changes in the capillary number. Capillary number represents the relative importance of viscous forces versus interfacial tension acting across an interface ($Ca = \eta_{matrix}\dot{\gamma}R/\Gamma$), where η_{matrix}, $\dot{\gamma}$, R and Γ represent the viscosity of the matrix, shear rate, average droplet radius and the interfacial tension, respectively. In a droplet/matrix type morphology, for capillary number less than a critical value (i.e., critical capillary number, Ca_{crit}), the droplet attains a steady shape and orientation, whereas above that critical value, the droplet eventually breaks-up. For a single Newtonian droplet in a Newtonian medium this value was measured by Grace,[45] and an empirical fit to Grace's data was proposed later by Bruijn.[46] In this work, the morphology change during the 1st *CW* step increases the capillary number and its ratio over the critical capillary number at the beginning of *CCW* step (Table 6.3). The increase is mainly through the conventional ratio of R/Γ (where *R*, the average radius of droplet in droplet/matrix type morphology is replaced by 1/*Q*). The mentioned ratio is a measure of deformability of the minor phase. At a fixed shear rate, composition and viscosity ratio, the larger this ratio is the more deformable would be the minor phase. Therefore, the absence of a significant overshoot during the *CCW* and the 2nd *CW* steps would possibly be explained by the decrease in the specific interfacial area and the presence of oriented stable fibers. Figure 6.9 shows the persistence of such an elongated morphology at the end of the 2nd

CW step. Although, multiple shearing sequences and rest times resulted in a decrease in the interfacial area through coalescence of the polymeric phases (Figure 6.10), their phase morphologies at the end of the 2nd *CW* step confirms the stability of a fibrilar morphology in such low interfacial tension blends.

Table 6.3. Capillary number for different non-plasticized and non-reactive blends during consecutive start-up experiments

EPDM, wt%	η_d/η_m [a] @ 0.075 s^{-1}	Ca_{crit} [c]	Ca_i/Ca_{crit} 1st *CW*	Ca_i/Ca_{crit} *CCW*
25	2.27	0.85	2.18	4.36
40	2.27	0.85	2.01	2.94
50[b]	2.27	0.85	2.03	2.50
	0.44	0.46	8.46	10.43
60	0.44	0.46	6.79	9.39
75	0.44	0.46	8.91	8.99

[a] Viscosity of minor phase over the major phase at ¾ of the rim of the parallel plate geometry.

[b] Due to co-continuity at this composition, both EPDM and PP can be considered minor phase.

[c] Critical capillary number calculated based on the viscosities of neat polymeric components using the empirical fit obtained by de Bruijn[46].

6.4.3.3 Reactive EPDM/PP Blends

As mentioned earlier, due to the intrinsic reactive nature of the curing agent no rest time and consequently no multiple start-up experiment could have been envisaged for the reactive TPEs and they were only subjected to single step start-up experiments. In contrast to the non-reactive blends, two simultaneous indistinguishable phenomena generally take place during the stress growth of reactive TPEs: the phase morphology evolution and the curing reaction of the elastomeric component. Figure 6.12 compares the stress growth curves of the non-plasticized and

plasticized reactive TPEs subjected to 0.1 s^{-1} for 450 s with their corresponding non-reactive counterparts. The presence of the curing agent in both non-plasticized and plasticized reactive TPEs results in an overall upward stress growth trend.

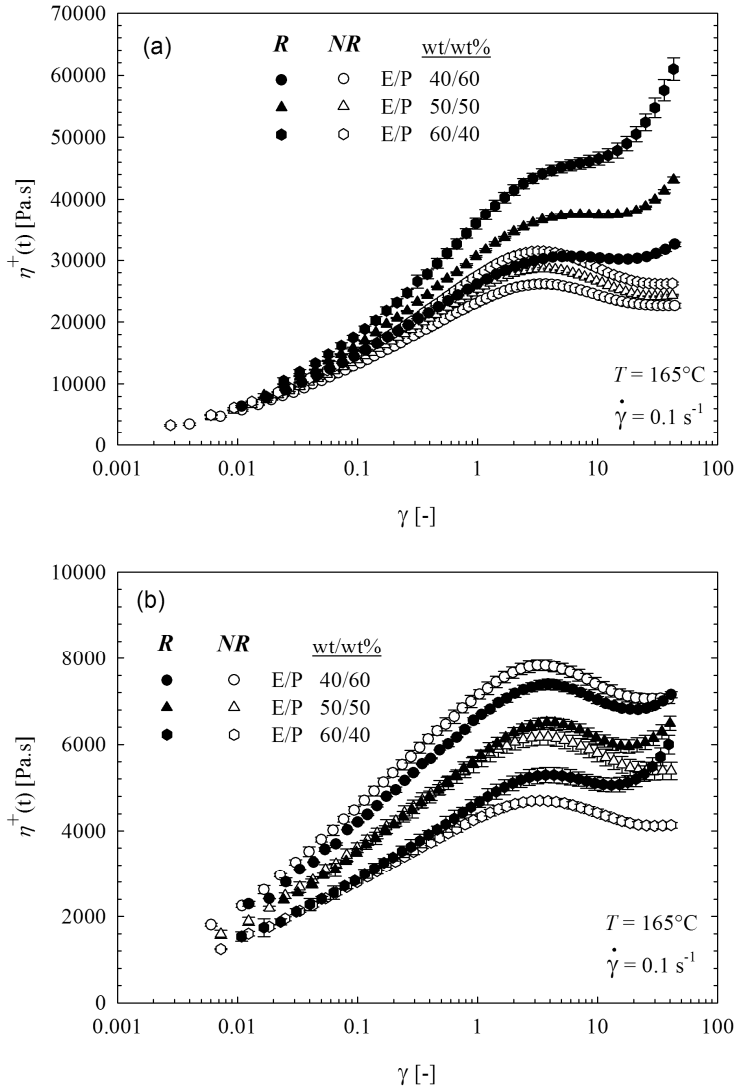

Figure 6.12. Single start-up (stress growth) curves of non-reactive and reactive TPEs for 450 s at 0.1 s^{-1}: (a) Non-plasticized, (b) Plasticized. (*NR*: non-reactive; *R*: reactive)

Furthermore, due to the continuous progression of the curing reaction, no tendency towards steady state conditions could be observed in the reactive blends. Regardless of plasticization, the difference between the final viscosities of non-reactive and reactive blends

increases with EPDM content. In the non-plasticized blends, the rapid increase in viscosity is clearly evident right from the beginning of the experiment (Figure 6.12a). The mentioned increase is faster in blends with larger EPDM content, containing larger amount of curing agent. Furthermore, in contrast to the non-reactive blends, the overshoot has disappeared and the blends passed through a plateau region. On the other hand, for the plasticized blends a different trend is observed (Figure 6.12b). Throughout the whole experiment, the viscosity of low EPDM content (40 wt% EPDM) reactive blend follows an identical trend as the non-reactive counterpart, with its viscosity being lower. Furthermore, no significant increase is observed at the end of the experiment. Hence one could conclude that no substantial curing has taken place for the low EPDM content reactive blends and the curing agent has mainly acted as an additional plasticizer during the mentioned period. By increasing the EPDM content, the differences between the non-reactive and reactive curves become increasingly evident and the overshoot is overshadowed by the curing reaction. Comparing the difference between the final viscosity values of the non-reactive and reactive TPEs with identical composition at the end of 450 s, the delaying effect of plasticizer became clearly evident. Generally during a specified time, the larger the viscosity difference is, the faster would have been the cross-linking reaction. The viscosity difference or increase at the end of 450 s of shearing in the 40, 50 and 60 wt% EPDM content non-plasticized TPEs were 44.3%, 78.9% and 135.1%, respectively. The corresponding values in the plasticized TPEs were 2.9%, 23.1% and 52.0% in the blends with 40, 50 and 60 wt% EPDM content, respectively. The AFM phase morphologies of reactive TPEs prior and after 450 s start-up experiments are shown in Figure 6.13.

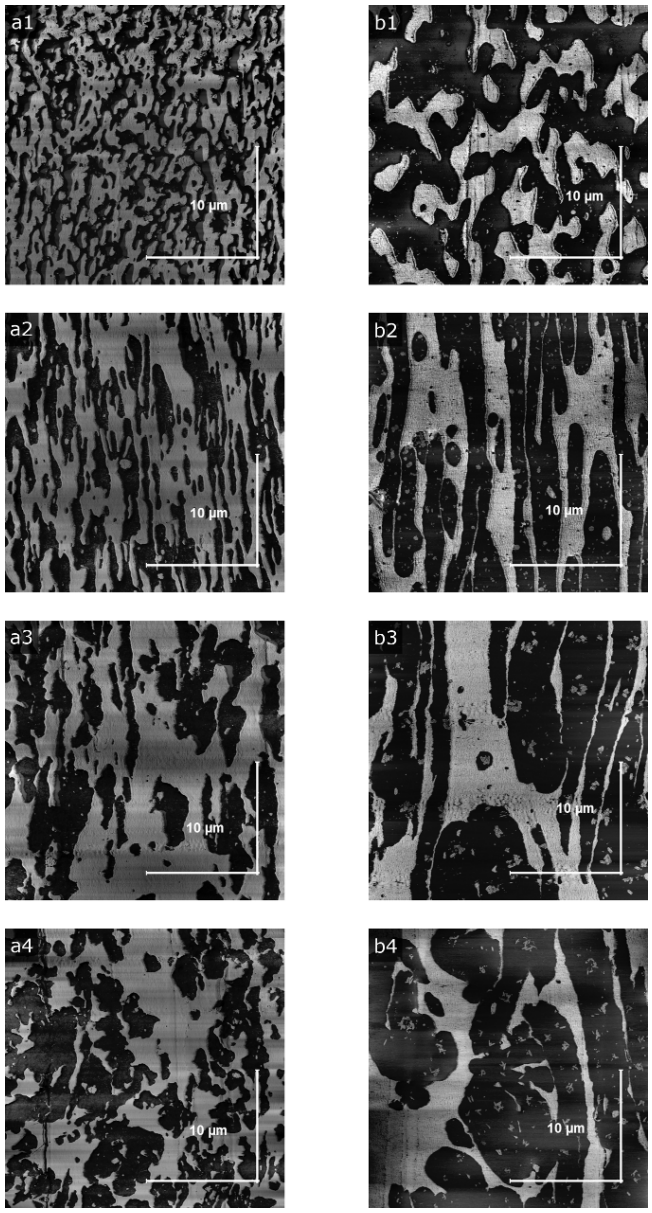

Figure 6.13. AFM phase morphologies of non-plasticized and plasticized reactive E/P 50/50 (wt/wt%) TPEs during start-up experiment at 0.1s^{-1} and 165°C: (1) Prior shearing, (2) After 450 s, (3) After 2700 s, (4) After 7200 s. (Column *a*: non-plasticized; Column *b*: plasticized; Dark phase: EPDM; Bright phase: PP)

These morphologies compared to non-reactive ones (Figure 6.9) prior to the start-up experiment have more irregular shape interfaces with disintegrated polymeric domains (especially in the case of the non-plasticized TPEs) resulting in larger initial specific interfacial

area (Figure 6.14). The probable limited cross-linking reaction that occurred during the blending step in the internal mixer and during the compression molding process might have caused the deference between the interfacial area of non-reactive and reactive TPEs prior to the start-up experiment.

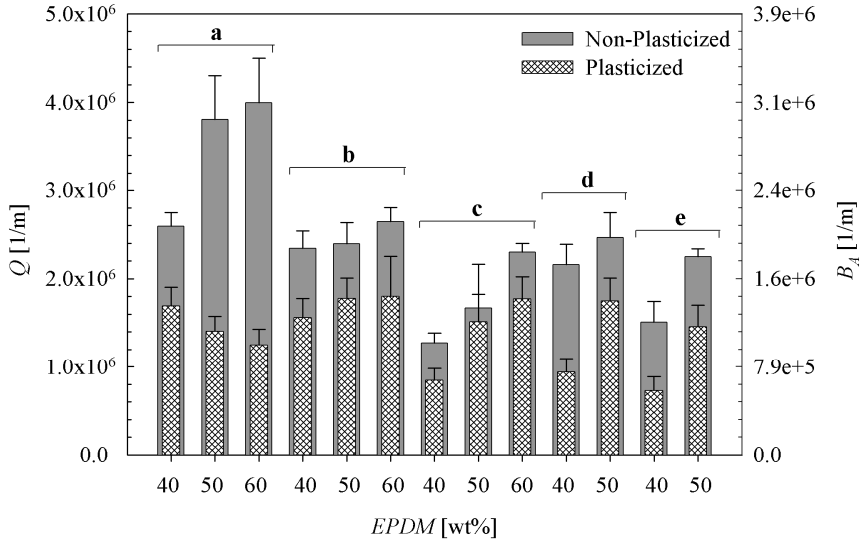

Figure 6.14. The evolution of specific interfacial areas (Q) of reactive TPEs prior and during start-up experiments at 0.1 s^{-1} and 165°C: (a) Prior shearing, (b) At the end of 450 s, (c) At the end of 2700 s, (d) At the end of 2700 s (at 180°C), (e) At the end of 7200 s.

Throughout the start-up experiment, the initial large interfacial area of the non-plasticized blends decreased through coalescence. Nevertheless, instead of uniform ellipsoidal shape or fibrilar morphologies seen in the non-reactive blends (Figure 6.9), an irregular elongated and distorted interface has been created at the end of this experiment (Figure 6.13). The mentioned irregular interface might be due to the cross-linking reaction of the elastomeric phase, which has transformed the molten elastomeric liquid into a thermoset solid type elastic substance with limited deformability under flow. The overall morphologies of the plasticized blends at the end of

the mentioned period are identical to non-reactive blends with slightly larger interfacial area (Figure 6.14).

To observe the effect of the curing reaction on the rheology and morphology of TPEs, start-up experiments with longer duration (2700 s and 7200 s) have been performed. Figure 6.15 represents the stress growth curves for the non-plasticized and plasticized TPEs subjected to 0.1 s^{-1} for 2700 s.

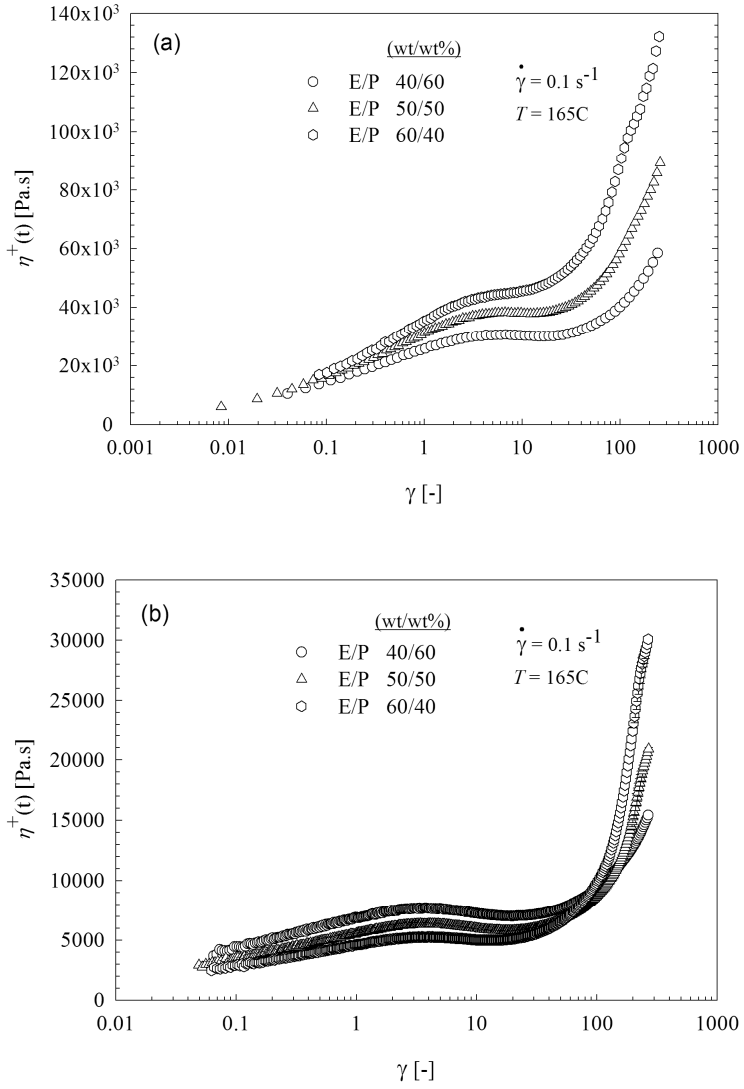

Figure 6.15. Single start-up (stress growth) curves of reactive TPEs for 2700 s at 0.1 s^{-1}: (a) Non-plasticized, (b) Plasticized.

The non-plasticized blends exhibit a uniform upward viscosity trend with no tendency to reach a steady state (Figure 6.15a). Similar to what was seen earlier, at shorter times an initial delayed reaction followed by a rapid increase of viscosity could be observed for the plasticized reactive TPEs (Figure 6.15b). During the initial stage (t < ~600 s) the high elastomer content blend has the lowest viscosity due to the presence of the plasticizer and the slow curing reaction of the elastomeric component. Following this period in Figure 6.15b, the curing reaction rapidly continues and after a cross over point the viscosity of high elastomer content blend (60 wt% EPDM) increases more rapidly compared to the low elastomer content one (40 wt% EPDM). At this stage, the cross-linking reaction of the elastomeric phase becomes the dominant factor in increasing the viscosity of the reactive TPEs. Interestingly, in contrast to the delaying effect of the plasticizer during the first ~600 s of the experiment; after the mentioned period the viscosity increased more rapidly in plasticized blends rather than non-plasticized ones. This could be clearly observed by comparing the viscosities of these blends at the end of 2700 s and 7200 s with respect to their corresponding values at the end of 450 s. For instance, the increase in viscosity after 2700 s and 7200 s shearing times in the non-plasticized EPDM/PP 50/50 wt/wt% TPE were 111.0% and 258.2% compared to 214.7% and 425.1% in the corresponding plasticized blend, respectively. The presence of the plasticizer at longer times might have facilitated the diffusion of the curing agent and resulted in its uniform distribution in the elastomeric phase. Accordingly, after the initial delaying period at the beginning of the start-up experiment (t < ~600 s), the increase in viscosity was more pronounced for the plasticized TPEs rather than in non-plasticized ones. Furthermore, after the mentioned periods, the morphologies of the reactive TPEs are no longer of elongated type structure (Figure 6.13). In the non-plasticised EPDM/PP 50/50 wt/wt% TPEs, coarsely dispersed cross-linked elastomeric domains encapsulated by the

thermoplastic phase could be observed (Figure 6.13 – column *a*). This phenomenon has also been observed for blends with larger elastomer content, i.e. 60 wt% of EPDM, where the major cross-linked elastomeric component has been encapsulated by the minor thermoplastic component and, therefore, could possibly be considered as the onset of phase inversion. Due to long shearing time, both flow induced coalescence and simultaneous cross-linking of the elastomeric phase affected the morphology development of these TPEs. At the early stage of cross-linking reaction, the approaching elastomeric domains in the low intensity flow field possibly coalesced and formed larger domains. However, as the cross-linking reaction proceeded, the viscosity of the elastomeric phase increased and the low viscosity thermoplastic phase encapsulated the high viscosity elastomeric phase. Generally in a flowing system of a binary immiscible blend, it is known that the low viscosity component tends to encapsulate the high viscosity one to minimize the energy dissipation.[47, 48] On the other hand, a similar encapsulation phenomenon was not observed in the plasticized reactive TPEs (Figure 6.13 – column *b*). This might be due to the presence of the plasticizer which delayed the cross-linking reaction at the early stage, resulting in more coalesced elastomeric domains. Furthermore, comparing to non-plasticized TPEs, the viscosity difference between the thermoplastic and the cross-linked elastomeric phases in the plasticized TPEs was possibly smaller in order to promote a similar encapsulation by the thermoplastic phase seen in the non-plasticized blends. Hence, the specific interfacial areas of these blends decrease between 450 s and 2700 s (Figure 6.14). On the other hand longer shearing times (7200 s) has no effect on the plasticized TPEs, whereas it slightly increases the interfacial area of non-plasticized blends probably through rupture and further encapsulation of the small cross-linked elastomeric domains. In addition to shearing time, the temperature effect on the morphology has also been investigated. As a result, reactive TPEs subjected to 2700 s but at higher temperature (180°C) possess slightly larger interfacial area with an identical irregular

interface (Figure 6.14). Furthermore, the temperature effect is more pronounced in non-plasticized blends. On the other hand, it was also observed that temperature had more significant effect on the increase of interfacial area than the shearing time (especially in the case of non-plasticized blends) (Figure 6.14). Consequently, to create large specific interfacial area in reactive blends subjected to relatively low intensity flow fields, one should operate at elevated temperature for shorter time to both rapidly promote the curing reaction and to hinder the coalescence of the polymeric phases.

6.4.4 Morphology Modeling

The morphology evolution of non-reactive TPEs expressed by their specific interfacial areas (Q) was compared with the predictions of Lee and Park constitutive equation.[28] The general concept of the mentioned constitutive equation was originally developed by Doi and Ohta for a mixture of two Newtonian fluids with identical viscosities, densities and volume fractions.[22] The authors used the anisotropy tensor (**q**),[23] and the specific interfacial area (Q) to characterize the morphological state of the interface. Both the stress response and morphological variables (i.e., **q** and Q) can be separately predicted using the rheological properties of the constituent polymers and the appropriate phenomenological parameters representing different interfacial phenomena such as coalescence, break-up, etc.

Few similar approaches have so far been employed to model the rheology/morphology relationship of concentrated immiscible blends with large deformation history.[24-26] However, in most studies the simultaneous predictions of the stress response parallel with the morphology evolution parameters were not satisfactory.[39] As a result, due to the separate and independent nature of time evolution equations written for stress tensor and morphological variables in the

original Lee and Park constitutive equation,[28] one could use the mentioned constitutive equation to merely predict the morphological state variables such as the specific interfacial area. Generally in an immiscible blend, the dynamics of morphology evolution, i.e. orientation, coalescence and break-up of the interface, are mainly controlled by the competition between the flow field enlarging and orienting the interface and the interfacial tension opposing these effects.[22] Accordingly, the following set of kinetic equations was originally proposed by Doi and Ohta for the time evolution of the morphological state variables,

$$\frac{\partial Q}{\partial t} = \left.\frac{\partial Q}{\partial t}\right|_{Flow} + \left.\frac{\partial Q}{\partial t}\right|_{\substack{Interfacial \\ tension}} \tag{6.2a}$$

$$\frac{\partial q_{\alpha\beta}}{\partial t} = \left.\frac{\partial q_{\alpha\beta}}{\partial t}\right|_{Flow} + \left.\frac{\partial q_{\alpha\beta}}{\partial t}\right|_{\substack{Interfacial \\ tension}} \tag{6.2b}$$

where, $q_{\alpha\beta}$ are the components of the orientation tensor (**q**). The authors neglected the effect of interfacial tension to evaluate the effect of flow in the first term and vice versa for the second term in Equation 6.2. For the first part expressing the effect of flow field, Doi and Ohta obtained the following equations mainly based on the geometric consideration,

$$\begin{aligned} \left.\frac{\partial Q}{\partial t}\right|_{Flow} &= -\kappa_{\alpha\beta} q_{\alpha\beta} \\ \left.\frac{\partial q_{\alpha\beta}}{\partial t}\right|_{Flow} &= -q_{\alpha\gamma}\kappa_{\gamma\beta} - q_{\beta\gamma}\kappa_{\gamma\alpha} + \frac{2}{3}\delta_{\alpha\beta}\kappa_{\mu\nu}q_{\mu\nu} - \frac{Q}{3}(\kappa_{\alpha\beta} + \kappa_{\beta\alpha}) + \frac{q_{\mu\nu}\kappa_{\mu\nu}}{Q} q_{\alpha\beta} \end{aligned} \tag{6.3}$$

where, $\kappa_{\alpha\beta} = \partial u_\alpha / \partial x_\beta$ are the components of the velocity gradient tensor and $\delta_{\alpha\beta}$ is the Kronecker delta. On the other hand, for the interfacial tension part, Doi and Ohta represented two main relaxation mechanisms expressing the tendency to reduce the interfacial area (size relaxation) and to make it more isotropic (shape relaxation).[22] This concept was further modified

by Lee and Park[28] by introducing a different additional mechanism by incorporating phenomena such as coalescence and breakup, involved in an immiscible blend. These authors proposed three different relaxation mechanisms: coalescence, shape and break-up mechanisms. Consequently by dimensional analysis, they obtained the following set of equations for the time evolution equation of the second term in Equation 6.2 (the part related to the effect interfacial tension),

$$\left.\frac{\partial Q}{\partial t}\right|_{\substack{Interfacial\\tension}} = -r_1 Q - r_3 q_{\alpha\beta}$$

$$\left.\frac{\partial}{\partial t}\left(\frac{q_{\alpha\beta}}{Q}\right)\right|_{\substack{Interfacial\\tension}} = -r_2\left(\frac{q_{\alpha\beta}}{Q}\right) \qquad (6.4)$$

$$r_1 = d_1\frac{\Gamma Q}{\eta_m} \quad , \quad r_2 = d_2\frac{\Gamma Q}{\eta_m} \quad , \quad r_3 = d_3\frac{\Gamma}{\eta_m}q_{\alpha\beta}$$

where, Γ is the interfacial tension and r_1, r_2 and r_3 are the relaxation rates representing coalescence, shape and break-up mechanisms, respectively with their corresponding dimensionless rate constants, i.e. d_1, d_2, d_3. To avoid the complete phase separation resulting in $Q = 0$,[22] Doi and Ohta had originally proposed the following alternative relaxation rate for the coalescence phenomenon,[22] guaranteeing the stop of the relaxation process after an isotropic morphology state has been reached,

$$r_1 = d_1\frac{\Gamma}{\eta_m}\sqrt{\sum q_{\mu\nu}{}^2} \qquad (6.5)$$

In this work, the above mentioned rate equation has been employed to avoid the possible complete phase separation in the simulation. Therefore, by rearranging Equations 6.4, the following set of equation has been obtained,

$$\left.\frac{\partial Q}{\partial t}\right|_{\substack{Interfacial\\tension}} = -c_1 c_2 \frac{\Gamma Q}{\eta_m}\sqrt{\sum q_{\mu\nu}{}^2} - c_1 c_3 \frac{\Gamma}{\eta_m} q_{\alpha\beta} q_{\alpha\beta}$$

$$\left.\frac{\partial q_{\alpha\beta}}{\partial t}\right|_{\substack{Interfacial\\tension}} = -c_1 c_2 \frac{\Gamma\sqrt{\sum q_{\mu\nu}{}^2}}{\eta_m} q_{\alpha\beta} - c_1 c_3 \frac{\Gamma}{\eta_m}\frac{\sum q_{\mu\nu}{}^2}{Q} q_{\alpha\beta} - c_1(1-c_2)\frac{\Gamma Q}{\eta_m} q_{\alpha\beta} \qquad (6.6)$$

$$c_1 = \mathrm{d}_1 + \mathrm{d}_2 \quad , \quad c_2 = \mathrm{d}_1/(\mathrm{d}_1 + \mathrm{d}_2) \quad , \quad c_3 = \mathrm{d}_3/(\mathrm{d}_1 + \mathrm{d}_2)$$

where the three dimensionless phenomenological parameters, c_1, c_2 and c_3 represent the extent of total, size and breakup/shape relaxations, respectively. Combining Equations 6.3 and 6.6 resulted in the following morphology evolution equation used in this work,

$$\left.\frac{\partial Q}{\partial t}\right| = -\kappa_{\alpha\beta} q_{\alpha\beta} - c_1 c_2 \frac{\Gamma Q}{\eta_m}\sqrt{\sum q_{\mu\nu}{}^2} - c_1 c_3 \frac{\Gamma}{\eta_m} q_{\alpha\beta} q_{\alpha\beta}$$

$$\left.\frac{\partial q_{\alpha\beta}}{\partial t}\right| = -q_{\alpha\gamma}\kappa_{\gamma\beta} - q_{\beta\gamma}\kappa_{\gamma\alpha} + \frac{2}{3}\delta_{\alpha\beta}\kappa_{\mu\nu} q_{\mu\nu} - \frac{Q}{3}(\kappa_{\alpha\beta} + \kappa_{\beta\alpha}) + \frac{q_{\mu\nu}\kappa_{\mu\nu}}{Q} q_{\alpha\beta}$$
$$- c_1 c_2 \frac{\Gamma\sqrt{\sum q_{\mu\nu}{}^2}}{\eta_m} q_{\alpha\beta} - c_1 c_3 \frac{\Gamma}{\eta_m}\frac{\sum q_{\mu\nu}{}^2}{Q} q_{\alpha\beta} - c_1(1-c_2)\frac{\Gamma Q}{\eta_m} q_{\alpha\beta} \qquad (6.7)$$

$$c_1 = \mathrm{d}_1 + \mathrm{d}_2 \quad , \quad c_2 = \mathrm{d}_1/(\mathrm{d}_1 + \mathrm{d}_2) \quad , \quad c_3 = \mathrm{d}_3/(\mathrm{d}_1 + \mathrm{d}_2)$$

In the following paragraphs, the specific interfacial areas (Q) of the non-plasticized/plasticized TPEs in the absence of curing agent (non-reactive blends) subjected to multiple start-up experiments were compared with the predictions of Equation 6.7. To resolve the Equation 6.7, the following initial conditions have been set: $q_{\alpha\beta}\big|_{t=0} = 0$ indicating an initial isotropic morphology,[22, 27, 39] and the experimental data of the specific interfacial area prior to shear as the initial condition for $Q\big|_{t=0}$. Among the three phenomenological parameters (i.e., c_1, c_2 and c_3), the size relaxation (c_2) and break-up and shape relaxation (c_3) parameters have been considered constant values. Since the EPDM/PP based TPEs possess a relatively low interfacial

tension (~0.3 mN/m), promoting the formation of extended stable fibrilar morphology, it possibly leads to slower shape relaxation in comparison to coalescence and break-up processes. As result the rate of shape relaxation (r_2) can be neglected (d_2=0) resulting in a constant size relaxation parameter c_2 = 1. On the other hand, by neglecting the shape relaxation, the parameter c_3 would represent the relative importance of the breakup over coalescence phenomenon (c_3=d_3/d_1). Considering the formation of elongated morphology in such blends, the break-up rate could be represented by the inverse of thread break-up time (t_b) of the filaments of minor phase, and the coalescence rate by the inverse of film drainage time (t_c) of the thin film of major phase. Since the viscosity ratios of TPEs encountered in this study do not deviate from unity, the film drainage process could be expressed based on the partially mobile interface (PMI) model.[13] Therefore, as a rough approximation, since the breakup and film drainage times are proportional to viscosities of the major (η_m) and the minor (η_d) phases, respectively,[49, 50] the break-up and shape relaxation parameter (c_3) can be expressed as follows,

$$c_3 = \frac{d_3}{d_1} \sim \frac{1/t_b}{1/t_c} \sim \frac{\eta_d}{\eta_m} \tag{6.8}$$

This value (viscosity ratio) could be directly obtained in non-plasticized blends. However, in plasticized TPEs, it was assumed that prior to transient experiments and throughout the molding step, the plasticizer was primarily distributed into the EPDM phase due to the crystallization of PP. Although this assumption is not necessarily accurate,[6] it has been considered as a rough estimation for the calculation of the viscosity ratio and consequently the breakup and shape relaxation parameters for the plasticized blends.

The remaining phenomenological parameter representing the total relaxation of the interface (c_1) has mainly been used as a fitting variable. The simulation consisted of five separate

steps identical to the experimental steps performed during multiple start-up experiments. The total relaxation parameter was set in such way so that the value of simulated specific interfacial area at the end of 1st *CW* step was equal to the experimental one. Subsequently, the remaining steps of simulation were continued with already set value of all the phenomenological parameters. In Figure 6.16, both the experimental and simulation results for the non-plasticized E/P 75/25 wt/wt% blend are shown. During the 1st *CW* step, the value of specific interfacial area rapidly increases, passes through an overshoot and reaches the experimental value. After cessation of the flow, coalescence effects result in an exponential decrease of specific interfacial area during the rest period. Subsequently, the interface once again is stretched in the reverse direction during the flow reversal or *CCW* step. This step is followed by a rest period resulting in coalescence and eventually the 2nd *CW* step where the interfacial area increases once again.

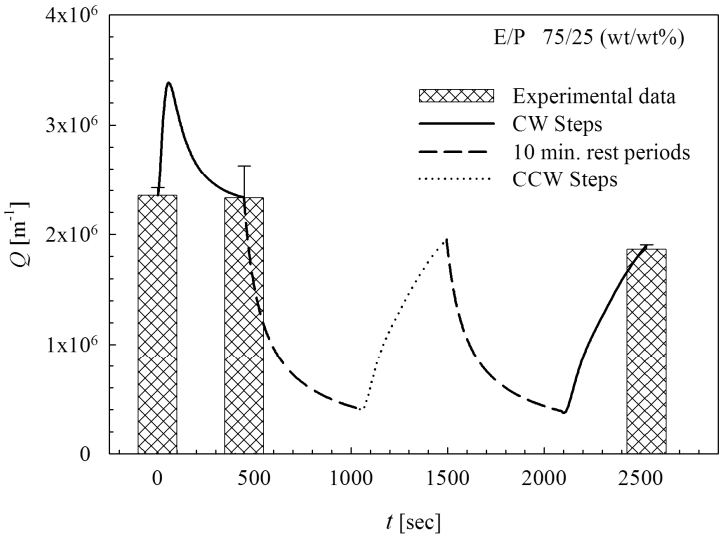

Figure 6.16. Experimental and model prediction of specific interfacial area for non-reactive and non-plasticized E/P 75/25 (wt/wt%) TPE blend subjected to multiple start-up experiment at 0.075 s^{-1}.

As it is clear, the specific interfacial area after each consequent shearing step slightly decreases indicating the predominant effect of coalescence phenomenon in comparison to break-up. In Figure 6.17, the final simulation results at the end of 2nd *CW* step along with the total relaxation parameter used in this work are compared with the experimental data of both non-plasticized and plasticized TPEs. Apart from the mid-composition range of non-plasticized blends (i.e., 40 and 50 wt% of EPDM) and high elastomer content range of plasticized one (i.e., 60 wt% of EPDM), the simulation fairly well predicts the final specific interfacial areas. Furthermore, one could observe that the value of total relaxation parameter uniformly decreases in non-plasticized blends and slightly increases in plasticized ones. The increase of this parameter indicates the importance of coalescence phenomenon reflecting the experimental specific interfacial areas.

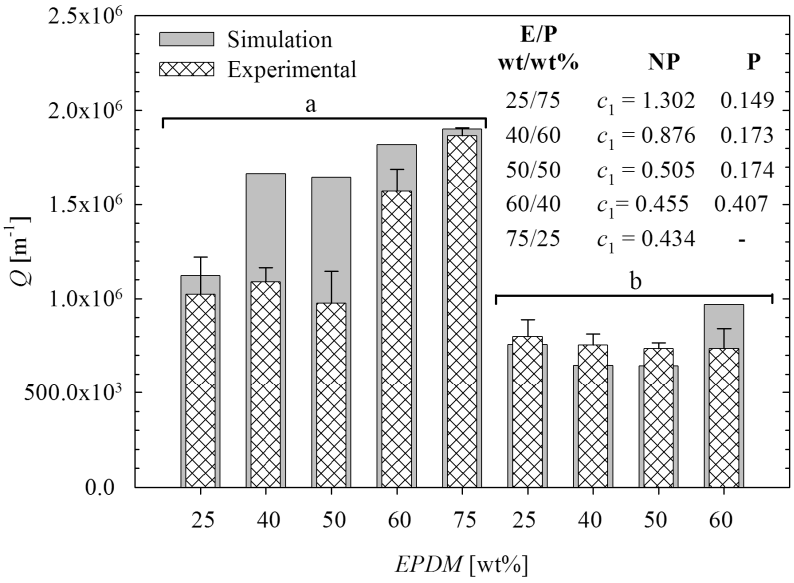

Figure 6.17. Experimental and model prediction of non-reactive TPEs subjected to multiple start-up experiments at 0.075 s^{-1}: (a) Non-plasticized or *NP*, (b) Plasticized or *P*.

The normalized specific interfacial areas of non-plasticized and plasticized TPEs during 1st *CW* step are shown in Figure 6.18. For all TPE compositions with an elastomer content more

than 25 wt% EPDM an initial overshoot was observed. Regardless of plasticization, the amplitude and the required time to reach steady state increases with elastomer content (except in the case TPEs with 60 wt% EPDM, which might be attributed to the experimental error). Furthermore, similar to what was observed for the evolution of transient viscosities during 1st *CW* step, the time required to reach the overshoot is slightly larger in the case of plasticized blends, indicating a slower interface orientation. Therefore, the total relaxation parameter not only reflects the coalescence phenomenon in this particular case, but also the deformation rate of the interface. The larger the total relaxation parameter is, the faster would possibly be the interface deformation.

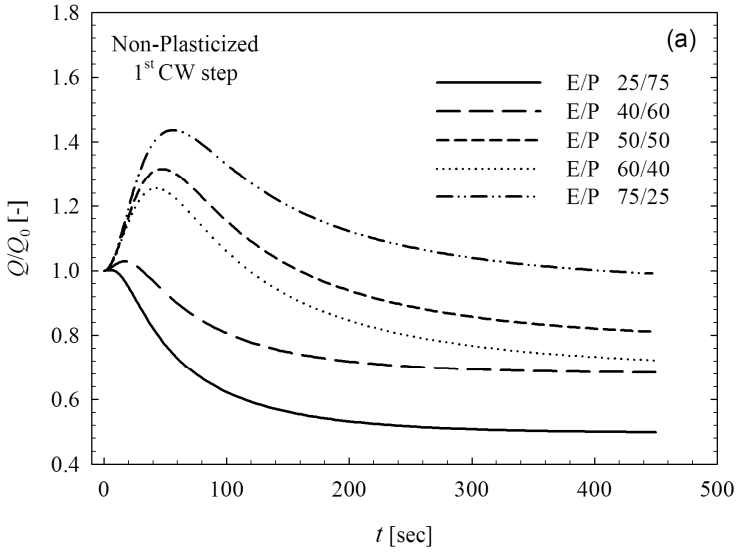

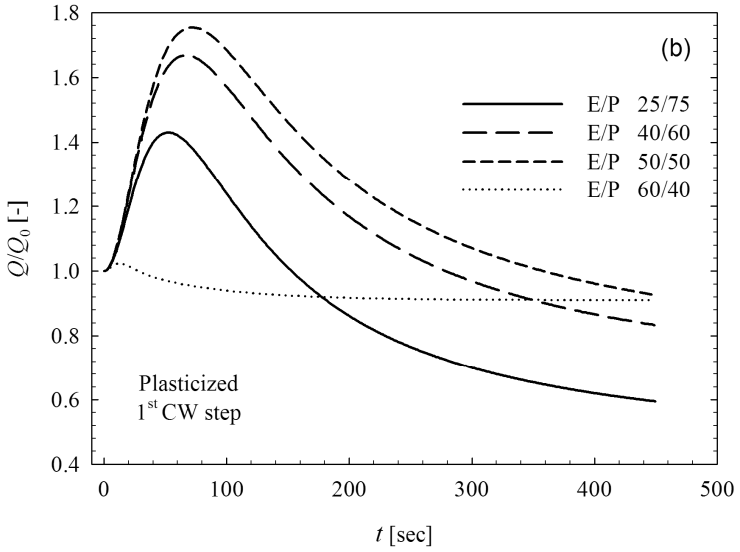

Figure 6.18. The evolution of specific interfacial area (Q) of non-reactive TPEs during the 1st CW step of multiple start-up experiment at 0.075 s^{-1}: (a) Non-plasticized, (b) Plasticized.

6.5 Conclusions

In this work, the non-linear viscoelastic behavior of the non-plasticized/plasticized EPDM/PP TPEs in the absence and presence of a curing agent was studied through single and multiple start-up transient (stress growth) experiments. The morphology evolution of these blends was also investigated by measuring their specific interfacial area (Q) prior and after shearing. The main concerns were to study the effects of the composition, plasticizer and curing system throughout the transient start-up flows and to predict the morphology evolution using a proper constitutive equation.

The presence of a small quantity of plasticizer (25 phr) in the neat polymeric components drastically reduced both the viscosity and elasticity. The linear viscoelastic properties of the non-reactive blends (in the absence of the curing agent) were enormously affected by the presence of a plasticizer due to its predominant distribution in the EPDM phase and the coarser initial

morphology of the plasticized blends prior to the rheological measurements. The initial trend of viscoelastic properties of non-reactive TPEs as a function of EPDM (the more viscous and elastic component) was reversed in the plasticized blends.

Furthermore, the presence of the plasticizer retarded the curing reaction of the EPDM. Regardless of the curing temperature, the gelling point (i.e., the crossover point of G' and G'') shifted to longer times in the plasticized blends. However, the presence of the plasticizer during the curing reaction at elevated temperatures ($T \geq 150°C$) resulted in a larger increase of the final viscoelastic properties. The mentioned delaying effect and its higher efficiency at longer times in the plasticized elastomer compared to the non-plasticized elastomer affected the morphology evolution of the reactive plasticized TPEs.

The TPE compositions studied in this work were in the range of 25 to 75 wt% of EPDM. In the non-reactive blends, during the single step startup or the 1st *CW* step of multiple startups, the magnitude of the normalized overshoot and the time required to reach the steady state increased with the elastomer content. At the end of this step, regardless of the plasticization, due to relatively low interfacial tension of EPDM/PP blends, a coalesced elongated morphology was obtained for all non-reactive blends. The coalescence effect was more pronounced in low elastomer content non-plasticized blends. On the other hand, due to higher shear stress of the elastomeric component in blends with larger elastomer content (especially in the non-plasticized TPEs), more elongated fibrilar morphology with less coalescence was obtained. Most importantly, although the specific interfacial area (Q) of the non-reactive blends decreased throughout the multiple start-up experiments, the elongated fibrilar morphology remained stable. As a result, neither interfacial instabilities and breakup, nor shape relaxation towards spherical shape was observed in the non-reactive blends.

The reactive TPEs on the other hand were subjected to single startups. In the plasticized reactive blends, in contrast to the non-plasticized ones, the presence of the plasticizer and its initial delaying effect during the first 600 s of the start-up experiment resulted in slower viscosity increase. During the mentioned period, due to the presence of the plasticizer, the viscosity of the blends with larger elastomer content was lower than low elastomer content blends. Therefore, the corresponding morphologies at the end of 450 s period were similar to their non-reactive counterparts. On the other hand, the morphologies of non-plasticized reactive counterparts consisted of irregular elongated with distorted interface. After the initial delaying period, the mentioned trend in the plasticized blends was reversed and the curing reaction rapidly increased the viscosity of high elastomer content blends. Furthermore, the level of viscosity increase at the end of 2700 s and 7200 s was greater in the case of the plasticized reactive blends compared to non-plasticized ones. After 2700 s, due to long shearing time, both flow induced coalescence and simultaneous cross-linking of the elastomeric phase affected the morphology development of the reactive TPEs. The long shearing times in the non-plasticized reactive blends with high elastomer content, i.e. 50 and 60 wt% EPDM, resulted in coarsely dispersed cross-linked elastomeric domains encapsulated by the minor thermoplastic phase. This was considered as a possible onset of phase inversion. In contrast, due to possibly the delayed cross-linking reaction in the plasticized blends and the smaller viscosity difference between the plasticized cross-linked elastomeric and the thermoplastic phases, a similar encapsulation phenomenon was not observed in the plasticized reactive TPEs.

Shearing times longer than 2700 s had nearly no effect on the plasticized reactive blends. However, it slightly increased the interfacial area of the non-plasticized blends through the probable rupture and further encapsulation of the elastomeric component. The increase in temperature was more effective in increasing more the interfacial area of the non-plasticized

blends rather than the plasticized ones. Therefore, in reactive blends subjected to relatively low intensity flow fields, elevated temperature and shorter reaction time would possibly lead towards the creation of larger interfacial area.

The specific interfacial areas of both the non-plasticized and plasticized non-reactive TPEs subjected to multiple start-up experiments were fairly well predicted using the phenomenological model proposed by Lee and Park.[28] According to the presence of stable elongated morphology and, therefore, extremely slow shape relaxation process in comparison to coalescence and break-up phenomena, a modified dimensionless breakup/shape relaxation parameter was proposed. The modification was based on the relative importance of the breakup over coalescence phenomena which appeared to be a proper approach for low interfacial tension immiscible blends such as EPDM/PP.

6.6 References

[1] P. Potschke and D. R. Paul, *J. Macromol. Sci., Polym. Rev.* **43**, 87 (2003).

[2] S. K. De and A. K. Bhowmick, "Thermoplastic elastomers from rubber-plastic blends," Ellis Horwood, 1990, New York.

[3] C. H. Lei, X. B. Huang, and F. Z. Ma, *Polym. Adv. Technol.* **18**, 999 (2007).

[4] M. van Duin, *Macromolecular Symposia*. **233**, 11 (2006).

[5] T. Abraham, N. G. Barber, and M. P. Mallamaci, *Rubber Chem. Technol.* **80**, 324 (2007).

[6] M. D. Ellul, *Rubber Chem. Technol.* **71**, 244 (1998).

[7] K. Jayaraman, V. G. Kolli, S.-Y. Kang, S. Kumar, and M. D. Ellul, *J. Appl. Polym. Sci.* **93**, 113 (2004).

[8] N. Nakajima and E. R. Harrell, *J. Rheol.* **26**, 427 (1982).

[9] W. G. F. Sengers, P. Sengupta, J. W. M. Noordermeer, S. J. Picken, and A. D. Gotsis, *Polymer.* **45**, 8881 (2004).

[10] D. R. Paul and C. B. Bucknall, "Polymer blends," John Wiley & Sons, Inc., 2000, New York.

[11] B. D. Favis, "Factors influencing the morphology of immiscible polymer blends in melt processing," in *Polymer Blends*, D.R. Paul and C.B. Bucknall, John Wiley & Sons, Inc., 2000, New York.

[12] F. A. Morrison, "Understanding rheology," Oxford University Press, 2001, New York.

[13] C. L. Tucker and P. Moldenaers, *Annu. Rev. Fluid Mech.* **34**, 177 (2002).

[14] I. Vinckier, P. Moldenaers, and J. Mewis, *J. Rheol.* **41**, 705 (1997).

[15] G. I. Taylor, Proceedings of the Royal Society of London, Series A: Mathematical, Physical and Engineering Sciences. **138**, 41 (1932).

[16] G. I. Taylor, Proceedings of the Royal Society of London, Series A: Mathematical, Physical and Engineering Sciences. **146**, 501 (1934).

[17] M. Bousmina, *Rheol. Acta*. **38**, 73 (1999).

[18] J. G. Oldroyd, Proceedings of the Royal Society of London, Series A: Mathematical, Physical and Engineering Sciences. **218**, 122 (1953).

[19] J. F. Palierne, *Rheol. Acta*. **29**, 204 (1990).

[20] P. Scholz, D. Froelich, and R. Muller, *J. Rheol. (N. Y.)*. **33**, 481 (1989).

[21] W. R. Schowalter, C. E. Chaffey, and H. Brenner, *J. Colloid Interface Sci.* **26**, 152 (1968).

[22] M. Doi and T. Ohta, *J. Chem. Phys.* **95**, 1242 (1991).

[23] A. Onuki, *Phys Rev A*. **35**, 5149 (1987).

[24] M. Bousmina, M. Aouina, B. Chaudhry, R. Guenette, and R. E. S. Bretas, *Rheol. Acta.* **40**, 538 (2001).

[25] M. Grmela and A. Ait-Kadi, *Journal of Non-Newtonian Fluid Mechanics*. **77**, 191 (1998).

[26] M. Grmela, M. Bousmina, and J. F. Palierne, *Rheol. Acta*. **40**, 560 (2001).

[27] G. K. Guenther and D. G. Baird, *J. Rheol.* **40**, 1 (1996).

[28] H. M. Lee and O. O. Park, *J. Rheol.* **38**, 1405 (1994).

[29] M. Bousmina, A. Ait-Kadi, and J. B. Faisant, *J. Rheol.* **43**, 415 (1999).

[30] ASTM Standard D2084-01, "Standard Test Method for Rubber Property - Vulcanization Using Oscillating Disk Cure Meter," *Annu. Book of ASTM Stand.* **09.01,** (2001).

[31] P. Martin, P. J. Carreau, B. D. Favis, and R. Jerome, *J. Rheol.* **44** (2000).

[32] J. C. Russ, "Practical stereology," Plenum Press, 1986, New York, NY.

[33] J. A. Galloway, M. D. Montminy, and C. W. Macosko, *Polymer*. **43** (2002).

[34] W. P. Cox and E. H. Merz, *Journal of Polymer Science*. **28**, 619 (1958).

[35] O. Chung and A. Y. Coran, *Rubber Chem. Technol.* **70**, 781 (1997).

[36] F. Marguerat, P. J. Carreau, and A. Michel, *Polym. Eng. Sci.* **42**, 1941 (2002).

[37] P. Cassagnau, M. Bert, V. Verney, and A. Michel, *Polym. Eng. Sci.* **32**, 998 (1992).

[38] J. M. G. Cowie, "Polymers: chemistry and physics of modern materials," Chapman and Hall, 1991, New York.

[39] P. H. P. Macaubas, N. R. Demarquette, and J. M. Dealy, *Rheol. Acta*. **44** (2005).

[40] C. Tufano, G. W. M. Peters, P. van Puyvelde, and H. E. H. Meijer, *J. Colloid Interface Sci.* **328**, 48 (2008).

[41] S. Shahbikian, P. J. Carreau, M.-C. Heuzey, M. D. Ellul, J. Cheng, P. Shirodkar, and H. Nadella, *Polym. Eng. Sci.* **In press**, (2010).

[42] P. A. Bhadane, M. F. Champagne, M. A. Huneault, F. Tofan, and B. D. Favis, *Polymer*. **47**, 2760 (2006).

[43] M. Hemmati, H. Nazokdast, and H. S. Panahi, *J. Appl. Polym. Sci.* **82**, 1129 (2001).

[44] H. Shariatpanahi, H. Nazokdast, B. Dabir, K. Sadaghiani, and M. Hemmati, *J. Appl. Polym. Sci.* **86**, 3148 (2002).

[45] H. P. Grace, *Chem. Eng. Commun.* **14**, 225 (1982).

[46] R. A. de Bruijn, *Deformation and breakup of drops in simple shear flows*. 1989, Eindhoven University of Technology.

[47] C. D. Han, "Multiphase flow in polymer processing," Academic Press, 1981, New York.

[48] L. E. Nielsen, "Polymer rheology," M. Dekker, 1977, New York.

[49] P. H. M. Elemans, J. M. H. Janssen, and H. E. H. Meijer, *J. Rheol.* **34**, 1311 (1990).

[50] I. Fortelny and A. Zivny, *Polymer*. **36**, 4113 (1995).

CHAPTER 7

MORPHOLOGY DEVELOPMENT OF EPDM/PP UNCROSS-LINKED AND DYNAMICALLY CROSS-LINKED BLENDS

S. Shahbikian,[1] P.J. Carreau,[1*] M.-C. Heuzey,[1] M. D. Ellul,[2] H. P. Nadella[3], J. Cheng,[3] P. Shirodkar[3]

[1] Center for Applied Research on Polymers and Composites (CREPEC), Department of Chemical Engineering, École Polytechnique de Montréal, Quebec H3T 1J4, Canada

[2] ExxonMobil Chemical Co., Global Specialty Polymers Technology, Akron, Ohio 44311, USA

[3] ExxonMobil Chemical Co., Global Specialty Polymers Technology, Baytown, Texas 77520, USA

*Corresponding author: pierre.carreau@polymtl.ca

Submitted to "*Polymer Engineering and Science*".

7.1 Abstract

Ethylene-propylene-diene-terpolymer (EPDM) and polypropylene (PP)-based uncross-linked and dynamically cross-linked blends were prepared both in an internal mixer and in a co-rotating twin-screw extruder. The aim of this study was to identify the effects of composition, mixing equipment and more specifically the plasticization effect on the morphology development and the final viscoelastic properties. In the uncross-linked blends, the plasticization resulted in a coarser morphology. Furthermore, it was shown that the majority of the plasticizer resided in the EPDM phase, enabling its deformation in the flow direction. In addition, the intensive mixing conditions inside the twin-screw extruder resulted in a finer morphology. In the dynamically cross-linked blends, the twin-screw extrusion process resulted in a higher level of gel content with larger EPDM domains. The plasticization showed again a coarsening effect, resulting in interconnected cross-linked EPDM domains. An interesting interfacial phenomenon was observed specially in the plasticized vulcanized blends where nanometer size occluded PP domains were stripped off and eroded into the EPDM phase. With the exception of the non-plasticized uncross-linked blends, the viscoelastic properties of all other blending systems were found to be directly affected by the morphology, gel content (in the case of cross-linked blends) and the presence of the plasticizer.

7.2 Introduction

Thermoplastic elastomers (TPEs) represent a large group of polymeric materials with thermoreversible cross-links, providing processability by conventional thermoplastic melt processing equipment and an elastic behavior similar to that of vulcanized (i.e., chemically cross-

linked) elastomers [1]. An important category of TPEs consists of a combination of polyolefin semi-crystalline thermoplastic and an amorphous elastomeric component. Within this category, TPEs based on polypropylene (PP) and ethylene-propylene-diene-terpolymer (EPDM) are commercially recognized for their unique physical and mechanical properties obtained by melt mixing mainly due to their phase compatibility [2-4]. Besides the rheological and interfacial properties of the constituent polymers, the morphology and ultimate physical and mechanical properties of these blends largely depends on the presence of various additives such as plasticizers and whether or not the elastomeric component is dynamically cross-linked during the melt processing step. Non-reactive TPE blends are known as thermoplastic polyolefins (TPOs), whereas reactive blends where the elastomeric component is selectively vulcanized during an in-situ cross-linking reaction or "dynamic vulcanization" are recognized as thermoplastic vulcanizates (TPVs) [5]. To achieve the desired elastic properties, the chosen EPDM/PP ratio is often larger than 50/50 (wt/wt%) and more specifically around 60/40 (wt/wt%) [1]. TPOs in the mentioned composition range possess a co-continuous morphology, which indeed is considered as the optimal morphological state for a dynamic vulcanization process [4]. According to Radusch [6], only an initial co-continuous phase morphology allows the effective transfer of shear and elongational stresses to one phase to the other and the breakup of the elastomeric component during the dynamic vulcanization stage, in which the initially continuous elastomeric phase is transformed into dispersed cross-linked particles in the range of 1 to 3 μm [7].

From a processing point of view, the mixing quality and the melt processing conditions are the key factors in achieving a specific microstructure with desired properties. They govern both the distribution and dispersion of the different components such as curing agents, stabilizers, fillers, plasticizer and possibly pigments. They further control the size of the polymeric domains

within the blend. As a result of these complex interactions, the majority of research works on the morphology development of TPEs have been mainly conducted in batch internal mixers by monitoring the effect of each component on the torque/temperature evolution of the blend. The batch mixing approach provides a unique capability in examining different phenomena such as dynamic vulcanization in TPVs [8-15]. A rigorous temperature control, sampling flexibility and wide choice of mixing residence time with comparably moderate flow dynamics within the internal mixer have considerably facilitated the assessment of various processing parameters on the morphology development of TPEs. Meanwhile, parallel efforts have been devoted to the TPE production through continuous mixers such as twin-screw extruders which are more beneficial and realistic from an industrial point of view [13,14,16-18]. However, due to the diversity of processing parameters and the complexity of the flow field, the rigorous design of a twin-screw extrusion process is comparably harder. Only recently, Goharpey et al. [19] attempted to set the operating conditions of twin-screw extrusion on the basis of the results obtained from internal mixer. These authors have obtained comparable viscoelastic and tensile mechanical properties for TPVs from both mixing sources.

In addition to the mixing aspect, both TPOs and TPVs share an additional level of complexity in the presence of a plasticizer. The use of a proper plasticizer (processing oil or extender oil) during the melt processing step has been a common practice in the TPE industry. They generally reduce the cost and improve the resistance to oil swell, heat stability, elastic recovery and permanent set of the TPEs, as well as the low temperature mechanical properties, melt processability and the final appearance of the products [3,20]. Furthermore, the addition of a plasticizer is indispensable to obtain softer thermoplastic elastomer compositions with a lower hardness in the range of 60 and 35 Shore A in the case of EPDM/PP-based TPOs and TPVs, respectively [7,21]. Due to the compatibility and small polarity difference between the plasticizer

and the polymeric components, the plasticizer is expected to be well distributed and to swell both phases in the molten state [3,22]. However, upon cooling the plasticizer is believed to be predominantly adsorbed by the EPDM phase due to the crystallization of the semi-crystalline PP phase, with some portion remaining in the amorphous regions of the PP component [22]. Several experimental studies have been devoted to the oil distribution between the EPDM and PP phases in both solid and melt states [3,23-28]. The outcome of the majority of these studies is an oil distribution coefficient that is the ratio of the oil concentration in the PP phase over that in the EPDM phase [23]. Although the values obtained for this coefficient were found to be less than unity, meaning that the plasticizer had a larger preference towards the EPDM phase, it appeared to be also dependent on the blend composition. In addition, a separate phase of plasticizer has also been reported in some studies based on EPDM/PP TPVs [24,28].

Considering all the above, both TPOs and TPVs shall be considered as highly complex multiphase blends with regards to their morphology development and ultimate physical and mechanical properties. The objective of this study is to investigate the combined effects of plasticizer and processing route on the morphology development and viscoelastic properties of EPDM/PP-based TPOs and TPVs.

7.3 Experimental

7.3.1 Materials

In this work, an ethylidene norbornene (ENB) based ethylene-propylene-diene-terpolymer (EPDM) and a polypropylene (PP), both provided by ExxonMobil Chemical Co., were used as the elastomeric and thermoplastic components, respectively. The nomenclatures and properties of these polymeric components are given in Table 7.1. TPOs and TPVs with different EPDM/PP

(wt/wt%) compositions ranging from 25 to 75 wt% EPDM were investigated. For selective cross-linking of the EPDM during the dynamic vulcanization step, 5 phr (parts per hundred parts of rubber) of an heat reactive octylphenol-formaldehyde resin (Schenectady® SP-1045) was used along with 1.26 phr of anhydrous stannous chloride ($SnCl_2$) and 2 phr of zinc oxide (ZnO) as halogen donor and hydrogen halide scavenger, respectively.

Table 7.1. Characteristics of the neat polymeric components

Polymer	*MFI,* dg/60 s (ASTM D-1238)	T_m °C	*Mooney Viscosity* (ASTM D-1646)	*ENB** wt%	C_2+ wt%
EPDM	-	-	76 (ML 1+4, @ 125°C)	5.8	45
PP	5.3 (230°C/2.16 kg)	165	-	-	-

* ENB: ethylidene norbornene.

+ C_2: ethylene content.

In the case of plasticized blends, 100 phr of paraffinic oil (Sunpar® 150M from Sunoco, Inc.) was used. Furthermore, in order to prevent the thermal degradation of the polymeric components during the melt mixing stage, an antioxidant, Irganox® B-225, (1 wt% based on the weight of EPDM + PP) was used.

7.3.2 Melt Mixing: Internal Mixer

The melt mixing of both TPOs and TPVs was carried out using a small scale laboratory internal mixer (Brabender® Plasti-corder®) at 180°C. A constant rotational speed was set to 100 rpm, which corresponds to an apparent shear rate of ~50 s^{-1} [29]. The process was carried out under a nitrogen atmosphere to prevent the thermal degradation of the polymeric components.

Depending on the blending system, the mixing time was set based on the required time to reach a steady state torque value.

For the TPOs, the mixing was performed for a period of 12 min. In the case of the plasticized TPOs, 75 wt% of the plasticizer was added during the first 8 min of the mixing process and the remaining was added during the latest mixing stage (the remaining 4 min).

Due to the reactive nature of the TPV blends, the mixing procedure was slightly different. In the non-plasticized TPVs the polymeric components along with the catalytic components of the curing system (i.e., $SnCl_2$ and ZnO) were incorporated during the first 8 min of the mixing process, followed by an extra 4 min of mixing for the curing process to occur, keeping the residence time identical to the processed TPOs. The mixing time was slightly longer for the plasticized TPVs due to the required time to reach steady state. Similarly to the non-plasticized TPVs, the polymeric components along with 75 wt% of the plasticizer and the catalytic components were incorporated during the first 8 min of the mixing process, followed by 8 min of curing time to reach steady conditions. The remaining 25 wt% of the plasticizer was subsequently added and the mixing was continued for an additional 4 min.

For the purpose of analyzing the curing kinetics EPDM, $SnCl_2$ and ZnO (and the plasticizer in the case of plasticized EPDM) were mixed at 100 rpm and 150°C for 8 min. The phenolic resin was subsequently added and the mixing proceeded for an additional 4 min.

At the end of the mixing process, the various blends were immediately quenched in liquid nitrogen to freeze the morphology and stop the curing reaction when applicable.

7.3.3 Melt Mixing: Twin-Screw Extruder

The melt mixing was also carried out using a Leistritz® ZSE 18HP (18 mm) tightly intermeshing co-rotating twin-screw extruder with an *L*/*D* of 40. Processing was carried out at 165 rpm, resulting in an apparent shear rate similar to that of the internal mixer in the final metering zone where the filling factor is equal to one [30]. The temperature profile and the screw configuration used in this work are shown in Figure 7.1. To obtain elastomeric pellets with a uniform size comparable to that of the PP for the melt mixing process, the EPDM was initially grinded in an industrial grinder and subsequently extruded at 100 rpm with the temperature profile shown in Figure 7.1.

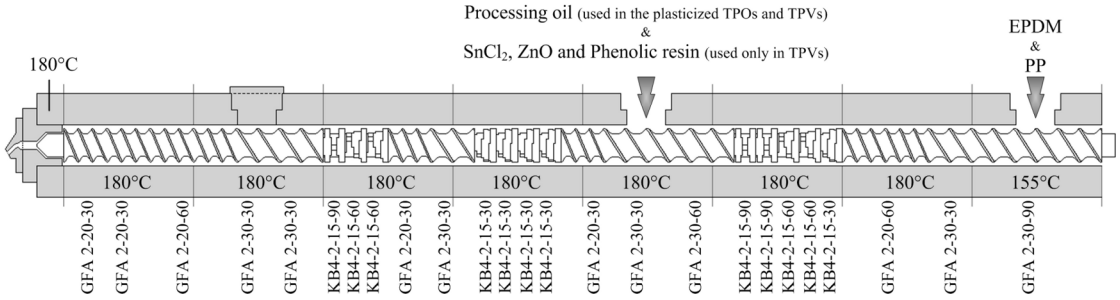

Figure 7.1. The schematic view of the screw configuration along with the temperature profile. (GFA: co-rotating conveying free-meshing elements, KB: kneading blocks; for details on screw element numbering refer to Leistritz® technical data sheets)

The obtained extrudate was dried and then pelletized. For the melt mixing process of TPOs and TPVs, the polymeric components along with the antioxidant were initially dry blended and fed into the feeder. To obtain a homogeneous blend, a two-pass extrusion process was carried out. During the first pass, the initially dry blended polymeric components were extruded. Meantime, depending on the system investigated, the whole amount of plasticizer required for the plasticized blends, and the catalytic components of the curing system (i.e., ZnO and $SnCl_2$) for

the reactive TPVs were added from the side feeder position (Figure 7.1). Subsequently, the extrudate was pelletized and reprocessed immediately for the second pass under the beforementioned operating conditions. During the second pass and merely for TPV compositions, 5 phr of phenolic resin dissolved in acetone were uniformly fed using a HPLC pump at a controlled rate (Figure 7.1). The final extrudate was pelletized for further characterization.

7.3.4 Rheological Measurements

The blends were compression molded at 180°C in the form of 25 mm diameter disks with ~1.5 mm thickness. The rheological measurements were carried out at 180°C using a stress controlled rheometer (TA Instruments® AR-2000) equipped with a parallel plate flow geometry and under a nitrogen atmosphere. Time sweep and frequency sweep experiments were both carried out in the linear viscoelastic range to characterize the thermal stability and the viscoelastic properties of the blends.

The curing behavior of non-plasticized and plasticized EPDM samples was investigated by time sweep experiments using a stress-controlled rheometer (TA Instruments® AR-2000). The EPDM samples were molded in the forms of disks at 165 °C for 4 min to minimize static curing during the molding step. The time sweep experiments were carried out at 10.43 rad/s (frequency stated in ASTM-D2084 for vulcanization of rubbery materials using Oscillatory disk cure meter) [31] with a strain $\gamma \leq 0.1$. The temperature range was set between 135 and 180°C (with 15°C intervals).

7.3.5 Gel Content Measurements

To evaluate the amount of cross-linked elastomer in the TPVs at any given composition, a boiling xylene extraction method was used. For each TPV composition, three pellet size specimens weighting between 0.17-0.20 g were cut and separately placed in 400-mesh size wire netting. Subsequently, each three specimens were directly immersed into a 500 ml round bottom boiling flask containing ~250 ml xylene and attached to a spiral condenser. The extraction was carried out for 6 h. Afterwards, the insoluble residues trapped in the wired mesh were taken out and dried in a vacuum oven at 60°C and weighted. Accordingly, the gel fraction of EPDM in the TPVs was established on the boiling xylene insoluble fraction after making suitable corrections based upon the knowledge of the ingredients. According to Abdou-Sabet and Fath [20], except the possible uncross-linked portion of the elastomeric component, the soluble ingredients used in the TPV formulation of this work are the plasticizer, the polypropylene and the phenolic resin. On the other hand, ingredients such as antioxidant and ZnO are considered as insoluble. As a result, the corrected final weight was obtained by subtracting the weight of the insoluble ingredients. Ultimately, the gel content was obtained using the following correlation:

$$\text{Gel content}\,[\%] = \frac{\text{Final weight}_{\text{corrected}}}{\text{Initial weight of EPDM}} \times 100 \tag{7.1}$$

7.3.6 Morphological Analyses

The blended samples were cryo-microtomed at -150~-170°C using a Leica® RM 2165 equipped with a Leica® LN 21 cryo-chamber. For the extruded samples, the parallel and perpendicular surfaces to the flow direction were both cryo-microtomed. Scanning electron microscopy (SEM) analyses were merely performed on the randomly cut surface of the non-

plasticized and plasticized TPOs after subjecting the samples to fresh *n*-heptane to create the necessary contrast by extracting the exterior EPDM phase. They were then dried and coated with a gold-palladium layer and the experiment was carried out using a Jeol® JSM 840 operated at 10 kV.

Atomic force microscopy (AFM) was as well used to characterize the final morphology of the non-plasticized and plasticized TPOs and TPVs obtained from both internal mixer and twin-screw extruder. The AFM imaging was performed on the cryo-microtomed sections using a Dimension™ 3100 system from Veeco Instruments in tapping mode. The test section in the case of extruded TPOs and TPVs consisted of a randomly cut surface, perpendicular to the flow direction. The experiments were carried out under ambient conditions using a scanning rate of ~0.3-0.7 (Hz), integral gain of ~0.3-0.7 and proportional gain of ~0.6-1.4. The height, phase and amplitude channels were recorded. The phase images of TPO blends were used for subsequent quantitative morphological analyses using a SigmaScan Pro Ver.5 image analysis software. A semi-automatic technique consisting of a digitalizing table was employed to trace the perimeter between the two polymeric phases and, therefore, the interface. The measured interface was then divided by the area of the micrograph to obtain the specific interfacial perimeter (B_A). To do so, between four to five AFM micrographs with various scan sizes ranging between 5 to 15 μm were employed. The specific interfacial perimeters obtained from each of those micrographs were further used to calculate the specific interfacial area, or the average interfacial area per unit volume (Q) of the blends according to the following correlation [32],

$$Q = \frac{4B_A}{\pi} \tag{7.2}$$

the calculated specific interfacial area holds for any cross-section orientation of imaged photos and for any type of non-lamellar morphology [33].

7.4 Results and Discussion

7.4.1 Rheology of Neat Polymers

The thermal stability of the unprocessed and processed pure polymeric components was examined by time sweep of the rheological properties in the linear viscoelastic domain, and all the materials were shown to be thermally stable. The complex viscosity and the storage modulus of the neat polymeric constituents are presented in Figure 7.2. It can be seen that the viscoelastic behavior of PP and EPDM at 180°C are significantly different. The storage modulus and complex viscosity of the PP exhibit a classical viscoelastic behavior with a tendency to reach the terminal zone at low frequencies, where G' is proportional to $\omega^{1.26}$ instead of the theoretical value of ω^2. In the same frequency range, the complex viscosity exhibits a tendency towards a Newtonian plateau.

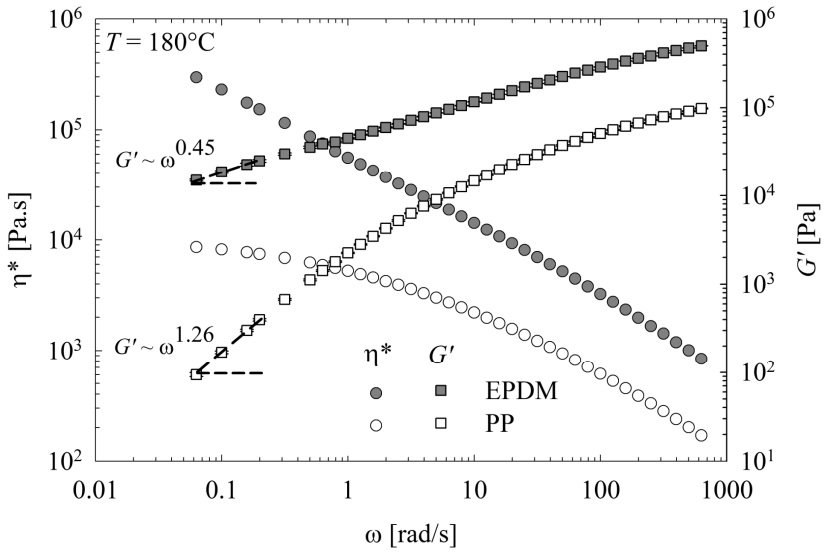

Figure 7.2. Complex viscosity (η^*) and storage modulus (G') of the neat polymeric components as a function of frequency.

This observed viscoelastic behavior is typical of most polyolefins of moderate molecular weight with a linear molecular structure. On the other hand, due to the high Mooney viscosity of the elastomer, the EPDM terminal zone is far from being reached even at the lowest frequency. The complex viscosity of the EPDM also shows a tendency towards a typical yield stress behavior. Therefore, the terminal zone for such a highly elastic substance shall be located at frequencies far below the experimental frequency window. Furthermore, throughout the whole frequency range the EPDM is more viscous and elastic than the PP. Assuming the Cox-Merz [34] relation to be valid for the neat polymeric components [35], the complex viscosity can be interpreted as the steady shear viscosity. Accordingly, at the apparent shear rate of the mixing equipments (i.e., ~50 s^{-1}), the viscosity ratio (η_{EPDM}/η_{PP}) of non-plasticized components is equal to 5.53. Hence, the EPDM phase in the blends shall always be considered less deformable than the PP phase.

7.4.2 TPOs Obtained from Internal Mixer and Twin-Screw Extruder

This section covers the rheology and morphology of TPOs obtained from both internal mixer and twin-screw extruder. The AFM morphologies of EPDM/PP 50/50 (wt/wt%) TPOs obtained from both mixing equipments are shown in Figure 7.3.

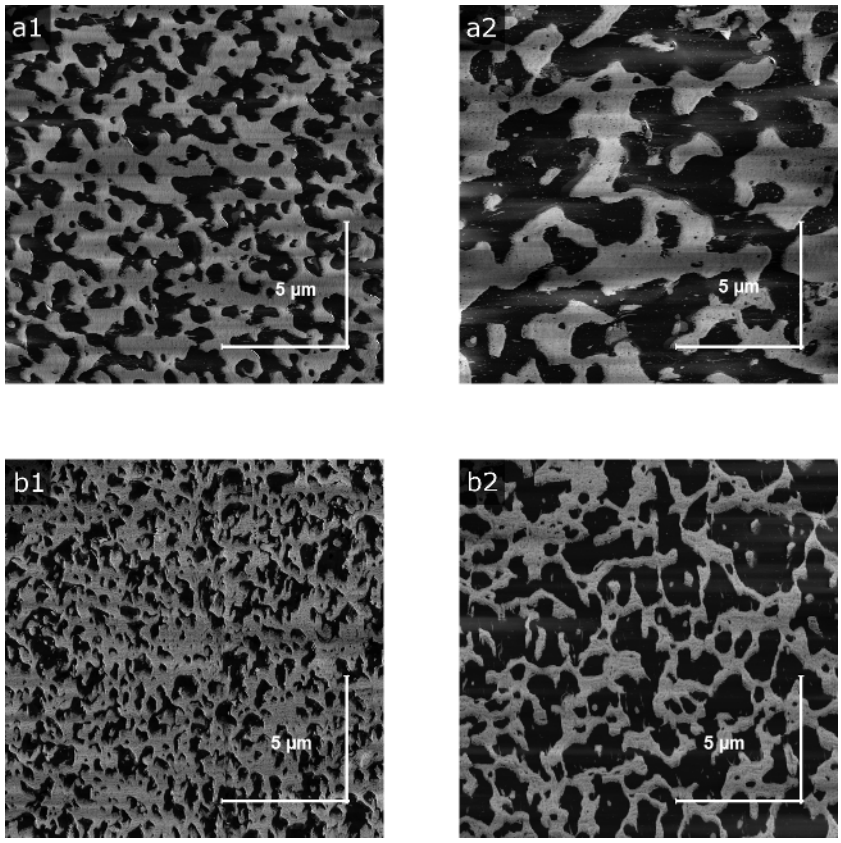

Figure 7.3. AFM phase micrographs of EPDM/PP 50/50 (wt/wt%) TPOs: (a) Internal mixer, (b) Twin-screw extruder. (Column 1: non-plasticized, Column 2: plasticized; Dark phase: EPDM; Bright phase: PP)

These morphologies are characteristics of an interconnected co-continuous structure where both polymeric components present a three-dimensional spatial continuity. The size of the domains is generally dictated by the rheological properties of the polymeric constituents, the mixing and operating conditions and as well by the presence of a plasticizer. Figure 7.3 shows

that the plasticization results in a coarser final morphology with swollen and coalesced elastomeric domains. On the other hand, TPOs prepared in the twin-screw extruder (Figure 7.3 - *row b*) possess a much finer morphology as compared to those prepared in the internal mixer (Figures 7.3 - *row a*). The mentioned differences are quantitatively characterized by the specific interfacial area of these blends (Figure 7.4).

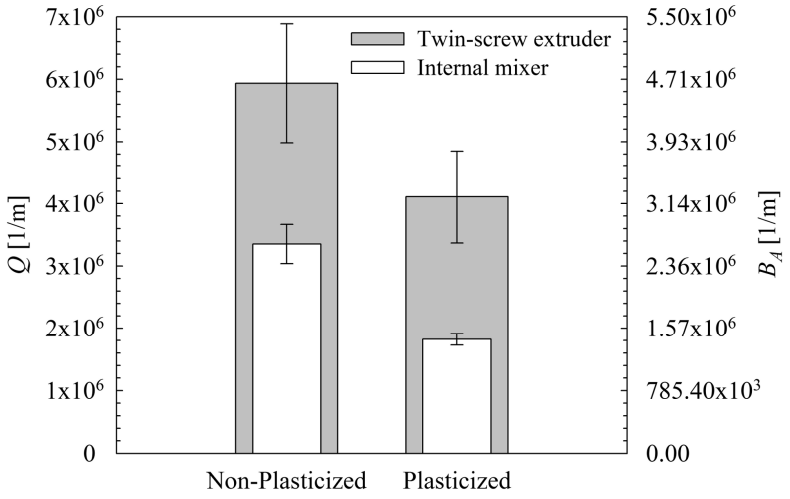

Figure 7.4. The specific interfacial areas (Q) and the specific interfacial perimeters (B_A) of EPDM/PP 50/50 (wt/wt%) TPOs obtained from internal mixer and twin-screw extruder.

Generally the larger the specific interfacial area is, the finer is the morphology. Regardless of plasticization or the type of mixing equipment, the presence of a large specific interfacial area in the TPOs can be largely attributed to the low interfacial tension between the polymeric components, i.e. ~0.3 mN/m @ 190°C [36-38]. Despite the large variability, the ratios of the average specific interfacial areas of the non-plasticized TPOs over the plasticized ones are 1.84 and 1.44 for the blends prepared in the internal mixer and extruder, respectively. The observed coarsening effect of the plasticizer during the melt mixing stage is partly related to the swelling of the EPDM by the plasticizer. According to Ponsard-Fillette et al. [39], a low molecular weight plasticizer diffuses into a highly entangled polymer, e.g. EPDM, and swells the

elastomer without inducing substantial disentanglement. In contrast to the Fickian diffusion process dominant in polypropylene, the former process known as elastic diffusion occurs when the characteristic relaxation time of the polymer is larger than the characteristic time of the diffusion process resulting in less disentanglement and more swelling [39,40]. In addition to the swelling effect of the plasticizer, according to Tufano et al. [41] the diffusion of low molecular weight species from one phase to another, in an extremely diffusive system, may also result in faster coalescence and coarser morphology. Besides the coarsening effect, the plasticization remarkably affects the morphologies of the plasticized extrudates where the elastomeric component is oriented in the flow direction. This can be clearly observed in the SEM micrographs of EPDM/PP 50/50 (wt/wt%) TPOs after the extraction of the EPDM phase as opposed to the non-plasticized TPOs with the same composition (Figure 7.5).

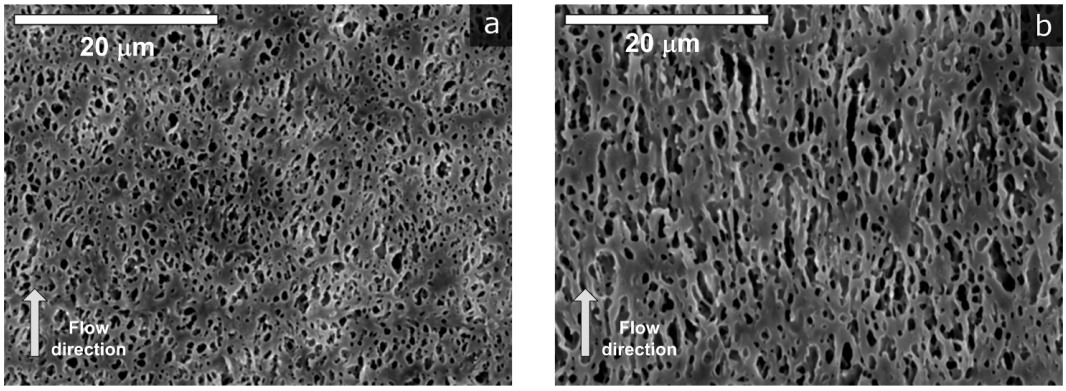

Figure 7.5. SEM micrographs of EPDM/PP 50/50 (wt/wt%) TPOs in the flow direction: (a) Non-plasticized, (b) Plasticized.

The oriented structure of EPDM in the plasticized extrudate at the end of the second pass may imply the predominant presence of the plasticizer in the elastomeric phase. This would result in a large drop of the viscoelastic properties of the elastomeric phase to approximately the same level as the PP phase; otherwise the PP would not be able to deform the highly viscous and elastic EPDM phase. As mentioned earlier, a two-pass extrusion process is used in this study and

after the first pass, the plasticizer may predominantly be redistributed in the elastomeric phase and remaining amorphous fraction of polypropylene due to cooling and PP crystallization [22]. Although in this study the distribution of the plasticizer could not be accurately measured, it is believed that its preferential redistribution into the elastomeric phase prior to the second pass, and its possibly incomplete redistribution into the PP phase during the second pass [39], could possibly lower the viscosity ratio (η_{EPDM}/η_{PP}). In the extreme hypothetical situation where the plasticizer would be completely redistributed in the EPDM phase, the viscosity ratio of plasticized EPDM over that of PP would drop from 5.53 (value for non-plasticized TPOs) to 0.68. This would reasonably explain the ease of interface deformation under flow conditions. However, it is noteworthy to mention that although the decrease in the viscoelastic properties of the elastomeric component and, therefore, the viscosity ratio (η_{EPDM}/η_{PP}) in the presence of a plasticizer should favor a finer morphology, the simultaneous swelling effect of the plasticizer has an opposing effect resulting in a final coarser morphology as depicted by Figure 7.3 - *column* 2.

The mixing equipment may also considerably affect the morphology. The ratios of the average specific interfacial areas of TPOs obtained from the twin-screw extruder over the ones prepared in the internal mixer are 1.77 and 2.25 for non-plasticized and plasticized TPOs, respectively. The twin-screw extrusion process is well known for the presence of significant elongational flow, particularly in the kneading block elements [42], which is highly efficient in deforming and increasing interfacial areas of immiscible blends [43]. Furthermore, the degree of filling inside the extruder channel has an important effect on the amount of shear transferred to the melt. Generally, as the degree of filling decreases, the mean effective channel depth to be taken into account becomes smaller and consequently results in higher local apparent shear rates

[44]. This is usually the condition after the kneading blocks where the pressure drops and the screws become starve fed. On the other hand, the flow field between the rotors and the wall in internal mixers has been regularly considered as simple shear flow [29,45]. Accordingly, the presence of elongation flow and local high shear rates along the screw axis compared to milder flow conditions in the internal mixer might result in larger specific interfacial area for the TPOs obtained from twin-screw extrusion.

To further understand the effect of plasticization and mixing equipment on the morphology and, therefore, on viscoelastic properties of these blends, the low frequency complex viscosity and storage modulus (not presented here) of these blends have been investigated and both show identical trends. The data presented in Figure 7.6 have been obtained at a frequency of 0.063 rad/s. Interestingly, despite the large differences between the morphologies of the non-plasticized TPOs obtained from the internal mixer and the twin-screw extruder, their viscoelastic properties appear to be independent of the mixing conditions.

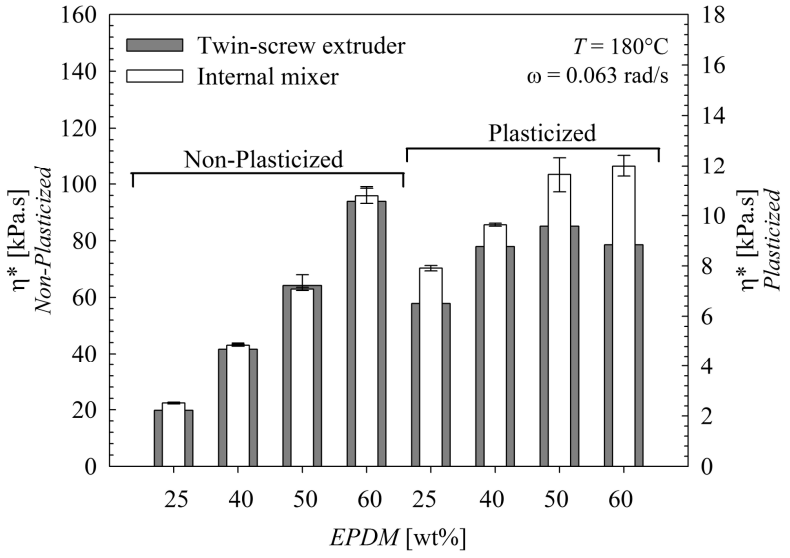

Figure 7.6. Complex viscosity (η^*) data of non-plasticized and plasticized TPOs at 180°C prepared in twin-screw extruder and internal mixer.

Goharpey et al. [19] observed a similar trend for their EPDM/PP-based TPOs. According to Sengers et al. [46], in a low interfacial tension blend the contribution to the elastic properties due to the deformation of the interface, which is directly proportional to the extent of interfacial area, can be overshadowed by the elasticity of the elastomeric phase. Hence, in contrast with typical immiscible blends with a high interfacial tension, for which the low frequency viscoelastic properties are strongly influenced by both composition and morphology, it is merely the EPDM content and its intrinsic viscoelastic properties that control the low frequency data for the non-plasticized EPDM/PP-based TPOs.

However, the former argument does not hold for the plasticized TPOs (Figure 7.6). Due to the likely preferential distribution of the plasticizer into the elastomeric component, the complex viscosity (as well as the storage modulus not reported here) of the EPDM phase may significantly decrease [47] and, therefore, the effect of the interfacial elasticity may become more pronounced at larger EPDM content. Moreover, the viscoelastic properties of TPOs obtained from different mixing equipments are significantly different. The blends obtained from the internal mixer are more viscous and elastic throughout the whole composition range. Furthermore, in contrast with the uniform increase of the viscoelastic properties with EPDM content observed in the non-plasticized TPOs, these properties tend to level off or decrease at high EPDM content. In a previous study conducted in our laboratory [48], an extremum appeared at 75 wt% EPDM for the plasticized TPOs prepared inside the internal mixer and it was attributed to the upper limit of the co-continuity interval. As a result, the appearance of an extremum at 50 wt% EPDM for the plasticized extruded TPOs might be an indication for the shift of the upper limit of co-continuity to a lower value.

7.4.3 Curing Behavior of Non-Plasticized/Plasticized EPDM

The curing behavior of the non-plasticized and plasticized EPDM has been characterized using rheological tools. The aim was to investigate the possible effect of the plasticizer on the curing behavior of EPDM. During the course of the curing reaction, a three dimensional network of chemically cross-linked chains is obtained. This increases the viscoelastic properties of the elastomer (i.e., η^* and G') by strongly affecting the molecular chain mobility. Figure 7.7 presents the evolution of the normalized storage modulus (G'/G'_{NR}) of the non-plasticized and plasticized EPDMs as a function of time.

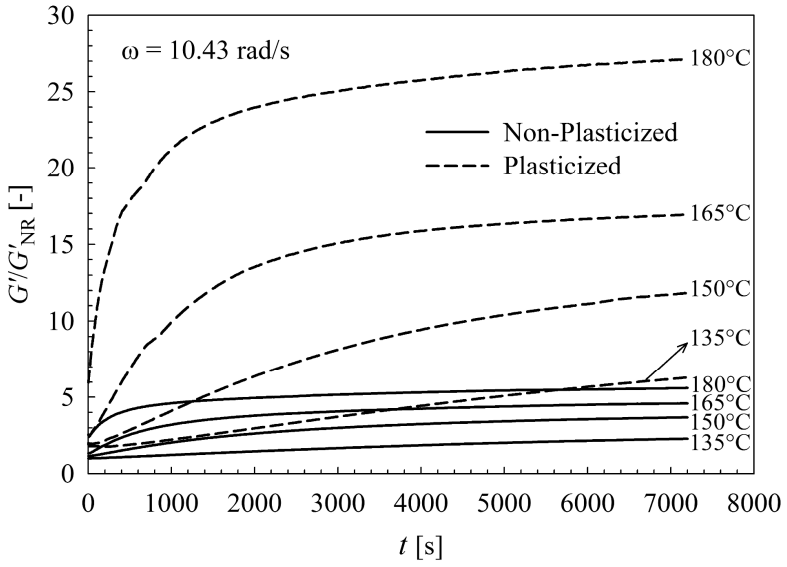

Figure 7.7. The time evolution of normalized storage modulus (G'/G'_{NR}) of non-plasticized and plasticized EPDMs at various temperatures, ω = 10.43 rad/s.

The data are normalized by the storage moduli of the non-reactive elastomer (G'_{NR}) at different temperatures. At the beginning of the rheological characterization, values of the normalized storage modulus larger than one may indicate the presence of a slightly cross-linked network, whereas values lower than unity might indicate the plasticization effect of the curing

system prior to the cross-linking reaction. As shown in Figure 7.7, regardless of plasticization the initial value of G'/G'_{NR} is always larger than unity. It further increases with temperature, demonstrating the heat reactive nature of the phenolic curing system. The effect of the plasticizer can be readily observed by larger initial values of G'/G'_{NR} as opposed to the non-plasticized EPDM. The difference might be directly related to the mixing conditions prior to the rheological experiments. Although the amount of phenolic resin added to the mixture of the plasticized EPDM is lower as compared to the non-plasticized one (as it is based on the total EPDM content), the diffusion of the phenolic resin throughout the sample may be enhanced in the presence of the plasticizer due to the lower viscosity, promoting the reaction with the elastomeric chains. As the curing reaction proceeds as shown in Figure 7.7, the viscoelastic properties rapidly increase and tend towards steady state values. The curing rate is also faster as the temperature increases. Concerning the effect of the plasticizer on the curing rate of EPDM, one shall compare the slope of G' rather than G'/G'_{NR}. The reason lies in the fact that the initial linear slope of G' in Figure 7.7 is divided by its corresponding G'_{NR}, which is lower for the plasticized non-reactive EPDMs. As a result the slope of the plasticized EPDMs appears to be steeper. Furthermore, reaching steady state appears to be faster in the non-plasticized EPDMs. This might be due to the relatively shorter distance between the molecules of the phenolic resin and the reactive sites of EPDM in the absence of the plasticizer, due to the coarser morphology.

To quantify the effect of the plasticizer on the curing rate of EPDM, the "Cure Rate Index" of non-plasticized and plasticized elastomers is obtained according to a procedure based on the ASTM-D2084 method [31]. It is characterized by the time required to reach 50 and 90% modulus increases (i.e., $G'_x = G'_0 + x(G'_f - G'_0)$ where G'_0 and G'_f represent the initial and final storage moduli, respectively with x being 0.5 and 0.9). The "Cure Rate Index" (i.e., $100/(t_x$-

scorch time), the scorch time has been considered zero in this case) of the non-plasticized and plasticized EPDM is presented in Figure 7.8.

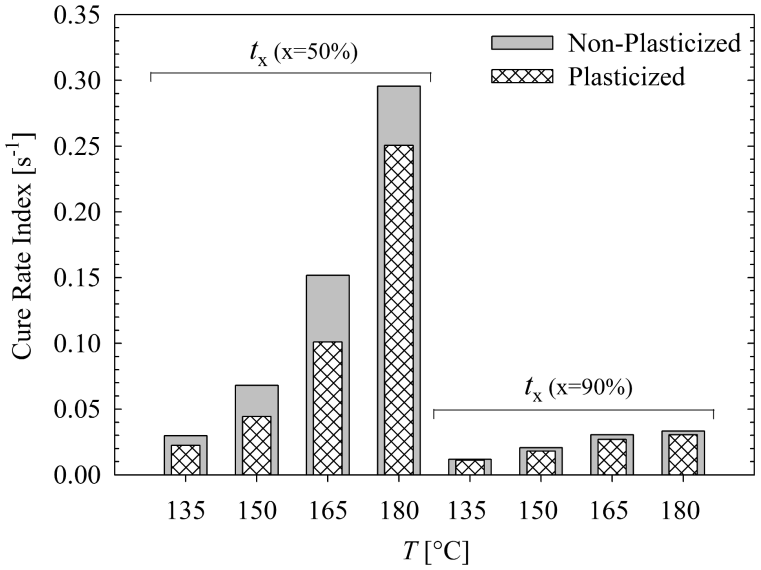

Figure 7.8. "Cure Rate Index" of non-plasticized and plasticized EPDMs calculated based on the time required to reach 50% and 90% modulus increase at various temperatures.

The differences between the "cure rate indices" of the non-plasticized and plasticized elastomers are not significantly different; however, they are slightly larger at $t_{x=50\%}$ as compared to $t_{x=90\%}$, indicating a slightly slower curing reaction in the presence of the plasticizer at an intermediate reaction stage of the curing process. Based upon the same data, the curing activation energies of the non-plasticized and plasticized EPDMs have been calculated. The required times to reach a certain G'_x value (i.e., t_x) at different temperatures ranging from 135 to 180°C follow an Arrhenius-type equation. Accordingly, the plots of $ln(1/t_x)$ vs $1/T$ result in linear curves with their corresponding slopes proportional to the activation energy (E_a). The activation energies for the non-plasticized and plasticized elastomers calculated at $x=50\%$ are 78.9 and 82.6 kJ/mol, respectively. Once again, the slight difference between the values implies a negligible effect of the plasticizer on the curing kinetics of the EPDM at an intermediate stage of the curing reaction.

Nevertheless, at the early stage of the curing reaction, e.g. x =10%, the activation energy was found to be comparably lower in the case of the non-plasticized elastomer, indicating a rapid curing initiation as compared to the plasticized counterpart.

7.4.4 TPVs Obtained from Internal Mixer and Twin-Screw Extruder

This section mainly covers the effects of plasticization and melt mixing processing on the morphology and linear viscoelastic properties of TPVs. In order to compare the cross-linking level of the EPDM phase in different TPVs, their gel content is presented in Figure 7.9. The level of fully cured EPDM has commonly been reported to be 97% [49]. According to Figure 7.9, the elastomeric phase is fully cured for all blend compositions above 50 wt% EPDM independently of plasticization and mixing equipment. It is noteworthy to mention that although the elastomeric chains above a gel content level of approximately 97% are part of a three dimensional cross-linked network, the gel content is known to be insensitive to the cross-link density at high level of cross-linking [13,17].

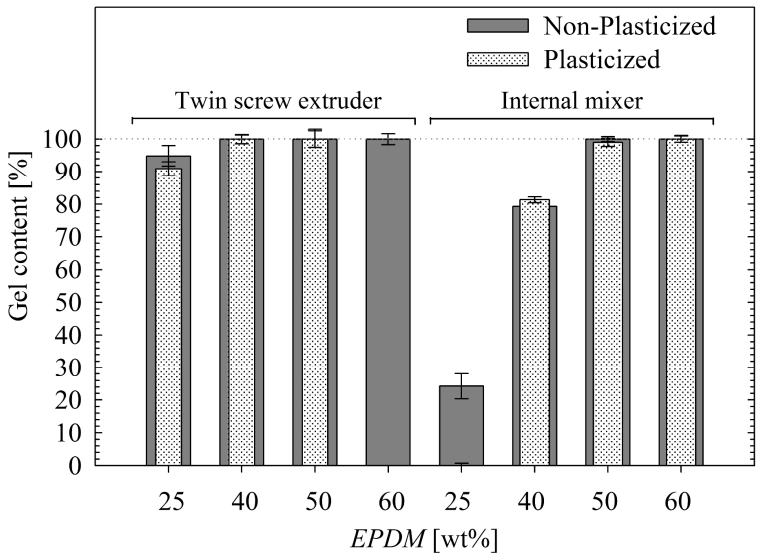

Figure 7.9. Gel content of the EPDM phase in the non-plasticized and plasticized TPVs obtained from different processing equipments.

As a result, the elastomeric chains mobility and, therefore, the deformability of the EPDM phase in TPVs with high level of gel content but different cross-link density shall differ as well. Consequently, despite the similarity of gel content in the TPVs with EPDM content above 50 wt%, their morphologies and viscoelastic properties shall be directly affected by the extent of the cross-linking reaction.

Below 50 wt% of EPDM, the gel content reported in Figure 7.9 is shown to be influenced by both plasticization and mixing procedure. However, the mixing equipment has comparably much larger effect on the final gel content level of the elastomeric phase. The effect of the plasticizer is only noticeable for TPVs containing 25 wt% EPDM prepared in the internal mixer for which the gel content was about zero. The lower level of gel content in these TPVs can be related to the small quantity of the phenolic resin and its distribution into the relatively small amount of the EPDM phase [17], and the dilution effect of the plasticizer. In addition, despite the shorter residence time, the TPVs containing 25 and 40 wt% EPDM prepared by twin-screw

extrusion present a higher level of gel content. This observation implies that the cross-linking reaction inside the twin-screw extruder proceeds relatively faster. This has an important consequence, especially for TPVs above 50 wt% EPDM for which the high gel content does not allow detecting the effect of the melt processing method on the curing reaction. According to the faster cross-linking reaction and the higher gel content level obtained for low EPDM content TPVs processed by extrusion compared to the internal mixer and due to the insensitivity of gel content to cross-link density at higher levels of gel content, it is reasonable to assume that the cross-link density of high EPDM content TPVs is relatively larger for blends prepared by twin-screw extrusion. In another study Sengupta and Noordermeer [13] have also reported a similar trend where higher cross-link density was found for TPVs obtained from twin-screw extrusion as opposed to internal mixer.

The AFM phase morphologies of non-plasticized and plasticized 50/50 (wt/wt%) EPDM/PP TPVs are presented in Figure 7.10. It is noteworthy to remind that TPVs containing 50 wt% EPDM or more have an identical gel content of approximately 100%. In contrast to the morphologies of the non-reactive TPOs consisting of uniform co-continuous structures (Figure 7.3), the morphologies of TPVs with the same level of EPDM content consist of mainly irregular shaped elastomeric domains heterogeneously dispersed in the PP phase.

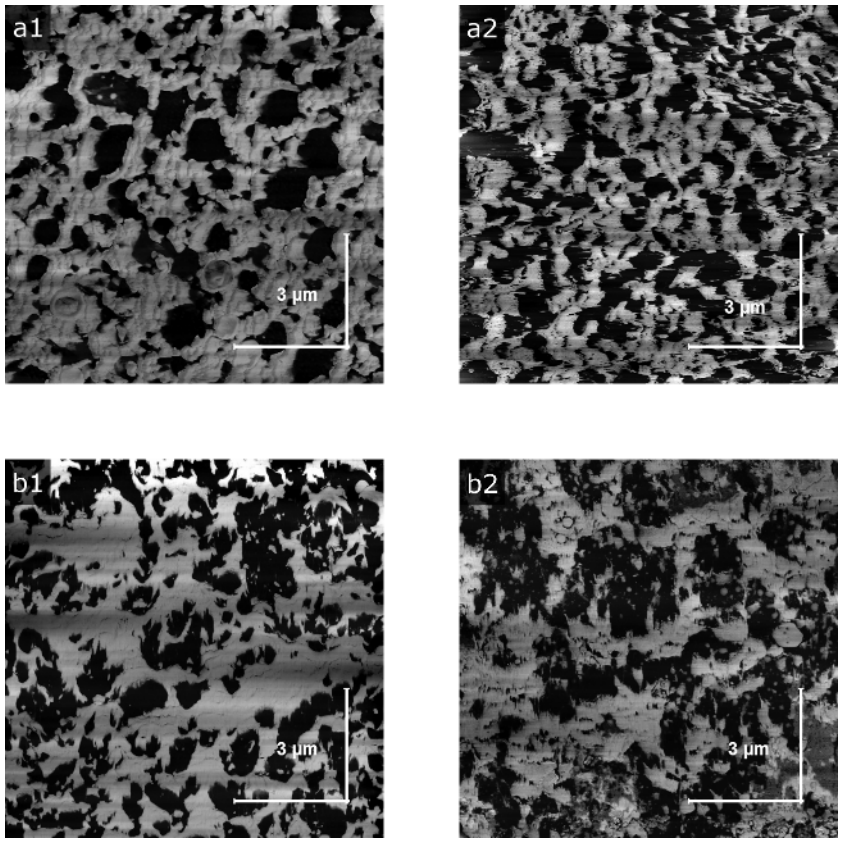

Figure 7.10. AFM phase micrographs of EPDM/PP 50/50 (wt/wt%) TPVs: (a) Internal mixer, (b) Twin-screw extruder. (Column 1: non-plasticized, Column 2: plasticized; Dark phase: EPDM; Bright phase: PP)

Depending on the composition and the processing equipments, the shape of the elastomeric domains in TPVs is known to be irregular with a broad size distribution [17,50]. Differences observed in the morphologies of TPVs in Figure 7.10 shall be seen as a consequence of both plasticization and melt processing conditions. Despite the transformation of the initial uniform co-continuous morphology to an irregular dispersed type during the dynamic vulcanization stage, in the plasticized TPVs (Figure 7.10 - *column* 2) the interconnections between the elastomeric domains are to some extent preserved resulting in larger elastomeric domains in comparison to their corresponding non-plasticized ones prepared through the same mixing equipment (Figure 7.10 - *column* 1). Hence, the non-plasticized TPVs are mainly

composed of distinct cross-linked elastomeric domains (Figure 7.10 - *column* 1), especially in TPVs obtained from the internal mixer (Figure 7.10a1). The rheological properties, the initial morphological state of the plasticized blends prior to dynamic vulcanization (i.e., plasticized TPOs) and the cross-linking rate may noticeably affect the morphology development and, therefore, the dispersion of the elastomeric component in the reactive blends. Compared to the non-plasticized blends, the morphologies of the plasticized TPOs are more of a coarser type co-continuous structure with swollen elastomeric phase (Figure 7.3). Moreover, the probable effect of plasticization on lowering the viscosity ratio prior to the cross-linking reaction may have hindered or delayed the complete dispersion process of EPDM during the dynamic vulcanization. As a result, the EPDM phase may to some extent preserve its continuity in the plasticized TPVs (Figure 7.10 - *column* 2).

On the other hand, similarly to what was observed in TPO morphologies, the melt mixing procedure influences the size of the EPDM domains in the TPVs. The size of the elastomeric domains in TPVs obtained from the internal mixer (Figures 7.10 - *row* a) is more uniform and less irregular in shape than the blends obtained from twin-screw extrusion (Figures 7.10 - *row* b). Sengupta and Noordermeer [13] have also observed uniformity in both size and shape of the elastomeric domains obtained from an internal mixer, and attributed this to the larger residence time inside the internal mixer and, therefore, a larger amount of total shear exerted on the TPVs. Along with the processing conditions, the dispersion of the cross-linked elastomeric component and, therefore, the morphology development in TPVs shall also be related to the degree and rate of the cross-linking reaction during the dynamic vulcanization stage. Martin et al. [51] investigated the importance of the gel content on the dispersion of precross-linked elastomeric domains in the thermoplastic phase. According to the authors, it is crucial to disperse the EPDM phase before its gel content reaches 70%. Beyond that, the cross-linked EPDM phase can no

longer be fragmented and finely dispersed into the PP phase. Studying the morphology development of in-situ cured epoxy in polystyrene (PS), Fenouillot and Perier-Camby [52] found that the morphology of epoxy coarsens drastically at gel content larger than 70% due to the lower deformability of the droplets, and also probably because of the coalescence and agglomeration phenomena. In another study, Deyrail and Cassagnau [53] investigated the extent of in-situ cross-linking of ethylene vinyl acetate (EVA) in poly(dimethylsiloxane) (PDMS) on the final morphology of the dispersed EVA phase. According to them, by adjusting the shear rate with respect to the curing rate, the already elongated EVA phase would have time to relax, disintegrate and form a nodular morphology provided that the level of cross-linking remains low. As a result, the simultaneous dispersion process and chemical cross-linking reaction have a dramatic effect on the final morphology development of TPVs during the dynamic vulcanization stage. According to the above discussion and based on the gel content reported in Figure 7.9, the coarser coalesced morphology observed in TPVs obtained from twin-screw extrusion process may be due to the rapid curing reaction, which inhibits the complete deformation and dispersion of the initial co-continuous EPDM phase into the thermoplastic one.

In addition to the major morphological features observed in Figure 7.10, the high magnification AFM phase morphologies of the TPVs in the micrographs of Figure 7.11 reveal an interesting interfacial phenomenon on the interface between the elastomeric and thermoplastic components.

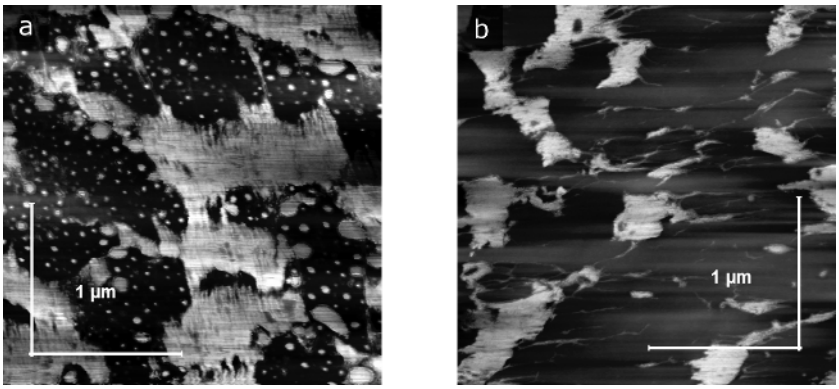

Figure 7.11. AFM phase micrographs of the plasticized EPDM/PP based TPVs: (a) 50/50 (wt/wt%) from twin-screw extruder, (b) 75/25 (wt/wt%) from internal mixer. (Dark phase: EPDM; Bright phase: PP)

During the dynamic vulcanization stage of plasticized systems, some of the PP is pulled out from the thermoplastic phase and form nanometre size PP domains encapsulated by the EPDM phase (Figure 7.11a). This phenomenon is mostly observed for plasticized TPVs prepared by twin-screw extrusion. The AFM micrographs of Figure 7.11 also show a tendency for the PP phase to be stripped off the interface and eroded. This phenomenon can be clearly seen in the plasticized high elastomer content cross-linked blend (75 wt% EPDM), where strings of the PP phase are eroded and pulled into the EPDM phase (Figure 7.11b). The erosion phenomenon and the formation of nanometric inclusions in reactive blends have mainly been reported for in-situ reactive compatibilized blends [54,55]. However, it has also been observed for thermoplastic vulcanizates. In TPVs, Yang et al. [56] have confirmed the presence of occluded PP particles in the dispersed EPDM. Huang et al. [50] have as well observed the same phenomenon where nylon (PA) droplets were formed and encapsulated by the elastomeric phase during the dynamic vulcanization process between maleic anhydride-grafted EPDM and PA. According to these authors, at low degree of cross-linking the thermoplastic PA phase may coalesce and form the continuous phase provided the residence time is long enough.

In the current study, both the viscosity and the elasticity of the elastomeric component increase during the dynamic vulcanization stage. As a result, the shearing stresses exerted by the elastomeric component and transferred through the interface increase. Since the shear stresses are known to progressively decrease as one moves from the interface into the core of the second phase [57], the surface of the PP phase in TPVs becomes less viscous than its core due to its shear-thinning behavior. Furthermore, according to Mighri and Huneault [57], when the shear stress exerted by one of the phases exceeds a critical value, normal stresses may be generated in the second phase and force the interface to grow in the vorticity direction. Moreover, the normal stresses exerted by the more elastic component on the less elastic one cause the latter to form sheets and to stretch perpendicularly to the shear direction [58]. Hence, the increase in the elasticity of the EPDM phase and the simultaneous decrease in the local viscosity of the surface layer of the PP, with the possible generation of normal stresses during the cross-linking reaction, may force the surface layer of PP to be stripped off and eroded. The intensity of this phenomenon may further increase in plasticized TPVs prepared through twin-screw extrusion, where the interface is less viscous due to the presence of the plasticizer and the faster cross-linking reaction and shorter residence time could result in trapped nanometre size PP domains inside the cross-linked EPDM phase.

In addition to the observed morphological features, the viscoelastic properties of TPVs reveal the complex effects of plasticizer, gel content and morphology of these materials. A comparison of the complex viscosities of non-plasticized and plasticized TPVs obtained from both mixing equipments is shown in Figure 7.12, where regardless of plasticization, the viscoelastic properties of the blends obtained from the twin-screw extruder are superior to the ones from the internal mixer.

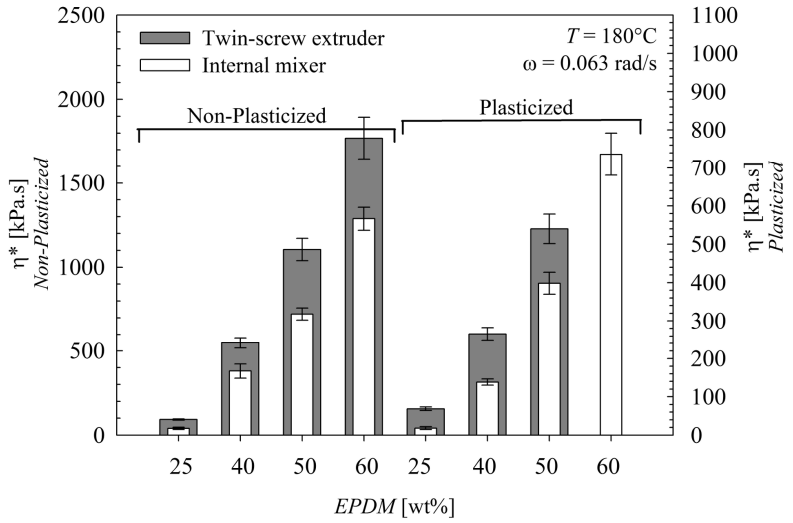

Figure 7.12. Complex viscosity (η^*) data of non-plasticized and plasticized TPVs at 180°C prepared in twin-screw extruder and internal mixer.

The higher gel content and possibly higher cross-link density of TPVs obtained in twin-screw extrusion (Figure 7.9) and their coarser interconnected cross-linked EPDM domains observed in the AFM micrographs (Figure 7.10) are probably responsible for the higher viscoelastic properties. Based on the same argument, comparing the complex viscosity ratio of TPVs over TPOs in Figure 7.13 (numbers appearing on the bars), the difference between the viscoelastic properties of TPVs and TPOs with the same composition is larger for the blends obtained from the twin-screw extruder. The plasticization further increases this ratio, probably due to the presence of swollen and coalesced large cross-linked EPDM domains.

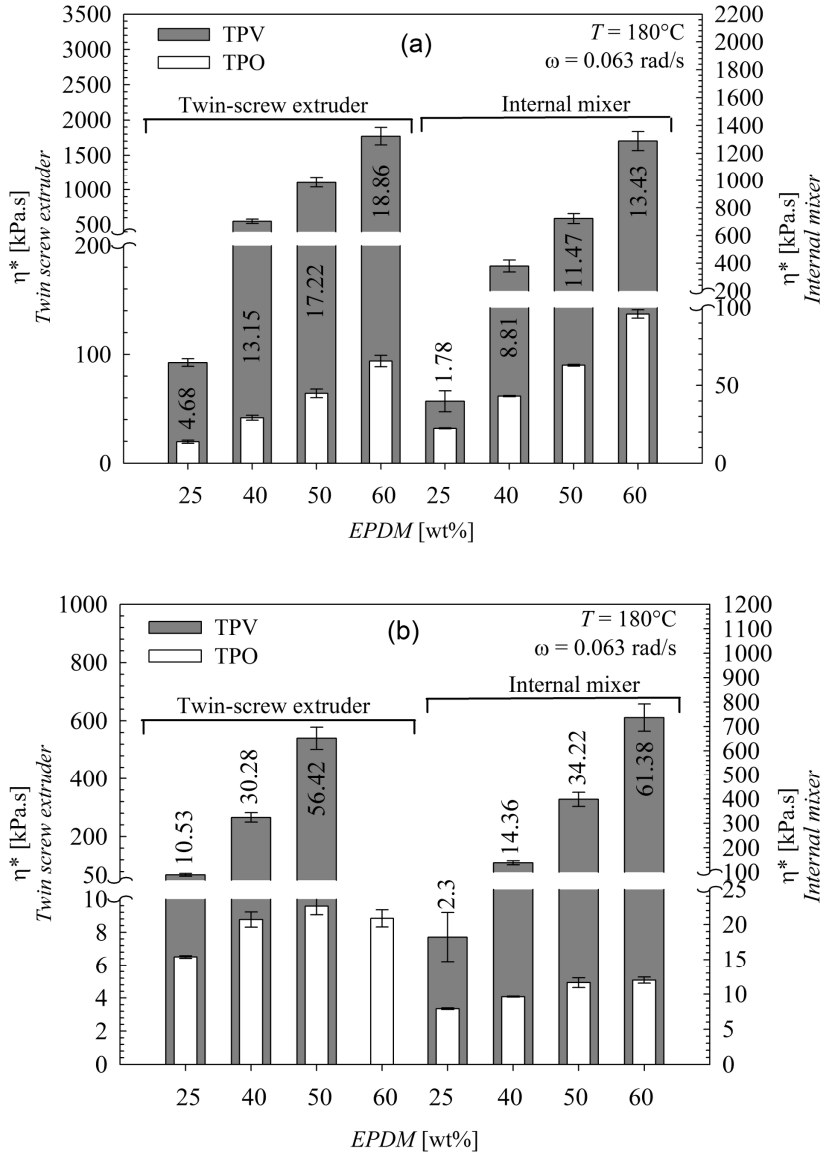

Figure 7.13. Comparison of complex viscosity (η^*) data of TPVs and TPOs at 180°C prepared in twin-screw extruder and internal mixer: (a) Non-plasticized, (b) Plasticized. (The numbers on each bar represent the ratio of complex viscosity of TPVs over TPOs)

7.5 Concluding Remarks

A comparative study on the morphology development and the viscoelastic properties of uncross-linked and cross-linked EPDM/PP-based TPEs is presented. The blends were prepared

using an internal mixer and a co-rotating twin-screw extruder. An AFM phase morphology imaging was used to investigate the effects of plasticizer and processing equipments on the morphology of these blends. In uncross-linked blends (TPOs), the presence of the plasticizer and its probable elastic diffusion into the elastomeric phase resulted in a swollen and coalesced EPDM phase and, therefore, a coarser TPO morphology. On the other hand, despite the similar average apparent shear rate used in both mixing equipments, the intensive flow field inside the twin-screw extruder resulted in a finer morphology in comparison to the internal mixer.

In dynamically cross-linked blends (TPVs), various factors such as plasticization, mixing intensity and more importantly the curing kinetics of the elastomeric component simultaneously affected the morphology development. Although the initial curing behavior of the neat EPDM studied during a static curing situation was slightly retarded in the presence of the plasticizer, its overall curing kinetics in the intermediate and final stage of the cross-linking reaction appeared to be independent of the plasticization. In addition, despite the shorter residence time inside the twin-screw extruder in comparison to the internal mixer, the cross-linking reaction was found to proceed comparably faster and resulted into more heterogeneous and larger cross-linked EPDM domains dispersed in the thermoplastic phase.

Finally, the combined effects of composition, plasticization, morphology and curing state were all reflected in the viscoelastic properties of the various systems. With the exception of the non-plasticized TPO blends, where the rheological properties appeared to be mostly controlled by the EPDM content rather than the phase morphology, the rheological behavior of the other blends was directly associated to phase morphology and the curing state of the elastomeric component.

Based on the results obtained in this study and due to the crucial role of the continuous extrusion process and the importance of achieving a finely dispersed elastomeric phase in TPVs, a multiple step plasticization and cross-linking reaction is recommended. A step wise addition of

the plasticizer along the extruder axis would probably result in a finer initial co-continuous morphology and, therefore, thinner elastomeric ligaments for the proper dispersion of the EPDM phase during the subsequent dynamic vulcanization stage, whereas a step wise curing reaction would possibly provide a gradual cross-linking and, therefore, the complete disintegration and finer dispersion of the elastomeric phase in the thermoplastic matrix.

7.6 References

1. J.G. Drobny, *Handbook of thermoplastic elastomers*, William Andrew Pub., Norwich, NY (2007).
2. A.Y. Coran, R.P. Patel, and D. Williams, *Rubber Chem. Technol.*, **55(1)**, 116-136 (1982).
3. C.H. Lei, X.B. Huang, and F.Z. Ma, *Polym. Adv. Technol.*, **18(12)**, 999-1003 (2007).
4. K. Naskar, and J.W.M. Noordermeer, *Prog. Rubber Plast. Tech.*, **21(1)**, 1-26 (2005).
5. A.M. Gessler, and W.H. Haslett, U.S. Patent, 3,037,954 (1962).
6. H.-J. Radusch, "Phase Morphology of Dynamically Vulcanized Thermoplastic Vulcanizates", C. Harrats, S. Thomas, and G. Groeninckx, In: *Micro- and nanostructured polymer blend systems: phase morphology and interfaces*, CRC/Taylor & Francis: Boca Raton, FL (2006).
7. G. Holden, *Understanding thermoplastic elastomers*, Hanser Gardner Pub., Inc., Cincinnati, OH (2000).
8. N. Dufaure, P.J. Carreau, M.C. Heuzey, and A. Michel, *J. Polymer Eng.*, **25(3)**, 187-216 (2005).
9. C. Joubert, P. Cassagnau, A. Michel, and L. Choplin, *Polym. Eng. Sci.*, **42(11)**, 2222-2233 (2002).
10. H.-J. Radusch, and T. Pham, *Kautsch. Gummi Kunstst.*, **49(4)**, 249-257 (1996).

11. F. Goharpey, A.A. Katbab, and H. Nazockdast, *J. Appl. Polym. Sci.*, **81(10)**, 2531-2544 (2001).

12. F. Goharpey, A.A. Katbab, and H. Nazockdast, *Rubber Chem. Technol.*, **76(1)**, 239-252 (2003).

13. P. Sengupta, and J.W.M. Noordermeer, *J. Elastomers Plast.*, **36(4)**, 307-331 (2004).

14. A. Verbois, P. Cassagnau, A. Michel, J. Guillet, and C. Raveyre, *Polym. Int.*, **53(5)**, 523-535 (2004).

15. A. Bouilloux, B. Ernst, A. Lobbrecht, and R. Muller, *Polymer*, **38(19)**, 4775-4783 (1997).

16. T. Pham, H.-J. Radusch, and T. Winkelmann, *Proceedings of the International conference 'Polymers in the Third Millenium'*, 123 (2001).

17. A. Machado, and M. van Duin, *Polymer*, **46(17)**, 6575-6586 (2005).

18. H.G. Fritz, U. Bolz, and Q. Cai, *Polym. Eng. Sci.*, **39(6)**, 1087-1099 (1999).

19. F. Goharpey, R. Foudazi, H. Nazockdast, and A.A. Katbab, *J. Appl. Polym. Sci.*, **107(6)**, 3840-3847 (2008).

20. S. Abdou-Sabet, and M.A. Fath, U.S. Patent, 4,311,628 (1982).

21. T. Abraham, K.-S. Shen, and N.G. Barber, U.S. Patent, 7,276,559 (2007).

22. M.D. Ellul, *Rubber Chem. Technol.*, **71(2)**, 244-276 (1998).

23. B. Ohlsson, H. Hassander, and B. Tornell, *Polym. Eng. Sci.*, **36(4)**, 501-510 (1996).

24. R. Winters, J. Lugtenburg, V.M. Litvinov, M. van Duin, and H.J.M. de Groot, *Polymer*, **42(24)**, 9745-9752 (2001).

25. K. Jayaraman, V.G. Kolli, S.-Y. Kang, S. Kumar, and M.D. Ellul, *J. Appl. Polym. Sci.*, **93(1)**, 113-121 (2004).

26. W.G.F. Sengers, M. Wubbenhorst, S.J. Picken, and A.D. Gotsis, *Polymer*, **46(17)**, 6391-6401 (2005).

27. V.M. Litvinov, *Macromolecules*, **39(25)**, 8727-8741 (2006).

28. T. Abraham, N.G. Barber, and M.P. Mallamaci, *Rubber Chem. Technol.*, **80(2)**, 324-339 (2007).

29. M. Bousmina, A. Ait-Kadi, and J.B. Faisant, *J. Rheol.*, **43(2)**, 415-433 (1999).

30. C. Rauwendaal, *Polymer extrusion*, Hanser Gardner Pub., Cincinnati, OH (2001).

31. In ASTM Standard D2084-01; Annu. Book of ASTM Stand., 2001.

32. J.C. Russ, *Practical stereology*, Plenum Press, New York, NY (1986).

33. J.A. Galloway, M.D. Montminy, and C.W. Macosko, *Polymer*, **43(17)**, 4715-4722 (2002).

34. W.P. Cox, and E.H. Merz, *J. Polym. Sci.*, **28**, 619-622 (1958).

35. O. Chung, and A.Y. Coran, *Rubber Chem. Technol.*, **70(5)**, 781-797 (1997).

36. H. Shariatpanahi, H. Nazokdast, B. Dabir, K. Sadaghiani, and M. Hemmati, *J. Appl. Polym. Sci.*, **86(12)**, 3148-3159 (2002).

37. M. Hemmati, H. Nazokdast, and H.S. Panahi, *J. Appl. Polym. Sci.*, **82(5)**, 1129-1137 (2001).

38. P.A. Bhadane, M.F. Champagne, M.A. Huneault, F. Tofan, and B.D. Favis, *Polymer*, **47(8)**, 2760-2771 (2006).

39. M. Ponsard-Fillette, C. Barres, and P. Cassagnau, *Polymer*, **46(23)**, 10256-10268 (2005).

40. J.S. Vrentas, and J.L. Duda, *J. Polym. Sci., Part B: Polym. Phys.*, **15(3)**, 441-453 (1977).

41. C. Tufano, G.W.M. Peters, P. van Puyvelde, and H.E.H. Meijer, *J. Colloid Interface Sci.*, **328(1)**, 48-57 (2008).

42. C. Harrats, S. Thomas, and G. Groeninckx, *Micro- and nanostructured polymer blend systems: phase morphology and interfaces*, CRC/Taylor & Francis, Boca Raton, FL (2006).

43. Z. Tadmor, and C.G. Gogos, *Principles of polymer processing*, Wiley-Interscience, Hoboken, NJ (2006).

44. H. Potente, J. Ansahl, and B. Klarholz, *Int. Polym. Process.*, **9(1)**, 11-25 (1994).

45. L. Adragna, F. Couenne, P. Cassagnau, and C. Jallut, *Ind. Eng. Chem. Res.*, **46(22)**, 7328-7339 (2007).

46. W.G.F. Sengers, P. Sengupta, J.W.M. Noordermeer, S.J. Picken, and A.D. Gotsis, *Polymer*, **45(26)**, 8881-8891 (2004).

47. N. Nakajima, and E.R. Harrell, *J. Rheol.*, **26(5)**, 427-458 (1982).

48. S. Shahbikian, P.J. Carreau, M.C. Heuzey, M.D. Ellul, J. Cheng, P. Shirodkar, and H.P. Nadella, *Polym. Eng. Sci.*, **In press** (2010).

49. S. Abdou-Sabet, and S. Datta, "Thermoplastic Vulcanizates", D.R. Paul, and C.B. Bucknall, In: *Polymer Blends*, Wiley: New York, NY (2000), pp 517.

50. H. Huang, T. Ikehara, and T. Nishi, *J. Appl. Polym. Sci.*, **90(5)**, 1242-1248 (2003).

51. G. Martin, C. Barres, P. Sonntag, N. Garois, and P. Cassagnau, *Eur. Polym. J.*, **45(11)**, 3257-3268 (2009).

52. F. Fenouillot, and H. Perier-Camby, *Polym. Eng. Sci.*, **44(4)**, 625-637 (2004).

53. Y. Deyrail, and P. Cassagnau, *J. Rheol.*, **48(3)**, 505-524 (2004).

54. H.Y. Kim, U. Jeong, and J.K. Kim, *Macromolecules*, **36(5)**, 1594-1602 (2003).

55. P.A. Bhadane, A.H. Tsou, J. Cheng, and B.D. Favis, *Macromolecules*, **41(20)**, 7549-7559 (2008).

56. Y. Yang, T. Chiba, H. Saito, and T. Inoue, *Polymer*, **39(15)**, 3365-3372 (1998).

57. F. Mighri, and M.A. Huneault, *J. Appl. Polym. Sci.*, **100(4)**, 2582-2591 (2006).

58. L. Levitt, C.W. Macosko, and S.D. Pearson, *Polym. Eng. Sci.*, **36(12)**, 1647-1655 (1996).

CHAPTER 8

GENERAL DISCUSSIONS

Due to the importance of phase morphology and plasticization in the thermoplastic elastomer industry, the main objective of this dissertation was to elucidate the effect of plasticization on the morphology development and rheological properties of the non-reactive (TPOs) and reactive (TPVs) EPDM/PP-based blends. To achieve this goal, two different mixing equipments such as internal mixer and twin-screw extruder, along with several characterization techniques such as solvent extraction, rheology, scanning electron microscopy (SEM) and atomic force microscopy (AFM) were employed. In the following paragraphs, a general discussion is provided to emphasize the essential role played by various factors as determined by the mentioned characterization techniques, especially the two most frequently used techniques, i.e. rheology and microscopy, throughout this study.

The combination of all the mentioned characterization tools have essentially been crucial to illustrate the effects of plasticization on the main morphological feature of the non-reactive TPOs, i.e. co-continuity interval, as the initial morphological state prior dynamic vulcanization step required to obtain EPDM/PP-based TPVs. The selective solvent extraction of the EPDM phase along with the AFM microscopy provided a comprehensive picture of how the plasticizer may coarsen the phase morphology and promote a rapid percolation by swelling and coalescing the elastomeric phase. The rheology and especially the linear viscoelastic properties of the TPOs on the other hand offered an alternative tool to characterize the co-continuity interval. However, despite the promising literature data on the use of rheology to determine the co-continuity interval, the viscoelastic properties of the TPOs appeared to be overshadowed by the elasticity of

the EPDM phase, which to some extent limited the use of rheology as a characterization tool. In addition, the possible existence of a plasticized interphase was also revealed through modeling the viscoelastic properties of the co-continuous plasticized TPOs.

The actual processing route for the production of TPOs and TPVs is generally through an industrial continuous mixing process, such as twin-screw extrusion, but the flow complexities inside such machinery have always hindered researchers from studying the effect of flow field on the morphology development. Hence, rheology and specifically transient rheological measurements have been exceptional characterization tools, capable of providing a homogenous flow field for structure development studies in emulsions and suspensions. Accordingly in this study, the transient start-up (stress growth) experiments performed on the non-reactive and reactive precursor EPDM/PP blends along with the AFM phase morphologies obtained from samples frozen at different shearing stages provided numerous valuable information. It appeared that even a low intensity homogenous shear flow field was capable of deforming and orienting the complex interfaces in highly viscous and elastic non-reactive blends, resulting in coalescence. The AFM phase morphologies further revealed the presence of highly elongated structure with no substantial interfacial instabilities in high elastomer content blends.

Interestingly in the reactive blends, rheology (dynamic rheological measurements) provided valuable information concerning the plasticization effect on the cross-linking kinetics of the elastomeric component, confirming a slower reaction in the presence of the plasticizer. Furthermore, the tendency of the elastomeric phase to be encapsulated by the thermoplastic phase was an additional appealing phenomenon captured by the AFM phase microscopy in the non-plasticized reactive blends subjected to longer shearing times. However, the observed phenomenon, i.e. the presence of highly elongated structures in the non-reactive and encapsulated

cross-linked elastomeric phase in the reactive blends, appeared to be considerably suppressed in the presence of the plasticizer.

As the final part of this research work, the SEM and AFM phase microscopy techniques assisted in distinguishing the morphological differences between non-plasticized/plasticized TPOs and TPVs prepared by two different mixing equipments, i.e. internal mixer and twin-screw extruder. In addition to the coarsening effect of the plasticizer observed previously by the AFM phase microscopy, the presence of elongated EPDM domains in the SEM micrographs of the extruded plasticized TPOs confirmed the idea of predominant distribution of plasticizer in the elastomeric component. Furthermore, in the AFM phase micrographs of dynamically cross-linked blends (TPVs), the plasticization appeared to hinder the complete disintegration and dispersion of the elastomeric component, preserving to some extent its coarser elastomeric continuous morphology. However, the most striking phenomenon captured by AFM phase microscopy was the surface layer erosion of the polypropylene in the plasticized TPVs, resulting in nanometre size occluded PP domains encapsulated by the cross-linked EPDM phase. On the other hand, the observed overall morphological trends in most TPOs and TPVs (along with the curing states in TPVs) have also been reflected in their dynamic rheological measurements, reassuring the morphology/rheology relationship in these blends.

As described above, among the aforementioned characterization techniques, rheology and AFM phase microscopy constituted the essential part of this research work, where their parallel use provided a unique capability of establishing the rheology/morphology relationship in the thermoplastic elastomers (TPEs).

CHAPTER 9

CONCLUSIONS AND RECOMMENDATIONS

9.1 Conclusions

This research work studied the morphology development of uncross-linked and cross-linked EPDM/PP-based thermoplastic elastomers in the presence and absence of a paraffinic plasticizer. The following conclusions have been drawn for each of the main three parts of the work.

PART I: The co-continuity interval and the linear viscoelastic response of the non-reactive EPDM/PP-based blends (TPOs) in the presence and absence of plasticizer.

1. The addition of plasticizer appears to swell and increase the interconnectivity of the elastomeric component (EPDM) and results in a coarser morphology. Consequently, it shifts the percolation threshold to a lower EPDM contents and slightly narrows the co-continuity interval.

2. The addition of the plasticizer reduces the elasticity, viscosity and the differences between the rheological properties of the pure polymeric components. Its presence further reduces the differences between the rheological properties of their corresponding TPO blends.

3. Due to the highly elastic nature of EPDM, the low frequency storage modulus data of the TPOs do not provide a quantitative measure of the co-continuity interval (either only one extremum or none). However, the loss tangent data based on the chemical gel approach

appears to be a comparably better measure of co-continuity especially in the plasticized TPOs.

4. Among the existing semi-empirical phase inversion models, only the viscosity ratio-based models with minimum dependency of the phase inversion composition to the viscosity ratio appeares to be the most appropriate.

5. The use of the Veenstra-D micro-mechanical model to predict the viscoelastic properties of co-continuous plasticized TPOs leads to the conclusion that a certain amount of plasticizer may be present at the interface between the polymeric components, resulting in a plasticized interphase.

PART II: The morphology development of non-reactive and reactive EPDM/PP-based blends in the absence and presence of plasticizer subjected to transient start-up (stress growth) experiments:

6. The specific interfacial area (Q) of the non-reactive EPDM/PP blends subjected to multiple start-up transient experiments reduces throughout the consecutive shearing steps. The coalescence appears to be more pronounced in the non-plasticized low EPDM content blends; and the plasticization results in a less elongated fibrillar morphology.

7. A highly elongated stable morphology is obtained for non-plasticized high elastomer content non-reactive blends subjected to multiple start-ups, with no substantial interfacial instabilities, break-up or shape relaxation towards sphericity.

8. The phenomenological Lee and Park model fairy well predicts the evolution of the specific interfacial areas (Q) of the non-reactive EPDM/PP blends throughout the multiple start-up transient experiments.

9. On the other hand, the interface in the reactive EPDM/PP-based blends subjected to single start-up transient experiments of various durations is transformed into less elongated domains with irregular interface, but of larger specific interfacial area (Q).

10. The EPDM phase in the non-plasticized high elastomer content reactive EPDM/PP-based blends is transformed into coarse cross-linked EPDM domains encapsulated by the thermoplastic phase at longer shearing times, showing a tendency towards phase inversion.

11. The plasticization results in delayed curing reaction, coagulated and coalesced cross-linked elastomeric domains at longer shearing times, with no tendency towards encapsulation or phase inversion.

PART III: The morphology development and rheological properties of non-plasticized and plasticized EPDM/PP-based TPOs and TPVs obtained from internal mixer and twin-screw extruder.

12. Regardless of the mixing equipment, the presence of the plasticizer results in a swollen and coalesced EPDM phase, reducing significantly the specific interfacial area (Q) of the uncross-linked blends (TPOs).

13. Regardless of plasticization, the TPOs prepared by twin-screw extrusion possess larger specific interfacial area (Q) and a finer morphology in comparison to the ones obtained from the internal mixer.

14. According to the AFM micrographs of extruded TPOs, the plasticizer appears to be predominantly distributed in the EPDM phase, enabling its deformation in the flow direction.

15. Dynamic cross-linking of the EPDM phase generally results in dispersed cross-linked EPDM domains dispersed in the thermoplastic phase. However, the plasticization once more shows a coarsening effect, leading towards cross-linked interconnected elastomeric domains as opposed to distinct ones observed in the non-plasticized TPVs.

16. Interestingly, despite the shorter residence time inside the twin-screw extruder in comparison to the internal mixer, the cross-linking reaction appears to proceed comparably faster during extrusion, resulting in a higher gel content.

17. The faster cross-linking reaction, the shorter residence time inside the twin-screw extruder and, therefore, the smaller total shear exerted on the TPVs hinders the dispersion of the EPDM phase, resulting in larger cross-linked elastomeric domains, heterogeneously dispersed in the PP phase.

18. In the plasticized TPVs, the surface of the PP phase appears to be eroded and stripped off, resulting in nanometre size PP domains encapsulated by the cross-linked EPDM phase. This interfacial phenomenon is attributed to the increase in the elasticity of the EPDM phase during dynamic cross-linking stage and the simultaneous decrease in the local viscosity of the polypropylene due to both its shear-thinning behavior and the presence of the plasticizer.

9.2 Recommendations

Following the findings of this work, the following recommendations are proposed.

1. In addition to what has been studied in this work by keeping a constant plasticizer content, i.e. 100 phr, it would be interesting to study the effect of plasticizer content on the morphology and rheological behavior of uncross-linked and cross-linked EPDM/PP blends at various constant EPDM/PP ratios.

2. As for the case of reactive EPDM/PP blends, it would be recommended to alter the composition of the curing system (kept constant throughout this study) and consequently to investigate its effect on the cross-linking reaction rate and, therefore, on the morphology development. It is believed that a slower reaction will favor a finer morphology of the TPVs.

3. Since the actual processing route for the preparation of TPOs and TPVs is through continuous extrusion process, it would be interesting to study the effects of screw configuration, feeding sequence and multiple step plasticization and cross-linking reaction (in the case of TPVs) on the final morphology.

4. It is recommended to carry out a detail study on the erosion phenomenon observed on the interface between EPDM and PP and the formation of the nanometric polypropylene inclusions in the reactive plasticized blends.

5. Concerning the morphology development in a homogenous flow field, in addition to the transient start-up (stress growth) experiments presented in this dissertation, it would be

recommended to study the transient behavior through creep experiments at various stress levels.

6. Concerning the morphological analyses, it would be interesting to quantify the anisotropy of the interface by obtaining the components of the anisotropy tensor (**q**). This information along with the specific interfacial area (Q) would provide a complete representation of the morphological state in an immiscible blend with complex interfaces.

REFERENCES

American Society for Testing and Materials (ASTM). (2001). *Standard Test Method for Rubber Property - Vulcanization Using Oscillating Disk Cure Meter*. Annual Book of ASTM Standards Vol. 09.01, ASTM Standard D2084-01.

The Freedonia Group, Inc. (2005). *World thermoplastic elastomers*. Cleveland, OH.: FREEDONIA GROUP, I.

ABDOU-SABET, S., & DATTA, S. (2000). Thermoplastic Vulcanizates. In PAUL, D. R., & BUCKNALL, C. B., *Polymer Blends* (Vol. 2: Performance, pp. 517). New York, NY: Wiley.

ABDOU-SABET, S., & FATH, M. A. (1982). *Thermoplastic elastomeric blends of olefin rubber and polyolefin resin*. US Patent 4,311,628.

ABDOU-SABET, S., PUYDAK, R. C., & RADER, C. P. (1996). Dynamically vulcanized thermoplastic elastomers. *Rubber Chemistry and Technology*, *69*(3), 476-494.

ABRAHAM, T., & BARBER, N. G. (2009). *Method for improving the compression set in thermoplastic vulcanizates*. US Patent 7,504,458.

ABRAHAM, T., BARBER, N. G., & MALLAMACI, M. P. (2007). Oil distribution in iPP/EPDM thermoplastic vulcanizates. *Rubber Chemistry and Technology*, *80*(2), 324-339.

ABRAHAM, T., SHEN, K.-S., & BARBER, N. G. (2007). *Soft thermoplastic elastomers*. US Patent 7,276,559.

ADRAGNA, L., COUENNE, F., CASSAGNAU, P., & JALLUT, C. (2007). Modeling of the complex mixing process in internal mixers. *Industrial & Engineering Chemistry Research*, *46*(22), 7328-7339.

ARAKI, T., & WHITE, J. L. (1998). Shear viscosity of rubber modified thermoplastics: Dynamically vulcanized thermoplastic elastomers and ABS resins at very low stress. *Polymer Engineering and Science*, *38*(4), 590-595.

ASTRUC, M., & NAVARD, P. (2000). Influence of the elasticity ratio on the point of phase inversion in an immiscible polymer blend. *Macromolecular Symposia*, *149*, 81-85.

AVGEROPOULOS, G. N., WEISSERT, F. C., BIDDISON, P. H., & BOEHM, G. G. A. (1976). Heterogeneous blends of polymers. Rheology and morphology. *Rubber Chemistry and Technology*, *49*(1), 93-104.

BATCHELOR, G. K. (1970). Stress system in a suspension of force-free particles. *Journal of Fluid Mechanics*, *41*(3), 545-570.

BHADANE, P. A., CHAMPAGNE, M. F., HUNEAULT, M. A., TOFAN, F., & FAVIS, B. D. (2006). Continuity development in polymer blends of very low interfacial tension. *Polymer*, *47*(8), 2760-2771.

BHADANE, P. A., CHAMPAGNE, M. F., HUNEAULT, M. A., TOFAN, F., & FAVIS, B. D. (2006). Erosion-dependant continuity development in high viscosity ratio blends of very low interfacial tension. *Journal of Polymer Science, Part B: Polymer Physics*, *44*(14), 1919-1929.

BHADANE, P. A., TSOU, A. H., CHENG, J., & FAVIS, B. D. (2008). Morphology Development and Interfacial Erosion in Reactive Polymer Blending. *Macromolecules*, *41*(20), 7549-7559.

BOUILLOUX, A., ERNST, B., LOBBRECHT, A., & MULLER, R. (1997). Rheological and morphological study of the phase inversion in reactive polymer blends. *Polymer*, *38*(19), 4775-4783.

BOURRY, D., & FAVIS, B. D. (1998). Cocontinuity and phase inversion in HDPE/PS blends: Influence of interfacial modification and elasticity. *Journal of Polymer Science, Part B: Polymer Physics*, *36*(11), 1889-1899.

BOUSMINA, M. (1999). Rheology of polymer blends: linear model for viscoelastic emulsions. *Rheologica Acta*, *38*(1), 73-83.

BOUSMINA, M., AIT-KADI, A., & FAISANT, J. B. (1999). Determination of shear rate and viscosity from batch mixer data. *Journal of Rheology*, *43*(2), 415-433.

BOUSMINA, M., AOUINA, M., CHAUDHRY, B., GUENETTE, R., & BRETAS, R. E. S. (2001). Rheology of polymer blends: non-linear model for viscoelastic emulsions undergoing high deformation flows. *Rheologica Acta*, *40*(6), 538-551.

BOUSMINA, M., & MULLER, R. (1993). Linear viscoelasticity in the melt of impact PMMA: influence of concentration and aggregation of dispersed rubber particles. *Journal of Rheology*, *37*(4), 663-679.

BU, W., & HE, J. (1996). Effect of mixing time on the morphology of immiscible polymer blends. *Journal of Applied Polymer Science*, *62*(9), 1445-1456.

CASSAGNAU, P., BERT, M., VERNEY, V., & MICHEL, A. (1992). A Rheological Method for the Study of Cross-Linking of Ethylene Acetate and Ethylene Acrylic Ester Copolymer in a Polypropylene Matrix. *Polymer Engineering and Science*, *32*(15), 998-1003.

CASTRO, M., CARROT, C., & PROCHAZKA, F. (2004). Experimental and theoretical description of low frequency viscoelastic behaviour in immiscible polymer blends. *Polymer*, *45*(12), 4095-4104.

CASTRO, M., PROCHAZKA, F., & CARROT, C. (2005). Cocontinuity in immiscible polymer blends: A gel approach. *Journal of Rheology*, *49*(1), 149-160.

CHAPUT, S., CARROT, C., CASTRO, M., & PROCHAZKA, F. (2004). Co-continuity interval in immiscible polymer blends by dynamic mechanical spectroscopy in the molten and solid state. *Rheologica Acta*, *43*(5), 417-426.

CHESTERS, A. K. (1991). The modeling of coalescence processes in fluid-liquid dispersions: a review of current understanding. *Chemical Engineering Research and Design*, *69*(A4), 259-270.

CHUNG, O., & CORAN, A. Y. (1997). The morphology of rubber/plastic blends. *Rubber Chemistry and Technology*, *70*(5), 781-797.

CHUNG, O., & NADELLA, H. P. (2001). Phase morphology and cure state characterization of soft thermoplastic vulcanizates (TPVs) by using atomic force microscopy (AFM). *ANTEC 2001 Plastics: 59th Annual Technical Conference Proceedings*, Dallas, TX, (Vol. 3, pp. 2926-2930). Society of Plastics Engineers.

CORAN, A. Y., & PATEL, R. (1981). Rubber-thermoplastic compositions. Part IV. Thermoplastic vulcanizates from various rubber-plastic combinations. *Rubber Chemistry and Technology*, *54*(4), 892-903.

CORAN, A. Y., PATEL, R. P., & WILLIAMS, D. (1982). Rubber-thermoplastic compositions. Part V. Selecting polymers for thermoplastic vulcanizates. *Rubber Chemistry and Technology*, *55*(1), 116-136.

COWIE, J. M. G., & ARRIGHI, V. (2008). *Polymers: chemistry and physics of modern materials* (3rd Ed.). Boca Raton, FL: CRC Press.

COX, W. P., & MERZ, E. H. (1958). Correlation of dynamic and steady flow viscosities. *Journal of Polymer Science*, *28*, 619-622.

DE BRUIJN, R. A. (1989). *Deformation and breakup of drops in simple shear flows*. Ph.D. Thesis, Eindhoven University of Technology, Eindhoven, Netherlands.

DE, S. K., & BHOWMICK, A. K. (1990). *Thermoplastic elastomers from rubber-plastic blends*. New York, NY: Ellis Horwood.

DEYRAIL, Y., & CASSAGNAU, P. (2004). Phase deformation under shear in an immiscible polymer blend: Influence of strong permanent elastic properties. *Journal of Rheology*, *48*(3), 505-524.

DOI, M., & OHTA, T. (1991). Dynamics and Rheology of Complex Interfaces .1. *Journal of Chemical Physics*, *95*(2), 1242-1248.

DROBNY, J. G. (2007). *Handbook of thermoplastic elastomers*. Norwich, NY: William Andrew Pub.

DUFAURE, N., CARREAU, P. J., HEUZEY, M. C., & MICHEL, A. (2005). Phase inversion in immiscible blends of PE and reactive EVA. *Journal of Polymer Engineering*, *25*(3), 187-216.

ELEMANS, P. H. M., JANSSEN, J. M. H., & MEIJER, H. E. H. (1990). The Measurement of Interfacial-Tension in Polymer-Polymer Systems - the Breaking Thread Method. *Journal of Rheology*, *34*(8), 1311-1325.

ELLUL, M. D. (1998). Plasticization of polyolefin elastomers, semicrystalline plastics and blends crosslinked in situ during melt mixing. *Rubber Chemistry and Technology*, *71*(2), 244-276.

ELMENDORP, J. J. (1986). *A study on polymer blending microrheology*. Ph.D. Thesis, Delft University of Technology, Delft, Netherlands.

EVERAERT, V., AERTS, L., & GROENINCKX, G. (1999). Phase morphology development in immiscible PP/(PS/PPE) blends influence of the melt-viscosity ratio and blend composition. *Polymer*, *40*(24), 6627-6644.

FAVIS, B. D. (1990). Effect of processing parameters on the morphology of an immiscible binary blend. *Journal of Applied Polymer Science*, *39*(2), 285-300.

FAVIS, B. D. (2000). Factors influencing the morphology of immiscible polymer blends in melt processing. In PAUL, D. R., & BUCKNALL, C. B., *Polymer Blends* (Vol. 1: Formulation, pp. 239-289). New York, NY: Wiley.

FAVIS, B. D., & CHALIFOUX, J.-P. (1987). Effect of viscosity ratio on the morphology of polypropylene/polycarbonate blends during processing. *Polymer Engineering and Science*, *27*(21), 1591-1600.

FAVIS, B. D., & CHALIFOUX, J.-P. (1988). Influence of composition on the morphology of polypropylene/polycarbonate blends. *Polymer*, *29*(10), 1761-1767.

FENOUILLOT, F., & PERIER-CAMBY, H. (2004). Formation of a fibrillar morphology of crosslinked epoxy in a polystyrene continuous phase by reactive extrusion. *Polymer Engineering and Science*, *44*(4), 625-637.

FORTELNY, I., & ZIVNY, A. (1995). Coalescence in Molten Quiescent Polymer Blends. *Polymer*, *36*(21), 4113-4118.

FRITZ, H. G., BOLZ, U., & CAI, Q. (1999). Innovative TPV two-phase polymers: Formulation, morphology formation, property profiles and processing characteristics. *Polymer Engineering and Science*, *39*(6), 1087-1099.

GALLOWAY, J. A., KOESTER, K. J., PAASCH, B. J., & MACOSKO, C. W. (2004). Effect of sample size on solvent extraction for detecting cocontinuity in polymer blends. *Polymer*, *45*(2), 423-428.

GALLOWAY, J. A., & MACOSKO, C. W. (2004). Comparison of methods for the detection of cocontinuity in poly(ethylene oxide)/polystyrene blends. *Polymer Engineering and Science*, *44*(4), 714-727.

GALLOWAY, J. A., MONTMINY, M. D., & MACOSKO, C. W. (2002). Image analysis for interfacial area and cocontinuity detection in polymer blends. *Polymer*, *43*(17), 4715-4722.

GESSLER, A. M., & HASLETT, W. H., JR. (1962). *Vulcanized blends of crystalline polypropylene and chlorinated butyl rubber*. US Patent 3,037,954.

GHODGAONKAR, P. G., & SUNDARARAJ, U. (1996). Prediction of dispersed phase drop diameter in polymer blends: The effect of elasticity. *Polymer Engineering and Science*, *36*(12), 1656-1665.

GOETTLER, L. A., RICHWINE, J. R., & WILLE, F. J. (1982). Rheology and processing of olefin-based thermoplastic vulcanizates. *Rubber Chemistry and Technology*, *55*(5), 1448-1463.

GOHARPEY, F., FOUDAZI, R., NAZOCKDAST, H., & KATBAB, A. A. (2008). Determination of twin-screw extruder operational conditions for the preparation of thermoplastic vulcanizates on the basis of batch-mixer results. *Journal of Applied Polymer Science*, *107*(6), 3840-3847.

GOHARPEY, F., KATBAB, A. A., & NAZOCKDAST, H. (2001). Mechanism of morphology development in dynamically cured EPDM/PP TPEs. I. Effects of state of cure. *Journal of Applied Polymer Science*, *81*(10), 2531-2544.

GOHARPEY, F., KATBAB, A. A., & NAZOCKDAST, H. (2003). Formation of rubber particle agglomerates during morphology development in dynamically crosslinked EPDM/PP

thermoplastic elastomers. Part 1: Effects of processing and polymer structural parameters. *Rubber Chemistry and Technology*, *76*(1), 239-252.

GOHARPEY, F., NAZOCKDAST, H., & KATBAB, A. A. (2005). Relationship between the rheology and morphology of dynamically vulcanized thermoplastic elastomers based on EPDM/PP. *Polymer Engineering and Science*, *45*(1), 84-94.

GRACE, H. P. (1982). Dispersion phenomena in high viscosity immiscible fluid systems and application of static mixers as dispersion devices in such systems. *Chemical Engineering Communications*, *14*(3-6), 225-277.

GRAEBLING, D., MULLER, R., & PALIERNE, J. F. (1993). Linear viscoelasticity of incompatible polymer blends in the melt in relation with interfacial properties. *Journal de Physique IV*, *3*(C7), 1525-1534.

GRMELA, M., & AIT-KADI, A. (1994). Comments on the Doi-Ohta theory fo blends. *Journal of Non-Newtonian Fluid Mechanics*, *55*(2), 191-195.

GRMELA, M., & AIT-KADI, A. (1998). Rheology of inhomogeneous immiscible blends. *Journal of Non-Newtonian Fluid Mechanics*, *77*(3), 191-199.

GRMELA, M., AIT-KADI, A., & UTRACKI, L. A. (1998). Blends of two immiscible and rheologically different fluids. *Journal of Non-Newtonian Fluid Mechanics*, *77*(3), 253-259.

GRMELA, M., BOUSMINA, M., & PALIERNE, J. F. (2001). On the rheology of immiscible blends. *Rheologica Acta*, *40*(6), 560-569.

GRMELA, M., & OTTINGER, H. C. (1997). Dynamics and thermodynamics of complex fluids. I. Development of a general formalism. *Physical Review E*, *56*(6), 6620-6632.

GUENTHER, G. K., & BAIRD, D. G. (1996). An evaluation of the Doi-Ohta theory for an immiscible polymer blend. *Journal of Rheology*, *40*(1), 1-20.

GUO, R., TALMA, A. G., DATTA, R. N., DIERKES, W. K., & NOORDERMEER, J. W. M. (2008). Solubility study of curatives in various rubbers. *European Polymer Journal*, *44*(11), 3890-3893.

HAN, C. D. (1981). *Multiphase flow in polymer processing*. New York, NY: Academic Press.

HAN, P. K., & WHITE, J. L. (1995). Rheological studies of dynamically vulcanized and mechanical blends of polypropylene and ethylene-propylene rubber. *Rubber Chemistry and Technology*, *68*(5), 728-738.

HARRATS, C., THOMAS, S., & GROENINCKX, G. (2006). *Micro- and nanostructured polymer blend systems: phase morphology and interfaces*. Boca Raton, FL: CRC/Taylor & Francis.

HEMMATI, M., NAZOKDAST, H., & PANAHI, H. S. (2001). Study on morphology of ternary polymer blends. I. Effects of melt viscosity and interfacial interaction. *Journal of Applied Polymer Science*, *82*(5), 1129-1137.

HEMMATI, M., NAZOKDAST, H., & PANAHI, H. S. (2001). Study on morphology of ternary polymer blends. II. Effect of composition. *Journal of Applied Polymer Science*, *82*(5), 1138-1146.

HO, R. M., WU, C. H., & SU, A. C. (1990). Morphology of plastic/rubber blends. *Polymer Engineering and Science*, *30*(9), 511-518.

HOLDEN, G. (2000). *Understanding thermoplastic elastomers*. Cincinnati, OH: Hanser Gardner Pub.

HUANG, H., IKEHARA, T., & NISHI, T. (2003). Observation of morphology in EPDM/nylon copolymer thermoplastic vulcanizates by atomic force microscopy. *Journal of Applied Polymer Science*, *90*(5), 1242-1248.

JAIN, A. K., GUPTA, N. K., & NAGPAL, A. K. (2000). Effect of dynamic cross-linking on melt rheological properties of polypropylene/ethylene-propylene-diene rubber blends. *Journal of Applied Polymer Science*, *77*(7), 1488-1505.

JANSSEN, J. M. H. (1993). *Dynamics of liquid-liquid mixing*. Ph.D. Thesis, Eindhoven University, Eindhoven, Netherlands.

JANSSEN, J. M. H. (1997). Emulsions: the dynamics of liquid-liquid mixing. In MEIJER, H. E. H., *Materials Science and Technology* (Vol. 18, Processing of Polymers, pp. 115-188). Weinheim, Germany: Wiley.

JANSSEN, J. M. H., & MEIJER, H. E. H. (1995). Dynamics of liquid-liquid mixing: A 2-zone model. *Polymer Engineering and Science*, *35*(22), 1766-1780.

JAYARAMAN, K., KOLLI, V. G., KANG, S.-Y., KUMAR, S., & ELLUL, M. D. (2004). Shear flow behavior and oil distribution between phases in thermoplastic vulcanizates. *Journal of Applied Polymer Science*, *93*(1), 113-121.

JORDHAMO, G. M., MANSON, J. A., & SPERLING, L. H. (1986). Phase continuity and inversion in polymer blends and simultaneous interpenetrating networks. *Polymer Engineering and Science*, *26*(8), 517-524.

JOUBERT, C., CASSAGNAU, P., MICHEL, A., & CHOPLIN, L. (2002). Influence of the processing conditions on a two-phase reactive blend system: EVA/PP thermoplastic vulcanizate. *Polymer Engineering and Science*, *42*(11), 2222-2233.

KARGER-KOCSIS, J., KALLO, A., & KULEZNEV, V. N. (1984). Phase structure of impact-modified polypropylene blends. *Polymer*, *25*(2), 279-286.

KERNER, E. H. (1956). The elastic and thermo-elastic properties of composite media. *Proceedings of the Royal Society of London, Series A: Mathematical and Physical Sciences*, (69, pp. 808-813).

KIM, H. Y., JEONG, U., & KIM, J. K. (2003). Reaction kinetics and morphological changes of reactive polymer-polymer interface. *Macromolecules*, *36*(5), 1594-1602.

KITAYAMA, N., KESKKULA, H., & PAUL, D. R. (2000). Reactive compatibilization of nylon 6/styrene-acrylonitrile copolymer blends. Part 1. Phase inversion behavior. *Polymer*, *41*(22), 8041-8052.

LACROIX, C., GRMELA, M., & CARREAU, P. J. (1999). Morphological evolution of immiscible polymer blends in simple shear and elongational flows. *Journal of Non-Newtonian Fluid Mechanics*, *86*(1-2), 37-59.

LAZO, N. D. B., & SCOTT, C. E. (1999). Morphology development during phase inversion of a PS/PE blend in isothermal steady shear flow. *Polymer*, *40*(20), 5469-5478.

LEE, H. M., & PARK, O. O. (1994). Rheology and Dynamics of Immiscible Polymer Blends. *Journal of Rheology*, *38*(5), 1405-1425.

LEI, C. H., HUANG, X. B., & MA, F. Z. (2007). The distribution coefficient of oil and curing agent in PP/EPDM TPV. *Polymers for Advanced Technologies*, *18*(12), 999-1003.

LEVITT, L., MACOSKO, C. W., & PEARSON, S. D. (1996). Influence of normal stress difference on polymer drop deformation. *Polymer Engineering and Science*, *36*(12), 1647-1655.

LI, J. M., MA, P. L., & FAVIS, B. D. (2002). The role of the blend interface type on morphology in cocontinuous polymer blends. *Macromolecules*, *35*(6), 2005-2016.

LITVINOV, V. M. (2006). EPDM/PP thermoplastic vulcanizates as studied by proton NMR relaxation: Phase composition, molecular mobility, network structure in the rubbery phase, and network heterogeneity. *Macromolecules*, *39*(25), 8727-8741.

LUCIANI, A., & JARRIN, J. (1996). Morphology development in immiscible polymer blends. *Polymer Engineering and Science*, *36*(12), 1619-1626.

LYNGAAE-JORGENSEN, J., RASMUSSEN, K. L., CHTCHERBAKOVA, E. A., & UTRACKI, L. A. (1999). Flow induced deformation of dual-phase continuity in polymer blends and alloys. Part I. *Polymer Engineering and Science*, *39*(6), 1060-1071.

MACAUBAS, P. H. P., DEMARQUETTE, N. R., & DEALY, J. M. (2005). Nonlinear viscoelasticity of PP/PS/SEBS blends. *Rheologica Acta*, *44*(3), 295-312.

MACHADO, A., & VAN DUIN, M. (2005). Dynamic vulcanisation of EPDM/PE-based thermoplastic vulcanisates studied along the extruder axis. *Polymer*, *46*(17), 6575-6586.

MARGUERAT, F., CARREAU, P. J., & MICHEL, A. (2002). Morphology and rheological properties of polypropylene/reactive elastomer blends. *Polymer Engineering and Science*, *42*(10), 1941-1955.

MARTIN, G., BARRES, C., SONNTAG, P., GAROIS, N., & CASSAGNAU, P. (2009). Morphology development in thermoplastic vulcanizates (TPV): Dispersion mechanisms of a pre-crosslinked EPDM phase. *European Polymer Journal*, *45*(11), 3257-3268.

MARTIN, P., CARREAU, P. J., FAVIS, B. D., & JEROME, R. (2000). Investigating the morphology/rheology interrelationships in immiscible polymer blends. *Journal of Rheology*, *44*(3), 569-583.

MEDSKER, R. E., GILBERTSON, G. W., & PATEL, R. P. (1999). *Preferred structure of phenolic resin cuartive for thermoplastic vulcanizate*. US Patent 5,952,425.

MEKHILEF, N., CARREAU, P. J., FAVIS, B. D., MARTIN, P., & OUHLAL, A. (2000). Viscoelastic properties and interfacial tension of polystyrene-polyethylene blends. *Journal of Polymer Science, Part B: Polymer Physics*, *38*(10), 1359-1368.

METELKIN, V. I., & BLEKHT, V. S. (1984). Formation of a continuous phase in heterogeneous mixtures of polymers. *Kolloidnyi Zhurnal*, *46*(3), 476-480.

MICHAELS, A. S., VIETH, W. R., & ALCALAY, H. H. (1968). The solubility parameter of polypropylene. *Journal of Applied Polymer Science*, *12*(7), 1621-1624.

MIGHRI, F., AJJI, A., & CARREAU, P. J. (1997). Influence of elastic properties on drop deformation in elongational flow. *Journal of Rheology*, *41*(5), 1183-1201.

MIGHRI, F., CARREAU, P. J., & AJJI, A. (1998). Influence of elastic properties on drop deformation and breakup in shear flow. *Journal of Rheology*, *42*(6), 1477-1490.

MIGHRI, F., & HUNEAULT, M. A. (2006). In situ visualization of drop deformation, erosion, and breakup in high viscosity ratio polymeric systems under high shearing stress conditions. *Journal of Applied Polymer Science*, *100*(4), 2582-2591.

MIKAMI, T., COX, R. G., & MASON, S. G. (1975). Breakup of extending liquid threads. *International Journal of Multiphase Flow*, *2*(2), 113-138.

MILES, I. S., & ZUREK, A. (1988). Preparation, structure, and properties of two-phase co-continuous polymer blends. *Polymer Engineering and Science*, *28*(12), 796-805.

MOLY, K. A., OOMMEN, Z., BHAGAWAN, S. S., GROENINCKX, G., & THOMAS, S. (2002). Melt rheology and morphology of LLDPE/EVA blends: Effect of blend ratio, compatibilization, and dynamic crosslinking. *Journal of Applied Polymer Science*, *86*(13), 3210-3225.

MORRISON, F. A. (2001). *Understanding rheology*. New York: Oxford University Press.

MULLER, R., GERARD, E., DUGAND, P., REMPP, P., & GNANOU, Y. (1991). Rheological characterization of the Gel point: a new interpretation. *Macromolecules*, *24*(6), 1321-1326.

NAKAJIMA, N., & HARRELL, E. R. (1982). Effect of extending oil on viscoelastic behavior of elastomers. *Journal of Rheology*, *26*(5), 427-458.

NASKAR, K., & NOORDERMEER, J. W. M. (2005). Thermoplastic elastomers by dynamic vulcanization. *Progress in Rubber Plastics Recycling Technology*, *21*(1), 1-26.

NIELSEN, L. E. (1974). Morphology and the elastic modulus of block polymers and polyblends. *Rheologica Acta*, *13*(1), 594-600.

NIELSEN, L. E. (1977). *Polymer Rheology*. New York: M. Dekker.

ODERKERK, J., & GROENINCKX, G. (2002). Morphology development by reactive compatibilisation and dynamic vulcanisation of nylon6/EPDM blends with a high rubber fraction. *Polymer*, *43*(8), 2219-2228.

ODIAN, G. G. (2004). *Principles of polymerization* (4th Ed.). Hoboken, NJ: Wiley.

OHLSSON, B., HASSANDER, H., & TORNELL, B. (1996). Blends and thermoplastic interpenetrating polymer networks of polypropylene and polystyrene-block-poly(ethylene-stat-butylene)-block-polystyrene triblock copolymer .1. Morphology and structure-related properties. *Polymer Engineering and Science*, *36*(4), 501-510.

OLDROYD, J. G. (1953). The elastic and viscous properties of emulsions and suspensions. *Proceedings of the Royal Society of London, Series A: Mathematical and Physical Sciences*, *218*, 122-132.

OMONOV, T. S., HARRATS, C., MOLDENAERS, P., & GROENINCKX, G. (2007). Phase continuity detection and phase inversion phenomena in immiscible polypropylene/polystyrene blends with different viscosity ratios. *Polymer*, *48*(20), 5917-5927.

ONUKI, A. (1987). Viscosity enhancement by domains in phase-seperating fluids near the critical point: Proposal of critical rheology. *Physical Review A*, *35*(12), 5149-5155.

OTTINGER, H. C., & GRMELA, M. (1997). Dynamics and thermodynamics of complex fluids. II. Illustrations of a general formalism. *Physical Review E*, *56*(6), 6633-6655.

PALIERNE, J. F. (1990). Linear rheology of viscoelastic emulsions with interfacial tension. *Rheologica Acta*, *29*(3), 204-214.

PAUL, D. R., & BARLOW, J. W. (1980). Polymer blends (or alloys). *Journal of Macromolecular Science, Reviews in Macromolecular Chemistry*, *C18*(1), 109-168.

PAUL, D. R., & BUCKNALL, C. B. (2000). *Polymer blends*. New York: Wiley.

PEON, J., VEGA, J. F., DEL AMO, B., & MARTINEZ-SALAZAR, J. (2003). Phase morphology and melt viscoelastic properties in blends of ethylene/vinyl acetate copolymer and metallocene-catalysed linear polyethylene. *Polymer*, *44*(10), 2911-2918.

PHAM, T., RADUSCH, H.-J., & WINKELMANN, T. (2001). Thermoplastic elastomers by reactive compounding. *Proceedings of the International conference 'Polymers in the Third Millenium'*, Montpellier, France, (pp. 123).

PONSARD-FILLETTE, M., BARRES, C., & CASSAGNAU, P. (2005). Viscoelastic study of oil diffusion in molten PP and EPDM copolymer. *Polymer*, *46*(23), 10256-10268.

PORTAL, J., CARROT, C., MAJESTE, J. C., COCARD, S., PELISSIER, V., BARAN, K., & ANSELME-BERTRAND, I. (2008). Coupling of various methods for the investigation of the morphology of blends of natural rubber and polybutadiene. *Polymer Engineering and Science*, *48*(6), 1068-1076.

POTENTE, H., ANSAHL, J., & KLARHOLZ, B. (1994). Design of tightly intermeshing co-rotating twin-screw extruders. *International Polymer Processing*, *9*(1), 11-25.

POTENTE, H., KRAWINKEL, S., BASTIAN, M., STEPHAN, M., & POTSCHKE, P. (2001). Investigation of the melting behavior and morphology development of polymer blends in the melting zone of twin-screw extruders. *Journal of Applied Polymer Science*, *82*(8), 1986-2002.

POTSCHKE, P., & PAUL, D. R. (2003). Formation of co-continuous structures in melt-mixed immiscible polymer blends. *Journal of Macromolecular Science - Polymer Reviews*, *43*(1), 87-141.

PROCHAZKA, F., DIMA, R., MAJESTE, J. C., & CARROT, C. (2003). Phase inversion and co-continuity domain in immiscible polyethylene/polystyrene blends. *E-Polymers*, *040*.

RADUSCH, H.-J. (2006). Phase Morphology of Dynamically Vulcanized Thermoplastic Vulcanizates. In HARRATS, C., THOMAS, S., & GROENINCKX, G., *Micro- and nanostructured polymer blend systems: phase morphology and interfaces*. Boca Raton, FL: CRC/Taylor & Francis.

RADUSCH, H.-J., & PHAM, T. (1996). Morphology formation in dynamic vulcanized PP/EPDM blends. *Kautschuk Gummi Kunststoffe*, *49*(4), 249-257.

RATNAGIRI, R., & SCOTT, C. E. (1998). Phase inversion during compounding with a low melting major component: Polycaprolactone/polyethylene blends. *Polymer Engineering and Science*, *38*(10), 1751-1762.

RAUWENDAAL, C. (2001). *Polymer extrusion* (4th Ed.). Cincinnati, OH: Hanser Gardner Pub.

REIGNIER, J., FAVIS, B. D., & HEUZEY, M. C. (2003). Factors influencing encapsulation behavior in composite droplet-type polymer blends. *Polymer*, *44*(1), 49-59.

ROLAND, C. M., & BOHM, G. G. A. (1984). Shear-induced coalescence in two-phase polymeric systems. I. Determination from small-angle neutron scattering measurements. *Journal of Polymer Science, Part B: Polymer Physics*, *22*(1), 79-93.

RUSS, J. C. (1986). *Practical stereology*. New York, NY: Plenum Press.

SARAZIN, P., & FAVIS, B. D. (2003). Morphology control in co-continuous poly(L-lactide)/polystyrene blends: A route towards highly structured and interconnected porosity in poly(L-lactide) materials. *Biomacromolecules*, *4*(6), 1669-1679.

SAROOP, M., & MATHUR, G. N. (1997). Studies on the dynamically vulcanized polypropylene (PP) butadiene styrene block copolymer (SBS) blends: Mechanical properties. *Journal of Applied Polymer Science*, *65*(13), 2691-2701.

SCHOLZ, P., FROELICH, D., & MULLER, R. (1989). Viscoelastic properties and morphology of two-phase polypropylene/polyamide 6 blends in the melt. Interpretation of results with an emulsion model. *Journal of Rheology (New York, NY, United States)*, *33*(3), 481-499.

SCHOWALTER, W. R., CHAFFEY, C. E., & BRENNER, H. (1968). Rheological behavior of a dilute emulsion. *Journal of Colloid and Interface Science*, *26*(2), 152-160.

SCOTT, C. E., & MACOSKO, C. W. (1991). Model experiments concerning morphology development during the initial stages of polymer blending. *Polymer Bulletin*, *26*(3), 341-348.

SCOTT, C. E., & MACOSKO, C. W. (1995). Morphology development during the initial stages of polymer-polymer blending. *Polymer*, *36*(3), 461-470.

SENGERS, W. G. F., SENGUPTA, P., NOORDERMEER, J. W. M., PICKEN, S. J., & GOTSIS, A. D. (2004). Linear viscoelastic properties of olefinic thermoplastic elastomer blends: melt state properties. *Polymer*, *45*(26), 8881-8891.

SENGERS, W. G. F., WUBBENHORST, M., PICKEN, S. J., & GOTSIS, A. D. (2005). Distribution of oil in olefinic thermoplastic elastomer blends. *Polymer*, *46*(17), 6391-6401.

SENGUPTA, P., & NOORDERMEER, J. W. M. (2004). Effects of composition and processing conditions on morphology and properties of thermoplastic elastomer blends of SEBS-PP-oil and dynamically vulcanized EPDM-PP-oil. *Journal of Elastomers and Plastics*, *36*(4), 307-331.

SHAHBIKIAN, S., CARREAU, P. J., HEUZEY, M.-C., ELLUL, M. D., CHENG, J., SHIRODKAR, P., & NADELLA, H. (2010). Rheology/morphology relationship of plasticized and non-plasticized thermoplastic elastomers based on ethylene-propylene-diene-terpolymer and propylene. *Polymer Engineering and Science*, *In press*.

SHARIATPANAHI, H., NAZOKDAST, H., DABIR, B., SADAGHIANI, K., & HEMMATI, M. (2002). Relationship between interfacial tension and dispersedphase particle size in polymer blends. I. PP/EPDM. *Journal of Applied Polymer Science*, *86*(12), 3148-3159.

SHI, D., KE, Z., YANG, J. H., GAO, Y., WU, J., & YIN, J. H. (2002). Rheology and morphology of reactively compatibilized PP/PA6 blends. *Macromolecules*, *35*(21), 8005-8012.

SHIH, C. K., TYNAN, D. G., & DENELSBECK, D. A. (1991). Rheological properties of multicomponent polymer systems undergoing melting or softening during compounding. *Polymer Engineering and Science*, *31*(23), 1670-1673.

STEEMAN, P., & ZOETELIEF, W. (2000). Rheology of TPVs. *ANTEC 2000 Plastics: 58th Annual Technical Conference Proceedings*, Orlando, FL, (Vol. 3, pp. 3297-3301). Society of Plastics Engineers.

STEINMANN, S., GRONSKI, W., & FRIEDRICH, C. (2001). Cocontinuous polymer blends: influence of viscosity and elasticity ratios of the constituent polymers on phase inversion. *Polymer*, *42*(15), 6619-6629.

STEINMANN, S., GRONSKI, W., & FRIEDRICH, C. (2002). Quantitative rheological evaluation of phase inversion in two-phase polymer blends with cocontinuous morphology. *Rheologica Acta*, *41*(1-2), 77-86.

SUNDARARAJ, U., DORI, Y., & MACOSKO, C. W. (1995). Sheet formation in immiscible polymer blends - model experiments on initial blend morphology. *Polymer*, *36*(10), 1957-1968.

SUNDARARAJ, U., MACOSKO, C. W., ROLANDO, R. J., & CHAN, H. T. (1992). Morphology development in polymer blends. *Polymer Engineering and Science*, *32*(24), 1814-1823.

TADMOR, Z., & GOGOS, C. G. (2006). *Principles of polymer processing* (2nd Ed.). Hoboken, NJ: Wiley.

TAYLOR, G. I. (1932). The viscosity of a fluid containing small drops of another fluid. *Proceedings of the Royal Society of London, Series A: Mathematical and Physical Sciences*, (138, pp. 41-48).

TAYLOR, G. I. (1934). The formation of emulsions in definable fields of flow. *Proceedings of the Royal Society of London, Series A: Mathematical and Physical Sciences*, (146, pp. 501-523).

THOMAS, S., & GROENINCKX, G. (1999). Nylon 6/ethylene propylene rubber (EPM) blends: Phase morphology development during processing and comparison with literature data. *Journal of Applied Polymer Science*, *71*(9), 1405-1429.

TOMOTIKA, S. (1935). On the instability of a cylindrical thread of a viscous liquid surrounded by another viscous fluid. *Proceedings of the Royal Society of London, Series A: Mathematical and Physical Sciences*, (150, pp. 322-337).

TUCKER, C. L., & MOLDENAERS, P. (2002). Microstructural evolution in polymer blends. *Annual Review of Fluid Mechanics*, *34*, 177-210.

TUFANO, C., PETERS, G. W. M., VAN PUYVELDE, P., & MEIJER, H. E. H. (2008). Transient interfacial tension and morphology evolution in partially miscible polymer blends. *Journal of Colloid and Interface Science*, *328*(1), 48-57.

UTRACKI, L. A. (1988). Analysis of Polymer Blends by Rheological Techniques. In KOHUDIC, M. A., *Advances in Polymer Blends and Alloys Technology, Vol. 1*. Lancaster, PA: Technomic Publishing Company, Inc.

UTRACKI, L. A. (1991). On the Viscosity-Concentration Dependence of Immiscible Polymer Blends. *Journal of Rheology*, *35*(8), 1615-1637.

UTRACKI, L. A. (1998). *Commercial polymer blends*. London ; New York: Chapman & Hall.

VAN DUIN, M. (2002). Chemistry of EPDM cross-linking. *Kautschuk Gummi Kunststoffe*, *55*(4), 150-156.

VAN DUIN, M. (2006). Recent developments for EPDM-based thermoplastic vulcanisates. *Macromolecular Symposia*, *233*, 11-16.

VAN OENE, H. (1972). Modes of dispersion of viscoelastic fluids in flow. *Journal of Colloid and Interface Science*, *40*(3), 448-467.

VAN PUYVELDE, P., & MOLDENAERS, P. (2006). Rheology-Morphology Relationships in Immiscible Polymer Blends. In HARRATS, C., THOMAS, S., & GROENINCKX, G., *Micro- and nanostructured polymer blend systems: phase morphology and interfaces*. Boca Raton, FL: CRC/Taylor & Francis.

VEENSTRA, H., VAN DAM, J., & DE BOER, A. P. (2000). On the coarsening of co-continuous morphologies in polymer blends: effect of interfacial tension, viscosity and physical cross-links. *Polymer*, *41*(8), 3037-3045.

VEENSTRA, H., VERKOOIJEN, P. C. J., VAN LENT, B. J. J., VAN DAM, J., DE BOER, A. P., & NIJHOF, A. (2000). On the mechanical properties of co-continuous polymer blends: experimental and modelling. *Polymer*, *41*(5), 1817-1826.

VERBOIS, A., CASSAGNAU, P., MICHEL, A., GUILLET, J., & RAVEYRE, C. (2004). New thermoplastic vulcanizate, composed of polypropylene and ethylene-vinyl acetate copolymer crosslinked by tetrapropoxysilane: evolution of the blend morphology with respect to the crosslinking reaction conversion. *Polymer International*, *53*(5), 523-535.

VINCKIER, I., MOLDENAERS, P., & MEWIS, J. (1997). Transient rheological response and morphology evolution of immiscible polymer blends. *Journal of Rheology*, *41*(3), 705-718.

VRENTAS, J. S., & DUDA, J. L. (1977). Diffusion in polymer-solvent systems - 3. Construction of deborah number diagrams. *Journal of Polymer Science, Part B: Polymer Physics*, *15*(3), 441-453.

WILLEMSE, R. C., DE BOER, A. P., VAN DAM, J., & GOTSIS, A. D. (1998). Co-continuous morphologies in polymer blends: a new model. *Polymer*, *39*(24), 5879-5887.

WILLEMSE, R. C., RAMAKER, E. J. J., VAN DAM, J., & DE BOER, A. P. (1999). Morphology development in immiscible polymer blends: initial blend morphology and phase dimensions. *Polymer*, *40*(24), 6651-6659.

WINTERS, R., LUGTENBURG, J., LITVINOV, V. M., VAN DUIN, M., & DE GROOT, H. J. M. (2001). Solid state C-13 NMR spectroscopy on EPDM/PP/oil based thermoplastic vulcanizates in the melt. *Polymer*, *42*(24), 9745-9752.

WU, S. (1987). Formation of dispersed phase in incompatible polymer blends: interfacial and rheological effects. *Polymer Engineering and Science*, *27*(5), 335-343.

WYPYCH, G. (2004). *Handbook of plasticizers*. Toronto; New York: ChemTec Pub.; William Andrew Pub.

XING, P. X., BOUSMINA, M., RODRIGUE, D., & KAMAL, M. R. (2000). Critical experimental comparison between five techniques for the determination of interfacial tension in polymer blends: Model system of polystyrene/polyamide-6. *Macromolecules*, *33*(21), 8020-8034.

YANG, Y., CHIBA, T., SAITO, H., & INOUE, T. (1998). Physical characterization of a polyolefinic thermoplastic elastomer. *Polymer*, *39*(15), 3365-3372.

YUAN, Z. H., & FAVIS, B. D. (2005). Coarsening of immiscible co-continuous blends during quiescent annealing. *Aiche Journal*, *51*(1), 271-280.

ZOETELIEF, W. (2001). Rheology and Processing of TPVs. *ANTEC 2001 Plastics: 59th Annual Technical Conference Proceedings*, Dallas, TX, (Vol. 3, pp. 2904-2908). Society of Plastics Engineers.

APPENDIX A

CHEMISTRY OF EPDM CROSS-LINKING IN TPVs

Several different cross-linking systems have already been reported to chemically cross link the EPDM phase in dynamically vulcanized EPDM/PP-based thermoplastic vulcanizates (TPVs): sulphur curing system, co-agent assisted peroxides, activated phenol formaldehyde resins (phenolic resin known as resol), platinum catalyzed hydrosiloxane, vinyltrialkoxysilane/moisture, catalyzed quinonedioxime and bisthiols and etc. (Naskar and Noordermeer, 2005) Each of the aforementioned curing systems has its own advantages and disadvantages, and the choice of the cross-linking system generally depends on many factors such as the cost of the chemicals used, the cure rate, the thermal stability of the crosslinks formed and etc. (Naskar and Noordermeer, 2005).

In this dissertation, a phenolic curing system and more specifically resol-type phenolic resin has been used mainly due to its importance and the extensive use for the cross-linking of the EPDM elastomer in TPV industry, which results in products with good high temperature properties (Naskar and Noordermeer, 2005). Phenolic resins in general are divided into two main groups, i.e. resols and novolacs (Odian, 2004). They are produced in different reaction conditions in terms of pH level and the molar ratio of the phenol:aldehyde reactants (Odian, 2004). Hence, they possess different chemical structure and reactivity. A typical chemical structure of resol-type phenolic resin used as cross-linking agent is shown in Figure A.1. Resols are generally characterized by the presence of reactive methylol groups, and two different types of structures between aromatic rings, i.e. dibenzyl ether and methylene bridges (Medsker et al., 1999; Naskar

and Noordermeer, 2005). On the contrary, novolacs do not possess any reactive methylol functionalities and, therefore, can not be used as a cross-linking agent.

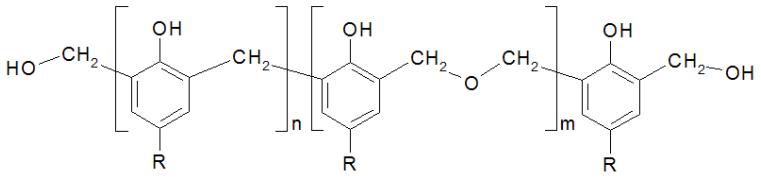

Figure A.1. The chemical structure of resol-type phenol formaldehyde resin. (Medsker et al., 1999)

Generally, those resol-type phenolic resins having high or exclusively methylene bridges (conventional resins) react faster and possess shorter cure time and are preferred for elastomer vulcanization in the thermoset rubber industry (Medsker et al., 1999). However during TPV production and, therefore, in dynamic vulcanization process, the elastomer phase can be more effectively cross-linked with a resol-type curing system containing 50 to ~90 dibenzyl ether links per 100 aromatic rings (Medsker et al., 1999). Furthermore, the high percentage of dibenzyl ether bridges are known to maintain their chemical activity for longer storage time and/or processing at elevated temperatures (Medsker et al., 1999).

In typical resol-type resins used in the thermoplastic elastomer industry, the sum of the repeating units containing dibenzyl ether and methylene bridges (i.e. $n+m$ in Figure A.1) generally varies between 1 to about 15. Moreover, the *para* position of the industrial resins designated with *R* in Figure A.1 is normally substituted by an alkyl group such as *t*-butyl, octyl or nonyl groups. The alkyl substitution is essential since it avoids the formation of methylol functionalities greater than two which upon heating would form thermoset resins, insoluble in elastomer and incapable of cross linking the elastomeric phase. The ordinary non-halogenated resol-type phenolic resin, e.g. heat reactive octylphenol-formaldehyde resin (Schenectady® SP-1045) used in this work, are more effective with a halogen donor. Metal halides from Bronsted

acid complexes such as stannous chloride, ferric chloride, zinc chloride or chlorinated polymers have been reported as activator or catalysts for this curing system (Medsker et al., 1999; Naskar and Noordermeer, 2005). In addition to the chlorinated compounds, it is recommended to use a halogen halide scavenger such as iron oxide, titanium oxide, magnesium oxide, magnesium silicate, silicone dioxide and most preferably zinc oxide (Medsker et al., 1999).

During the cross-linking reaction in the presence of acidic activators, the ether bridges are first split and, therefore, the oligomeric structure of the resol curing system is completely broken (Van Duin, 2002; Naskar and Noordermeer, 2005). The activated resol-type cross-linking reaction is known to proceed via a carbo-cationic mechanism, where the benzylic cations are formed and subsequently react with the ENB co-monomer of EPDM (Van Duin, 2002). The overall main cross-linking steps are shown in Figure A.2. Cross-link cationic precursors consist of phenolic units attached to ENB on one side and on the other side to reactive dimethylene ether units or methylol end groups.

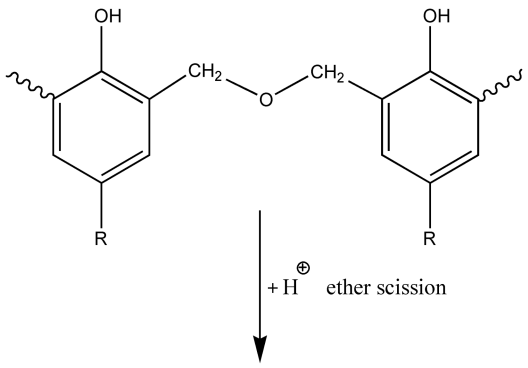

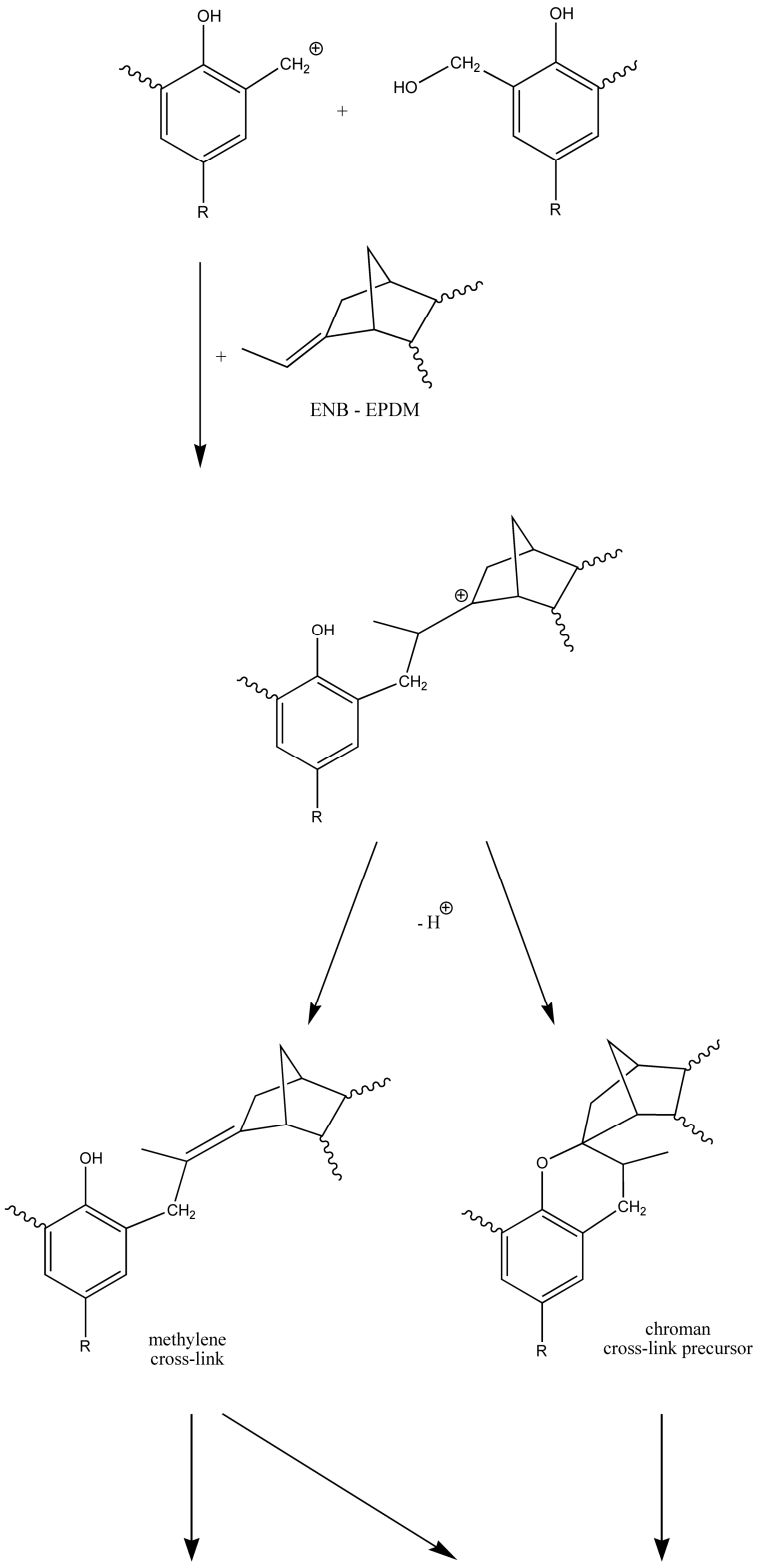
OH
CH2
R
HO
ENB - EPDM
- H
methylene
cross-link
chroman
cross-link precursor
O

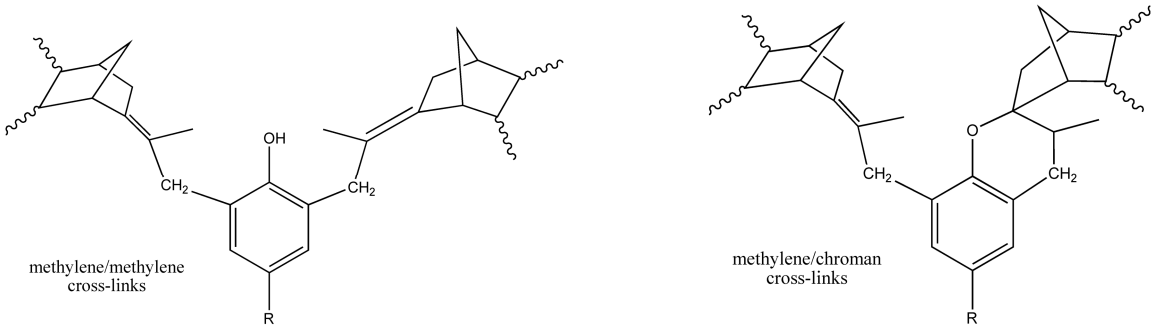

Figure A.2. Reaction mechanism of activated resol cross-linking of EPDM. (Van Duin, 2002)

As it is shown in Figure A.2, this mechanism results in two different types of mono phenolic cross-links: methylene/methylene and/or methylene/chroman cross-links. However, it has to be mentioned that depending on the initial structure of the phenolic resin, i.e. the presence of methylene bridges besides the dibenzyl ether bridges and their corresponding ratio, di-phenolic and tri-phenolic precursors and cross-links may be also formed.